UNIVERSITAT DE BARCELONA

Investigations in animal models of anti-NMDAR encephalitis

Anna García Serra

Investigations in animal models of anti-NMDAR encephalitis

Doctoral thesis presented by

Anna García Serra

Doctoral Programme in Biomedicine. Research area of Neuroscience

Barcelona, June 2021

Director and tutor of thesis

Josep Dalmau Obrador, MD, PhD

UNIVERSITAT DE BARCELONA

IDIBAPS Institut D'Investigacions Biomèdiques August Pi i Sunyer

FUNDACIÓ CLÍNIC BARCELONA

Cover and back cover design and layout by Silvia Vicente Rizo @silviavicenterizo
www.artstation.com/silviavicenterizo

Report for the contribution of Anna García-Serra to the publications that form part of this thesis

Below please find my comments on the publications of Anna García-Serra as part of the group of reports that comprise her doctoral thesis entitled "Investigations in animal models of anti-NMDAR encephalitis". The comments include my assessment on her level of participation as well as the journal impact factor.

Paper I. Pregnancy outcomes in anti-NMDA receptor encephalitis: Case series

Bastien Joubert, Anna García-Serra, Jesús Planagumà, Eugenia Martínez-Hernandez, Andrea Kraft, Frederick Palm, Takahiro Iizuka, Jérôme Honnorat, Frank Leypoldt, Francesc Graus, and Josep Dalmau

Neurol Neuroimmunol Neuroinflamm. 2020 Jan 16;7(3):e668

Impact factor JCR 2020 (percentile): 8.485 (D1)

PhD candidate contribution: The PhD candidate participated in the conceptual and experimental design of this study, and provided assistance for the recollection of data. She participated in the initial drafting of the manuscript.

This article is not expected to be included in any other doctoral thesis.

Paper II. Placental transfer of NMDAR antibodies causes reversible alterations in mice

Anna García-Serra, Marija Radosevic, Anika Pupak, Veronica Brito, José Ríos, Esther Aguilar, Estibaliz Maudes, Helena Ariño, Marianna Spatola, Francesco Mannara, Marta Pedreño, Bastien Joubert, Silvia Ginés, Jesús Planagumà,* and Josep Dalmau* *These authors are joint senior authors

Neurol Neuroimmunol Neuroinflamm. 2020 Nov 10;8(1):e915

Impact factor JCR 2020 (percentile): 8.485 (D1)

PhD candidate contribution: The PhD candidate participated in the experimental design of the study and in most of the experiments including the development of the model, neurodevelopmental and behavioural assessment, obtaining and processing of brain and blood samples, immunohistochemical studies, and analysis of the dendritic spines. She performed the statistics of the immunohistochemical and electrophysiological experiments, drafted the manuscript, including figures, and supplemental material, and wrote the original and revised versions of the manuscript.

This article is not expected to be included in any other doctoral thesis.

Paper III. Blocking placental IgG transfer prevents NMDAR antibody effects in newborn mice

Anna García-Serra, Marija Radosevic, José Ríos, Esther Aguilar, Estibaliz Maudes, Jon Landa, Lidia Sabater, Eugenia Martínez-Hernandez, Jesús Planagumà,* and Josep Dalmau* *These authors are joint senior authors

Neurol Neuroimmunol Neuroinflamm. 2021

Impact factor JCR 2021 (percentile): In press. The available IF from 2020 is 8.485 (D1)

PhD candidate contribution: The PhD candidate participated in the conceptual and experimental design of the study and in most of the experiments including development of the model, neurodevelopmental and behavioural assessment, and in obtaining and processing of brain and blood samples. She performed the statistics of the immunohistochemical and electrophysiological experiments, drafted the manuscript and figures, and in wrote the original and revised versions of the manuscript.
This article is not expected to be included in any other doctoral thesis.

Paper IV. Allosteric modulation of NMDA receptors prevents the antibody effects of patients with anti-NMDAR encephalitis

Francesco Mannara,* Marija Radosevic,* Jesús Planagumà,* David Soto, Esther Aguilar, Anna García-Serra, Estibaliz Maudes, Marta Pedreño, Steven Paul, James Doherty, Michael Quirk, Jing Dai, Xavier Gasull, Mike Lewis,[$] and Josep Dalmau.[$] *,[$]These authors contributed equally

Brain. 2020 Sep 1;143(9):2709-2720

Impact factor JCR 2020 (percentile): 13.501 (D1)

PhD candidate contribution: The PhD candidate participated in the design and development of the following experiments: animal behaviour tests, administration of the treatment, removal of mouse brains, and tissue processing for immunohistochemistry. She participated in the initial drafting of the manuscript.
This article is expected to be used for the PhD thesis of Estibaliz Maudes.

Josep Dalmau MD, PhD

"En los anaqueles de las bibliotecas aguardan juntos libros escritos en países enemigos, incluso en guerra unos con otros. Manuales de fotografía y de interpretación de los sueños. Ensayos que hablan de microbios y galaxias. La autobiografía de un general al lado de las memorias de un desertor. La obra optimista de un autor incomprendido y la obra oscura de un autor de éxito. Los apuntes de una escritora viajera junto a los cinco tomos que necesita un escritor sedentario para contar con pelos y señales sus ensoñaciones. El libro impreso ayer y, a su lado, el que acaba de cumplir veinte siglos. Ahí no se conocen fronteras temporales ni geográficas. Y, por fin, estamos todos invitados a entrar: extranjeros y locales, gente con gafas, con lentillas o con legañas, hombres que llevan moño o mujeres que llevan corbata. Eso se parece a una utopía."

El infinito en un junco. Irene Vallejo
Filóloga y escritora (1979-actualidad)

¿Se puede? ¿Se puede?
Señoras, señores, discúlpenme
si me presento a mí mismo.
Soy el Prólogo.
[…]
El autor
ha intentado aprehender
un trozo natural de la vida.
Su máxima es que el artista
es un hombre y, es para él, como tal,
para quien debe escribir.
Por ello se inspira en la realidad.
Un nido de recuerdos,
en el fondo de su alma,
un día decidió cantar, y,
con lágrimas verdaderas los escribió
y, suspiros y sollozos
le marcaban el compás.

Así, verán amar,
tal como se aman los seres humanos,
verán del odio los tristes frutos.
De dolor, espasmos,
¡gritos de rabia oirán, y cínicas risas!
Y, ustedes, más que nuestros
pobres gabanes de histriones,
nuestras almas consideren,
pues somos hombres y mujeres
de carne y hueso,
y de este huérfano mundo,
como ustedes, respiramos igual aire!
El concepto les he dicho;
ahora, escuchen
cómo se desenvuelve.

(gritando hacia la escena)
¡Vamos! ¡Comenzad!

Prólogo de Pagliacci, ópera de Ruggero Leoncavallo
Compositor italiano (1857-1919)

Abbreviations

AE	Autoimmune encephalopathies
AMPAR	α-amino-3-hydroxy-5-methyl-4-isoxazolepropionic acid receptor
BBB	Blood-brain barrier
CBA	Cell-based assay
CNS	Central nervous system
CSF	Cerebrospinal fluid
FcRn	Neonatal Fc [fragment, crystallizable] receptor
HEK	Human embryonic kidney
HSE	Herpes simplex encephalitis
IgG	Immunoglobulin class G
LE	Limbic encephalitis
LEMS	Lambert-Eaton myasthenic syndrome
MG	Myasthenia gravis
MRI	Magnetic resonance imaging
nAChR	Nicotinic acetylcholine receptor
NLE	Neonatal lupus erythematosus
NMDAR	N-methyl-D-aspartate receptor
PCD	Paraneoplastic cerebellar degeneration
PERM	Progressive encephalomyelitis with rigidity and myoclonus
PNS	Paraneoplastic neurological syndrome
SCLC	Small-cell lung cancer
VGCC	Voltage-gated calcium channels

Table of Contents

ABSTRACT

Background: Anti-N-methyl-D-aspartate receptor (NMDAR) encephalitis is a neuronal antibody-mediated disease that associates with prominent neuropsychiatric symptoms and predominantly affects women of childbearing age. Animal models of this disease have enabled the demonstration that patients' antibodies are pathogenic as they bind to NMDARs and cause their internalization, resulting in a decrease of synaptic levels of these receptors, impairment of synaptic plasticity, memory deficits, and depressive-like and psychotic-like behaviors. These antibodies are class G immunoglobulins (IgG); thus, they can be transferred across the placenta in pregnant patients with anti-NMDAR encephalitis and potentially be detrimental for the fetus/newborn. On the other hand, novel therapeutic strategies to accelerate patients' recovery are of interest.

Objectives: 1) Report the effects of anti-NMDAR encephalitis in pregnant patients and their babies, 2) develop an animal model of placental transfer of IgG antibodies from patients with anti-NMDAR encephalitis to determine their potential pathogenic effects in the fetus and offspring, 3) investigate whether treatment with a neonatal Fc receptor (FcRn) inhibitor prevents the placental transfer of patients' IgG and abrogates the antibody-mediated alterations in the previously developed mouse model, and 4) study the potential therapeutic use of a positive allosteric modulator (PAM) of NMDAR (i.e., SGE-301) in a reported mouse model of cerebroventricular infusion of patients' cerebrospinal fluid (CSF) antibodies.

Methods: Clinical data of patients with anti-NMDAR encephalitis during pregnancy was retrospectively collected from consultations to our group and reviewed from the English literature between 2010 and 2019. To develop the animal model, pregnant C57BL/6J mice were administered via tail vein patients' or controls' IgG from serum on days 14, 15 and 16 of gestation, when the placenta is able to transport IgG and the immature fetal blood-brain barrier is less restrictive to IgG crossing. Using this model, an antibody able to block FcRn-IgG binding required for placental IgG transcytosis was administered via tail vein six hours prior to patients' or controls' IgG injections on days 14-16 of gestation to determine whether it could prevent antibody-mediated effects in fetus/offspring. To assess the potential therapeutic effect of SGE-301, adult mice receiving cerebroventricular infusion of patients' CSF through mini-osmotic pumps during 14 days were treated with a daily subcutaneous administration of this NMDAR PAM. An extensive combination of techniques was used for these studies, including immunocytochemistry with HEK cells or dissociated rat hippocampal neurons, brain immunohistochemical staining, confocal microscopy, electrophysiology on acute hippocampal

sections, and comprehensive panels of standardized developmental and behavioral tasks. All studies were conducted with sets of mice at different time points during fetal or postnatal development into adulthood, or during and after antibody infusion.

Results: (1) Up to 90% of newborns from patients who develop anti-NMDAR encephalitis during pregnancy or become pregnant during recovery are healthy at birth, and only 3 of 16 infants had transient neurologic or respiratory symptoms. All of the babies who had assessable follow-up (7–96 months) had normal development.

(2) IgG antibodies from patients with anti-NMDAR encephalitis intravenously injected to pregnant mice are transferred across the placenta, reach fetal brain and cause a decrease in NMDAR clusters and in cortical plate thickness, along with a reduction of cell-surface and synaptic NMDAR levels, increased dendritic arborization, a decrease of mature (mushroom-shaped) spine density, microglial activation, thinning of brain cortical layers II–IV with cellular compaction, a delay in innate reflexes and eye opening, depressive-like behavior, deficits in nest building, poor motor coordination, and impaired social-spatial memory and hippocampal plasticity after birth. Remarkably, all these paradigms progressively improved (becoming similar to those of controls) during follow-up without further implications in mature adulthood.

(3) In pregnant mice that receive patients' IgG, treatment with FcRn antibody prevents the IgG from reaching the fetal brain, abrogating the decrease of NMDAR clusters and the reduction of cortical plate thickness that were observed in fetuses from untreated pregnant mice. Moreover, among the offspring exposed *in utero* to patients' IgG, those whose mothers are treated with FcRn antibody do not develop the alterations that occur in offspring of untreated mothers, including impairment in hippocampal plasticity, delay in innate reflexes, and visuospatial memory deficits.

(4) In mice infused with patients' CSF, daily subcutaneous administration of SGE-301 prevents the hippocampal memory impairment and synaptic alterations caused by NMDAR antibodies from patients with anti-NMDAR encephalitis.

Conclusions: My studies have contributed to gain insight into the outcome of babies from pregnant patients with anti-NMDAR encephalitis and to unravel the antibody-mediated synaptic alterations underlying the transient developmental and behavioral impairment using a mouse model of placental transfer of patients' IgG. Overall, these findings have provided potential therapeutic strategies in antibody-mediated diseases of the CNS during pregnancy (i.e., FcRn inhibitor) or in an adult mouse model of anti-NMDAR encephalitis (SGE-301).

INTRODUCTION

1. Autoimmune encephalopathies

Autoimmune encephalopathies (AEs) are a new category of neurological diseases mediated by autoantibodies against cell-surface and synaptic proteins. Most AEs manifest as a rapidly progressive encephalitis[1] but can also occur as a cerebellar syndrome[2] or a chronic encephalopathy resembling a degenerative process.[3] These neuropsychiatric syndromes were previously considered idiopathic or not even suspected to be immune-mediated but investigations in the last 15 years have revealed their autoimmune etiology completely changing the clinical diagnosis and thus, converting AEs from potentially lethal to now treatable diseases.[4]

The discovery of AEs stemmed from clinical observations of patients with unusual syndromes that improved after immunotherapy, or whose cerebrospinal fluid (CSF) and brain magnetic resonance imaging (MRI) findings were consistent with an inflammatory disorder, which led to the detection of autoantibodies against neuronal cell-surface proteins in patients' CSF.[5,6] Studies show that patients' antibodies can directly alter the target antigen function, by impairing the surface dynamics of the receptors and eliminating them from synapses, blocking the function of the antigens without changing their synaptic density, interfering with synaptic protein-protein interactions, altering synapse formation, or by unclear mechanisms that may cause a new form of tauopathy. These autoantibody effects impair memory, cognition, and behavior, and may result in psychosis, seizures, and other neurological symptoms that are reversible after removing the antibodies or the antibody-producing cells.[4]

There are currently 19 AEs characterized by autoantibodies directed against excitatory or inhibitory neuronal receptors or proteins involved in somatodendritic signal integration, clustering and modulation of receptors, synaptic vesicle reuptake, or synaptogenesis (Table 1; Figure 1).[4,7,8] AEs can occur in patients with or without cancer. The frequency and type of cancer vary according to the autoantibody. The clinical features, main symptoms, and antibody effects associated to each autoantigen are summarized in Table 1.

Table 1. Antibodies to neuronal cell-surface proteins and synaptic receptors associated to AEs

Target antigen	*Clinical features*	*Main presenting symptoms and tumor*	*Main IgG isotype*	*Antibody effects*
NMDA receptor	80% female, median age 21 yrs (2mo – 85yrs)	Psychiatric symptoms, cognitive impairment, seizures, abnormal movements, and coma Ovarian teratoma (58% in women 18-45 yrs)	IgG1	Displacement from synapse and internalization of NMDA receptors[9,10] Memory and behavioral deficits *in vivo*[11,12]
AMPA receptor	70% female, median age 56 yrs (23-81 yrs)	Limbic encephalitis (LE) with memory loss, psychiatric features Small-cell lung cancer (SCLC), thymoma, breast	IgG1	Decrease in the total surface and synaptic GluA1 and GluA2, and decrease of AMPAR-mEPSC[13]
$GABA_B$ receptor	60% male, median age 61 yrs (16-77 yrs)	LE with severe seizures, memory loss SCLC	IgG1	Block activation of $GABA_BR$ by baclofen[14]
LGI1	65% male, median age 60 yrs (30-80 yrs)	LE, memory loss, fasciobrachial dystonic seizures No tumor associated	IgG4	Disruption of LGI1-Adam binding, and decrease GluR1 of AMPAR.[15] Reduced Kv1.1 and AMPAR, neuronal hyperexcitability, impaired LTP and memory in mice[16]
CASPR2	85% male, median age 60 yrs (46-77 yrs)	Neuromyotonia, muscle spasms, fasciculations, LE, memory loss Thymoma	IgG4	Decrease Gephyrin clusters at inhibitory synaptic contacts[17]
$GABA_A$ receptor	50% female, median age 40 yrs (2.5mo-88yrs)	Status epilepticus No tumor associated	IgG1	Decrease synaptic $GABA_AR$[18]
DPPX	70% male, median age 57 yrs (36-69 yrs)	Confusion, diarrhea, hyperplexia No tumor associated	IgG4/IgG1	Decrease of surface DPPX clusters and Kv4.2 (ref. 19)
Dopamine-2 receptor	50% female, median age 5,5 yrs (1,6-15 yrs)	Dystonia, chorea No tumor associated	Unknown	Internalization of D2R in HEK293 cells[20]
mGluR5	60% male, median age 29 yrs (6–75yrs)	LE, memory loss Hodgkin lymphoma	IgG1	Decrease density of mGluR5 (ref. 21)

Neurexin-3α	80% female, median age 44 yrs (23-50 yrs)	Confusion, seizures, and decreased level of consciousness No tumor associated	IgG1	Decrease expression of neurexin-3α on synapsis; and decrease synapse formation[22]
IgLON5	50 % male, median age 64 yrs (46–83 yrs)	REM and NREM parasomnia with sleep breathing problems, brainstem dysfunction, and gait instability No tumor associated	IgG4	Decrease of surface IgLON5, disruption of cytoskeletal organization in cultured neurons[3,23]
Amphiphysin	100% female, median age 58 yrs (39–73 yrs)	Stiff person syndrome, encephalomyelitis SCLC, breast cancer	IgG1	Disrupt vesicle endocytosis in cultures of neurons.[24] *In vivo* motor neuron hyperactivity, stiffness, and muscle spasms[25]
DNER (Tr)	78% male, median age 61 yrs (14 - 75 yrs)	Paraneoplastic cerebellar degeneration (PCD) Hodgkin's lymphoma	IgG1 (ref. 26)	Unknown
mGluR1	50% male, median age 58 yrs (33–81 yrs)	Severe cerebellar syndrome, cerebellar atrophy Hodgkin's lymphoma	IgG1	Reduction of basal activity of Purkinje cells[2,27] Decrease of mGluR1 clusters in cultured neurons. *In vivo*, transient ataxia[2]
P/Q-type VGCC	52% female, median age 57 yrs (9–87 yrs)	Lambert-Eaton Myasthenic Syndrome (LEMS) SCLC, Hodgkin's lymphoma	Unknown	Reduction of VGCC, and inhibit Ca^{2+} influx.[28] Intrathecal injection in mice cause transient ataxia[29,30]
Glycine receptor (GlyR)	60% male, median age 47 yrs (1-75 yrs)	Hyperekplexia, muscle spasms and cramps, stiff-person syndrome, exaggerated startle, PERM No tumor associated	IgG1	Internalization of GlyR,[31] direct antagonism of glycinergic transmission by Fab fragments,[32] and disturbed escape behavior in zebrafish[33]
SEZ6LP2	50% female, median age 62 yrs (54–69 yrs)	Subacute cerebellar syndrome with frequent extrapyramidal symptoms	IgG4 (ref. 7)	Unknown
mGluR2	2 reported cases; both female, 78 and 3 yrs	Paraneoplastic cerebellar ataxia	IgG1 (ref. 8)	Unknown
GluK2	62,5% male, median age 28 yrs (14–75 yrs)	Encephalitis with prominent cerebellar involvement No tumor associated	IgG1	Internalization of GluK2 receptors in neurons[34]

Since the identification of the first autoimmune encephalopathy, studies aimed at better understanding these rare diseases have investigated the antibody pathogenicity at cellular, synaptic, and circuitry levels.

Figure 1. Rat brain immunostaining with autoantibodies of patients targeting neuronal cell-surface and synaptic proteins.
Sagittal and coronal sections of rat brain immunostained with 13 autoantibodies against neuronal cell-surface and synaptic proteins. Each antibody immunostains rat brain neuropil in a characteristic pattern. For DNER and mGluR1, which predominantly react with cerebellum, the coronal section has been replaced by a sagittal section of cerebellum. Technique of immunostaining was reported in[5]. All tissue sections have been mildly counterstained with hematoxylin. Scale bars: all panels = 2 mm.[4,35]

The concept that some CNS diseases can be mediated by neuronal autoantibodies has evolved over the years influenced by the study of two groups of disorders: the paraneoplastic syndromes and the myasthenic syndromes.

Paraneoplastic neurological syndromes (PNSs)

Paraneoplastic neurological syndromes (PNSs) comprise a group of disorders that are associated with cancer and can affect any part of the nervous system. These disorders are not caused by metastatic or local effects of cancer on the nervous system and, instead, are mediated by cancer-induced immune responses against neuronal proteins.[36,37]

PNSs are usually severe, often disabling, and sometimes lethal.[38] Some PNSs affect only a single area (e.g., limbic encephalitis [LE], which causes memory loss and seizures) or a single cell type (e.g., the Purkinje cells of the cerebellum); whereas in other instances, multiple levels of the nervous system are involved (e.g., encephalomyelitis).[36] PNSs are rare, occurring in <1% of patients with cancer.[37] The neurologic disorder usually appears before the diagnosis of the underlying tumor, which is often asymptomatic, at an early or limited stage, and sometimes occult; it is the neurologic symptoms that take the patient to the doctor.[36]

The onset in PNSs is generally subacute.[37] The neurologic symptoms develop progressively over days or weeks, rapidly leading to severe disability within a few months.[36] CSF examination reveals a mild pleocytosis (30 to 40 white cells per cubic millimeter), a slightly elevated protein level (50 to 100 mg per deciliter), and an elevated immunoglobulin G (IgG) level. Pleocytosis is usually apparent only early in the course of the disease and disappears within several weeks to months. The elevated IgG level may, however, persist. Most patients with PNSs have antibodies in their serum and CSF that are reactive to the nervous system and to an occult tumor.[39] The detection of these so called onconeural autoantibodies is highly predictive of the presence of an underlying cancer.[40]

Whole-body positron-emission tomography – computed tomography (PET-CT) is the best screening method for locating the unidentified cancer based on its hypermetabolic activity[41] and reveals the underlying tumor in up to 95% of patients with PNS at first evaluation.[42,43] Notably, failure to find the antigen in the cancer of a patient with paraneoplastic antibodies should prompt a search for a second cancer.[38] At the time of diagnosis, the tumors of patients with PNS are usually small but may be heavily infiltrated with inflammatory cells[44–46] and often have already spread to the regional lymph nodes.[47] The combination of an indolent tumor and severe neurologic disability suggests effective antitumor immunity coupled with autoimmune brain degeneration.[36]

Ectopic expression of a neuronal protein (onconeural antigen) by a tumor not involving the nervous system triggers an antitumor immune response that in some patients is misdirected against the nervous system.[4] Apoptotic tumor cells are phagocytized by dendritic cells that

migrate to lymph nodes, where they activate onconeural antigen-specific $CD4^+$, $CD8^+$, and B cells.[36,47] B cells mature into plasma cells that produce antibodies against the tumor antigen (onconeural antibodies).[36] It has been shown that apoptosis of tumor cells in PNSs strongly activates tumor-specific T cells. Indeed, these patients develop prominent cytotoxic T-cell responses that slow the growth of the tumor, but which also react against neurons expressing the onconeural antigen in the peripheral or in the CNS if they cross the blood–brain barrier (BBB).[36] Autopsy studies of patients show extensive infiltrates of cytotoxic T cells surrounding neurons and causing degeneration via perforin and granzyme B mechanisms.[48–50] Analysis of CSF cells in patients with paraneoplastic cerebellar degeneration (PCD) through fluorescent-activated cell sorting has revealed that the predominant cell type (over 75 percent) is T cells, with a small component (less than 10 percent) of B cells and natural killer cells.[39] Such cytotoxic T cells could trigger a feedback loop by inducing apoptosis and hence amplification of the antitumor immune response.[36]

Recent studies provide evidence that the onconeural antigens expressed by tumor cells are not identical to those expressed in the nervous system.[51,52] In fact, these genetic mutations generate peptides predicted to bind more strongly to class I antigen-presenting major histocompatibility complex (MHC) than the wild-type ones[52] which are believed to be responsible for breaking immune tolerance towards the onconeural autoantigens.[37] The presence of antigen-specific cytotoxic T cells in PNSs was clearly documented after a patient with acute PCD and anti-Yo antibodies was found to have activated T cells in her blood that were able to lyse target cells presenting the Yo (also called CDR2) antigen *in vitro*.[36,47] Documentation of the expression of MHC class I and MHC class II in neurons supports the possibility that T cells recognize intracellular antigens presented to them as an MHC–peptide complex and thereby kill neurons.[36,53]

Testing for neuronal autoantibodies in serum and CSF has been an important advance in the diagnosis of PNSs. Detection of onconeural antibodies is a robust biomarker of PNSs or cancer, and not only reliably predicts that the neurological syndrome is paraneoplastic but can also help in guiding the search for the underlying tumor.[37] Each type of onconeural antibody is mainly associated with one or a few tumor histologies; therefore, if the underlying tumor is found to be different from the histological type expected, the possibility of a second, occult tumor must be considered.[37] Hu autoantibodies, also known as type 1 antineuronal nuclear antibodies (ANNA1), are the most frequent onconeural autoantibodies detected in patients with PNS encephalomyelitis caused by small-cell lung cancer (SCLC).[37,38] Also, onconeural Yo autoantibodies almost always occur in women with PCD and breast or ovarian cancer,[26,44] and

the same is true for autoantibodies against the delta and notch-like epidermal growth factor-related receptor (DNER) in patients with PCD and Hodgkin's lymphoma.[26,44] In young men (aged < 40 years) with paraneoplastic limbic or brainstem encephalitis, the detection of Ma2 autoantibodies predicts the presence of a testicular germ cell tumor, whereas these antibodies are associated with non-small cell lung cancer (NSCLC) and gastrointestinal tumors in older patients.[54] Ri (ANNA2) autoantibodies occur in patients with opsoclonus myoclonus syndrome (OMS) or brainstem encephalitis in association with breast, lung or gynecological adenocarcinomas.[55]

Onconeural immune responses do not always result in PNSs, as some onconeural autoantibodies can occur in patients with cancer but without neurological dysfunction.[56,57] For example, up to 16% of patients with SCLC without a PNS harbor Hu or SOX1 autoantibodies.[58,59] In patients with a previous history of cancer, the development of PNSs often heralds tumor recurrence.[38]

Despite the high diagnostic value of onconeural antibodies in PNSs, these diseases are predominantly caused by T cell responses. In fact, the term 'onconeural antigen' is typically used only for intracellular autoantigens;[40] and studies using cultures of live neurons have demonstrated that onconeural antibodies cannot reach their intracellular antigen; thus, they do not have pathogenic effects.[60]

Since PNSs are mediated by T-cell immunity, patients with these syndromes rarely respond to immunotherapies focused on removing the autoantibodies or the autoantibody-producing cells. Thus, removal of the tumor as the source of the antigen and drugs directed at suppressing T-cell proliferation, such as tacrolimus or mycophenolate mofetil, may be effective.[36,61,62] However, most of these patients already have irreversible deficits when they are diagnosed with the disease. Many reports suggest that patients with PNSs have a better prognosis than patients with histologically identical tumors that are not associated with PNSs.[63–65]

Autoimmune myasthenic syndromes

In contrast to PNSs, there is a group of neurological diseases that are long known to be antibody-mediated: the myasthenic syndromes. Patients with myasthenic syndromes harbor autoantibodies directed at cell-surface antigens of the synapse between a motor neuron and a muscle fiber, namely the neuromuscular junction (NMJ).[66,67]

Neuromuscular transmission depends on an action potential in the motor neuron that allows the entry of calcium ion (Ca^{2+}) through activated voltage-gated calcium channels (VGCC), leading to the fusion of acetylcholine (ACh)-containing presynaptic vesicles with the membrane. In the synaptic cleft, released ACh binds and activates the postsynaptic nicotinic acetylcholine receptor (nAChR) on the muscle membrane, which results in sodium (Na^{+}) influx and muscle contraction. ACh is immediately eliminated from the NMJ by the enzyme acetylcholinesterase, and the neuron repolarizes.[68] Other proteins such as muscle-specific receptor tyrosine kinase (MuSK), provide a structural scaffold to cluster nAChRs on the membrane (Figure 2).[69]

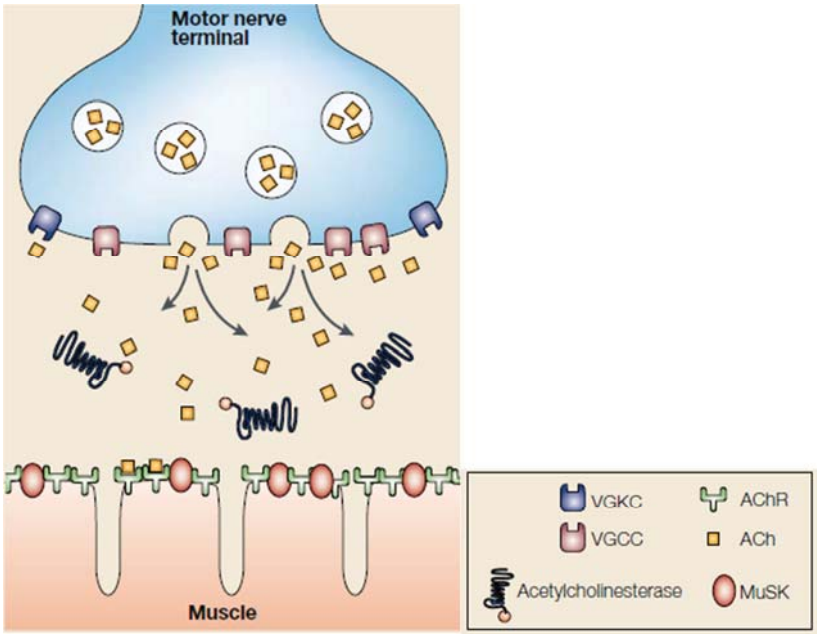

Figure 2. Synaptic component at the neuromuscular junction
Presynaptic vesicles at the motor nerve terminal contain acetylcholine (ACh). Action potential activates voltage-gated calcium channels (VGCCs) and induces ACh release to the synaptic cleft. At the postsynaptic muscle terminal, ACh binds to nicotinic acetylcholine receptors (nAChRs) to generate muscle contraction. Acetylcolinesterase rapidly eliminates ACh from the synapse, and voltage-gated potassium channels (VGKCs) contribute to the repolarization of the presynaptic terminal. Muscle-specific receptor tyrosine kinase (MuSK) acts as a scaffold protein for clustering nAChRs at the NMJ. From[70]

The autoantibodies underlying myasthenic syndromes target nAChR or MuSK in myasthenia gravis (MG), and P/Q type VGCC in the Lambert-Eaton myasthenic syndrome (LEMS). Animal experiments of passive and active immunization confirmed the autoimmune etiology of myasthenic syndromes and revealed that serum autoantibodies in these patients not only reach the cell-surface antigens at the NMJ, but also have direct pathogenic effects: (1)

crosslinking, internalizing and increasing degradation of the receptors, (2) blocking ACh binding to nAChR, and (3) causing the lysis of the postsynaptic muscle membrane through activation of the complement system.[66,67,71,72] The antibody-mediated impairment of neuromuscular transmission results in progressive painless weakness and fatigue of voluntary muscles, which are the main symptoms of myasthenic syndromes.[73] In contrast to PNSs there is no involvement of the CNS as the antigens in myasthenic syndromes are expressed in the NMJ.

Due to the antibody-mediated etiology of myasthenic syndromes, immunotherapy directed at removing the autoantibodies or the antibody-producing cells is an effective treatment for patients with these diseases. Moreover, better understanding the physiopathology of the neuromuscular transmission led to new treatment approaches with the use of compounds that compensated or antagonized the antibody effects (e.g., acetylcholinesterase inhibitors prolong the action of ACh, or 3,4-diaminopyridine that enhances the presynaptic release of ACh).[74,75]

As AEs, myasthenic syndromes may occur with or without cancer. MG associates with thymoma in about 10% of patients, usually between the ages of 40 and 60, whereas LEMS strongly associates with SCLC, in about 60% of the patients. In tumor-associated LEMS patients, SCLC cells express P/Q-type VGCC,[76] and although none of the targets of MG-associated antibodies seems to be present intact in the thymoma tissue itself, tumor cells do seem to express individual subunits of the nAChR.[77,78] There is evidence that thymoma in MG patients contributes to the generation of both $CD4^+$ and $CD8^+$ T cells[79,80] which might have become sensitized to thymoma antigens; probably triggering the humoral immune response in the peripheral lymph nodes.[81] Similar to PNSs, ectopic expression of the antigen is a trigger of the autoimmune myasthenic response.

Anti-NMDAR encephalitis

In this context, clinical observation of patients with unusual encephalitis similar to PNSs involving the CNS, but without either cancer or antibodies against intracellular proteins, and who frequently responded to immunotherapy, suggested an autoimmune etiology analogous to that of myasthenic syndromes or with antibodies against cell-surface proteins.[4]

In 2005, a syndrome with prominent neuropsychiatric symptoms, seizures, memory deficits, decreased level of consciousness, and central hypoventilation was described in a cohort of four young women.[82] All of them had inflammatory markers in the CSF, and an underlying ovarian teratoma. Further investigations revealed the presence in CSF and serum of antibodies that

reacted to the cell surface of live neurons and produced a characteristic staining of hippocampus in rat brain neuropil (Figure 3).[82] Soon after that, the antibodies were found to be directed against subunits of the N-methyl-D-aspartate receptor (NMDAR); hence naming the disorder anti-NMDAR encephalitis.[83]

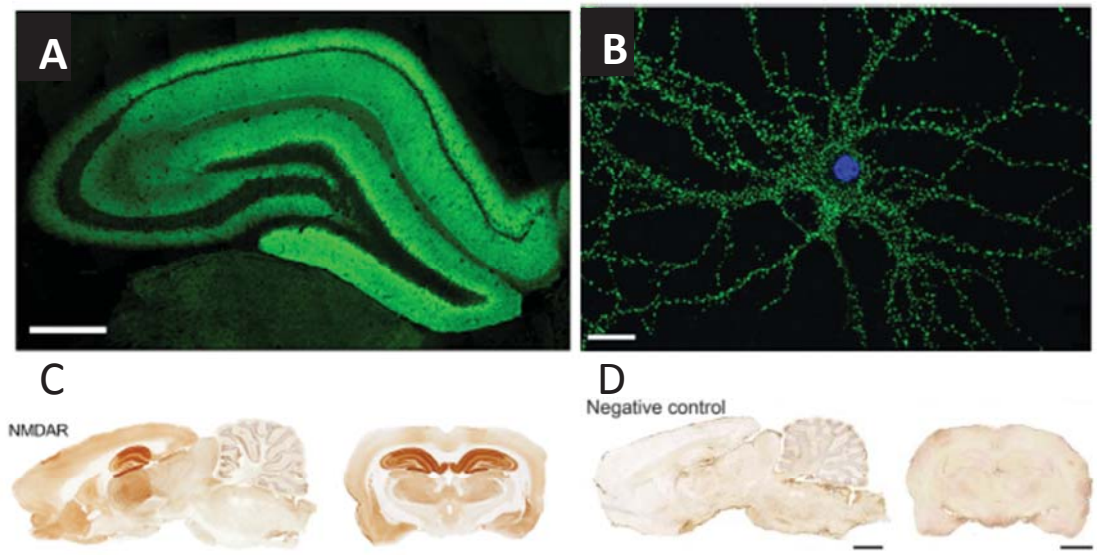

Figure 3. Brain and neuronal reactivity of antibodies against a cell surface
(A) Coronal section of rat hippocampus immunolabeled with an autoantibody against NMDAR from a patient with anti-NMDAR encephalitis showing intense reactivity. (B) The NMDAR autoantibody reacts with cultures of dissociated nonpermeabilized live rat hippocampal neurons, indicating that the antigen is accessible in the cell-surface of the neuron. (C and D) sagittal and coronal rat brain sections showing reactivity of NMDAR antibodies from a patient with anti-NMDAR encephalitis compared to a negative control CSF sample (immunoperoxidase technique). Scale bars: A = 500 µm, B = 10 µm, C and D = 2 mm; NMDAR = NMDA receptor. Adapted from[4]

Therefore, anti-NMDAR encephalitis was different from the previously known PNSs as (1) the associated antibodies were directed against an extracellular antigen, (2) the disease was not associated to malignant tumors or cytotoxic T-cell immunity, and (3) patients were responsive to immunotherapy (Figure 4).[4,83] The accessibility of the cell-surface antigen to circulating antibodies and the reversibility of patients' symptoms after removing the antibodies or antibody-producing cells suggested a direct pathogenic role of the antibodies, a hypothesis that was later confirmed in *in vitro* and *in vivo* models.

Anti-NMDAR encephalitis is the most frequent neuronal antibody-mediated encephalitis with an estimated incidence of ~1.5 per million population per year.[84] This encephalitis affects individuals of all ages (from 8 months to 85 years), but patients are usually children and young

adults (37% younger than 18 years old, and 58% between 18 and 44 years old).[85] The median age at disease onset is 21 years with a clear predominance in women (female to male ratio around 4:1).[85,86] Although the disease may occur without the presence of an underlying tumor, in young female patients anti-NMDAR encephalitis is highly associated to ovarian teratoma (~50%).[85,87]

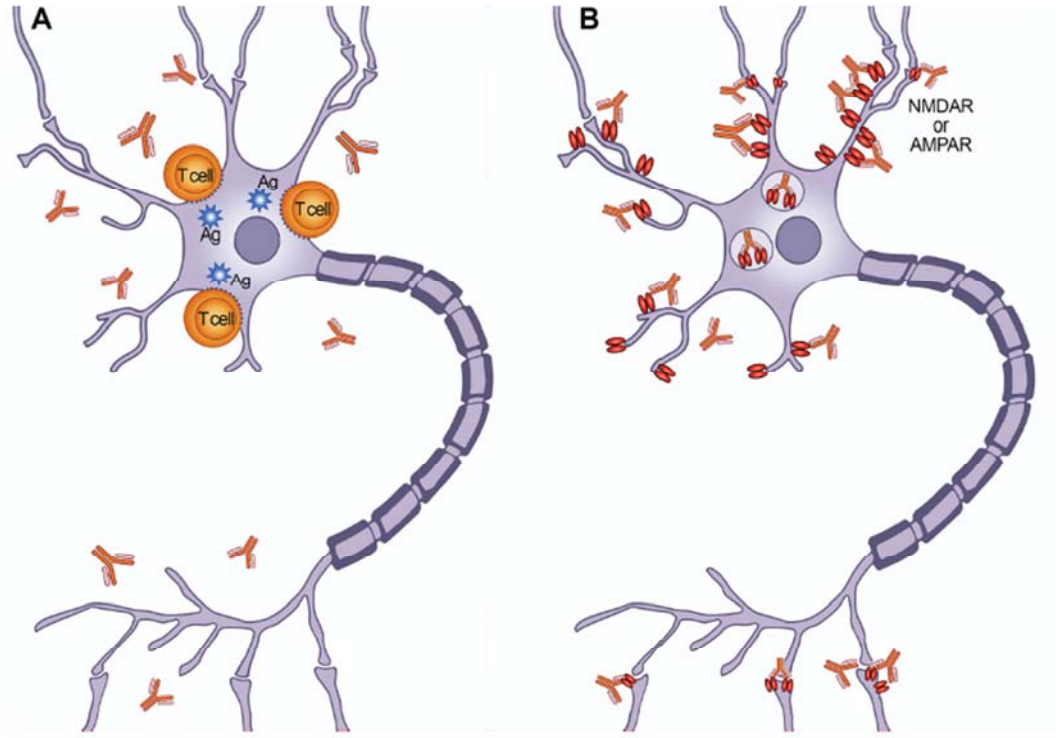

Figure 4. Comparison of autoantibodies in classic PNSs and in AEs
(A) In classic paraneoplastic syndromes of the CNS, the autoantibodies are directed against intracellular onconeural proteins that are not accessible, thus the autoantibodies *per se* are not pathogenic. Biopsy and autopsy studies of these patients show prominent inflammatory infiltrates of cytotoxic T-cells surrounding and indenting neurons, and causing neuronal degeneration (e.g., perforin or granzyme B cytotoxic mechanisms). (B) In contrast, the autoantibodies in autoimmune encephalopathies target antigens exposed on the neuronal cell-surface. Many patients with AE do not have an underlying tumor, and the autoantibodies have a direct pathogenic effect on the target neuronal proteins. In contrast to PNSs, patients with these syndromes often respond to treatments aimed to remove the autoantibodies or antibody-producing cells. From[4]

The clinical signs of anti-NMDAR encephalitis usually develop in a sequential manner. The onset is acute; in a matter of a few days or weeks patients develop behavioral changes and severe psychiatric symptoms. These symptoms are followed by rapid neurological deterioration, memory deficit, seizures, dyskinesias, decreased level of consciousness, and central hypoventilation, often requiring admission to an intensive care unit (Figure 5).[84,88]

There is a slight variation in symptom manifestation according to age: in children the most common features are seizures and movement disorders, whereas in adult patients memory deficits and central hypoventilation occur more often.[85]

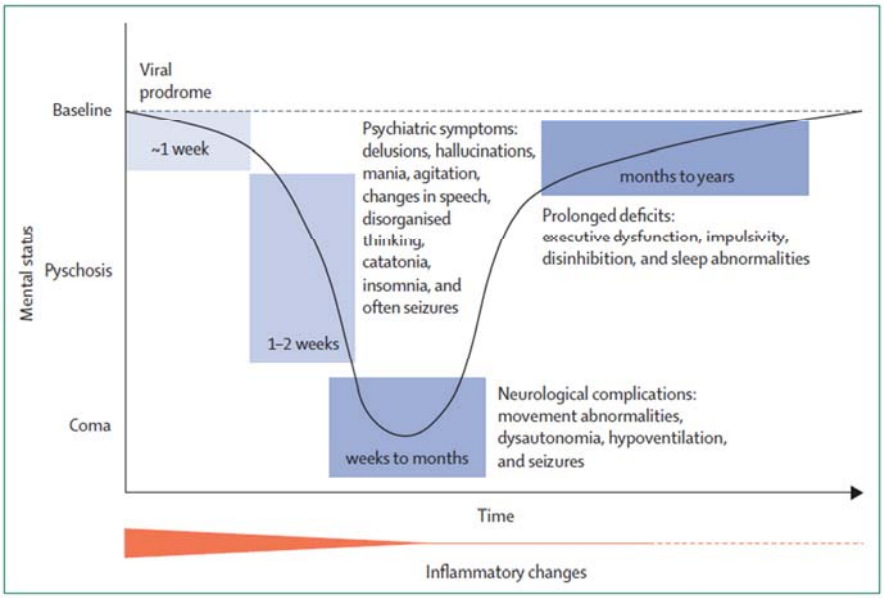

Figure 5. Temporal progression of symptoms in patients with anti-NMDAR encephalitis
This graphic representation shows the typical course of symptoms in a young adult with full-fledged anti-NMDA receptor encephalitis, with predominance of psychiatric symptoms at the disease onset. These symptoms are usually accompanied or followed by neurological alterations (abnormal movements, seizures, dysautonomia, or coma) that eventually improve or resolve, and lead to a prolonged phase of recovery with prominent involvement of executive functions. The intensity of inflammatory changes (which is usually reflected by the presence of pleocytosis in the CSF or suggested by the brain MRI findings), is shown by the thickness of the red line, which decreases over time until becoming a thin line and then a dotted line (minimal or undetectable inflammatory changes). Except in young male patients and children, the progression of symptoms is remarkably similar in most patients. Milder forms of the disorder, without symptoms requiring intensive support care, are becoming more frequent as the disease is better known and diagnosed and treated earlier. From [84,88]

In the first phase, brain magnetic resonance imaging (MRI) is abnormal in ~30% of the cases, with fluid-attenuated inversion recovery (FLAIR) showing alterations in cortical and subcortical or cerebellar regions;[85,89] whereas 90% of patients present diffuse slowing in the electroencephalogram.[83,85] Pleocytosis or high protein concentration in the CSF are markers of CNS inflammation usually present in these patients at disease onset (90%),[85] suggesting an immune-related etiology. The diagnosis of anti-NMDAR encephalitis is confirmed by the detection of CSF antibodies against the GluN1 subunit of the NMDAR by a specific cell-based assay (CBA).[84]

Due to the severe psychiatric symptoms at onset, most patients are first admitted to psychiatric institutions instead of neurological units. Moreover, some clinical features may also occur in other antibody-mediated encephalitis such as a change in behavior, psychosis, seizures, memory and cognitive deficits, or decreased level of consciousness.[4,90] Therefore, it is important to recognize the particular syndrome of autoimmune encephalitis (including anti-NMDAR) in order to differentiate it from psychiatric conditions, and then provide the appropriate treatment.

Previous knowledge of the antibody-mediated pathogenesis in myasthenic syndromes helped to understand that NMDAR antibodies present in the CSF and/or serum of patients with anti-NMDAR encephalitis can alter synaptic function. Upon binding to the neuronal receptor, they cause a specific reduction of total cell-surface and synaptic density of NMDAR clusters. These antibodies are mainly of the immunoglobulin G class (IgG), therefore they crosslink the NMDARs altering their surface dynamics and leading to their internalization by endocytosis. These antibody effects result in a decrease of the NMDAR-mediated currents in live cultured neurons;[91] and in impaired memory and behavioral alterations in an animal model of the disease.[11] The epitope recognized by the NMDAR encephalitis antibodies is located at the amino terminal domain of the GluN1 subunit, in a specific region around the residues N368/G369.[92,93]

As every other autoimmune disease, the development of anti-NMDAR encephalitis implies an alteration of the immunologic self-tolerance. There are two clearly identified triggers of anti-NMDAR encephalitis.

First, up to 58% of the young female patients have an ovarian teratoma. These tumors contain mature and immature nervous tissue that ectopically expresses NMDAR, which is recognized by these patients' antibodies.[85] The role for this tumoral NMDAR expression in initiating the autoimmune response is further supported by histological studies showing extensive inflammatory cell infiltrates in teratomas from patients with anti-NMDAR encephalitis, compared with teratomas from individuals not affected by the disease.[94,95] The frequency of tumors in children and men is lower and the histology different (e.g., older men and women have carcinomas instead of teratomas). Twenty-three percent of patients older than 45 years have underlying tumors, which are usually carcinomas rather than teratomas.[85] Moreover, African-American female patients are more likely to have an ovarian teratoma than patients from other ethnic groups.[96]

Second, in a small subset of patients (less than 5%), the trigger of the disease is herpes simplex

encephalitis (HSE). Twenty-seven percent of patients with HSE develop neurological relapses within a few weeks up to 2 months after successful treatment of the viral infection.[97] Detection of antibodies to NMDAR and other neurotransmitter receptors 3 weeks after the diagnosis of HSE is associated with the development of autoimmune encephalitis. The anti-NMDAR encephalitis that occurs post-HSE is more frequent in children than adults, and whereas children present with predominant choreoathetoid movements, impaired level of consciousness, and refractory seizures (often with infantile spasms); adults more frequently show psychiatric and cognitive alterations.[98]

The pathogenesis of anti-NMDAR encephalitis post-HSE is unclear. In the context of extensive inflammatory infiltrates, it has been proposed that either the viral-induced release of NMDAR and other neuronal cell-surface proteins or mechanisms of molecular mimicry, such as similarity between NMDAR and herpes simplex virus proteins can trigger the autoimmune response.[4] The high frequency of antibodies against several different neuronal antigens supports the first possibility[99] but does not rule out that molecular mimicry might also be involved.

Anti-NMDAR encephalitis is a severe and potentially lethal disease, but investigations in the last fifteen years have made it a treatable neurological syndrome. The current approach to the treatment of anti-NMDAR encephalitis is immunotherapy and removal of the associated tumor, when applicable.[85] The immunotherapy is directed to remove the autoantibodies (first-line) and the antibody-producing B-cells (second-line; i.e., rituximab, cyclophosphamide). In clinical practice, most patients are treated with first-line glucocorticoids, intravenous immunoglobulins (IVIg), plasma exchange, or a combination of these, changing to second-line immunotherapy when first-line treatments fail.[85]

Despite the severity of the disease, most patients with anti-NMDAR encephalitis respond to immunotherapy. In a series of 577 patients with anti-NMDAR encephalitis, 53% showed clinical improvement within four weeks, and 81% showed substantial recovery (mild or no residual symptoms) at the last follow-up.[85] Early treatment and no need of intensive care were factors associated with good outcome.[85]

In contrast to the acute onset, the recovery in anti-NMDAR encephalitis is usually slow, over months and may take even more than two years.[96] Patients gradually improve from severe neurological complications reverting the stages of symptom presentation, but remaining with executive function deficits and behavioral alterations for long time.[96]

Relapses occur in about ~20-25% of cases, even many years after the first episode, sometimes triggered by reduction or discontinuation of medication or tumor recurrence.[86,100] Relapses are usually less severe than previous episodes (67%); and as in the initial episodes, immunotherapy and treatment of the tumor usually result in improvement.[85]

Overall, anti-NMDAR encephalitis is an antibody-mediated disease of the CNS: patients' autoantibodies are directed against a neuronal surface antigen and do have a direct pathogenic effect.

2. Pregnancy in antibody-mediated diseases

Physiological fetal development

Maternofetal immunization across the placenta and FcRn

Antibodies are the hallmark components of humoral immunity that link specific antigen recognition to different effector mechanisms of the immune system. Antibodies have two functional domains, the Fab (fragment of antigen binding) and the Fc (crystallizable fragment) region. The Fab region is responsible for antigen recognition, whereas the Fc region couples the antibody to immune effector pathways (Figure 6).[101] The process of antibody class switching enables B cells to vary their expression of the heavy-chain constant region, and thereby the Fc region, that results in the production of antibodies with different effector functions. Differing localization of B-cell blasts and plasma cells that express these different heavy chains confers different tissue localization and effector-cell recognition to the five classes of antibodies — IgA, IgD, IgE, IgG and IgM.[101]

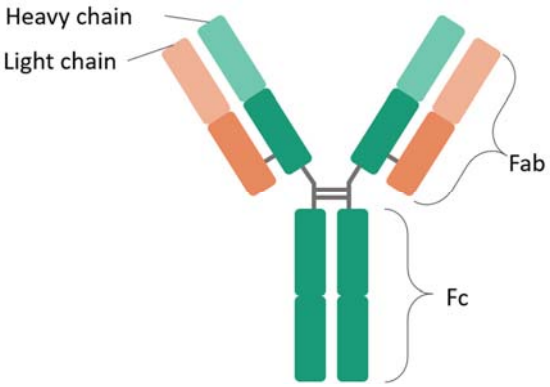

Figure 6. Structure of mammalian immunoglobulin
This diagram shows schematic representation of and antibody, which consists of two larger heavy chains (green) and two shorter light chains (pink). Each rectangle represents a globular domain, and the lighter domains are those which are variable. Fab (antigen binding) and Fc (crystallizable) fragments are also indicated.

Of the five antibody classes, IgG is the most prevalent class in the serum and non-mucosal tissues.[101] Compared to the other Ig classes, IgG has the longest half-life in the circulation, ranging from 7 to 21 days in healthy humans.[102–104] IgG antibodies have an important role in protective immunity against a wide range of pathogens and toxins.[101] Attesting to its important role in protective immunity, IgG has long been known to be the only class of antibody that is actively transferred from mother to offspring to confer short-term passive immunity.[101,105,106] This specific transport of IgG is carried out by the neonatal Fc receptor (FcRn).[107,108]

The FcRn-mediated mechanism of IgG transfer from mother to offspring for passive humoral immunity differs between rodents and humans (Figure 7). In rodents, FcRn functions most efficiently in the neonatal period when it transports maternal IgG contained in ingested milk across the epithelial-cell layer of the proximal small intestine.[109] By contrast, in humans, FcRn

expressed by syncytiotrophoblasts transports the majority of maternal antibodies to the fetus antenatally, across the placenta.[101,110,111]

The FcRn-IgG interaction is crucial to understand the mechanism for directional transport of IgG at these sites. The Fc portion of IgG binds with high affinity to FcRn at an acidic pH (i.e., <6.5) but not at physiological pH (i.e., 7.4).[101,107,109,112] In an acidic environment, histidine residues of IgG Fc are protonated and then can form salt-bridges with anionic residues on FcRn, stabilizing the hydrophobic interactions.[113–115] FcRn – IgG interaction is inhibited by bacterial protein A, localizing the binding site of IgG Fc on the CH_2-CH_3 domain interface, different from other Fc receptors.[116,117]

FcRn is highly expressed in the gut of neonatal rodents, on the cell-surface brush border of enterocytes.[107] Shortly after birth, rodent pups ingest maternal milk containing IgG. After passing through the stomach, ingested IgG bind to the FcRn on the brush border in the acidic milieu of the lumen of the duodenum. Upon binding, FcRn transcytoses IgG and releases it at neutral pH on neonatal blood at the basolateral side.[101,109] In humans, most materno fetal IgG transfer in humans occurs antenatally across the syncytiotrophoblasts of the placenta. The syncytiotrophoblast internalizes fluid containing maternal IgG into endosomes; the IgG-containing endosome is then gradually acidified thereby allowing IgG to bind tightly to FcRn present in this compartment. Then, the vesicle fuses with the membrane on the fetal side of the syncytiotrophoblast, where the physiological pH promotes the dissociation of IgG from FcRn.[101,110,111,118] The FcRn molecule may be recycled to the maternal membrane to perform additional rounds of transcytosis.[101,119,120] Therefore, the pH-dependent binding of IgG to FcRn allows for IgG transcytosis through a polarized cell layer and down a concentration gradient of IgG (Figure 7).[101]

FcRn is not specific for materno fetal transport of IgG, instead is expressed in various tissues in adults. Throughout life, FcRn contributes to effective humoral immunity by protecting IgG from lysosomal catabolism and then recycling IgG back into circulation, thus extending its serum half-life.[101,121] The vascular endothelium is proposed to be the main site of IgG recycling, but myeloid-derived antigen-presenting cells also contribute significantly to extend the serum half-life of IgG (Figure 7).[122] FcRn is also expressed in the BBB,[123] in the alveolar macrophages of the lungs,[124,125] and in glomerular epithelial cells (podocytes), which form the main filtration barrier of the kidney.[126]

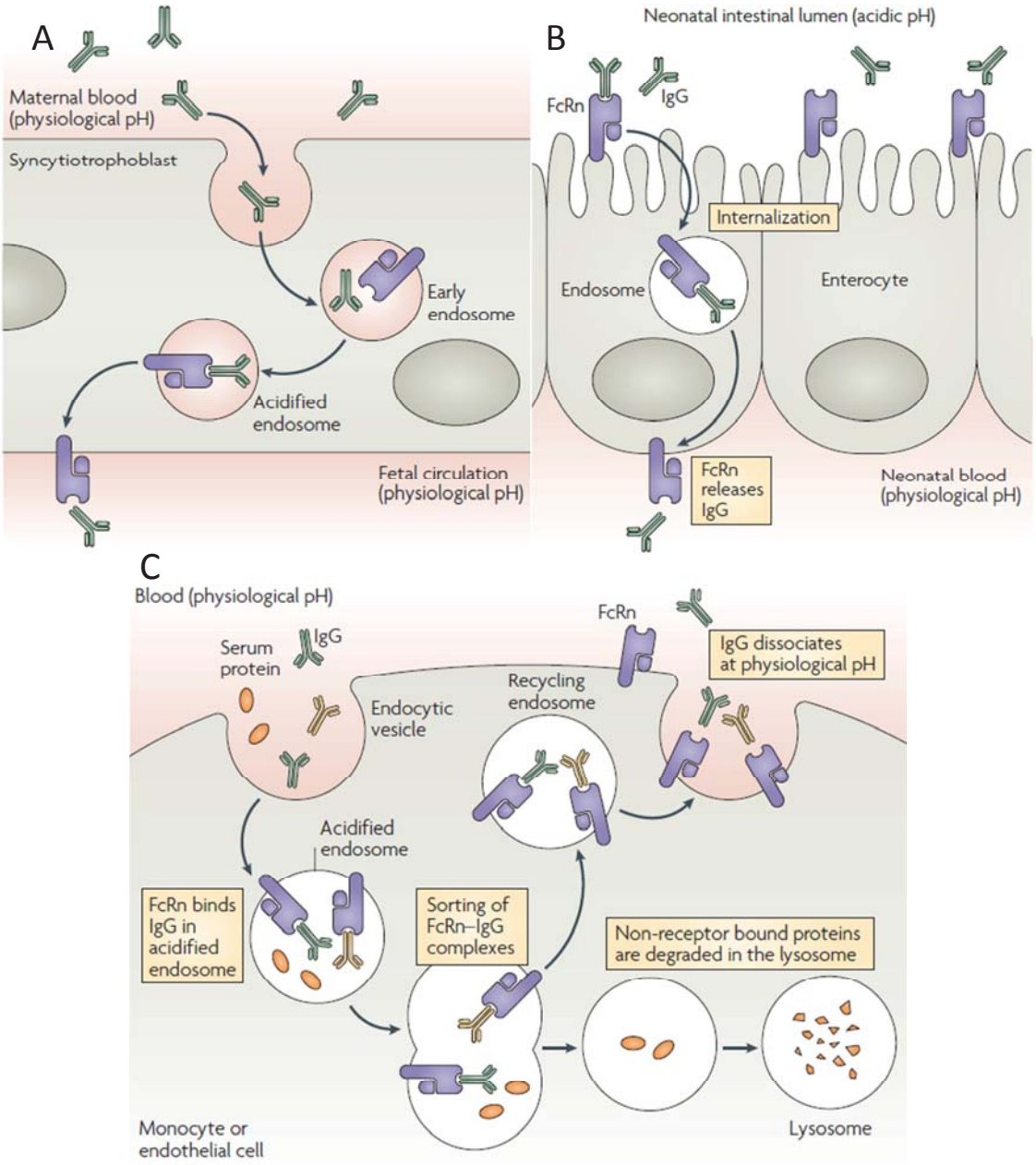

Figure 7. FcRn prolongs IgG half-life in serum and mediates perinatal transfer of IgG
(A) In mammals, FcRn mediates maternal immunization of the fetus across the placenta antenatally or (B) in the neonatal gut through ingested breast milk by different pH-dependent transcytosis mechanisms. (C) FcRn expressed in endothelial cells and circulating monocytes recycle IgG back to circulation avoiding lysosomal degradation, thus extending its serum half-life. From[101]

FcRn is highly expressed in CNS vascular endothelial cells in the BBB.[123] It may have a role in limiting CNS inflammation in pathological situations.[101] Therefore, rather than transporting IgG into the CNS, FcRn probably mediates reverse transcytosis of IgG from the CNS back into the

bloodstream.[101] IgG molecules injected into the brain parenchyma are rapidly transported back into the circulation in an Fc-dependent manner.[101,127]

FcRn is a heterodimer consisting of an MHC-class-I-like heavy chain and a β_2-microglobulin (β_2m) light chain, which is the common obligate light chain for all MHC class I molecules.[101,108] Despite its structural similarity to MHC class I molecules, the gene encoding the heavy chain of FcRn is outside the MHC gene complex and FcRn does not present peptide antigens to T cells since its analogous "peptide-binding" groove is occluded.[113,128] FcRn binds to IgG with a 2:1 stoichiometry, with two receptor molecules binding to a single Fc fragment.[101,129–132]

The affinity of the FcRn–IgG interaction is highly dependent on the species and isotype of IgG.[133] Consequently, transgenic mice expressing human FcRn transgenes are required for the initial evaluation of the pharmacokinetics of recombinant human IgG therapeutics before more focused testing in primate systems.[101]

The critical role of FcRn in the long half-life of IgG has prompted the proposal that inhibitors of FcRn may be useful in the treatment of autoimmune diseases. Indeed, competition with autoantibodies for FcRn binding results in lysosomal degradation or clearance of the pathogenic antibodies.[134] One possible way to interfere with the function of FcRn is to overload it with "innocuous" IgG, saturating the receptor resulting in clearance of pathogenic antibodies.[135] Furthermore, more specific inhibitors of FcRn have been investigated as a possible way to modulate IgG half-lives. Such inhibitors could have possible applications in reducing autoantibody levels in autoimmune disease states[102] as well as preventing placental transfer of pathogenic IgG antibodies.[136]

Perinatal pathologies associated to maternal antibody-mediated diseases

FcRn-mediated placental transfer of maternal IgG antibodies to the fetus is an important mechanism that provides protection to the infant while its immune system is still immature. However, in pregnant patients with autoimmune antibody-mediated diseases, pathogenic IgG antibodies from maternal circulation may also cross the placenta and harm the fetus.[136] This is the case for some autoimmune disorders that can generate passively acquired perinatal alterations. These include neonatal MG,[137] neonatal lupus erythematosus (NLE),[138] immune bullous dermatoses (including pemphigus and epidermolysis bullosa acquisita),[139] and fetal and neonatal immune thrombocytopenia[140,141] (Table 2).

Table 2. Perinatal pathologies associated to maternal antibody-mediated diseases				
Disease	***Maternal disease***	***Fetal/Neonate symptoms***	***Target autoantigen***	***Fetal/neonatal animal model***
Neonatal myasthenia gravis	Myasthenia gravis; weakness and fatigability in voluntary muscles	Generalized hypotonia, poor sucking/swallowing and respiratory difficulties Arthrogryposis multiplex congenita – joint contractures[137]	Antigens of the NMJ: nAChR or MuSK	Arthrogryposis multiplex congenita in mice fetuses exposed to plasma from patients with myasthenia gravis (nAChR)[142]
Neonatal lupus erythematosus (NLE)	Systemic lupus erythematosus	Cutaneous rash, atrioventricular heart block[138]	Ro/SSA, La/SSB, or U1-Ribonucleoprotein	Monoclonal antibody derived from patients with lupus caused thinned cortical plate[143]
Neonatal alloimmune bullous dermatoses	Autoimmune bullous dermatoses	Transient flaccid blisters and erosions on the skin and the mucosa[139]	Desmosomal or dermal-epidermal junction antigens: e.g. desmoglein 3, collagen XVII (also known as BP180), laminin 5, and collagen VII	Blistering skin disease similar to bullous pemphigoid induced by maternally transferred antibodies against humanized collagen XVII in the skin of transgenic mice[144]
Immune thrombocytopenic purpura (ITP)	Platelet destruction by opsonization, and miscarriage	Intracranial hemorrhage, neurologic sequelae and death[140,141]	Adult or fetal platelet antigens: Glycoprotein Integrin αIIbβ3 (GPIIb/IIIa) and the GPIbα or IX complex	Autoantibodies against β3 integrin are transferred from pregnant mice to the fetuses/newborns and induce platelet destruction[145]

As described before (section 1, Autoimmune myasthenic syndromes, page 24), the underlying cause of the muscle weakness and fatigue in MG patients are serum IgG antibodies directed to nAChR on the NMJ. Since these pathogenic IgG can be transferred across the placenta to the fetus, some newborns from patients with MG also present muscle weakness. Similarly, some infants born to mothers with lupus erythematosus develop the characteristic cutaneous lesions, whereas children from patients with autoimmune bullous dermatoses, which are caused by antibodies against structural proteins of the skin from the desmosomal or the dermal-epidermal junctions, have mucosal or epidermal symptoms similar to their mothers. Patients with immune thrombocytopenic purpura harbor antibodies against several platelet antigens that cause its destruction by opsonization. In a context of pregnancy, these antibodies can result in miscarriage, intracranial hemorrhage with neurologic sequelae or even fetal death.

Despite the diversity of these disorders, they share common features: (1) mothers have specific autoantibodies in the bloodstream, (2) these antibodies can bind to the antigen and cause pathogenic effects related to disease symptoms, and (3) they are of the IgG class, thus can be transferred across the placenta to the fetus.

The diagnosis of the neonatal affectation is based on clinical observations but confirmed with the detection of specific antibodies in maternal and/or in the newborn sera. Animal models of autoantibody-mediated diseases have been crucial for demonstrating the pathogenicity of these antibodies. Passive transfer of purified patients' autoantibodies to experimental animals reproduces the disease, and symptoms correlate with the presence and titer of autoantibodies. Additional experimental evidence comes from active immunization with autoantigen epitopes to produce the autoantibodies and the development of the associated pathology in immunized animals or in their offspring (Table 2).

In most clinical cases, the effects in the newborn are transient, and infants improve as pathogenic maternal IgG are naturally cleared from circulation; similar to the reversibility in passive transfer animal models of antibody-mediated diseases. However, in other instances, there are severe rare variants of the disease in which the damage caused to the fetus/newborn is irreversible and can be lethal. In some pregnant patients with MG, antibodies against a nAChR subunit specific for the fetal isoform of the receptor result in impaired neuromuscular transmission, decreased fetal movement (fetal akinesia) and subsequent arthrogryposis multiplex congenita, defined as contractures in more than two joints and in multiple body areas. Likewise, affected children born to mothers with systemic lupus

erythematosus usually present reversible cutaneous lesions and hepatic dysfunction. Moreover, about 30% of children from mothers containing Ro antibodies develop congenital, mostly complete, atrioventricular heart block despite having a structurally normal heart.

It is unclear why only a few babies of mothers with autoimmune antibody-mediated diseases develop the associated neonatal pathology. As the symptoms are usually mild and transient, some clinical cases might be underreported. The antibody epitope specificity has been proposed to be a major factor (e.g., fetal-specific γ subunit of nAChRs and arthrogryposis multiplex congenita in babies of MG patients). Strikingly, an increased recurrence rate and severity of the neonatal pathology in subsequent pregnancies has been observed in most of these antibody-mediated diseases.

All the antibodies present in the antibody-mediated pathologies collected in Table 2 are directed against systemic antigens, which are easily accessible to maternal antibodies if these reach fetal circulation. However, pathogenic autoantibodies in AEs, including anti-NMDAR encephalitis, target neuronal antigens only expressed in the CNS.

Blood-brain barrier formation

The CNS is a site of immune privilege. The blood-brain barrier (BBB) is a multicellular vascular structure that separates the CNS from the peripheral blood circulation. The BBB excludes serum IgG from the CNS interstitium and circulating cerebrospinal fluid.

Compared with endothelial cells in different tissues, endothelial cells of the BBB possess unique features: continuous intercellular tight junctions that prevent the passive diffusion of macromolecules across barrier in the absence of specific transporters, lack fenestrations and undergo extremely low rates of transcytosis, which greatly limits both the paracellular and transcellular movement of molecules through the EC layer. By tightly controlling the passage of molecules and ions with a series of specific transporters, BBB maintains an environment that allows neurons to function properly. This structure protects the brain from toxins and pathogens, and delivers nutrients and oxygen according to current neuronal needs. In addition, endothelial cells have low expression of leukocyte adhesion molecules, abrogating extensive immune cell infiltration into the healthy CNS (Figure 8).

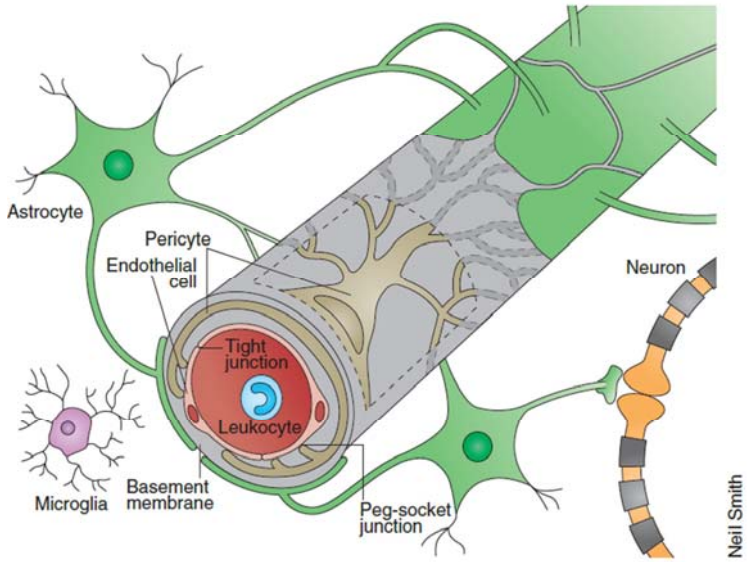

Figure 8. Cellular components of the mature BBB
Endothelial cells establish tight junctions to form the lumen of the capillary. Pericytes and astrocytes ensheath with their processes the endothelial cells. All the components of the BBB and the signaling crosstalk among them is crucial for an efficient barrier function to protect and maintain the homeostasis of the CNS. Author: Neil Smith. From[146]

To exert maintenance of brain homeostasis, regulation of influx and efflux transport, and protection from harm, the BBB is a multicellular structure where every constituent cell type makes an indispensable contribution to the BBB's integrity. If one member of the BBB fails, the disruption of the barrier can cause or contribute to neurological disease. There are two main contexts of CNS vulnerability: in a pathological situation able to disrupt the BBB integrity, or during embryogenesis and development of CNS while the BBB is not fully formed and sealed.

The development of the BBB is a multistep process regulated by multiple signaling pathways. BBB formation begins with angiogenesis. Neural progenitor cells secrete factors that guide endothelial progenitor cells to invade the embryonic neuroectoderm and give rise to sprouting new vessels. At this point, endothelial cells contain large numbers of transcytotic vesicles, show high expression of leukocyte adhesion molecules, and start expressing nutrient transporters and proteins for tight junction formation.

In the next stage, the endothelial cells recruit pericytes and astrocytes to the forming BBB. The signaling crosstalk between these cellular components promotes barrier properties in endothelial cells: tight junctions start to establish, transcytosis decreases, and expression of leukocyte adhesion molecules is downregulated.[147] Pericytes ensheath the abluminal surfaces of cerebral vessel walls including those of capillaries, precapillary arterioles and postcapillary

venules,[148] deposit extracellular matrix components for basement membrane formation, and regulate capillary diameter and blood flow, controlling BBB integrity and function.[149] Adhesion between cerebral endothelial cells and pericytes is required for maintenance of BBB integrity. Pericyte detachment is associated with increased microvessel diameters, increased BBB permeability and hemorrhage.[150] During BBB formation, astrocytic foot processes are directed to the endothelial tube, and subsequently initiate proper end-foot polarization.

The last step for a mature BBB is sealing of the barrier by interendothelial tight junctions, which has to be maintained throughout life. Astrocytes and pericytes signal for upregulation of the expression of tight junction proteins in endothelial cells, thus enhancing barrier tightness.[146,151] Perivascular astrocytic end feet are highly specialized and polarized structures which encircle the abluminal side of cerebral vessels. Astrocytes provide nutrition for neurons, regulate extracellular potassium balance, carry out neurotransmitter clearance and recycling, and control immune reactions.[152]

Timings of fetal BBB formation and sealing differ between murine and human embryogenesis. In mouse embryonic development, angiogenesis occurs around at embryonic day (E) 9,[153] proper vessel morphology at E11.5-12.5,[154–156] and vessel sealing at E11-13.5.[157] In humans, the BBB of the fetus starts to become more restrictive to the passage of albumin (and likely Igs) to the brain at approximately 12–13 weeks of pregnancy.[158]

The time window between placental transfer of IgG and BBB sealing determines the accessibility of pathogenic antibodies in maternal circulation to reach the fetal brain. In women who develop anti-NMDAR during pregnancy, their pathogenic antibodies are IgGs directed to an antigen in the CNS; thus, if transferred across the placenta while the BBB of the fetus is not fully restrictive to IgG, they can potentially damage the developing fetal brain.

The NMDA receptor and glutamate signaling during development

Autoantibodies in anti-NMDAR encephalitis are IgG able to cause a specific pathogenic hypofunction on their target: the NMDA receptor.

The NMDA receptor

The *N*-methyl-D-aspartate receptor (NMDAR) belongs to the family of ionotropic glutamate receptors. When activated, these receptors undergo a series of conformational changes that open the ion pore of the channel and allow the flux of Ca^{2+} or Na^{+} ions inside the cell (down

their concentration gradient), which result in electrical changes of the membrane potential and in the activation of downstream signaling pathways.[159]

Compared to other two known ionotropic receptors that respond to the excitatory neurotransmitter glutamate (i.e., α-amino-3-hydroxy-5-methyl-4-isoxaasolepropionic acid [AMPA] and kainate receptors) the NMDAR has particular features that make it especially interesting: (1) it is highly permeable to Ca^{2+},[160] (2) has slow activation and deactivation kinetics,[161] and (3) its activation requires binding not only of the ligand (glutamate) and a co-agonist (glycine) but also depolarization of the membrane, acting as a coincident detector of both signals.[159,162–164]

Therefore, NMDARs are both ligand- and voltage-gated channels. At resting membrane potential, the ion pore of the receptor is blocked by extracellular Mg^{2+}.[165] In glutamatergic synapses, neuronal action potential in the presynaptic terminal releases vesicular glutamate to the synaptic cleft activating its ionotropic and metabotropic receptors in the postsynaptic terminal. Glutamate firstly activates AMPARs due to their fast kinetics. AMPAR-mediated membrane depolarization induces the voltage-dependent unbinding of Mg^{2+}, so that the NMDARs can be activated in the simultaneous presence of glutamate and glycine.[166]

The structure of NMDAR is a heterotetramer.[167] There are three GluN subunits (GluN1 – GluN3), with eight different isoforms of GluN1 generated from alternative splicing, four GluN2 (A-D) subunits encoded in four different genes, and two of GluN3 (A-B) from two distinct genes.[159] Each subunit has two extracellular globular domains in the amino-terminal region, three transmembrane domains (S1, S3, and S4), a membrane loop (S2), and an intracellular carboxyl-terminal domain (CTD). In the extracellular part of the subunit there are two bilobed clamshell-shaped structures: the amino-terminal domain (NTD, the one farther from the cell membrane) and the agonist-binding domain (ABD, closer to the transmembrane region).[168,169] The binding site for the co-agonist glycine is in the ABD of GluN1 and GluN3 subunits, while glutamate interacts with the ABD of GluN2 subunits.[170,171] Most allosteric modulation occurs in the NTD or in the cleft between NTD and ABD, supporting the role of the extracellular domains in regulating the receptor function according to changes in the environment.[159] The intracellular CTD connects the receptor to scaffold proteins and downstream signaling transducers (e.g. The Ca^{2+} sensor calmodulin directly binds to the CTD of GluN1).[172]

A functional NMDAR must contain two GluN1 subunits within the tetramer. These two GluN1 subunits bind in an alternating pattern to either two GluN2 (e.g., 1-2-1-2) or to a combination of GluN2 and GluN3 subunits (Figure 9).[168,173] The assembling GluN2 or GluN3 subunits will

determine the biophysical properties of the receptor (gating kinetics, ion permeabilities, binding affinities, conductance, intracellular interactors, etc.).[174–176] Changes in the number, the subunit composition, or the subcellular location of these receptors (due to trafficking, internalization, or lateral diffusion) confer NMDARs an extraordinary fine-tuned functional regulation demonstrated to be responsible for mechanisms behind long-term plasticity. This activity-dependent strengthening or weakening of synaptic connections is the cellular paradigm for complex brain processes such as memory formation and cognition.[177]

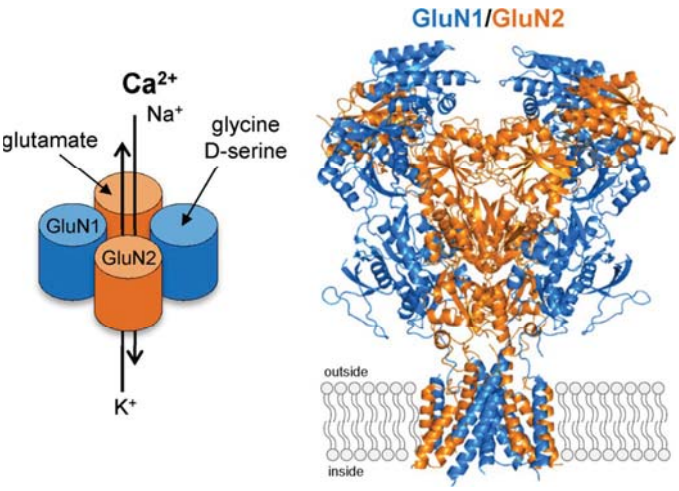

Figure 9. N-methyl-D-aspartate receptor subunit arrangement
The most abundant form of the NMDA receptor contains two GluN1 and two GluN2 subunits in an alternating manner as indicated. The channel pore generated is permeable to cations. The ligand glutamate binds to GluN2 subunits, whereas glycine (or D-serine) which act as co-agonists bind to the mandatory GluN1 subunits. Each subunit has two extracellular globular domains in which there are the binding sites (the NTD and the ABD). This knowledge was provided by the crystal structure of NMDAR (4PE5; ref. [168]). The intracellular domains of the subunits have been omitted. From[178]

NMDAR composition is controlled by regional and temporal differential expression of the subunits. The mandatory GluN1 subunit is ubiquitously expressed in the CNS of rodents from embryonic stage E14 to adulthood, but major changes occur in the expression of the other NMDAR subunits, especially of the four glutamate-binding GluN2A-D during development (Figure 10).[179,180]

Along with GluN1, the expression of GluN2B and GluN2D subunits starts prenatally starting at E14 (ref. [180]). In contrast, GluN2A and GluN2C are first detected after birth, at postnatal days 3 and 10 respectively. Whereas GluN2D peaks around postnatal day 7, GluN2B expression is maintained at high levels after birth. GluN2A-C reach highest expression at postnatal day 20, then decreasing to adult levels in the brain, where GluN2A is widely and abundantly expressed in all CNS with predominance in the hippocampus and the cerebral cortex, GluN2B is mainly restricted to the telencephalon and the thalamus, GluN2C to the cerebellum, and GluN2D to midbrain structures.

During development, NMDAR composition switches from primarily containing GluN2B subunits to predominantly containing GluN2A subunits throughout the CNS. The increased contribution of GluN2A subunits is accompanied by several distinctive changes in NMDAR-mediated synaptic currents, including a marked acceleration in decay time kinetics and a consequent change in the temporal integration properties which explain synapse maturation, circuit refinement and acquisition of learning abilities. The postnatal developmental subunit switch appears to be driven by neuronal activity and evolutionary conserved.

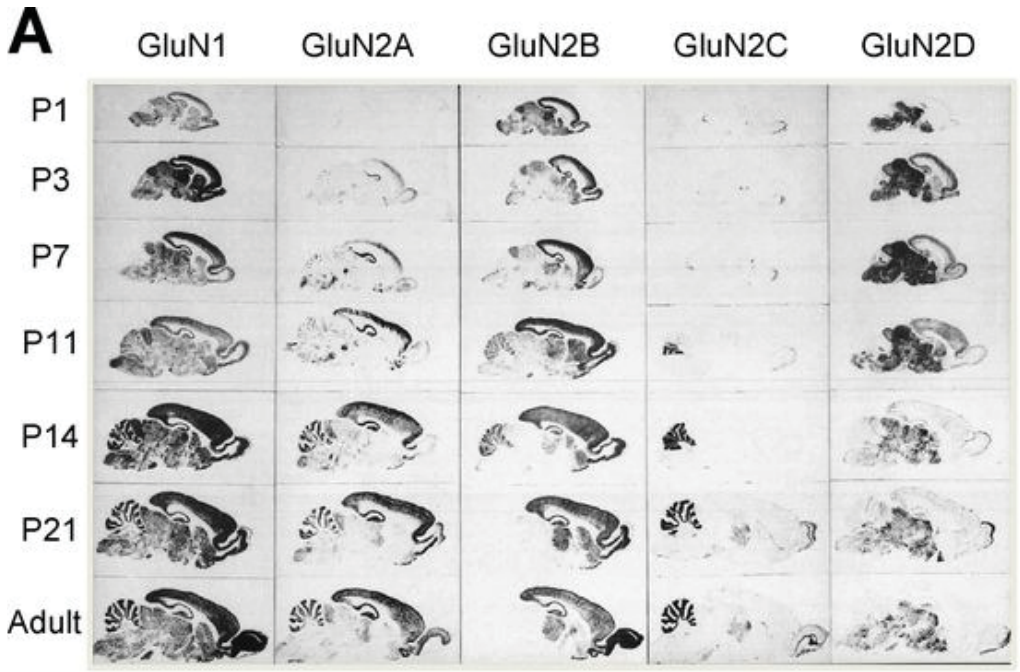

Figure 10. Expression of NMDA receptor subunits
Autoradiograms obtained by in situ hybridizations of oligonucleotide probes to parasagittal sections of rat brain at indicated postnatal (P) days showing the distributions of mRNAs of GluN1, and GluN2A-D reveal distinct regional and developmental expression of NMDAR subunits. Modified from[181] in[178]

Moreover, the expression profile of the GluN3A subunit, peaking at early postnatal stages, suggests a role in the developmental maturation of synaptic NMDARs. Studies pointed to GluN3A as a molecular break during neuronal development limiting premature synaptic maturation.

NMDAR subunit composition is plastic. Changes in the assembling subunits are not exclusive to the developmental period but underlie mechanisms of plasticity in response to neuronal activity or sensory experiences also in adult synapses.

In the adult brain, the triheteromeric NMDAR composed by GluN1/GluN2A/GluN2B becomes the most abundant synaptic receptor, particularly in the hippocampus and cortex,[182,183] indicating that they have central roles in synaptic function and plasticity.

3. Cellular and animal models of anti-NMDAR encephalitis

Antibody pathogenicity: from *in vitro* to *in vivo* models

By the time anti-NMDAR encephalitis was first described in 2005[82] (and the target antigen characterized two years later[83]), previously characterized neuronal autoantibodies were mainly associated with PNSs. Investigations using cultured neurons or *in vivo* models had failed to demonstrate the pathogenicity of these autoantibodies, which are directed against intracellular antigens (e.g., anti-Hu, anti-Yo);[60,184] thus their presence was considered a useful biomarker for an underlying tumor. However, along with the discovery of anti-NMDAR encephalitis, the identification of CSF antibodies that reacted with the cell surface of live neurons, the clinical response to immunotherapy, and resemblance of patients' clinical features with those caused by genetic or pharmacological hypofunction of NMDAR led to hypothesize that these autoantibodies were directly pathogenic.[82,83]

Initial studies using dissociated rat hippocampal neurons incubated for 3–7 days with patients' antibodies showed a selective and reversible decrease of NMDAR surface density and synaptic localization that correlated with the titers of antibodies present in patients' serum or CSF samples (Figure 11).[9,89] These effects were not observed using Fab fragments derived from the autoantibodies, but subsequent crosslinking of the Fab fragments with Fab antibodies recapitulated the antibody-induced reduction of cell-surface and synaptic NMDARs.[9] These findings suggested that patients' antibodies were able to internalize NMDARs by a mechanism of crosslinking.

As a result, whole cell patch-clamp recordings of mEPSCs in cultured neurons showed that patients' antibodies specifically decreased synaptic NMDAR-mediated currents, without altering the AMPA receptor-mediated currents.[9] In contrast to the marked effects on the levels of NMDARs, patients' antibodies did not alter other synaptic proteins (e.g., GluA2/3, GABAa), number of synapses, dendritic spines, dendritic complexity, or neuronal cell survival.[9]

To determine if the autoantibodies also had effects *in vivo*, CSF from patients with high-titer GluN1 antibodies or control CSF from individuals without these antibodies was infused directly into the hippocampus of adult rats for two weeks, followed by analysis of tissue-bound human IgG and levels of NMDARs. Rats infused with patients' but not control CSF showed deposits of human IgG in the hippocampus in a pattern that was dependent on NMDAR density (e.g., high density in proximal dendrites of dentate gyrus).[9] This pattern was similar to that identified in the hippocampus of two patients who had died of anti-NMDAR encephalitis. Moreover, no

neuronal death or deposits of complement were observed, which is also similar to the autopsy findings of the patients even though the autoantibodies are predominantly IgG1 and potentially able to fix complement.[9] Overall, results from these studies provided a compelling link between the clinical syndrome and the presence of these antibodies, strongly suggesting they have a pathogenic role in the disease.

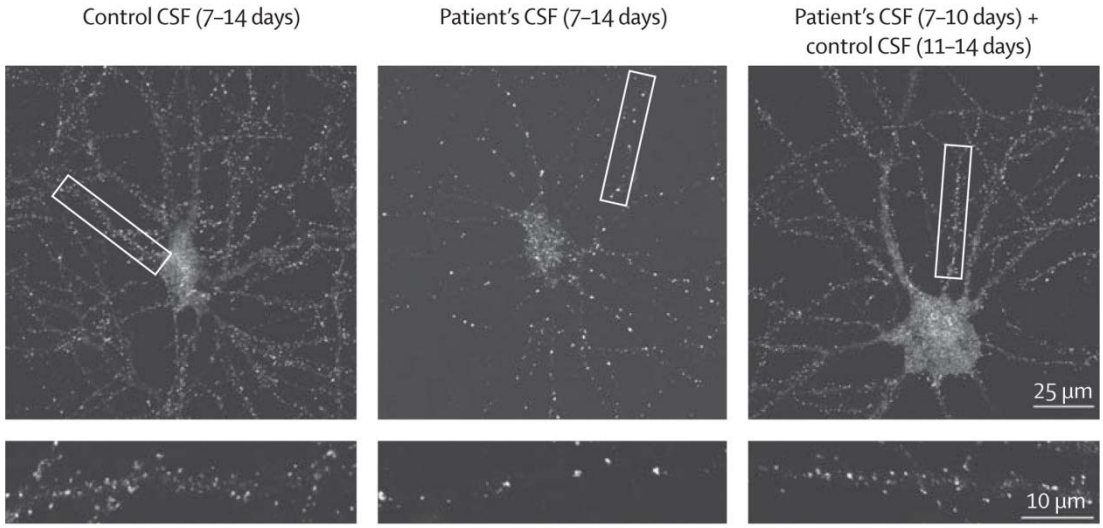

Figure 11. Patient's antibodies decrease the number of clusters of NMDAR in live neurons
Representative images of hippocampal neurons cultured with control CSF or patients' CSF from day 7 to day 14 *in vitro* (7-day treatment; *left* and *center*), or with patients' CSF from day 7 to day 10 *in vitro* followed by control CSF from day 11 to day 14 *in vitro* (3-day treatment and 4-day recovery; *right*), then immunostained for GluN1 subunit of NMDAR. Boxed areas for dendrites are shown below at higher magnification. Fewer NR1-labelled clusters were found in cultures treated with patient's CSF for 7 days (*center*) compared with those treated with control CSF (*left*) or cultures treated for 3 days with patient's CSF followed by 4 days recovery (*right*). From[89]

The dynamics of antibody-induced internalization of receptors were investigated in cultured neurons exposed for 15 minutes to 48 hours to patients' IgG.[185] Although a progressive decrease of NMDAR density started to be noted 2 hours after exposure to the patients' antibodies, the most significant effects were noted at 12 hours with no further reduction of NMDARs with longer treatment. In parallel, the internalized NMDAR clusters followed the same time course. Similar studies using Fab fragments did not cause significant effects.[185] In addition, cultured neurons treated with an NMDAR blocker were used to demonstrate that the mechanism by which patients' antibodies induced internalization was independent of the receptor function.[185]

Studies using nanoparticle/molecule tracking showed that in neurons treated with patients' IgG the lateral diffusion of the GluN2-NMDAR was dramatically increased compared with GluA1-AMPAR (that was mildly increased), and the α2-$GABA_A$R and potassium channel Kv1.3 which were unaffected.[10] It is believed that increased lateral diffusion, and consequent NMDAR escape from the synapse to extra-synaptic sites, precedes receptor internalization. Additional studies using neurons transfected with either the GluN2A or GluN2B subunit tagged with SEP [a pH-sensitive variant of enhanced green fluorescent protein (GFP) that exhibits bright fluorescence when exposed to the exterior of the cell], showed that the exposure to patients' NMDAR antibodies caused a decrease of the surface GluN2A- and GluN2B-containing receptors.[10] These changes were not caused by loss of synaptic contacts, since the overall number of glutamatergic synapses was not affected, consistent with the findings of Hughes et al.[9] Further studies using co-labeling of internalized antibody-bound NMDARs with recycling endosomal and lysosomal biomarkers (Rab11, Lamp1) showed that a greater percentage of internalized receptors colocalized with recycling endosomes rather than lysosomes, similar to the trafficking observed in other conditions (e.g., exposing neurons to picrotoxin, NMDA/glycine).[185]

Besides the ability of patients' antibodies to internalize NMDARs, they do not modulate receptor function as shown by whole cell patch-clamp recording of mEPSCs from primary neurons after short (30 minutes) or prolonged exposure (24 hours) to either patients' and control CSF, or to patients' Fab fragments.[185] However, neurons exposed to patients' CSF antibodies, but not control CSF for 20 hours, failed to increase the synaptic content of GluA1-AMPA receptor after undergoing chemically induced LTP,[186] suggesting that patients' antibodies reduced potentiation of glutamatergic synapses.

Considering the altered subcellular localization of NMDARs caused by patients' antibodies, further studies focused on the effects of the antibodies on direct partners of the NMDAR at the extracellular level, such as the Ephrin B2 receptor (EphB2). EphB2 is a member of a family of receptor tyrosine kinases that modulate LTP probably through their interaction with NMDARs that results in stabilization and clustering of these receptors in the postsynaptic membrane.[187–190] Ephrin signaling, such as ephrin-B2 ligand binding to the EphB2, is important to establish LTP in CA3-CA1 synapses, but downstream kinase signaling is not critical since LTP remains unaltered with intracellular truncated forms of EphB2.[188,191] In neurons exposed to patients' NMDAR antibodies, the tracking of EphB2 using quantum dots showed that the antibodies caused a marked increase of EphB2 diffusion at the synapse. These findings coupled to a reduction of coimmunoprecipitated EphB2/NMDAR when neurons were exposed to

patients' but not control IgG suggest that the antibodies prevent the surface interaction between EphB2 and NMDARs leading to a lateral diffusion of both EphB2 and synaptic NMDARs. Notably, activation of EphB2 by ephrin-B2 ligand prevented the increased surface diffusion and lateral synaptic escape of NMDARs induced by patients' antibodies.[10] Similar protective effects of ephrin-B2 ligand were suggested *in vivo* after injection of patients' antibodies in the dorsal hippocampus in rats. In this setting, the decrease of NMDAR immunostaining (attributed to a decrease of density of receptors) was abrogated when patient antibodies were coinjected with ephrin-B2 ligand.[10] These data provided evidence that patients' antibodies alter the interaction between NMDAR and EphB2 displacing them from synaptic to extrasynaptic sites before the NMDARs are internalized, which can be potentially prevented by EphB2 stimulation.

Mouse model of cerebroventricular transfer of patients' CSF antibodies

Combined data from these reports demonstrated that anti-NMDAR encephalitis fulfilled most of the redefined Koch-Witebsky criteria to be an antibody-mediated disease[192] (including the presence of circulating autoantibodies, and the identification of the related autoantigen). Only the transfer of symptoms to animals was pending. To develop such a model in C57BL/6J mice, Planagumà et al.[11] used bilateral ventricular catheters connected to subcutaneous osmotic pumps to deliver a continuous infusion of patients' or control CSF for 14 days. During and after the infusion period, tasks for memory (novel object recognition), anhedonic behaviors (sucrose preference test), depressive-like behaviors (tail suspension, force swimming test), anxiety (black and white, elevated plus maze tests), aggressiveness (resident-intruder test), and locomotor activity were investigated, and the potential association with brain antibody binding and levels of NMDARs were examined.

The infusion of patients' but not control CSF caused progressive memory deficits, along with anhedonic and depressive-like behaviors, without affecting locomotor activity.[11] The most dramatic effects occurred in the novel object recognition (NOR) task that was maximally impaired on day 18 (4 days after the ventricular infusion stopped) and recovered over one week (Figure 12 panel C). Brain tissue studies confirmed the progressive presence of brain-bound human IgG (maximal on day 18, mainly in hippocampus). Extraction and characterization of this IgG confirmed it to be NMDAR antibodies. Additionally, analysis of NMDAR clusters in the hippocampus showed a progressive decrease of the density of cell-surface and synaptic NMDARs (maximum on day 18; Figure 12 panels A and B) without

affecting the density of AMPA receptors or PSD95. These effects developed in parallel with memory and other behavioral alterations and gradually improved after day 18, with reversibility of symptoms, progressive reduction of brain-bound antibodies, and reestablishment of the normal levels of cell-surface and synaptic NMDARs. Pathological studies did not reveal inflammatory infiltrates or deposits of complement.[11] These findings provided robust evidence that antibodies from patients with anti-NMDAR encephalitis alter memory and behavior through reduction of cell-surface and synaptic NMDARs.

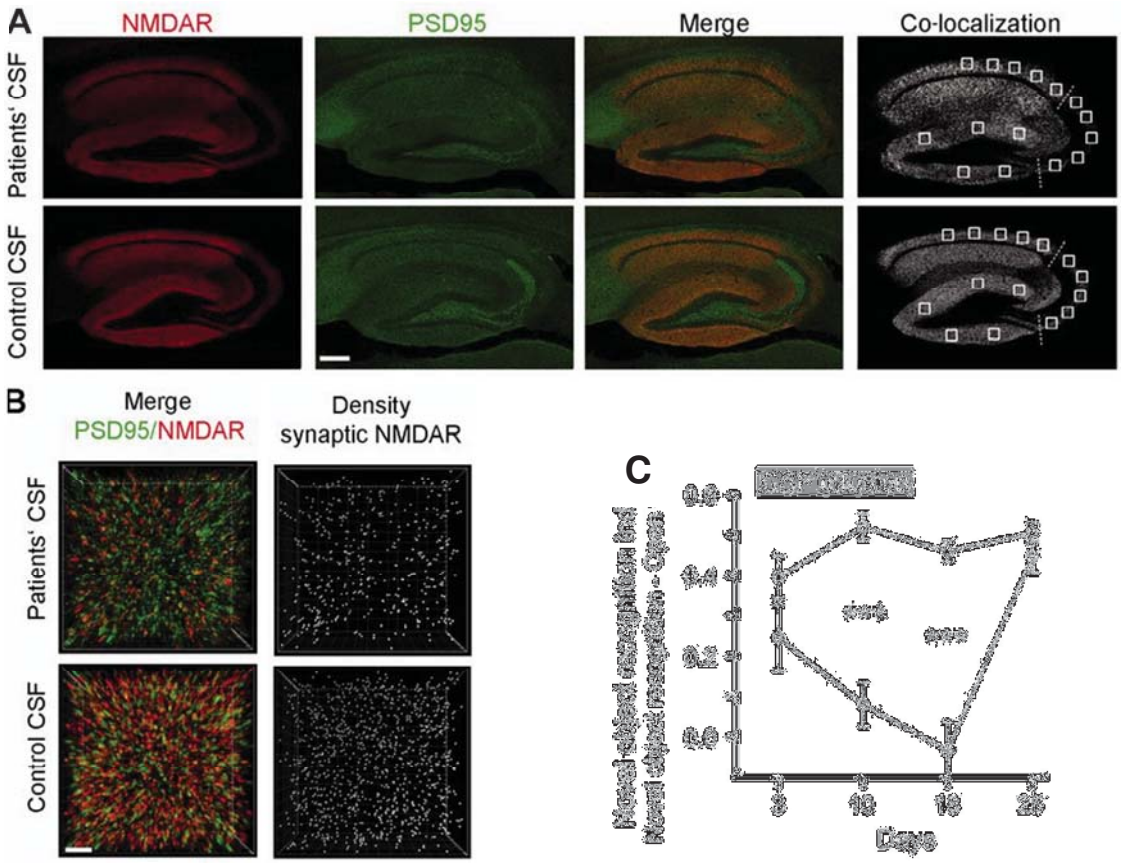

Figure 12. Patients' NMDAR antibodies selectively reduce the density of total and synaptic NMDAR clusters in hippocampus and impair visuospatial memory in mice

(A) Representative images of hippocampus of mice infused for 14 days (Day 18) with patients' CSF (upper row) or control CSF (lower row) immunolabelled for PSD95 and NMDAR. Images were merged (merge) and post-processed to demonstrate co-localizing clusters (co-localization). Squares in 'co-localization' indicate the analyzed areas in CA1, CA3 and dentate gyrus of hippocampus. Scale bar = 200 µm. (B) Three-dimensional projection of the density of total clusters of PSD95 and NMDAR, and analysis of synaptic clusters of NMDAR (defined as NMDAR clusters colocalizing with PSD95) in a representative CA3 region (square in A 'co-localization'). Scale bar = 2 µm. (C) Novel object recognition index in an open field arena of animals infused with patients' CSF (grey circles) or control CSF (white circles). A high index indicates better object recognition memory. From[11]

Findings from this model are in line with the concept that anti-NMDAR encephalitis is predominantly an antibody-mediated disease; which is supported by detection of high levels of B-cell attracting chemokines (e.g., CXCL13) in the CSF,[193] and autopsy or biopsy studies showing absent or very rare neuronophagic T-cell infiltrates, but abundant plasma cells or deposits of IgG.[49,194]

Considering previous studies that showed that stimulation of EphB2 by ephrin-B2 ligand antagonized the effects of the antibodies, Planagumà et al. used the passive transfer model to investigate the effects on synaptic plasticity (e.g., induction of LTP by stimulation and recording of the Schaffer collateral-CA1 pathway in acute brain sections from infused mice) and to determine whether the antibody-induced memory and behavioral deficits could be prevented by administration of soluble ephrin-B2 ligand.[12] Mice were infused with patients' or control CSF with or without ephrin-B2 ligand added to the osmotic pumps. Animals that received patients' antibodies without ephrin-B2 ligand developed a phenotype identical to that described above, along with severe impairment of long-term hippocampal synaptic plasticity and memory formation. These findings resembled those obtained in hippocampal CA1 region-specific GluN1 knockouts which also show deficits of memory and learning accompanied by severe impairment of LTP in the Schaffer collateral-CA1 synapse, demonstrating the role of NMDARs in establishing synaptic plasticity and memory formation.[195,196] Moreover, in contrast to the dramatic effects observed in mice receiving patients' antibodies without ephrin-B2 ligand, the coadministration of ephrin-B2 ligand antagonized the pathogenic effects of the antibodies at all levels, including memory, depressive-like behavior, density of cell-surface and synaptic NMDARs, and significantly restored the long-term synaptic plasticity.[12]

Overall, taking into account the clinical experience with this disorder and the extensive data generated from modeling the effects of antibodies *in vitro* and *in vivo*, there is compelling evidence that anti-NMDAR encephalitis is an antibody-mediated disease. Moreover, the identification that ephrin-B2 ligand antagonizes the pathogenic effects of the antibodies provides a potential strategy beyond immunotherapy on how to treat this disease (e.g., small molecule ephrin-B2 ligand-like agonists able to cross the BBB). Such an approach may shorten the duration of symptoms by antagonizing the antibody effects while immunotherapy would eliminate the antibodies or antibody-producing plasma cells.

Modeling placental transfer of NMDAR antibodies

Considering the pathogenicity of autoantibodies from patients with anti-NMDAR encephalitis, transplacental transfer of these IgG from pregnant patients to embryos can potentially result in neurological deficits in neonates.[197,198] Experience and number of reports on pregnant patients with anti-NMDAR encephalitis are limited, and the effects of the immune response on patients and offspring are largely unknown.

During the course of this thesis, Jurek et al. established a murine model of in utero exposure to recombinant monoclonal GluN1 antibodies derived from a patient with anti-NMDAR encephalitis to determine whether maternal autoantibodies are a risk factor for impaired brain development in the neonate.[199] Pregnant C57BL/6J mice were intraperitoneally injected on embryonic days 13 and 17 with 240 µg of recombinant monoclonal NR1-reactive IgG antibodies. After confirming that systemically administered antibodies to pregnant mice were transferred across the placenta and bound to synaptic structures within the neonatal brain, they showed that in utero exposure to this monoclonal antibody resulted in 27% postnatal mortality, reduced NMDAR density, and hippocampal electrophysiological properties were altered in early postnatal life. Maternal anti-NMDAR antibodies also delayed neurodevelopment in neonates, reduced anxiety behavior, and impaired prepulse inhibition in adult offspring. Mice in utero exposed to GluN1 antibodies had reduced volumes of cerebellum, midbrain, and brainstem structures at 10 months of age, from which they concluded that the antibody caused long-lasting neuropathological effects.

Searching for an application of these findings to a clinical setting, the authors determined the presence of NMDAR antibodies in serum of asymptomatic mothers of patients with neuropsychiatric disorders and mothers of healthy children (MCs) serving as controls. None of the mothers had a history of anti-NMDAR encephalitis, and their serum was tested 4 to 20 years after pregnancy. The authors found a spectrum of NMDAR antibodies slightly higher in mothers of patients with neuropsychiatric disorders than in mothers of healthy persons, and suggested that antibodies of asymptomatic seropositive pregnant women (without evidence of anti-NMDAR encephalitis) could be transferred to the fetus and caused developmental and cognitive deficits causing lifelong neuropsychiatric morbidity in the affected children.

However, the authors did not provide any experimental evidence that the antibodies from asymptomatic mothers of children with cognitive or neurodevelopmental deficits were pathogenic. Considering the experience with humans, these conclusions were premature and

could be distressing for patients with a history of anti-NMDAR encephalitis who remain antibody-positive for a long time after recovery.

Guided rationale

In order to develop a mouse model of placental transfer of antibodies from patients with anti-NMDAR encephalitis, we first pooled IgG from serum samples of patients with the disease. In contrast to a recombinant monoclonal antibody, these IgG better represent the antibody repertoire of patients with anti-NMDAR encephalitis. Pooled IgG from serum samples of healthy blood donors was used as controls' IgG.

Then we had to restrict patients' IgG administration to pregnant mice to the window of time in which the neonatal receptor (FcRn), which allows transplacental transfer of IgG, is expressed in placental tissue, and the immature fetal blood-brain barrier (BBB) does not restrict the crossing of IgG (e.g., around gestational day 16 the BBB becomes significantly more restrictive to maternal antibody penetration into the fetal brain).[200] Therefore, pooled IgG was administered on days 14, 15 and 16 of gestation.

On these days, pooled IgG from patients or controls was injected via the tail vein to pregnant mice. The intravenous route of administration was chosen not only because blood circulating IgG better modelled the situation of pregnant patients with anti-NMDAR encephalitis, but also, intraperitoneal administration in pregnant mice at late gestation may imply a risk for fetal damage.

Patients with anti-NMDAR encephalitis present with severe memory deficits. Consequently, this cognitive impairment was successfully reproduced in the mouse model of the disease by cerebroventricular infusion of patients' CSF. In fact, poor performance in the novel object recognition (NOR) task was the most prominent effect in mice infused with patients' CSF compared to those with control CSF. Consequently, within the battery of behavioral tests designed to determine the effects of in utero exposure to patients' antibodies a task to assess visuospatial memory had to be included.

After proper animal handling and habituation to the arena, the NOR test consists of two phases: an acquisition phase and a recognition test phase, separated by a delay also known as retention time. In the acquisition phase, two identical objects are placed near two opposite corners of the arena (10 cm from each adjacent wall) (Figure 13). The animal is placed into the arena and allowed a total of 9 minutes of exploration of the two objects. At test phase, after

the retention time, the animal is placed in the arena for 9 minutes where two objects are positioned in the opposite corners of those used in the acquisition phase. In this phase, the animal is presented to one object identical to the objects used in the acquisition phase and the other is a novel object, significantly different from the familiar one. The time the mice spends exploring each object is recorded. Exploratory behavior is defined as the animal directing its nose toward the object at a distance of <2 cm. Other behaviors such as looking around while sitting on or resting against the object are not considered as exploration. A discrimination index is calculated as the difference of the time spent exploring the novel and the time spent exploring the familiar object divided by the total time exploring both objects. A higher discrimination index is considered to reflect greater memory retention for the familiar object.[201,202] Varying the NOR retention time allows to assess short-term or long-term memory.

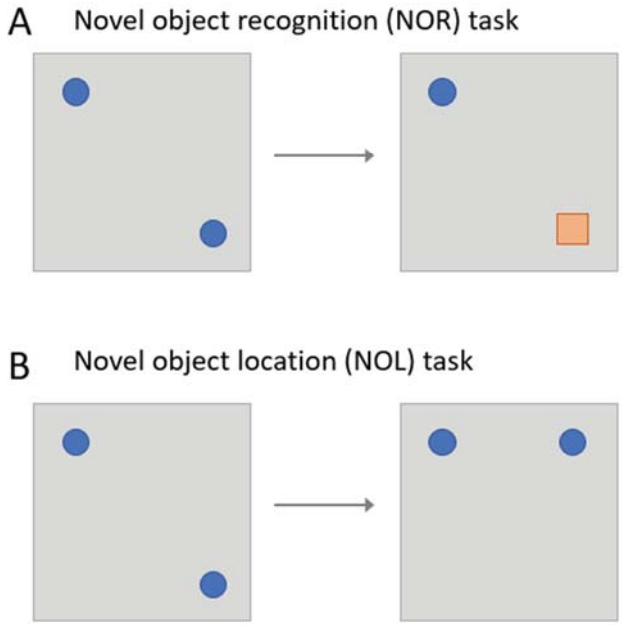

Figure 13. Schematic representation of object recognition memory tasks
Diagram of object presentation in a square-shaped open field arena during the acquisition phase (*left*) and the test phase (*right*) after the retention time (*indicated by the arrows*) for (A) the novel object recognition and (B) the novel object location tasks. Blue circles indicate identical objects, orange square represents an object significantly different from the familiar one.

In the first study of the cerebroventricular transfer model of NMDAR antibodies,[11] the NOR test was performed using two different shaped arenas for different groups of animals: an open field and a V-maze. On the day of osmotic pump implantation (considered day 1), before surgery, mice were habituated for 30 minutes in the open field arena, or 9 minutes in the V-maze. During and after antibody infusion, on days 3, 10, 18 and 25, mice were put back into

the open field arena or into the V-maze for the acquisition and test phases, with a retention time of 3 hours, as described above. During the test phase of the open field paradigm, the objects were positioned in the opposite corners of those used in the training phase, and the novel object was presented in 50% of trials on the right and in 50% of trials on the left side. For the study of the potential antagonistic effect of ephrin-B2 administration using the same animal model, the behavioral paradigm of memory was NOR, this time only in the open-field squared-shaped arena.[12]

However, NMDAR is mainly expressed in the hippocampus, and the role of the hippocampus in several paradigms of spontaneous object-location recognition memory tasks based on familiarity is controversial. Indeed, hippocampal bilateral lesions in rats revealed that the hippocampus is crucial for novel object location (NOL), but not for the NOR task. Instead, the latest was demonstrated to be more dependent on the perirhinal cortex.[203] Therefore, in the experimental design of this mouse model of placental transfer of IgG from patients with anti-NMDAR encephalitis we decided to use the NOL paradigm for the assessment of visuospatial memory.

The NOL task consists of the same phases as the NOR, and is manly performed in a squared-shaped open field arena. During the acquisition phase, animals are placed into the arena in the presence of two equal objects positioned at two opposite corners of the arena (Figure 13). The animal is allowed to freely explore both objects for 9 minutes. After a retention time of 3 hours, the animal is reintroduced to the arena for the test phase, where one of the two objects has been moved to a different corner. Thus, in the test phase both objects are equally familiar, but one of them is in a new location. The animal is allowed to explore both objects for 9 minutes and the time of exploration of each object is recorded. The criteria to define object exploration is the same as for the NOR test. A discrimination index (NOL Index) is calculated using the following formula: the difference between the time of exploration of the moved object minus the time of exploration of the not moved object divided by total time of exploration of both objects. As in NOR test, a higher discrimination index indicates a better memory of the position of both objects.

HYPOTHESES

Based on the concepts previously described, anti-NMDAR encephalitis is considered the most common autoimmune encephalitis and a severe but treatable disease that affects predominantly women of childbearing age. Patients' NMDAR antibodies have been demonstrated to be pathogenic in cellular and animal models, causing reduction of total cell-surface and synaptic NMDAR clusters, as well as impaired hippocampal long-term potentiation, memory deficits and depressive-like behavior. Moreover, the reversibility of these NMDAR antibody-mediated alterations has been proven to correlate with antibody clearance, either in patients who respond to immunotherapy, or in animal models after stopping antibody infusion. However, during embryogenesis there is a critical time window for proper development of the nervous system. At the beginning of my thesis, the number of reported clinical cases of pregnant patients with anti-NMDAR encephalitis was limited and the outcome of the mothers and babies largely unknown; thus, there was a need for retrospective data collection and for an experimental approach that resembled the human disease to further study this condition.

Therefore, I postulated that if circulating patients' antibodies are able to reach the parenchyma of the developing fetal brain, their pathogenic effect might be detrimental for the fetus/newborn. To investigate whether in utero exposure to patients' IgG resulted in developmental alterations or impaired memory and behavior after birth, I would need to develop an animal model of placental transfer of IgG antibodies from patients with anti-NMDAR encephalitis.

On the other hand, although currently anti-NMDAR encephalitis is a treatable disease, it often takes several months or more than one year for treated patients to return to most of their activities. Novel therapeutic strategies for a faster improvement are of interest. Given that most symptoms in anti-NMDAR encephalitis are associated with NMDAR hypofunction, it was reasonable to postulate that a potent and selective positive allosteric modulator of this receptor could potentially abrogate the pathogenic effects of patients' antibodies.

Therefore, considering all the above I hypothesized that:

1) Placental transfer of patients' NMDAR antibodies in mice should model the alterations observed in the clinical cases of pregnant patients with anti-NMDAR encephalitis and their offspring.

2) In a mouse model of placental transfer of IgG from patients with anti-NMDAR encephalitis, FcRn blockade is likely to prevent materno-fetal transfer of antibodies and thus, to abrogate the potential synaptic and neurodevelopmental alterations caused by patients' IgG in the offspring.

3) Treatment with a positive allosteric modulator of NMDAR is likely to prevent, at least partially, the antibody-mediated alterations described in a reported mouse model of passive cerebroventricular transfer of patients' CSF antibodies.

OBJECTIVES

The **objectives** of this thesis are:

1. Retrospectively collect clinical data from cases of anti-NMDAR encephalitis during pregnancy to report the effects of the disease and the outcome in patients and their babies.

2. Develop an animal model of placental transfer of IgG antibodies from patients with anti-NMDAR encephalitis by intravenous administration of patients' IgG to pregnant mice to determine their potential pathogenic effects in neurodevelopment and behavior, and synaptic function in the fetus and offspring.

3. Investigate whether treatment with an FcRn inhibitor prevents the placental transfer of patients' IgG and abrogates the antibody-mediated alterations in a mouse model of materno-fetal transfer of IgG from patients with anti-NMDAR encephalitis.

4. Study the potential therapeutic use of SGE-301, a positive allosteric modulator of NMDAR, in a reported mouse model of passive cerebroventricular transfer of patients' CSF antibodies.

GENERAL METHODS

The general methods that have been used in the enclosed publications are briefly summarized below and can be found described in more detail in the corresponding manuscripts included in this thesis. Additional methods of particular interest for each individual project are only described in the published manuscripts.

1) Determination of presence of NMDAR antibodies in serum and CSF samples

    a. Rat brain tissue immunohistochemistry

    b. Immunolabeling of cultured live hippocampal neurons

    c. Cell-based assay

2) Determination of antibody effects in cultured neurons

3) Cerebroventricular infusion of patients' CSF

4) Determination of the effects of antibodies in mice, including

    a. Development, memory and behavior

    b. Hippocampal electrophysiological studies

    c. Immunohistochemistry and confocal microscopy

1. Determination of presence of NMDAR antibodies in serum and CSF samples

Serum and CSF samples derived from patients with anti-NMDAR encephalitis and control individuals were used in these projects.

First, patients were selected according to clinical criteria developed by Drs. Graus and Dalmau, published in the Lancet Neurology 2016. Clinical information was provided by the treating physicians and collaborators who sent serum and CSF of patients to the laboratory of Dr. Dalmau. Then, three laboratory techniques are routinely performed with these collected samples to confirm the diagnosis of anti-NMDAR encephalitis by determining presence of specific NMDAR autoantibodies. These tests were used for selection criteria of patients' samples for the projects, validation of pooled patients' samples, and also for determination of NMDAR antibodies in mice serum samples.

a. Rat brain tissue immunohistochemistry

This technique is relevant to confirm the characteristic staining pattern, predominantly hippocampal, of autoantibody-containing serum or CSF from patients with anti-NMDAR encephalitis against rat brain tissue.

The immunohistochemistry is performed with non-perfused rat brain, that after being removed from the animal is split sagittally, fixed by immersion in 4% paraformaldehyde for 1 hour at 4°C, and cryoprotected by immersion with 40% sucrose for 48 hours. The tissue is then embedded in freezing compound, snap frozen in isopentane chilled with liquid nitrogen, and cut into 7-µm sections using a cryostat. Sections of tissue are then incubated overnight with serum or CSF using the indicated dilutions, and the reactivity developed with a standard immunoperoxidase technique (avidin-biotin peroxidase) and diaminobenzidine.

b. Immunolabeling of cultured live hippocampal neurons

To determine whether any sample reactivity identified with tissue immunostaining is directed against neuronal surface antigens, we used immunolabeling of primary cultures of rodent dissociated hippocampal neurons. Briefly, hippocampi are isolated from rat fetuses at embryonic day 18 (E18), homogenized with trypsin and seeded in P35 plates with poly-L-lysine coated coverslips. Neurons are cultured in neurobasal medium for 15-21 days *in vitro* at 37°C, 5% CO_2, 95% humidity, incubated with serum or CSF for 1 hour, fixed with 4% paraformaldehyde, developed with a fluorescent secondary antibody and observed under a fluorescent microscope.

c. Cell-based assay

To confirm the specificity of sample reactivity for NMDAR we performed cell-based assays (CBAs). This test consists on an immunocytochemistry with HEK293T cells transfected with a plasmid encoding for the target antigen and incubated with the patients' sample.

Antibodies from patients with anti-NMDAR encephalitis are directed to the GluN1 subunit of the receptor. In brief, HEK293T cells are seeded in plates containing poly-D-lysine coated coverslips, and 24 hours later, when the confluency is approximately 80%, cells are co-transfected with lipofectamine and GluN1 and GluN2 plasmids. If co-transfected with GluN1/GluN2B they need ketamine to avoid excitotoxicity (ketamine is not needed if HEK cells are only transfected with GluN1). Twenty-four hours after transfection, cells are incubated with patients' serum or CSF

either before (live CBA) or after (fixed CBA) fixation with 4% paraformaldehyde. A commercial antibody against a different epitope of the antigen is used as control for the transfection. The reactivity of patients' and commercial antibodies is then developed with the appropriate fluorescent secondary species-specific antibodies and observed under a fluorescent microscope.

2. Determination of the effect of patients' antibodies in cultured neurons

The potential effect of patients' antibodies on cultured neurons was assessed measuring the alteration of the levels of NMDAR at synaptic and extrasynaptic sites, using confocal microscopy. In brief, neurons were isolated and cultured as described above. Neurons at 14-17 days in vitro were exposed to patients' CSF or serum for 12 hours. The effect of patients' antibodies on specific receptors or synaptic proteins was then assessed with commercially available biomarkers against the receptor or protein of interest and quantified with confocal microscopy (Zeiss LSM710) using software Imaris (Bitplane).

3. Cerebroventricular infusion patients' antibodies to mice

To study a potential treatment for the behavioral and synaptic effects of patients' antibodies, we have used the mouse model of cerebroventricular infusion of patients' CSF. In brief, bilateral intraventricular catheters connected to two osmotic minipumps each containing 100 µl of patients' CSF are used to infuse patients' antibodies for 14 days at a constant flow rate of 0.25 ml/h (Figure 14).

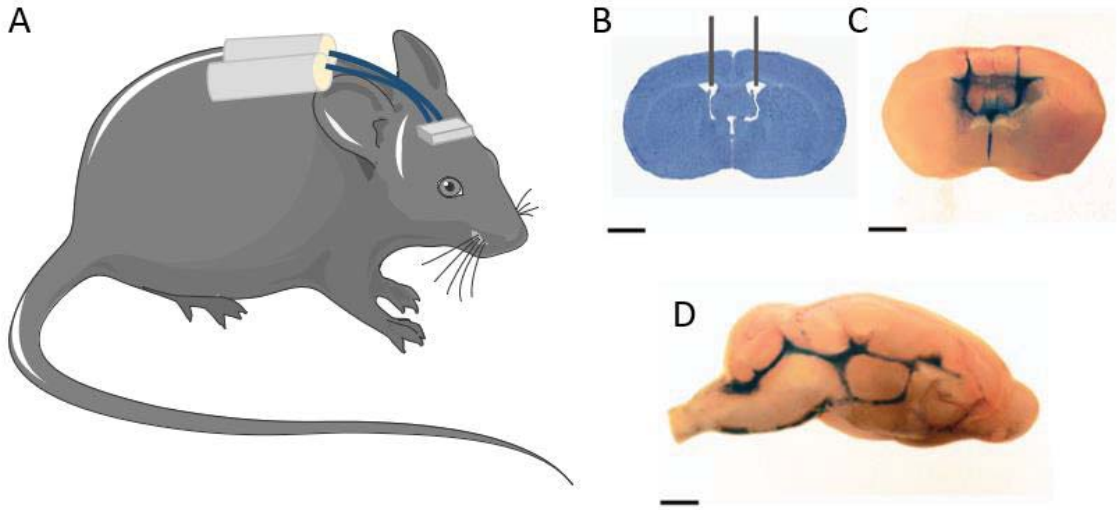

Figure 14. Cerebroventricular infusion patients' antibodies to mice
(A) Schematic representation of a mouse implanted with intraventricular catheters connected to osmotic minipumps subcutaneously placed on the back of the animal. (B) Representative coronal mouse brain section with catheter placement. (C and D) Coronal and sagittal mouse brain sections demonstrating cerebroventricular diffusion of methylene blue after ventricular infusion. Scale bar in B, C and D =2mm. Adapted from[11]

4. Determination of the pathogenic effects of the antibodies in mice

At different time points, the effects of patients' antibodies in mice (either by cerebroventricular infusion or intravenous injection to pregnant mice) were assessed using a) a battery of behavioral tests, summarized in Table 3; b) hippocampal electrophysiological studies, and c) immunohistochemistry and confocal microscopy.

a. Development, memory and behavior

Table 3. Behavioral tests used for the study of the pathogenicity of antibodies in mice		
Test	Assessment	Basis
Neurobehavioral assessment: body weight, ear detachment, eye opening, and innate reflexes	Developmental milestones	From birth to breastfeeding withdrawal, the animal undergoes drastic physical change and develops innate reflexes
Novel object location test (NOL)	Visuospatial memory	Animals tend to spend more time exploring an object in a novel rather than in a familiar location
Horizontal and vertical activity assessment	Locomotor activity	Ability to move in all planes
Prepulse inhibition of the acoustic startle response (PPI)	Sensorimotor gating	The animal does not startle when an intense acoustic stimulus is preceded by a less intense one
Nest building test (NB)	Welfare and social behavior	Healthy animals use the material to build a nest
Five-trial social interaction test (SIT)	Sociability and social memory	Animals tend to spend more time exploring a novel rather than a familial mouse
Accelerating rotarod test (ARR)	Balance and motor coordination	Ability of the animal not to fall on an accelerating rod
Tail suspension test (TST)	Depressive-like behavior	The animal will try to escape from an aversive stimulus such as an inescapable situation

b. Hippocampal electrophysiological studies

Assessment of functional effects of patients' antibodies on long-term potentiation was performed in acute hippocampal slices obtained from mice at different time points by recording field excitatory postsynaptic potentials after proper stimulation of the Schaffer collateral-CA1 pathway.

c. Immunohistochemistry and confocal microscopy

At different time points, representative sets of mice were sacrificed, and the extracted brain was processed as described for rat brain tissue immunohistochemistry. The presence of antibodies bound to tissue and specific target binding was assessed by anti-human IgG immunolabeling (and immunoprecipitation with fresh brain tissue). In addition, the effects of antibodies were assessed with confocal microscopy including quantification of the levels of the target antigens (e.g., NMDAR, Homer1, Bassoon, Cux1, FoxP2) using specific antigen and synaptic markers (e.g., PSD95 as post-synaptic marker) antibodies.

PUBLICATIONS

Paper I

Pregnancy outcomes in anti-NMDA receptor encephalitis: Case series

Bastien Joubert, Anna García-Serra, Jesús Planagumà, Eugenia Martínez-Hernandez, Andrea Kraft, Frederick Palm, Takahiro Iizuka, Jérôme Honnorat, Frank Leypoldt, Francesc Graus, and Josep Dalmau

Neurol Neuroimmunol Neuroinflamm. 2020 Jan 16;7(3):e668

Impact factor JCR 2020 (percentile): The available IF from 2019 is 7.724 (D1)

ARTICLE OPEN ACCESS

Pregnancy outcomes in anti-NMDA receptor encephalitis

Case series

Bastien Joubert, MD, Anna García-Serra, MSc, Jesús Planagumà, PhD, Eugenia Martínez-Hernandez, MD, PhD, Andrea Kraft, MD, Frederick Palm, MD, Takahiro Iizuka, MD, PhD, Jérôme Honnorat, MD, PhD, Frank Leypoldt, MD, PhD, Francesc Graus, MD, PhD, and Josep Dalmau, MD, PhD

Correspondence
Dr. Dalmau
jdalmau@clinic.cat

Neurol Neuroimmunol Neuroinflamm 2020;7:e668. doi:10.1212/NXI.0000000000000668

Abstract

Objective

To report the effects of anti-NMDA receptor (NMDAR) encephalitis in pregnant patients and their babies.

Methods

We studied a retrospective cohort of patients who developed anti-NMDAR encephalitis during pregnancy or became pregnant while recovering from the encephalitis. In addition, we reviewed the English literature between 2010 and 2019 related to this topic.

Results

We studied 11 patients; 6 developed anti-NMDAR encephalitis during pregnancy, and 5 became pregnant while recovering. There were no obstetrical complications, but 6 (55%) babies were premature. Ten newborns were healthy, and 1 (9%) developed transient respiratory distress. Nine infants had assessable follow-up (median 18 months; range, 7–96 months), and all showed normal development. We identified 21 cases in the English literature. Obstetrical complications occurred in 7 (33%) pregnancies. Two patients died of septic shock (1 baby successfully delivered), another 2 had miscarriages, and in 2, the pregnancy was terminated. Sixteen babies (76%) were delivered, 9 (56%) premature. At birth, 13/16 (81%) newborns were healthy, 2/16 (13%) had transient neurologic or respiratory symptoms, and 1 (6%) died of brain edema. Follow-up (median 12 months; range, 6–36 months) was reported for 8 children: 7 (88%) showed normal development and behavior, and 1 (13%) cortical dysplasia. Immunotherapy was used during pregnancy in 7 (64%) of our patients and 18 (86%) of the reported cases, including rituximab in 4 cases, without adverse effects.

Conclusions

Patients who develop anti-NMDAR encephalitis during pregnancy or become pregnant during recovery often have obstetrical complications, but most of the newborns are healthy and appear to have normal development.

From the Neuroimmunology Program (B.J., A.G.-S., J.P., E.M.-H., F.G., J.D.), Institut d'Investigacions Biomèdiques August Pi i Sunyer (IDIBAPS), Hospital Clínic, Universitat de Barcelona, Spain; Department of Neurology (A.K.), Martha-Maria Hospital, Halle, Germany; Department of Neurology (F.P.), Helios Hospital, Schleswig, Germany; Department of Neurology (T.I.), Kitasato University School of Medicine, Sagamihara, Japan; French Reference Center on Paraneoplastic Neurological Syndromes (B.J., J.H.), Hospices Civils de Lyon, SynatAc Team, Institut NeuroMyoGène, INSERM U1217/CNRS UMR 5310, Université de Lyon, Université Claude Bernard Lyon 1; France; Neuroimmunology Section (F.L.), Institute of Clinical Chemistry, University Hospital Schleswig-Holstein, Kiel/Lübeck, Germany; Department of Neurology (F.L.), Christian-Albrechts-University, Kiel, Germany; Institució Catalana de Recerca i Estudis Avançats (ICREA) (J.D.), Barcelona, Spain; and Department of Neurology (J.D.), University of Pennsylvania, PA.

Go to Neurology.org/NN for full disclosures. Funding information is provided at the end of the article.

The Article Processing Charge was funded by *Neurology: Neuroimmunology & Neuroinflammation*.

Glossary

IVIg = IV immunoglobulin; **mRS** = modified Rankin Scale; **NMDAR** = NMDA receptor.

Anti-NMDA receptor (NMDAR) encephalitis is a severe but treatable autoimmune neurologic disease that often results in psychotic symptoms, seizures, dyskinesias, decreased level of consciousness, dysautonomia, or central hypoventilation.[1] About 60% of patients are young women, and some develop the disease during pregnancy.[1,2] Several reports have suggested that dysautonomia, seizures, or central hypoventilation play important roles in the potential complications that pregnant patients may develop.[3–7] Other studies proposed that transplacental transfer of NMDAR antibodies can result in acute encephalopathy or death of the newborn or eventually result in autistic-spectrum disorders.[3,8–10] In a study based in an experimental animal model of transplacental transfer of a human monoclonal NMDAR antibody, Jurek et al.[11] suggested that antibodies of asymptomatic seropositive pregnant women (without evidence of anti-NMDAR encephalitis) caused developmental and cognitive deficits in the offspring. However, the authors did not provide any experimental evidence that the antibodies from asymptomatic mothers of children with cognitive or neurodevelopmental deficits were pathogenic. The best human model to examine the postulate of these authors is pregnant patients with anti-NMDAR encephalitis who all have clear evidence of pathogenic NMDAR antibodies. In fact, the experience and number of reports on pregnant patients with this disease are limited, and the effects of the immune response on patients and offspring are largely unknown. Here, we report 11 new patients and review 21 previously reported cases, describing the effects of the disease on the mothers and babies and the treatments used and outcome.

Methods

Data collection

Patients whose serum or CSF were examined for NMDAR antibodies in 3 referral centers (Barcelona, Spain; Lyon, France; and Kiel/Lübeck, Germany) and who were pregnant when they developed anti-NMDAR encephalitis or became pregnant while recovering from the disease were included in the study. Clinical information was retrospectively provided by the treating physicians, patients, and families using a structured questionnaire. We focused on the age and neurologic symptoms of the mothers, presence of an underlying tumor, immunotherapies used during pregnancy, duration of the pregnancy, and type of delivery. Mothers' neurologic outcomes were assessed using the modified Rankin Scale (mRS).[12] The short-term outcomes of the infants were obtained from records of obstetricians or midwives and the APGAR score 5 minutes after delivery. We reviewed whether the babies were later found to have developmental problems or alterations of behavior and social interaction.

Literature search

Previously reported cases were identified through MEDLINE search using the following keywords: "NMDAR," "N-methyl-D-aspartate," "antibodies," "autoimmune encephalitis," and "pregnancy," published between January 1, 2010, and August 15, 2019.

Standard protocol approvals, registrations, and patient consents

We obtained written informed consent from all patients. The study was approved by the local institutional review boards of Hospices Civils de Lyon (CPP SUD-EST II, US registration number 11263) and Hospital Clínic de Barcelona (registration number HCB/2018/0192). All data are available on request at Neuroimmunology Program, IDIBAPS Institute, Barcelona (Spain).

Data availability

Any data not published within the article are available and will be shared anonymously by request from any qualified investigator.

Results

Patients of the current series

We retrospectively assessed the information of 11 cases, including 6 patients (55%) who developed anti-NMDAR encephalitis during pregnancy (3 in the 1st trimester, 2 in the 2nd trimester, and 1 in the 3rd trimester), and 5 (45%) who became pregnant during recovery (median time from onset of recovery: 5 months [range, 1–42 months]; median mRS score at the onset of pregnancy: 1 [range, 1–2]). The main clinical features are shown in table 1 (further individual information in Supplemental Material, links.lww.com/NXI/A185). Median age was 23 years (range, 19–37 years), and all patients had combinations of symptoms typical for anti-NMDAR encephalitis, 7 of them (64%) requiring intensive care. An ovarian teratoma was found and removed in 4 (36%) patients. All patients survived, and at the last visit (median follow-up 28 months; range, 6–144 months), 8/11 (73%) had minor neurologic disability (mRS score ≤2). None of the 11 patients had obstetric complications, and all pregnancies were continued until delivery (table 2). A caesarean section was performed in 4 (36%) patients because of the severity of the neurologic disease, but there was no case of fetal distress. The postpartum period was uneventful in all cases.

Infants of the current series

In total, 11 children were born (5 females and 6 males), 6 (55%) preterm (table 3). Ten newborns (90%) were reported healthy after delivery, and the 5-minute APGAR score was

Table 1 Clinical features of the patients

	Present series	Literature
No. of cases	11	21
Median age (range)	23 (19–37)	25 (18–36)
NMDAR encephalitis during pregnancy, n (%)	6 (55)	21 (100)
Pregnancy onset during recovery phase, n (%)	5 (45)	0 (0)
Teratoma, n (%)	4 (36)	10 (48)
Clinical presentation		
First episode, n (%)	11 (100)	20 (95)
Relapse, n (%)	0 (0)	1 (5)
Symptoms, n (%)		
Psychotic symptoms	11 (100)	17 (81)
Anterograde amnesia	7 (64)	9 (43)
Seizures	6 (55)	13 (62)
Dyskinesia	7 (64)	14 (67)
Disintegration of speech	7 (64)	3 (14)
Impairment of consciousness	7 (64)	17 (81)
Central hypoventilation	3 (27)	9 (43)
Autonomic symptoms	5 (45)	9 (43)
Insomnia	2 (18)	3 (14)
Combination of ≥3 symptoms, n (%)	11 (100)	18 (86)
Psychotic and cognitive symptoms only, n (%)	0 (0)	2 (10)
Seizures only, n (%)	0 (0)	1 (5)
Admission in ICU, n (%)	7 (64)	18 (86)
Neurologic symptoms at the onset of pregnancy		
None, n (%)	6 (55)	21 (100)
Anterograde amnesia, n (%)	2 (18)	0 (0)
Depressed mood/anxiety, n (%)	2 (18)	0 (0)
Behavioral disturbances, n (%)	2 (18)	0 (0)
Reduced attention span, n (%)	1 (9)	0 (0)
Reduced speech fluency, n (%)	1 (9)	0 (0)
Immunotherapy during pregnancy		
Steroids, n (%)	4 (36)	17 (81)
IVIg, n (%)	4 (36)	11 (52)
Plasma exchange, n (%)	1 (9)	9 (43)
Rituximab, n (%)	1 (9)	3 (14)
Cyclophosphamide, n (%)	0 (0)	1 (5)
None, n (%)	4 (36)	3 (14)
Neurologic outcomes		
No. (%) with available follow-up	10 (91)	13 (68)
Median follow-up, mo (range)	28 (6–144)	9 (6–18)
Median mRS score at last follow-up (range)	1 (0–4)	1 (0–3)

Abbreviations: ICU = intensive care unit; IVIg = IV immunoglobulin; mRS = modified Rankin Scale; NMDAR = NMDA receptor.

normal in 6/6 (100%) (not provided for the other 5 newborns). One newborn, whose mother had developed NMDAR encephalitis at 20 weeks of gestation, presented with respiratory distress immediately after delivery (APGAR score not provided). This was considered an adverse effect of the antiepileptic and sedative drugs that had been administered to the mother, and the baby recovered spontaneously in less than 24 hours. Among 9 (81%) infants with follow-up (median 18 months; range, 7–96 months), no developmental abnormality, atypical behavior, or abnormal interaction was reported. Only 1 newborn was tested for serum NMDAR antibodies and was found positive; he was reported healthy at birth and at the last follow-up (18 months) showed normal development and behavior.

Review of previously reported patients

A review of the English literature identified 19 publications reporting 21 cases of anti-NMDAR encephalitis during pregnancy (table 1).[2–8,13–24] Median maternal age was 25 years (range, 18–36 years), and 18 (85.7%) patients required intensive care. A teratoma was found and removed in 10/21 (47.6%) patients. Two patients (10%) died of septic shock during intensive care, one of them after the delivery of a baby (case with cortical dysplasia). Follow-up was provided for 13/19 (68.4%) survivors, and 12 (92.3%) of them had good neurologic outcomes (final mRS score ≤ 2). Obstetrical complications were reported in 7/19 (36.8%) patients (table 2). Two patients had miscarriages during the first trimester, and in another 2 patients, the pregnancy was terminated.[2,17–19]

Review of outcomes of previously reported children

In total, 16 children were born, 9 (56%) preterm. A cesarean section was performed in 8 (50%) mothers, either because their clinical status was deteriorating (n = 5) or there was fetal distress (n = 3). Thirteen of 16 (81.3%) newborns were considered healthy. The APGAR score at 5 minutes was normal in 5/9 infants (56%; not provided for the other 7). One infant (mother's encephalitis at 7 weeks of gestation) had transient movement disorders after birth (5-minute APGAR score: 7/10) and during follow-up showed developmental delay and epilepsy due to cortical dysplasia.[13] Another infant (mother's encephalitis at 37 weeks of gestation) was born

Table 2 Obstetrical outcomes in pregnancies concomitant with NMDA receptor encephalitis

	Present series	Literature
No. cases	6	21
Median age, range	23 (19–37)	24.5 (18–36)
Disease onset		
First trimester, n (%)	3 (50)	11 (52)
Second trimester, n (%)	2 (33)	7 (33)
Third trimester, n (%)	1 (17)	3 (14)
Complications		
Death from septic shock, n (%)	0 (0)	2 (10)
Obstetrical complications, n (%)	0 (0)	7 (33)
Spontaneous miscarriage	0 (0)	2 (10)
Uteroplacental insufficiency	0 (0)	1 (5)
Eclampsia	0 (0)	1 (5)
Hemorrhagic shock from vaginal bleeding	0 (0)	1 (5)
Unexplained fetal distress	0 (0)	2 (10)
Delivery		
No. (%) children born	6 (100)	16 (76)
Spontaneous miscarriage, n (%)	0 (0)	2 (10)
Death of the mother before delivery, n (%)	0 (0)	1 (5)
Medical termination of pregnancy, n (%)	0 (0)	2 (10)
Cesarean section, n (%)	4 (67)	8 (50)
Maternal indication[a]	4 (100)	5 (63)
Fetal indication[b]	0 (0)	3 (37)

[a] Treatment or procedures used to treat the mother may affect the fetus.
[b] The clinical status of the mother (e.g., severe autonomic dysfunction and uncontrolled seizures) is harmful to the fetus.

with hypotonia, hypoventilation, and seizure-like abnormal movements (5-minute APGAR score: 2/10).[3] Brain MRI showed diffuse brain edema attributed to maternal antibody-mediated encephalitis, and he died 3 weeks after birth. Another infant (mother's encephalitis at 20 weeks of gestation) had transient neuromuscular symptoms and respiratory depression (APGAR score: 4/10) likely related to sedative drugs administered to the mother.[8] Follow-up was available in 10 children (63%; median, 12 months; range, 6–36 months). All of them had normal development and behavior, except for the child with cortical dysplasia. Serum anti-NMDAR antibodies were tested in 6 newborns and found positive in 3, all with complications at birth (1 lethal encephalopathy; 1 cortical dysplasia with epilepsy and developmental delay, and 1 transient neuromuscular and respiratory deficit).

Immunotherapy during pregnancy

Immunotherapy was used in 7 (64%) patients studied by us and in 18 (86%) of the previously reported patients (table 1). No adverse effect was reported in any of the patients or infants. Twenty-one patients received IV steroids, 15 IV immunoglobulin (IVIg), and 10 plasma exchange. In addition, rituximab was administered to 4 patients (1 from our cohort and 3 from the literature). Rituximab was started during the first trimester (2 patients) or the second trimester (2 patients), at a median of 21 weeks (range, 19–33 weeks) before delivery. In all 4 patients, rituximab was well tolerated and associated with clinical improvement. One of these patients also received IV cyclophosphamide 6 weeks before delivery. In all 4 cases, the babies were healthy without malformations, hypogammaglobulinemia, or leukopenia. None of the patients studied by us or previously reported who had a low 5-minute APGAR score, or any symptoms at birth, were exposed to rituximab or cyclophosphamide during pregnancy.

Discussion

In this study, we aimed to assess the effects of anti-NMDAR encephalitis on pregnancy, focusing on the obstetrical complications and outcome of mothers and babies. Because it has been suggested that transplacental transfer of maternal NMDAR antibodies may be harmful to the fetus, we focused on 2 settings associated with maternal levels of serum NMDAR antibodies: (1) pregnant women who developed anti-NMDAR encephalitis and (2) women who became pregnant while they were recovering from anti-NMDAR encephalitis.[25] Placental transfer of maternal antibodies is critical for fetal protection against infections and begins at 12–13 weeks of pregnancy.[26–28] However, at approximately the same time the blood-brain barrier of the fetus develops the ability to prevent the passage of endogenous albumin (and likely immunoglobulins) to the brain. Therefore, the amount of maternal antibodies that can actually reach the developing brain is unclear.[29–31]

Despite in utero exposure to NMDAR antibodies (in some cases from the first trimester onward), up to 90% of infants studied by us were healthy at birth, and all of those who had assessable follow-up (7–96 months) had normal development. Premature birth was common due to the frequent indication of cesarean section, although without obvious adverse effects on the babies. Moreover, review of the literature shows that only 3 of 16 infants whose mothers had anti-NMDAR encephalitis during pregnancy developed neonatal encephalopathy.[3,8,9] In 1 study, based in a single patient, the authors suggested that neonatal encephalopathy due to passive transfer of maternal NMDAR antibodies can potentially occur several years after the mother has recovered from the encephalitis as long as she remains anti-NMDAR seropositive.[9] Other authors proposed that the absence of serum NMDAR antibodies in the mother (e.g., only detected in CSF) decreases the risk of problems in the newborn.[5]

Table 3 Children outcomes

	Present series	Literature
No. children	11	16
Term of delivery		
Full term, n (%)	4 (36)	3 (19)
Early term, n (%)	1 (9)	4 (25)
Preterm, n (%)	5 (45)	9 (56)
Extreme preterm, n (%)	1 (9)	0
Health status at birth		
Healthy, n (%)	10 (91)	13 (81)
Neuromuscular/respiratory depression, n (%)	1 (9)	1 (6)
Transient abnormal movements, n (%)	0 (0)	1 (6)
Severe encephalopathy and death, n (%)	0 (0)	1 (6)
APGAR score 5 min following delivery		
No. (%) with data	6 (54)	9 (56)
7–10, n (%)	6 (100)	5 (56)
4–6, n (%)	0 (0)	3 (33)
0–3, n (%)	0 (0)	1 (11)
Outcome at last visit		
No. (%) with available follow-up	9 (81)	10 (63)
Median follow-up, mo (range)	18 (7–96)	12 (6–36)
Healthy child with normal development, n (%)	9 (100)	7 (88)
Cortical dysplasia, epilepsy, and mental retardation, n (%)	0 (0)	1 (12)

Although all 3 reported infants with detectable NMDAR antibodies at birth had neurologic symptoms, in our series, the only newborn that tested positive was healthy. It is likely that the neurologic symptoms described in those infants resulted from a combination of factors that may include the potential pathogenic effects of the antibodies (usually transient) along with the side effects of sedatives, antiepileptics, and other drugs used during the pregnancy. Except for 1 previously reported baby with cortical dysplasia (along with delayed global development and seizures) who was the product of a pregnancy with multiple complications, uteroplacental insufficiency, and delivery at gestational age 34 weeks, we have not identified other infants with neurodevelopmental disorders.[13]

In addition to the infants' outcomes, we reviewed the importance of obstetrical complications in patients who develop anti-NMDAR encephalitis during pregnancy. Although in our series we did not identify obstetrical complications, about one third of reported patients had pathologic pregnancy or spontaneous miscarriage that are likely related to the severe neurologic and medical problems of patients with this disease, often requiring intensive care admissions. Because pregnant patients with other diseases that may require prolonged intensive care are relatively infrequent in obstetrical cohorts, the comparison with those with anti-NMDAR encephalitis is difficult, and we have not been able to determine whether this disease causes more obstetric complications than other diseases that associate with similar degree of neurologic and systemic symptoms.[32,33] Therefore, although the exact cause of these complications and their relation with anti-NMDAR encephalitis are unclear, autonomic dysfunction or seizures could have played a role. In late stages of pregnancy, uteroplacental blood flow comprises a large part of the maternal cardiac output, making the fetus particularly sensitive to variations of maternal blood pressure.[34] For example, 3 patients underwent emergency cesarean sections due to signs of fetal distress, resulting in good outcome in 2 of them.

In most pregnant patients, the immunotherapies used are those described as first-line treatments (steroids, IVIg, and plasma exchange). Our experience and that reported in the literature indicate that these treatments are usually well tolerated. The experience with rituximab (which is often considered a second-line treatment) is limited to a few patients, and it was well tolerated. Previous retrospective studies and literature reviews on pregnant patients with autoimmune demyelinating diseases treated with rituximab did not show adverse effects on patients or newborns.[35,36] Low B-cell counts may be observed in the infants, but they usually normalize spontaneously in the first 6 months without increased infection rates.

This study has limitations posed by its retrospective nature and the small number of cases available. The short follow-up of the infants (median 18 months in our series and 12 months in the literature) and the lack of systematic neuropsychological assessment may have potentially missed neurologic complications. On the other hand, the current frequency of complications identified in the literature, despite being small, probably represents a reporting bias whereby cases with complications are more likely to be reported. Over the years, we have learned of additional cases (not included in this report, and unable to track) of pregnant patients with anti-NMDAR encephalitis who delivered healthy babies.

Despite these limitations, the current findings are important to report in light of a recent study by Jurek et al.,[11] suggesting that in asymptomatic pregnant women (without evidence of previous history of anti-NMDAR encephalitis), transplacental transfer of serum NMDAR antibodies results in neuropsychiatric symptoms in the offspring. This study is very disconcerting for patients and families of patients with anti-NMDAR encephalitis because during the disease, these patients have high levels of NMDAR antibodies that usually remain detectable (albeit at low titer) for many months or years after recovery. However, the conclusions

of Jurek et al.[11] are based in a model of passive transfer of high amounts (0.48 mg) of a monoclonal antibody derived from a patient with classic anti-NMDAR encephalitis to pregnant mice that resulted in 27% neonatal mortality and multiple symptoms during the postnatal and adult stages of the mice. This monoclonal antibody does not reflect the antibody repertoire of patients with anti-NMDAR encephalitis and, even less so, the antibodies of asymptomatic mothers of children with neurocognitive deficits. Moreover, there is no evidence that the antibodies of asymptomatic pregnant women (without a previous history of anti-NMDAR encephalitis) are the same as those antibodies occurring in anti-NMDAR encephalitis or have similar pathogenicity.

Overall, the current findings and previously reported cases suggest that in pregnant patients with anti-NMDAR encephalitis, fetal exposure to maternal NMDAR antibodies infrequently associates with overt neurologic deficits. Acute neonatal encephalopathy or neurodevelopmental disorders appear to be infrequent, and in such cases, other factors, not necessarily antibody related (e.g., drugs used during pregnancy, seizures or autonomic dysfunction of the mother, uteroplacental insufficiency, and premature delivery), may play a role. Obstetrical complications pose a serious threat to pregnant patients with NMDAR encephalitis, suggesting that these patients need to be monitored closely in intensive care units dedicated to high-risk pregnancies and treated early with first-line immunotherapy (e.g., steroids and IVIg). Considering our findings and those of larger series of patients with other CNS autoimmune disorders, rituximab is a potential treatment option in severely ill pregnant who fail first-line therapies.[35] Our results suggest that pregnancy is not contraindicated in women with a history of anti-NMDAR encephalitis. An important question to clarify is whether serum antibody titers in the mother and newborn correlate with the likelihood of neurologic deficits and developmental abnormalities. Future multi-institutional investigations on patients who develop anti-NMDAR encephalitis during pregnancy, or become pregnant after the acute phase of the disease, are needed. These studies should include neuropsychological assessments of the children with sufficient follow-up (24–36 months) to detect any delay in skill acquisition.

Study funding

This study was supported in part by Instituto Carlos III/FEDER (JR17/00012, E.M.-H.; FIS 17/00234 and PIE 16/00014, J.D.); CIBERER (15/00010, J.D.); AGAUR-Generalitat de Catalunya (2019FI B1 00212, A.G.-S.); Pla Estratègic de Recerca i Innovació en Salut (PERIS SLT002/16/00346, J.P.); La Caixa Foundation Health Research (J.D.); and Fundació CELLEX (J.D.).

Disclosure

B. Joubert, A. García-Serra, J. Planagumà, E. Martínez-Hernandez, and A. Kraft report no disclosures. T. Iizuka received a grant from The Japan Epilepsy Research Foundation and financial support from Astellas Pharma Inc. J. Honnorat reports no disclosure. F. Leypoldt reports having received speakers honoraria from Roche, Novartis, Bayer, Fresenius, and Grifols, serving as an advisory board member to Roche and Biogen, and working for an academic institute offering commercial autoantibody testing to third parties. F. Graus receives royalties from Euroimmun for the use of IgLON5 as an autoantibody test. J. Dalmau receives royalties from Athena Diagnostics for the use of Ma2 as an autoantibody test and from Euroimmun for the use of NMDA, GABAB receptor, GABAA receptor, DPPX and IgLON5 as autoantibody tests. He is editor of *Neurology® Neuroimmunology & Neuroinflammation*. Go to Neurology.org/NN for full disclosures.

Publication history

Received by *Neurology: Neuroimmunology & Neuroinflammation* November 19, 2019. Accepted in final form December 19, 2019.

Appendix Authors

Name	Location	Role	Contribution
Bastien Joubert, MD	University of Barcelona	Author	Designed and conceptualized the study; analyzed the data; and drafted the manuscript for intellectual content
Anna García-Serra, MSc	University of Barcelona	Author	Revised the manuscript for intellectual content
Jesús Planagumà, PhD	University of Barcelona	Author	Revised the manuscript for intellectual content
Eugenia Martínez-Hernandez, MD, PhD	University of Barcelona	Author	Revised the manuscript for intellectual content
Andrea Kraft, MD	Martha-Maria Hospital, Halle	Author	Major role in the acquisition of data
Takahiro Iizuka, MD, PhD	Kitasato University School of Medicine, Sagamihara	Author	Major role in the acquisition of data
Jérôme Honnorat, MD, PhD	Hospices Civils de Lyon	Author	Major role in the acquisition of data
Frank Leypoldt, MD, PhD	Christian-Albrechts-University, Kiel	Author	Major role in the acquisition of data
Francesc Graus, MD, PhD	University of Barcelona	Author	Revised the manuscript for intellectual content
Josep Dalmau, MD, PhD	University of Barcelona	Author	Designed and conceptualized the study; analyzed the data; and drafted the manuscript for intellectual content

References

1. Dalmau J, Lancaster E, Martinez-Hernandez E, Rosenfeld MR, Balice-Gordon R. Clinical experience and laboratory investigations in patients with anti-NMDAR encephalitis. Lancet Neurol 2011;10:63–74.
2. Kumar MA, Jain A, Dechant VE, et al. Anti-N-methyl-D-aspartate receptor encephalitis during pregnancy. Arch Neurol 2010;67:884–887.
3. Chourasia N, Watkins MW, Lankford JE, Kass JS, Kamdar A. An infant born to a mother with anti-N-methyl-d-aspartate receptor encephalitis. Pediatr Neurol 2018;79:65–68.
4. Liao Z, Jiang X, Ni J. Anesthesia management of cesarean section in parturient with anti-N-methyl-D-aspartate receptor encephalitis: a case report. J Anesth 2017;31: 282–285.
5. Ueda A, Nagao R, Maeda T, et al. Absence of serum anti-NMDAR antibodies in anti-NMDAR encephalitis mother predicts having healthy newborn. Clin Neurol Neurosurg 2017;161:14–16.
6. Xiao X, Gui S, Bai P, et al. Anti-NMDA-receptor encephalitis during pregnancy: a case report and literature review. J Obstet Gynaecol Res 2017;43:768–774.
7. McCarthy A, Dineen J, McKenna P, et al. Anti-NMDA receptor encephalitis with associated catatonia during pregnancy. J Neurol 2012;259:2632–2635.
8. Lamale-Smith LM, Moore GS, Guntupalli SR, Scott JB. Maternal-fetal transfer of anti-N-methyl-D-aspartate receptor antibodies. Obstet Gynecol 2015;125:1056–1058.
9. Hilderink M, Titulaer MJ, Schreurs MWJ, Keizer K, Bunt JEH. Transient anti-NMDAR encephalitis in a newborn infant due to transplacental transmission. Neurol Neuroimmunol Neuroinflamm 2015;2:e126. doi: 10.1212/NXI.0000000000000126.
10. Coutinho E, Jacobson L, Pedersen MG, et al. CASPR2 autoantibodies are raised during pregnancy in mothers of children with mental retardation and disorders of psychological development but not autism. J Neurol Neurosurg Psychiatry 2017;88:718–721.
11. Jurek B, Chayka M, Kreye J, et al. Human gestational NMDAR autoantibodies impair neonatal murine brain function. Ann Neurol 2019;86:656–670.
12. Banks JL, Marotta CA. Outcomes validity and reliability of the modified Rankin scale: implications for stroke clinical trials: a literature review and synthesis. Stroke 2007;38: 1091–1096.
13. Jagota P, Vincent A, Bhidayasiri R. Transplacental transfer of NMDA receptor antibodies in an infant with cortical dysplasia. Neurology 2014;82:1662–1663.
14. Shahani L. Steroid unresponsive anti-NMDA receptor encephalitis during pregnancy successfully treated with plasmapheresis. BMJ Case Rep 2015;2015:bcr2014208052.
15. Mathis S, Pin JC, Pierre F, et al. Anti-NMDA receptor encephalitis during pregnancy: a case report. Medicine (Baltimore) 2015;94:e1034.
16. Lu J, Samson S, Kass J, Ram N. Acute psychosis in a pregnant patient with Graves' hyperthyroidism and anti-NMDA receptor encephalitis. BMJ Case Rep 2015;2015: bcr2014208823.
17. Kim J, Park SH, Jung YR, Park SW, Jung DS. Anti-NMDA receptor encephalitis in a pregnant woman. J Epilepsy Res 2015;5:29–32.
18. Chan LW, Nilsson C, Schepel J, Lynch C. A rare case of anti-N-methyl-D-aspartate receptor encephalitis during pregnancy. N Z Med J 2015;128:89–91.
19. Kokubun N, Komagamine T, Hirata K. Pregnancy and delivery in anti-NMDA receptor encephalitis survivors. Neurol Clin Pract 2016;6:e40–e43.
20. Kalam S, Baheerathan A, McNamara C, Singh-Curry V. Anti-NMDAR encephalitis complicating pregnancy. Pract Neurol 2019;19:131–135.
21. Grewal KS, Bhatia R, Singh N, Singh R, Dash D, Tripathi M. Confusional state in a pregnant woman: a case of NMDA receptor encephalitis during pregnancy. J Neuroimmunol 2018;325:29–31.
22. Keskin AO, Tanburoglu A, Idiman E, Ozturk V. Anti-N-methyl-d-aspartate receptor encephalitis during pregnancy: a case report. J Obstet Gynaecol Res 2019;45: 935–937.
23. Mizutamari E, Matsuo Y, Namimoto T, Ohba T, Yamashita Y, Katabuchi H. Successful outcome following detection and removal of a very small ovarian teratoma associated with anti-NMDA receptor encephalitis during pregnancy. Clin Case Rep 2016;4:223–225.
24. Demma L, Norris S, Dolak J. Neuraxial anesthesia in a patient with anti-N-methyl-D-aspartate receptor encephalitis in pregnancy: management for cesarean delivery and oophorectomy. Int J Obstet Anesth 2017;31:104–107.
25. Gresa-Arribas N, Titulaer MJ, Torrents A, et al. Diagnosis and significance of antibody titers in anti-NMDA receptor encephalitis, a retrospective study. Lancet Neurol 2014; 13:167–177.
26. Simister NE. Placental transport of immunoglobulin G. Vaccine 2003;21:3365–3369.
27. Dancis J, Lind J, Oratz M, Smolens J, Vara P. Placental transfer of proteins in human gestation. Am J Obstet Gynecol 1961;82:167–171.
28. Malek A, Sager R, Kuhn P, Nicolaides KH, Schneider H. Evolution of maternofetal transport of immunoglobulins during human pregnancy. Am J Reprod Immunol 1996;36:248–255.
29. Virgintino D, Robertson D, Benagiano V, et al. Immunogold cytochemistry of the blood–brain barrier glucose transporter GLUT1 and endogenous albumin in the developing human brain11Published on the World Wide Web on 24 August 2000. Dev Brain Res 2000;123:95–101.
30. Virgintino D, Errede M, Robertson D, et al. Immunolocalization of tight junction proteins in the adult and developing human brain. Histochem Cell Biol 2004;122: 51–59.
31. Saunders NR, Dziegielewska KM, Møllgård K, Habgood MD. Physiology and molecular biology of barrier mechanisms in the fetal and neonatal brain. J Physiol (Lond) 2018;596:5723–5756.
32. Seppänen PM, Sund RT, Uotila JT, Helminen MT, Suominen TM. Maternal and neonatal characteristics in obstetric intensive care unit admissions. Int J Obstet Anesth 2019. doi:10.1016/j.ijoa.2019.07.002.
33. Chantry AA, Deneux-Tharaux C, Bonnet M-P, Bouvier-Colle M-H. Pregnancy-related ICU admissions in France: trends in rate and severity, 2006-2009. Crit Care Med 2015;43:78–86.
34. Crozier TME. General care of the pregnant patient in the intensive care unit. Semin Respir Crit Care Med 2017;38:208–217.
35. Das G, Damotte V, Gelfand JM, et al. Rituximab before and during pregnancy. Neurol Neuroimmunol Neuroinflamm 2018;5:e453. doi: 10.1212/NXI.0000000000000453.
36. Chakravarty EF, Murray ER, Kelman A, Farmer P. Pregnancy outcomes after maternal exposure to rituximab. Blood 2011;117:1499–1506.

Pregnancy outcomes in anti-NMDA receptor encephalitis: Case series

Bastien Joubert, Anna García-Serra, Jesús Planagumà, et al.

Neurol Neuroimmunol Neuroinflamm 2020;7;
DOI 10.1212/NXI.0000000000000668

Paper II

Placental transfer of NMDAR antibodies causes reversible alterations in mice

Anna García-Serra, Marija Radosevic, Anika Pupak, Veronica Brito, José Ríos, Esther Aguilar, Estibaliz Maudes, Helena Ariño, Marianna Spatola, Francesco Mannara, Marta Pedreño, Bastien Joubert, Silvia Ginés, Jesús Planagumà,* and Josep Dalmau*
*These are joint senior authors

Neurol Neuroimmunol Neuroinflamm. 2020 Nov 10;8(1):e915

Impact factor JCR 2020 (percentile): The available IF from 2019 is 7.724 (D1)

ARTICLE OPEN ACCESS

Placental transfer of NMDAR antibodies causes reversible alterations in mice

Anna García-Serra, MSc, Marija Radosevic, PhD, Anika Pupak, MSc, Veronica Brito, PhD, José Ríos, MSc, Esther Aguilar, BS, Estibaliz Maudes, MSc, Helena Ariño, MD, PhD, Marianna Spatola, MD, PhD, Francesco Mannara, PhD, Marta Pedreño, PhD, Bastien Joubert, MD, PhD, Silvia Ginés, PhD, Jesús Planagumà, PhD,* and Josep Dalmau, MD, PhD*

Correspondence
Dr. Dalmau
jdalmau@clinic.cat

Neurol Neuroimmunol Neuroinflamm 2021;8:e915. doi:10.1212/NXI.0000000000000915

Abstract

Objective

To determine whether maternofetal transfer of NMDA receptor (NMDAR) antibodies has pathogenic effects on the fetus and offspring, we developed a model of placental transfer of antibodies.

Methods

Pregnant C57BL/6J mice were administered via tail vein patients' or controls' immunoglobulin G (IgG) on days 14–16 of gestation, when the placenta is able to transport IgG and the immature fetal blood-brain barrier is less restrictive to IgG crossing. Immunohistochemical and DiOlistic (gene gun delivery of fluorescent dye) staining, confocal microscopy, standardized developmental and behavioral tasks, and hippocampal long-term potentiation were used to determine the antibody effects.

Results

In brains of fetuses, patients' IgG, but not controls' IgG, bound to NMDAR, causing a decrease in NMDAR clusters and cortical plate thickness. No increase in neonatal mortality was observed, but offspring exposed in utero to patients' IgG had reduced levels of cell-surface and synaptic NMDAR, increased dendritic arborization, decreased density of mature (mushroom-shaped) spines, microglial activation, and thinning of brain cortical layers II–IV with cellular compaction. These animals also had a delay in innate reflexes and eye opening and during follow-up showed depressive-like behavior, deficits in nest building, poor motor coordination, and impaired social-spatial memory and hippocampal plasticity. Remarkably, all these paradigms progressively improved (becoming similar to those of controls) during follow-up until adulthood.

Conclusions

In this model, placental transfer of patients' NMDAR antibodies caused severe but reversible synaptic and neurodevelopmental alterations. Reversible antibody effects may contribute to the infrequent and limited number of complications described in children of patients who develop anti-NMDAR encephalitis during pregnancy.

*These authors are joint senior authors.

From the Institut d'Investigacions Biomèdiques August Pi i Sunyer (IDIBAPS) (A.G.-S., M.R., A.P., V.B., E.A., E.M., H.A., M.S., F.M., M.P., B.J., S.G., J.P., J.D.), Hospital Clínic, Universitat de Barcelona; Departament de Biomedicina (A.P., V.B., S.G.), Facultat de Medicina, Institut de Neurociències, Universitat de Barcelona; Centro de Investigación Biomédica en Red sobre Enfermedades Neurodegenerativas (CIBERNED) (A.P., V.B., S.G.), Madrid; Medical Statistics Core Facility (J.R.), IDIBAPS and Hospital Clínic, Barcelona; Biostatistics Unit (J.R.), School of Medicine, Universitat Autònoma de Barcelona; Centro de Investigaciones Biomédicas en Red de Enfermedades Raras (CIBERER) (J.D.), Madrid, Spain; Department of Neurology (J.D.), University of Pennsylvania, Philadelphia; and Institució Catalana de Recerca i Estudis Avançats (ICREA) (J.D.), Barcelona, Spain.

Go to Neurology.org/NN for full disclosures. Funding information is provided at the end of the article.

The Article Processing Charge was funded by the ISCIII.

Glossary

BBB = blood-brain barrier; **CBA** = cell-based assay; **fEPSP** = field excitatory postsynaptic potential; **GEE** = generalized estimated equation; **GLM** = generalized linear model; **IgG** = immunoglobulin G; **LTP** = long-term potentiation; **NMDAR** = NMDA receptor; **NMDAR-ab** = NMDAR antibody; **NOL** = novel object location; **PD** = postnatal day; **PPI** = prepulse inhibition; **PSD95** = postsynaptic density protein 95.

Anti-NMDA receptor (NMDAR) encephalitis is a neuronal antibody-mediated disease that associates with prominent neurologic and psychiatric symptoms.[1] Most clinical series show that 60%–80% of patients are women of childbearing age[2–4] who sometimes develop the encephalitis during pregnancy.[5,6] In addition to the obstetric complications that can arise from the severity of the disease,[5–7] there is the concern that patient's antibodies can reach the fetal brain and cause synaptic and neurodevelopmental alterations. This concern is supported by the demonstration of the pathogenicity of the antibodies in cultured neurons[8–10] and in a mouse model of cerebroventricular transfer of patients' antibodies.[11] Moreover, peritoneal injection of a human NMDAR monoclonal antibody to pregnant mice resulted in high neonatal mortality and long-lasting irreversible neurodevelopmental deficits in the offspring.[12]

Therefore, considering the severity of patients' symptoms, pathogenicity of the antibodies, and the fact that NMDAR signaling regulates neuronal maturation,[13] migration,[14] and synaptogenesis,[15] one would expect severe abnormalities in the offspring of patients with anti-NMDAR encephalitis. However, the clinical experience is markedly different; other than a few exceptional cases,[16] most reports indicate that the offspring of these patients appear to have good outcomes.[6] Indeed, among the limited number of problems reported in the babies, most are described as transient[17] or attributed to medications.[6] These discrepancies led us to investigate in a model of maternofetal transfer of patients' immunoglobulin G (IgG) antibodies, the effects on synaptic NMDAR, dendritic complexity, cortical development, and microglial activation in fetal and postnatal brains. We also determined whether mice exposed in utero to patients' IgG had impairment of memory, behavior, and hippocampal long-term plasticity and whether the antibody effects persisted or resolved from newborn to adulthood stages.

Methods

Most of the methods and techniques used here have been previously reported[11,18] and are described in appendix e-1 (links.lww.com/NXI/A341).

Human serum samples, IgG purification, and immunoabsorption

IgG was isolated by ammonium sulfate precipitation from serum of 7 patients with anti-NMDAR encephalitis and 7 healthy blood donors. All patients with anti-NMDAR encephalitis were women (median age 20 years, range 16–26 years) with anti-NMDAR encephalitis. The presence of NMDAR antibodies (NMDAR-abs) was determined with rat brain immunohistochemistry and a cell-based assay (CBA).[1] To rule out the presence of other antibodies, pooled IgG from patients was immunoabsorbed with HEK293T cells expressing GluN1/2B, and the reactivity determined with brain immunohistochemistry, CBA of GluN1/2B, and live neurons, showing with all 3 techniques abrogation of reactivity.[10,18] We confirmed that immunoabsorbed patients' IgG no longer decreased the levels of NMDARs after 12-hour incubation, as reported.[19]

Animals, infusion of IgG, tissue processing, and determination of antibodies in blood from pregnant mice and fetuses

Animal care and processing of brain of fetuses and offspring were performed as reported.[11] Overall, 54 pregnant C57BL/6J mice, 165 fetuses, and 187 pups were used for behavioral, electrophysiologic, morphologic, and synaptic brain studies.

Pooled IgG (800 μg) from patients or controls was injected via tail vein to pregnant mice on days 14, 15, and 16 (E14, E15, and E16) of gestation (figure 1A). These experiments were planned according to the window of time in which the neonatal receptor (FcRn), which allows IgG transplacental transfer, is expressed in placental tissue, and the immature fetal blood-brain barrier (BBB) does not restrict the crossing of IgG (by day E16, the BBB becomes more restrictive).[20] The presence of human NMDAR-abs in blood from pregnant mice and fetuses was demonstrated with immunolabeling of live rat hippocampal neurons in culture and conventional CBA.[1] Antibody titers were obtained by serial sample dilution using CBA.

Determination of human IgG, NMDAR clusters, and cortical plate thickness in fetal brain tissue

To determine whether human NMDAR-abs injected to pregnant mice reached the brain of fetuses, 5-μm-thick fetal brain sections were immunostained for human IgG using Alexa Fluor 488 goat anti-human IgG, as above. Quantification of fluorescence intensity was performed using the public domain Fiji ImageJ software (fiji.sc/Fiji).[8] Confirmation that patients' IgG was bound to NMDAR was done by immunoprecipitation.[18]

The effects of patients' antibodies on total cell-surface and synaptic NMDAR clusters and postsynaptic density protein 95 (PSD95) were examined using immunohistochemistry

Figure 1 Patients' antibodies intravenously administered to pregnant mice reach fetal brain and bind to NMDAR

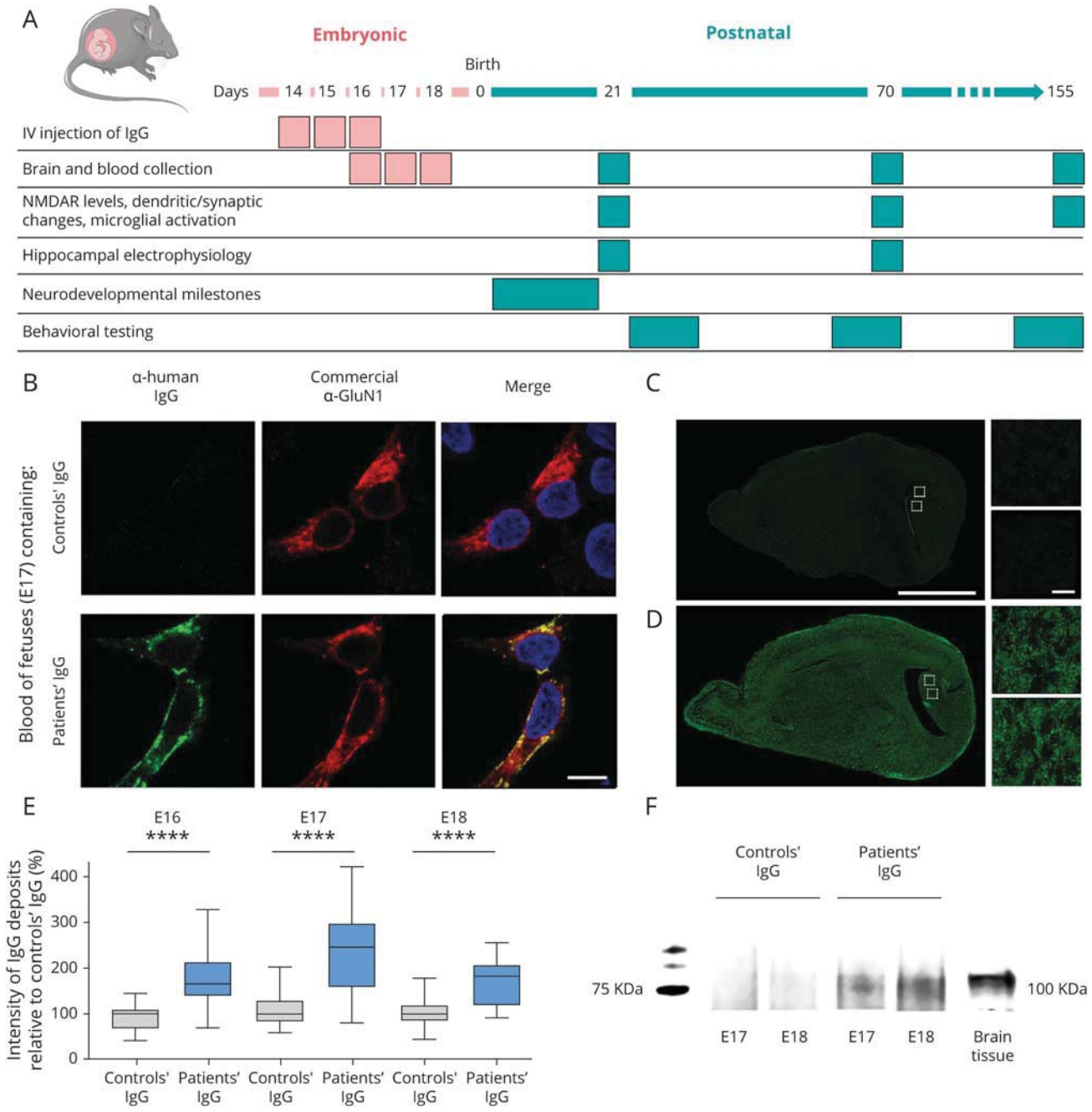

(A) Diagram of the experimental design. IV injection of pooled IgG was performed on gestational days E14, E15, and E16. Brain and blood samples from the fetus or offspring were collected on E16, E17, and E18 and PD 21, PD 70, and PD 155; blood samples of pregnant mice were collected on E16–E18. Brain tissue studies were performed on the same time points and electrophysiology on PD 21 and PD 70. Newborns were assessed daily for neurodevelopmental milestones from birth until PD 21. After breastfeeding withdrawal, mice underwent a battery of behavioral tests at age 1, 2, and 4 months. Gestational period is marked in pink and postnatal period in green. (B) Representative images of HEK293T cells expressing GluN1/2B immunolabeled with human IgG contained in serum of fetuses (E17) exposed to controls' or patients' IgG. Scale bar = 10 μm. (C and D) Representative human IgG immunolabeling in E17 fetal brain sections of animals exposed in utero to controls' (C) or patients' (D) IgG; the 2 insets (small squares in C and D, developing hippocampus) are shown enlarged on the right of each panel. Scale bar whole brain = 100 μm, insets = 10 μm. (E) Quantification of human IgG immunofluorescence intensity in the developing hippocampus of fetal brains obtained on gestational days E16-E18 exposed to controls' IgG or patients' IgG. Controls' IgG, E16, n = 5; E17, n = 13; E18, n = 8; patients' IgG, E16, n = 9; E17, n = 16; E18, n = 8. Median intensity of IgG immunofluorescence in brain of mice exposed to controls' IgG was defined as 100%. Data presented in box plots show the median, 25th, and 75th percentiles; whiskers indicate minimum and maximum. Significance of treatment effect was assessed by the Mann-Whitney *U* test. ****$p < 0.0001$. (F) Immunoprecipitated NMDAR-bound IgG from E17 and E18 brains of fetuses exposed in utero to controls' or patients' IgG. Lane brain tissue corresponds to homogenate of mouse brain used here as control. The band at ~100 KDa corresponds to the GluN1 subunit of the NMDAR. Each lane corresponds to the immunoprecipitation of the brains from 4 fetuses, per each indicated condition. IgG = immunoglobulin G; NMDAR = NMDA receptor; PD = postnatal day.

and confocal microscopy.[11] The thickness of the cortical plate was measured using 4', 6-diamidino-2-phenylindole (DAPI)-stained fetal brain sections and quantified using Fiji ImageJ software.

Determination of human IgG, NMDAR clusters, synaptic density, cortical layer thickness, and microglial activation in offspring

The presence of human IgG in the brain of offspring and the density of NMDAR were examined as indicated for fetal brains (time points shown in figure 1A). NMDAR clusters were quantified from a total of 15 images acquired from CA1, CA3, and dentate gyrus of the hippocampus (5 different areas per region).

The density of glutamatergic synapses was assessed with immunohistochemistry using presynaptic (Bassoon) and postsynaptic (Homer1) markers and the corresponding secondary antibodies (appendix e-1, links.lww.com/NXI/A341).

Cortical layer thickness was measured in sections of brains immunostained with specific cortical layer markers including a monoclonal mouse anti-CUTL1 for layers II–IV, and a polyclonal sheep anti-FoxP2 for layer VI, followed by the appropriate secondary antibodies. The layers' thickness was quantified using Fiji ImageJ software. Cell density in CUTL1-labeled layers was measured on brain sections using DAPI staining with spots algorithm in Imaris software.

Microglial activation was assessed in brain sections using a monoclonal rat antibody against CD68 (pan-macrophage) and a polyclonal rabbit antibody against Iba-1 (activated microglia). The CD68- or Iba-1–stained surface density was quantified using Imaris software.

Dendritic complexity and spine morphology analysis

These studies were performed using DiOlistic (gene gun delivery of fluorescent dye) staining and confocal microscopy (appendix e-1, links.lww.com/NXI/A341). Dendritic complexity was examined with Sholl analysis in cortical and CA1 hippocampal pyramidal neurons.[21] Spine morphology was examined in DiI-labeled segments of apical secondary dendrites of cortical and CA1 pyramidal neurons. Quantification of mushroom-shaped dendritic spines was performed with the spine classification algorithm (Imaris software).

Field potential recordings, hippocampal long-term potentiation, and paired-pulse facilitation

Acute sections of the hippocampus of the offspring were used to determine long-term plasticity by the classical paradigm of stimulation at the Schaffer collateral pathway and recording the field potentials at CA1 synapses.[19]

Neurobehavioral assessment in postnatal and adult stages

From birth to weaning (defined as breastfeeding withdrawal on postnatal day [PD] 21), mice were assessed daily for achievement of developmental milestones using a modified Fox battery, similar to that previously reported.[22] From weaning to adulthood (155 days), subsets of mice underwent a comprehensive battery of memory and behavioral tests (appendix e-1, links.lww.com/NXI/A341, and figure e-1, links.lww.com/NXI/A342).

Statistical analysis

Comparison of human IgG intensity, confocal densities of NMDAR, PSD95, Homer1, Bassoon, Iba-1, CD68, and mushroom-shaped spines between mice exposed to patients' IgG vs controls' IgG was performed with the Mann-Whitney *U* test as non-normally distributed parameters. Comparison of cortical plate thickness, cortical layers II–IV and VI, cortical cell density, and electrophysiologic field excitatory postsynaptic potential (fEPSP) slope changes between the 2 experimental groups was performed using independent sample *t* tests. Sholl analysis data were analyzed with a generalized linear model (GLM) for global and time point effects. For behavioral paradigms, longitudinal analyses were performed by generalized estimated equations (GEEs) using an AR(1) matrix to account for intraindividual correlations. All models include litter size, group, and group by time as fixed factors. Time to rooting, ear detachment, auditory startle, and eye opening were analyzed with the Mann-Whitney *U* test. All experiments were assessed for outliers with the ROUT method applying $Q = 1\%$. In all analyses, we used a 2-sided type I error of 5%. All tests were performed using GraphPad Prism (version 8; GraphPad Inc., San Diego, CA) or SPSS (version 25; IBM Corp., Armonk, NY) for GLM and GEE models. Mean values or estimated mean values (body weight, righting reflex, and negative geotaxis for the GEE model) were presented with ±SEM.

Ethical approval

Written informed consent was obtained from all patients; the study was approved by the local institutional review board at Hospital Clínic, Barcelona (HCB/2018/0192). Animal studies were approved by the Ethical Committee of the University of Barcelona (2010/63/UE) and Spanish (RD 53/2013) regulations.

Data availability

Data supporting these findings are available on reasonable request.

Results

Presence of human NMDAR-abs in serum of pregnant mice and fetuses

Serum samples collected on E16, E17, and E18 from pregnant mice and fetuses exposed to patients' IgG, but not those exposed to controls' IgG, showed human IgG binding to cell surface of live hippocampal neuronal cultures and HEK293T cells expressing GluN1/GluN2B (figure 1B). The human NMDAR antibody titer (obtained by serial dilution of samples in CBA) was 1:160–1:320 in pregnant mice and 1:80–1:160 in fetuses (data not shown).

Patients' IgG reach fetal brain, causing a reduction of synaptic NMDAR and thinning of the cortical plate

On days E16–18, fetuses exposed to patients' IgG showed increased human IgG fluorescence in the developing hippocampus compared with those exposed to controls' IgG (figure 1, C–E). Immunoprecipitation experiments confirmed the presence of NMDAR bound to IgG in the brain precipitate (figure 1F). Analysis of the density of NMDAR clusters showed that fetuses harboring patients' IgG had a significant decrease in cluster density of total cell-surface and synaptic NMDARs (figure 2, A and D). The cortical plate of these fetuses was also thinner on E17 and E18 compared with that of controls (figure 2, G and J).

Offspring exposed in utero to patients' IgG have decreased NMDAR and synaptic density, thinning of cortical layers, and microglial activation

On PD 21 and 70, mice exposed in utero to patients' IgG no longer had significant brain deposits of IgG (not shown). Despite this, the reduction of total cell-surface NMDAR clusters persisted until day 70 (figure 2, B and C) with subsequent normalization, so that by day 155, the levels were similar to those of controls (not shown). In contrast, the levels of synaptic NMDAR normalized faster; they were decreased on day 21 (figure 2E), but were normal on days 70 and 155 (figure 2F, not shown). PSD95 cluster density was not affected at any time point (data not shown).

Mice exposed to patients' IgG, but not controls' IgG, showed thinning of cortical layers II–IV (assessed with CUTL1/FoxP2 staining) on PD 21 (figure 2, H and K) that was no longer present on PD 70 (figure 2, I and L). This transient thinning of cortical layers II–IV was associated with an increase in cell density in these layers on PD 21 ($p = 0.0065$, data not shown).

On PD 21, the density of glutamatergic synapses (assessed by colocalization of Homer1/Bassoon clusters) was decreased in mice exposed in utero to patients' IgG (figure 3, A and B). These effects were no longer seen on day 70 (not shown).

On PD 21 and 70, there was an increase of 57% and 53% in activated microglia (assessed by expression of Iba-1 in somatosensory cortex) in mice exposed in utero to patients' IgG (figure 3, C and D). This difference in activated microglia was no longer present on PD 155 (not shown). No significant difference in the total number of microglial cells (assessed by expression of CD68) was noted between groups of mice at any time point examined (figure 3E).

Exposure to patients' IgG causes alterations in dendritic complexity, spine density, and spine morphology in cortical and hippocampal pyramidal neurons

Dendritic arborization was assessed by Sholl analysis (figure 4, A and B). On PD 21, the Sholl analysis in cortical and hippocampal areas showed a higher dendritic arborization in mice exposed in utero to patients' IgG (figure 4, C and D, left). No differences were noted on PD 70 (figure 4, C and D, right).

The density of mushroom-shaped (mature) dendritic spines was assessed in the cerebral cortex and hippocampus using the Imaris standard parameters for dendritic spine classification (example shown in figure 4, E–G). On PD 21, the density of these spines was significantly decreased in mice exposed in utero to patients' IgG (cortex, figure 4H, left; hippocampus, figure 4I, left). The changes were no longer seen on PD 70 (cortex, figure 4H, right; and hippocampus, figure 4I, right).

Intrauterine exposure to patients' IgG causes a reversible impairment in hippocampal long-term potentiation formation

Assessment of fEPSPs showed that on PD 21, mice that had been exposed in utero to patients' IgG had impairment in long-term potentiation (LTP) formation compared with mice exposed in utero to controls' IgG (figure e-2, A–C, links.lww.com/NXI/A343). This change in LTP formation was no longer detected on PD 70 (figure e-2, D–F). Paired-pulse facilitation studies at 50 and 100 milliseconds of interstimuli interval (which assess presynaptic release mechanisms) were not different between groups of animals (data not shown).

Neurodevelopmental delay due to in utero exposure to NMDAR-abs

Newborn pups exposed in utero to patients' IgG showed multiple alterations including transient decrease of weight (figure 5A); longer times for proper body righting (figure 5B) and negative geotaxis (figure 5C); delayed eye opening (figure 5D); and longer time in open field locomotion (not shown, $p < 0.01$). Neonatal mortality occurred in litters of mice exposed in utero to controls' IgG (26%) or patients' IgG (25%), which is in line with general litter loss in laboratory mice.[23] No significant differences were observed in ear detachment, tactile rooting response, and auditory startle (data not shown).

Spontaneous reversal of behavioral alterations from early to mature adulthood

At age 1 month, mice exposed in utero to patients' IgG showed a significant decrease in the novel object location (NOL) index indicating impairment in visuospatial memory (figure 5E), a higher amount of unused material for nest building (figure 5F), and a longer time of exploration of a familiar intruder mouse indicating impairment in social memory (figure 5G, trial 4). Assessment of motor coordination and balance showed that mice exposed in utero to patients' IgG had shorter times on the accelerating rotarod (figure 5H). No significant differences were noted in prepulse inhibition (PPI) of acoustic startle reaction, locomotor activity, or adult body weight at age 1 month (data not shown).

At age 2 months, the alterations of NOL, nest building, and social interaction in mice that had been exposed to patients'

Figure 2 Intrauterine exposure to patients' IgG causes a transient reduction of cell-surface NMDARs and thinning of the cortical plate and cortical layers II–IV

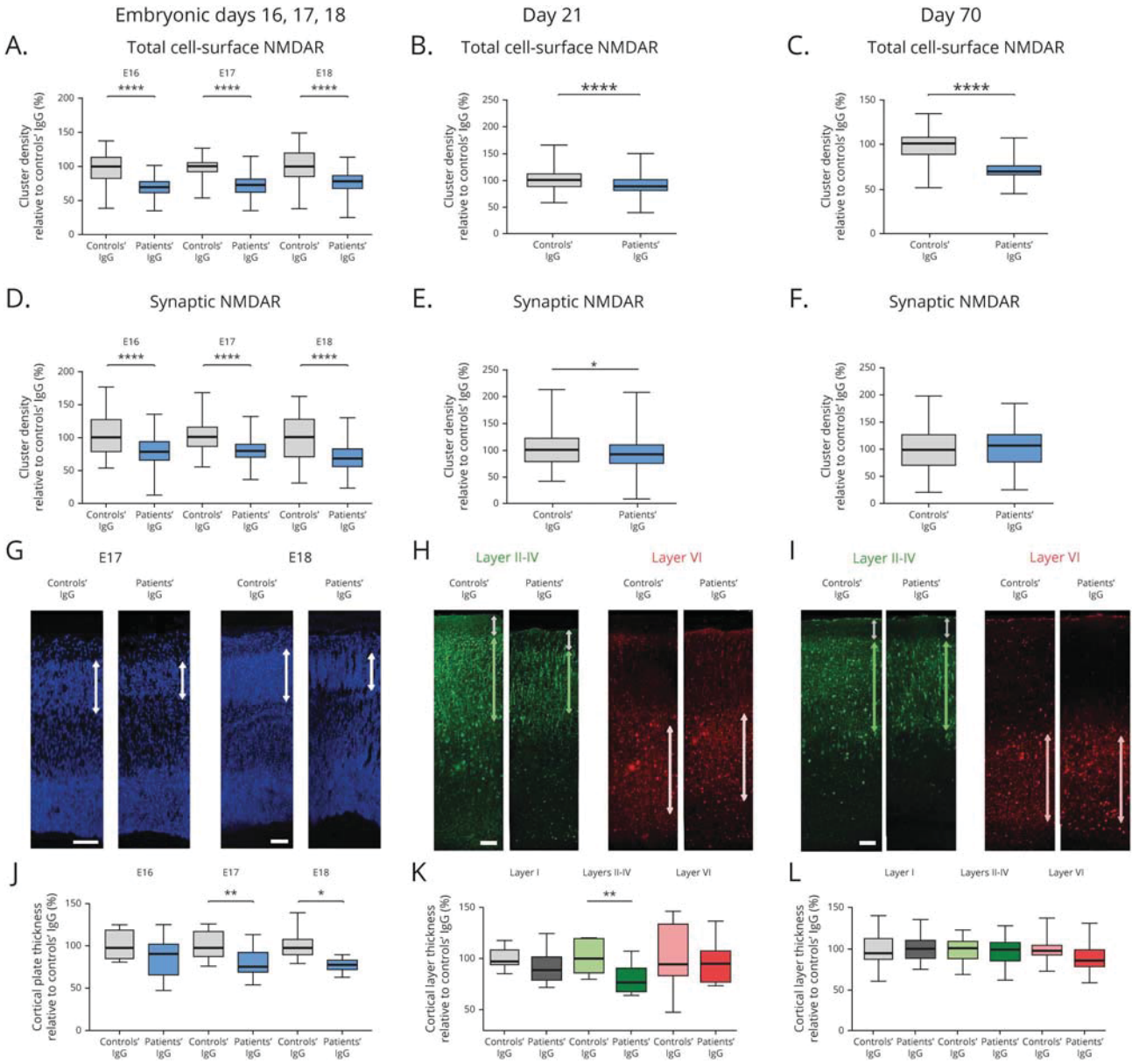

(A–F) Quantification of total cell-surface (A–C) and synaptic (D–F) NMDAR cluster density in brains obtained on gestational days E16, E17, and E18 (A and D), PD 21 (B and E), and PD 70 (C and F) from animals exposed in utero to controls' IgG or patients' IgG. Median of NMDAR clusters in mice exposed to controls' IgG was defined as 100%. Controls' IgG, E16, n = 6; E17, n = 15; E18, n = 7; PD 21, n = 11; PD 70, n = 9; patients' IgG, E16, n = 13; E17, n = 21; E18, n = 5; PD 21, n = 14; PD 70, n = 10. (G) Representative cortical plate thickness (assessed with DAPI) in E17 and E18 brains of fetuses exposed in utero to controls' or patients' IgG. Scale bars = 100 µm. (H–I) Representative sections of the somatosensory cortex (H, PD 21; I, PD 70) of animals exposed in utero to controls' or patients' IgG, showing cortical layers II–IV (CUTL1 positive, green fluorescence) and cortical layer VI (FoxP2 positive, red fluorescence); arrows indicate the thickness of the indicated layers. Scale bars = 100 µm. (J) Quantification of cortical plate thickness in E16, E17, and E18 brains of fetuses exposed in utero to controls' IgG or patients' IgG. Controls' IgG, E16, n = 4; E17, n = 11; E18, n = 10; patients' IgG, E16, n = 8; E17, n = 14; E18, n = 8. (K and L) Quantification of the indicated cortical layers' thickness (K, PD 21; L, PD 70) in animals exposed to controls' IgG or patient's IgG. Controls' IgG, PD 21, n = 7; PD 70, n = 8; patients' IgG, PD 21, n = 15; PD 70, n = 10. For J–L, the mean thickness of the cortical plate or the indicated cortical layers in mice exposed in utero to controls' IgG was defined as 100%. Data presented in box plots show the median, 25th, and 75th percentiles; whiskers indicate minimum and maximum. Significance of treatment effect was assessed by the Mann-Whitney *U* test in A–F and independent sample *t* test in J–L. *$p < 0.05$, **$p < 0.01$, ****$p < 0.0001$. IgG = immunoglobulin G; NMDAR = NMDA receptor; PD = postnatal day.

IgG were no longer present (figure 5, I and J; social interaction not shown). PPI and locomotor activity remained unaffected at age 2 months (not shown). However, mice exposed in utero to patients' IgG showed a shorter time on the accelerating rotarod (data not shown, $p = 0.0292$) and longer time of immobility in the tail suspension test (which assesses core helplessness) (figure 5K).

At age 4 months (adulthood), no significant difference was noted between mice exposed in utero to patients' IgG and

Figure 3 Intrauterine exposure to patients' IgG causes a reversible decrease in synaptic density and increase in activated microglia

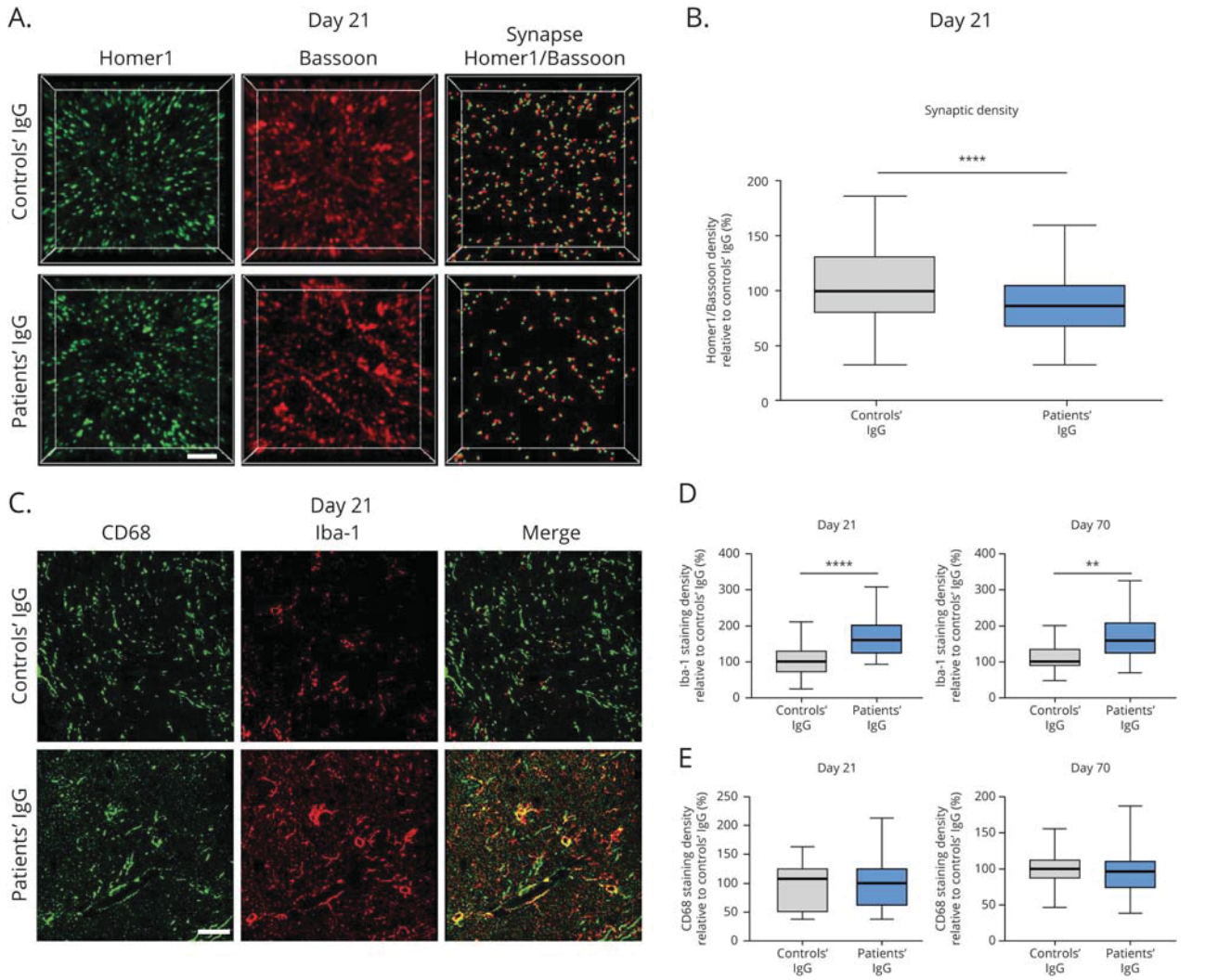

(A) Representative *z*-stacks of brain sections obtained on PD 21 from mice exposed in utero to controls' or patients' IgG immunostained for Homer1 and Bassoon expression. Colocalization of both markers is defined as a glutamatergic synapse. Scale bar = 2 μm. (B) Quantification of synaptic density (Homer1/Bassoon colocalization) in brains obtained on PD 21 from animals exposed in utero to controls' IgG or patients' IgG. Median density of Homer1/Bassoon synapses in mice exposed in utero to controls' IgG was defined as 100%. Controls' IgG, n = 11; patients' IgG, n = 14. (C) Representative CD68 (macrophage specific) and Iba-1 (activated microglia specific) immunostainings in brains obtained on PD 21 from mice exposed in utero to controls' or patients' IgG. Scale bar = 20 μm. (D and E) Quantification of Iba-1 (D) and CD68 (E) immunostaining in brains obtained at PD 21 and PD 70 from mice exposed to controls' IgG or patients' IgG. Median surface density of immunostaining in mice exposed in utero to controls' IgG was defined as 100%. Controls' IgG, PD 21, n = 11; PD 70, n = 9; patients' IgG, PD 21, n = 14; PD 70, n = 10. Data presented in box plots show the median, 25th, and 75th percentiles; whiskers indicate the minimum and maximum. Significance of treatment effect was assessed by the Mann-Whitney *U* test. $^{**}p < 0.01$, $^{****}p < 0.0001$. IgG = immunoglobulin G; PD = postnatal day.

those exposed to controls' IgG in any of the following tests: tail suspension (figure 5L), rotarod, locomotor activity, NOL, PPI, nest building, and social interaction (not shown).

Discussion

We show that antibodies from patients with anti-NMDAR encephalitis infused to pregnant mice reached the fetal brain, caused multiple alterations ranging from NMDAR synaptic changes to delayed neurodevelopment and behavioral deficits in the offspring, and that all these alterations progressively resolved after birth (summary in table e-1, links.lww.com/NXI/A341). As expected from previous experience with adult mice in which patients' IgG was infused in the cerebroventricular system,[11,19] we observed a robust antibody-mediated decrease in NMDAR clusters in the brain of the fetuses. These effects occurred quickly (noted 2 days after injecting the antibodies to the mothers), and the observed reduction of NMDAR clusters and impairment of memory and hippocampal long-term plasticity were detectable during the first postnatal month.

In addition, hippocampal and cortical neurons from mice exposed in utero to patients' IgG showed an increase in dendritic arborization accompanied by a reduction of mature

Figure 4 Intrauterine exposure to patients' IgG causes a transient increase in dendritic complexity and decrease in spine density

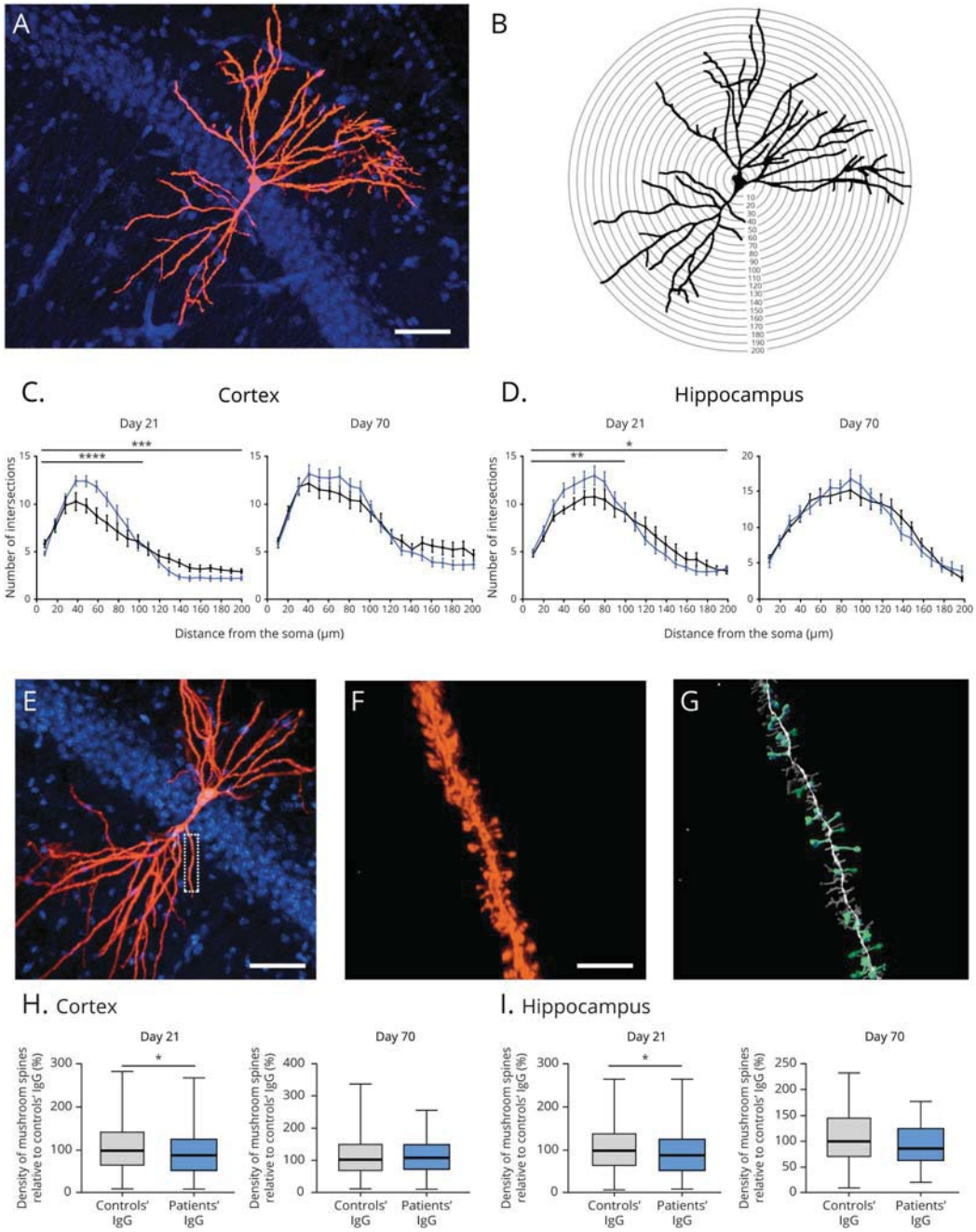

(A and B) Representative confocal image (A) and Sholl analysis (B) of a DiI-stained CA1 hippocampal pyramidal neuron showing in B the 10-µm spaced concentric rings used for quantification of dendritic complexity. Scale bar in A = 50 µm. (C and D) Number of dendrite intersections according to the indicated distance to the neuronal soma in cortical and hippocampal neurons examined at PD 21 and PD 70 of mice exposed in utero to controls' (Black) or patients' (blue) IgG. Number of mice exposed in utero to controls' IgG, PD 21, n = 6; PD 70, n = 4; number of mice exposed in utero to patients' IgG, PD 21, n = 6; PD 70, n = 4. Per each animal, condition, and brain region, 4 neurons were examined. Data presented as mean ± SEM. Significance of treatment effect was assessed by a generalized lineal model. *p < 0.05, **p < 0.01, ***p < 0.001, ****p < 0.0001. (E–G) Representative images by confocal microscopy of a DiI-stained CA1 hippocampal pyramidal neuron (E) and a secondary apical dendrite (F), with morphologically classified dendritic spines (G, mushroom-shaped spines in green); Scale bar in E = 50 µm; scale bar in F = 5 µm. (H and I) Quantification of mushroom dendritic spine density in cortical and hippocampal neurons examined at PD 21 and PD 70 in mice exposed in utero to controls' or patients' IgG. The median density of mushroom spines (number of spines/µm) in mice exposed to controls' IgG was defined as 100%. Total number of dendrites examined/total number of mice exposed to controls' IgG: PD 21, cortex n = 122/6, hippocampus n = 120/6; PD 70, cortex n = 81/4, and hippocampus n = 81/4. Total dendrites/mice exposed to patients' IgG: PD 21, cortex n = 141/6, hippocampus n = 148/6; PD 70, cortex n = 70/4, and hippocampus n = 72/4. Data presented in box plots show the median, 25th, and 75th percentiles; whiskers indicate minimum and maximum. Significance of treatment effect was assessed by the Mann-Whitney U test in H and I. *p < 0.05. IgG = immunoglobulin G; PD = postnatal day.

Figure 5 Intrauterine exposure to patients' IgG causes transient developmental delay and behavioral alterations in offspring

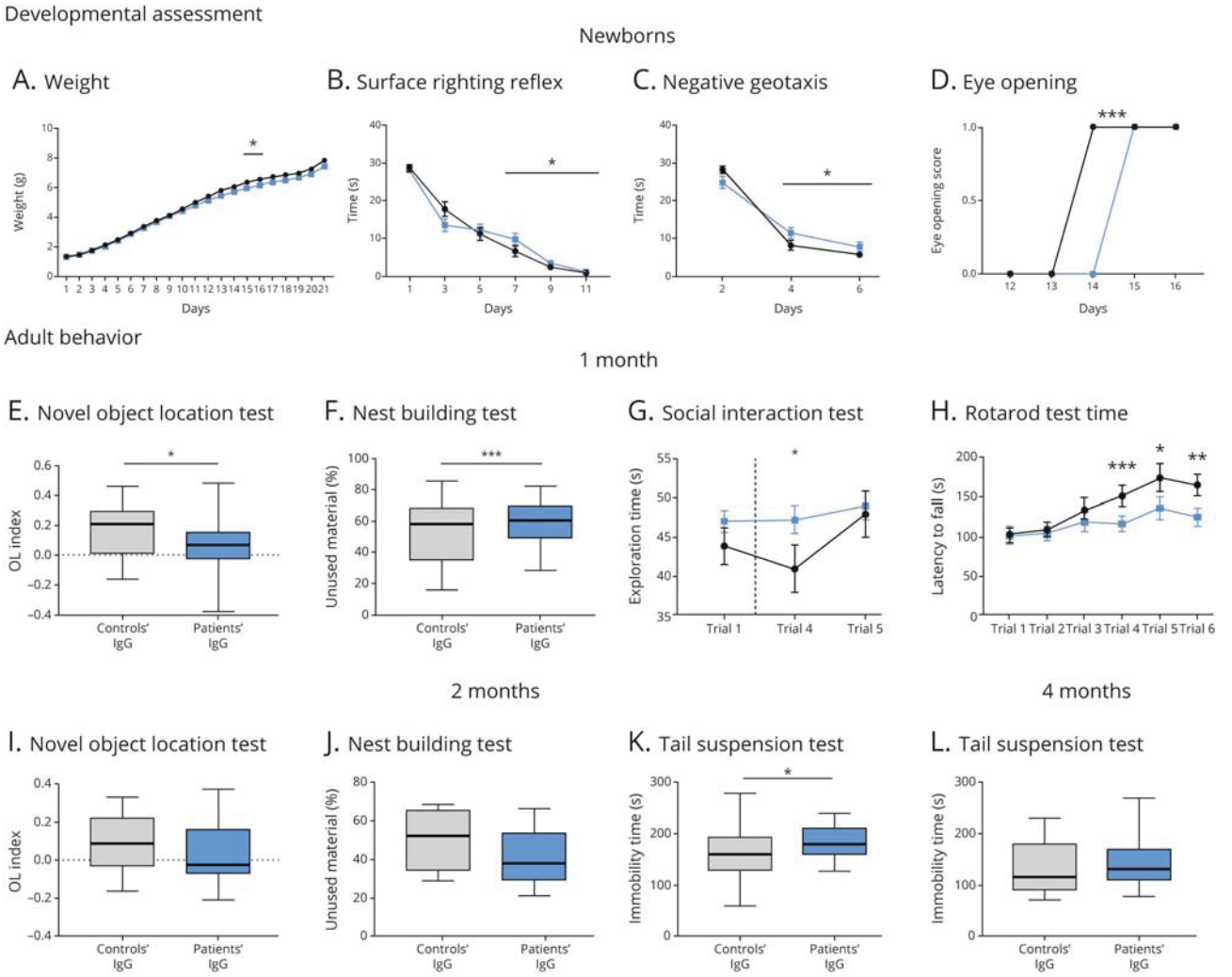

(A–D) Developmental milestone assessment (from birth to PD 21) in mice that were exposed in utero to controls' (Black) or patients' (blue) IgG including (A) body weight, (B) time needed for body righting using the surface righting reflex test (PD 1, 3, 5, 7, 9, and 11), (C) time needed for 180° turning to head up position using the negative geotaxis reflex (PD 2, 4, and 6), and (D) scored eye opening (PD 12–16). Number of mice exposed in utero to controls' IgG = 36; number of mice exposed to patients' IgG = 40. Data from A–C are represented as estimated mean ± SEM inferred by the GEE models described in Methods and in D are represented as median. Significance of treatment effect was assessed by a GEE adjusted model (A–C) and Mann-Whitney *U* test (D). **p* < 0.05, ****p* < 0.001. (E–L) Battery of behavioral tests performed at the indicated time points including novel object location index (E, 1 month; I, 2 months), nest building test (F, 1 month; J, 2 months), social interaction test (G, 1 month), rotarod test (H, 1 month), and tail suspension test (K, 2 months; L, 4 months). For E–I and K, number of mice exposed to controls' IgG = 18 and mice exposed to patients' IgG = 18. For J and L, number of mice exposed to controls' IgG = 8 and mice exposed to patients' IgG = 9. Data from panels E, F, and I–L are represented as box plots with median, 25th, and 75th percentiles; whiskers indicate minimum and maximum values; data from G and H are represented as mean ± SEM. For all behavioral tests, significance of treatment effect was assessed by GEE. **p* < 0.05, ***p* < 0.01, ****p* < 0.001. GEE = generalized estimated equation; IgG = immunoglobulin G; PD = postnatal day.

(mushroom-shaped) dendritic spines and synaptic density. These alterations have not been reported in previous models of immunodepletion of NMDAR and likely contributed to the impairment of hippocampal LTP. The effect of NMDAR hypofunction on dendritic arborization and the morphology of the spines are not well understood. In a cortex-specific GluN1 knockout model, the cortical neurons in layer IV elaborated exuberant dendritic specializations[24]; however, in a study using MK801 (an NMDAR antagonist) during early postnatal development, there was a transient decrease in dendritic arborization in hippocampal pyramidal neurons that reversed when MK801 was discontinued.[25] Our findings resemble those of the cortex-specific GluN1 knockout, although in our immune model, the alterations were reversible.

We believe that the increased dendritic arborization observed in animals exposed in utero to patients' IgG was likely caused by the reduction of NMDAR levels along with microglial activation. Any perinatal immune challenge such as the binding of antibodies to NMDAR in the fetal brain can result in microglial activation[26] and consequently affect microglia-mediated synaptic pruning. This normal microglial function is also triggered by neural activity in the developing brain.[27,28] For example, impaired microglia-neuron interactions in

CX3CR1-deficient mice showed delayed synaptic functional maturation[29] and immature and redundant connectivity, the latter attributed to reduced synaptic pruning.[30] These alterations spontaneously reverted by PD 30–40,[29,30] similar to our findings.

In our model, the brain of fetuses and offspring exposed in utero to patients' IgG had a reduction in the thickness of the cortical plate and cortical layers II–IV. In mice, glutamate serves as a chemoattractant for neurons in the developing cortex, signaling cells to migrate into the cortical plate through receptor activation.[14] Studies with NMDAR antagonists (MK801 or APV) have shown that they block neuronal cell migration from the ventricular zone into the cortical plate, delaying neuronal migration to the upper cortical layers (II–III).[14,31] In our immune-mediated model, the transient decrease in thickness of cortical layers II–IV was associated with an increase in cell density in the upper cortical layers that likely contributed to the restoration of the cortical layer thickness after PD 21. These findings are somewhat similar to those obtained in models of genetic disruption of other proteins and receptors where the decrease in cortical thickness is reversible and associates with an increase in cell density in the upper cortical layers.[32,33] For example, loss of MeCP2 in the Rett syndrome model results in a reduction in thickness of somatosensory cortical layers II–III and VI, with a total rescue of thickness after treatment with mirtazapine during PD 28–42.[33] In another model based on a constitutive reduction in central serotonin ($VMAT2^{sert\text{-}cre}$ mice), the total cortical thickness reduction at PD 7 spontaneously recovered by PD 14.[32] Like this model, our anti-NMDAR model associates with a temporary delay in the development of the upper cortical layers along with increased compaction of these layers.

Preceding the indicated memory deficit, the newborn pups exposed in utero to patients' IgG showed impaired innate reflexes and developmental delay. Similar impairment of native reflexes and developmental delay have been reported in GluN1 gene-manipulated mice,[34] and newborn rats treated with a competitive NMDAR antagonist.[35]

A previous model of transplacental transfer of a human-derived NMDAR monoclonal antibody showed high neonatal mortality (27%), impairment of native reflexes, and long-lasting neuropathologic alterations without evidence of reversibility.[12] In contrast, we did not observe increased neonatal mortality, and the symptoms and developmental alterations spontaneously improved. Moreover, although the monoclonal antibody model did not assess dendritic arborization, spine density, cortical development, and number of cell surface and synaptic NMDAR clusters, we found that patients' IgG antibodies robustly altered all these paradigms, along with a dramatic decrease in NMDAR clusters and hippocampal LTP. Thus, the reversibility of these alterations and associated symptoms cannot be attributed to a milder phenotype. The reasons for the discrepancies between our model, in which serum NMDAR-abs representative of several patients were used, and the model in which a human monoclonal NMDAR-ab was used are unclear. It is likely that the monoclonal antibody model, lacking the repertoire NMDAR-abs of patients, is less representative of the disease. Nevertheless, the outcome of newborns from pregnant patients with anti-NMDAR encephalitis[6] is remarkably different from that obtained with the mouse monoclonal antibody model.[12]

Our study does not allow generalization of the notion that anti-NMDAR encephalitis during pregnancy does not represent a risk for serious effects in the offspring. For example, our model does not associate with encephalitis of the mothers, which in our experience[6] is the most important risk factor for obstetric complications and potential brain damage of the newborns. However, the low frequency of antibody-mediated complications in newborns of patients with anti-NMDAR encephalitis is puzzling and may also be related to the timings of IgG placental transfer and BBB restriction properties for IgG crossing into the brain. In humans, placental transfer of maternal antibodies starts at 12–13 weeks of pregnancy[36–38] that is approximately the same time the BBB of the fetus starts to become more restrictive to the passage of albumin (and likely Igs) to the brain.[39] It is unknown whether this time window and the efficiency of the fetal BBB are affected by the presence of maternal encephalitis or systemic inflammation. Future studies with pregnant patients who develop anti-NMDAR encephalitis and close follow-up of the babies are needed to determine the frequency of deficits (if present, mostly overlooked until now) and the timing of improvement. Keeping these limitations in mind, the current model suggests that reversibility of some of the antibody-mediated alterations can potentially occur. Moreover, the model can be manipulated to assess the effects of systemic inflammation and provides also the possibility to determine whether inhibitors of FcRn have potential utility in preventing the potential neonatal abnormalities reported here.

Acknowledgment

The authors thank Dr. Myrna R. Rosenfeld (IDIBAPS, University of Barcelona) for critical review of the manuscript and useful suggestions and Mercedes Alba, Eva Caballero, and Araceli Mellado (IDIBAPS, Hospital Clínic, University of Barcelona) for their technical support.

Study funding

This study was funded by Plan Nacional de I+D+I and cofinanced by the Instituto de Salud Carlos III (ISCIII)—Subdirección General de Evaluación y Fomento de la Investigación Sanitaria and the Fondo Europeo de Desarrollo Regional (ISCIII-FEDER; 17/00234); Project Integrative of Excellence (PIE 16/00014); Centro de Investigación Biomédica en Red de Enfermedades Raras (CIBERER; #CB15/00010); "La Caixa" Foundation (ID 100010434, under the agreement LCF/PR/HR17/52150001); The Safra Foundation (J.D.), and Fundació CELLEX (J.D.); Centres de Recerca de Catalunya (CERCA) program by La Generalitat

de Catalunya (J.R.); Pla Estratègic de Recerca i Innovació en Salut (PERIS, SLT002/16/00346, J.P.); Ministerio de Economia y Competitividad (RTI2018-094374-B-I00, S.G.); Basque Government Doctoral Fellowship Program (PRE_2019_1_0255; E.M.); and Agència de Gestió d'Ajuts Universitaris i de Recerca (FI-AGAUR) grant program by La Generalitat de Catalunya (2018FI_B_00487 A.P.; 2019FI_B1 00212, A.G.-S.).

Disclosure

A. García-Serra, M. Radosevic, A. Pupak, V. Brito, J. Ríos, E. Aguilar, E. Maudes, H. Ariño, M. Spatola, F. Mannara, M. Pedreño, B. Joubert, S. Ginés, and J. Planagumà report no disclosures. J. Dalmau receives royalties from Athena Diagnostics for the use of Ma2 as an autoantibody test and from Euroimmun for the use of NMDA, GABAB receptor, GABAA receptor, DPPX and IgLON5 as autoantibody tests. Go to Neurology.org/NN for full disclosures.

Publication history

Received by *Neurology: Neuroimmunology & Neuroinflammation* July 13, 2020. Accepted in final form August 26, 2020.

Appendix Authors

Name	Location	Contribution
Anna García-Serra, MSc	IDIBAPS, Hospital Clínic, Universitat de Barcelona, Spain	Major role in the acquisition of data; analyzed the data; and drafted the manuscript for intellectual content
Marija Radosevic, PhD	IDIBAPS, Hospital Clínic, Universitat de Barcelona, Spain	Major role in the acquisition of data; analyzed the data; and revised the manuscript for intellectual content
Anika Pupak, MSc	IDIBAPS, Hospital Clínic, and Institut de Neurociències, Universitat de Barcelona; and CIBERNED, Madrid, Spain	Major role in the acquisition of data and revised the manuscript for intellectual content
Veronica Brito, PhD	IDIBAPS, Hospital Clínic, and Institut de Neurociències, Universitat de Barcelona; and CIBERNED, Madrid, Spain	Major role in the acquisition of data and revised the manuscript for intellectual content
José Ríos, MSc	Medical Statistics Core Facility, IDIBAPS and Hospital Clínic, Barcelona; and Biostatistics Unit, Faculty of Medicine, Universitat Autònoma de Barcelona, Spain	Analyzed the data and revised the manuscript for intellectual content
Esther Aguilar, BS	IDIBAPS, Hospital Clínic, Universitat de Barcelona, Spain	Major role in the acquisition of data and revised the manuscript for intellectual content
Estibaliz Maudes, MSc	IDIBAPS, Hospital Clínic, Universitat de Barcelona, Spain	Major role in the acquisition of data and revised the manuscript for intellectual content
Helena Ariño, MD, PhD	IDIBAPS, Hospital Clínic, Universitat de Barcelona, Spain	Performed IV administrations and revised the manuscript for intellectual content
Marianna Spatola, MD, PhD	IDIBAPS, Hospital Clínic, Universitat de Barcelona, Spain	Performed immunoprecipitation technique and revised the manuscript for intellectual content
Francesco Mannara, PhD	IDIBAPS, Hospital Clínic, Universitat de Barcelona, Spain	Revised the manuscript for intellectual content
Marta Pedreño, PhD	IDIBAPS, Hospital Clínic, Universitat de Barcelona, Spain	Revised the manuscript for intellectual content
Bastien Joubert, MD, PhD	IDIBAPS, Hospital Clínic, Universitat de Barcelona, Spain	Revised the manuscript for intellectual content
Silvia Ginés, PhD	IDIBAPS, Hospital Clínic, and Institut de Neurociències, Universitat de Barcelona; and CIBERNED, Madrid, Spain	Revised the manuscript for intellectual content
Jesús Planagumà, PhD	IDIBAPS, Hospital Clínic, Universitat de Barcelona, Spain	Major role in the acquisition of data; designed and conceptualized the study; and revised the manuscript for intellectual content
Josep Dalmau, MD, PhD	IDIBAPS, Hospital Clínic, Universitat de Barcelona, ICREA; CIBERER, Madrid, Spain; and University of Pennsylvania, Philadelphia	Designed and conceptualized the study and drafted the manuscript for intellectual content

References

1. Dalmau J, Gleichman AJ, Hughes EG, et al. Anti-NMDA-receptor encephalitis: case series and analysis of the effects of antibodies. Lancet Neurol 2008;7:1091–1098.
2. Titulaer MJ, McCracken L, Gabilondo I, et al. Treatment and prognostic factors for long-term outcome in patients with anti-NMDA receptor encephalitis: an observational cohort study. Lancet Neurol 2013;12:157–165.
3. Irani SR, Bera K, Waters P, et al. N-methyl-D-aspartate antibody encephalitis: temporal progression of clinical and paraclinical observations in a predominantly non-paraneoplastic disorder of both sexes. Brain 2010;133:1655–1667.
4. Viaccoz A, Desestret V, Ducray F, et al. Clinical specificities of adult male patients with NMDA receptor antibodies encephalitis. Neurology 2014;82:556–563.
5. Kumar MA, Jain A, Dechant VE, et al. Anti-N-methyl-D-aspartate receptor encephalitis during pregnancy. Arch Neurol 2010;67:884–887.
6. Joubert B, Garcia-Serra A, Planaguma J, et al. Pregnancy outcomes in anti-NMDA receptor encephalitis: case series. Neurol Neuroimmunol Neuroinflamm 2020;7:e668.
7. Xiao X, Gui S, Bai P, et al. Anti-NMDA-receptor encephalitis during pregnancy: a case report and literature review. J Obstet Gynaecol Res 2017;43:768–774.
8. Hughes EG, Peng X, Gleichman AJ, et al. Cellular and synaptic mechanisms of anti-NMDA receptor encephalitis. J Neurosci 2010;30:5866–5875.
9. Mikasova L, De Rossi P, Bouchet D, et al. Disrupted surface cross-talk between NMDA and Ephrin-B2 receptors in anti-NMDA encephalitis. Brain 2012;135:1606–1621.
10. Moscato EH, Peng X, Jain A, Parsons TD, Dalmau J, Balice-Gordon RJ. Acute mechanisms underlying antibody effects in anti-N-methyl-D-aspartate receptor encephalitis. Ann Neurol 2014;76:108–119.
11. Planaguma J, Leypoldt F, Mannara F, et al. Human N-methyl D-aspartate receptor antibodies alter memory and behaviour in mice. Brain 2015;138:94–109.
12. Jurek B, Chayka M, Kreye J, et al. Human gestational N-methyl-d-aspartate receptor autoantibodies impair neonatal murine brain function. Ann Neurol 2019;86:656–670.
13. Hirasawa T, Wada H, Kohsaka S, Uchino S. Inhibition of NMDA receptors induces delayed neuronal maturation and sustained proliferation of progenitor cells during neocortical development. J Neurosci Res 2003;74:676–687.

14. Behar TN, Scott CA, Greene CL, et al. Glutamate acting at NMDA receptors stimulates embryonic cortical neuronal migration. J Neurosci 1999;19:4449–4461.
15. Tolias KF, Bikoff JB, Burette A, et al. The Rac1-GEF Tiam1 couples the NMDA receptor to the activity-dependent development of dendritic arbors and spines. Neuron 2005;45:525–538.
16. Jagota P, Vincent A, Bhidayasiri R. Transplacental transfer of NMDA receptor antibodies in an infant with cortical dysplasia. Neurology 2014;82:1662–1663.
17. Hilderink M, Titulaer MJ, Schreurs MW, Keizer K, Bunt JE. Transient anti-NMDAR encephalitis in a newborn infant due to transplacental transmission. Neurol Neuroimmunol Neuroinflamm 2015;2:e126.
18. Planaguma J, Haselmann H, Mannara F, et al. Ephrin-B2 prevents N-methyl-D-aspartate receptor antibody effects on memory and neuroplasticity. Ann Neurol 2016;80:388–400.
19. Mannara F, Radosevic M, Planaguma J, et al. Allosteric modulation of NMDA receptors prevents the antibody effects of patients with anti-NMDAR encephalitis. Brain 2020;143:2709–2720.
20. Braniste V, Al-Asmakh M, Kowal C, et al. The gut microbiota influences blood-brain barrier permeability in mice. Sci Transl Med 2014;6:263ra158.
21. Ferreira TA, Blackman AV, Oyrer J, et al. Neuronal morphometry directly from bitmap images. Nat Methods 2014;11:982–984.
22. Hill JM, Lim MA, Stone MM. Developmental milestones in the newborn mouse. In: Gozes I, ed. Neuromethods. Totowa: Humana Press; 2008:131–149.
23. Weber EM, Algers B, Wurbel H, Hultgren J, Olsson IA. Influence of strain and parity on the risk of litter loss in laboratory mice. Reprod Domest Anim 2013;48:292–296.
24. Datwani A, Iwasato T, Itohara S, Erzurumlu RS. NMDA receptor-dependent pattern transfer from afferents to postsynaptic cells and dendritic differentiation in the barrel cortex. Mol Cell Neurosci 2002;21:477–492.
25. Elhardt M, Martinez L, Tejada-Simon MV. Neurochemical, behavioral and architectural changes after chronic inactivation of NMDA receptors in mice. Neurosci Lett 2010;468:166–171.
26. Paolicelli RC, Ferretti MT. Function and dysfunction of microglia during brain development: consequences for synapses and neural circuits. Front Synaptic Neurosci 2017;9:9.
27. Schafer DP, Lehrman EK, Kautzman AG, et al. Microglia sculpt postnatal neural circuits in an activity and complement-dependent manner. Neuron 2012;74:691–705.
28. Zuo Y, Yang G, Kwon E, Gan WB. Long-term sensory deprivation prevents dendritic spine loss in primary somatosensory cortex. Nature 2005;436:261–265.
29. Hoshiko M, Arnoux I, Avignone E, Yamamoto N, Audinat E. Deficiency of the microglial receptor CX3CR1 impairs postnatal functional development of thalamocortical synapses in the barrel cortex. J Neurosci 2012;32:15106–15111.
30. Paolicelli RC, Bolasco G, Pagani F, et al. Synaptic pruning by microglia is necessary for normal brain development. Science 2011;333:1456–1458.
31. Reiprich P, Kilb W, Luhmann HJ. Neonatal NMDA receptor blockade disturbs neuronal migration in rat somatosensory cortex in vivo. Cereb Cortex 2005;15:349–358.
32. Narboux-Neme N, Angenard G, Mosienko V, et al. Postnatal growth defects in mice with constitutive depletion of central serotonin. ACS Chem Neurosci 2013;4:171–181.
33. Bittolo T, Raminelli CA, Deiana C, et al. Pharmacological treatment with mirtazapine rescues cortical atrophy and respiratory deficits in MeCP2 null mice. Sci Rep 2016;6:19796.
34. Single FN, Rozov A, Burnashev N, et al. Dysfunctions in mice by NMDA receptor point mutations NR1(N598Q) and NR1(N598R). J Neurosci 2000;20:2558–2566.
35. Mikulecka A, Mares P. NMDA receptor antagonists impair motor performance in immature rats. Psychopharmacology (Berl) 2002;162:364–372.
36. Malek A, Sager R, Kuhn P, Nicolaides KH, Schneider H. Evolution of maternofetal transport of immunoglobulins during human pregnancy. Am J Reprod Immunol 1996;36:248–255.
37. Simister NE, Story CM, Chen HL, Hunt JS. An IgG-transporting Fc receptor expressed in the syncytiotrophoblast of human placenta. Eur J Immunol 1996;26:1527–1531.
38. Dancis J, Lind J, Oratz M, Smolens J, Vara P. Placental transfer of proteins in human gestation. Am J Obstet Gynecol 1961;82:167–171.
39. Virgintino D, Robertson D, Benagiano V, et al. Immunogold cytochemistry of the blood-brain barrier glucose transporter GLUT1 and endogenous albumin in the developing human brain. Brain Res Dev Brain Res 2000;123:95–101.

Placental transfer of NMDAR antibodies causes reversible alterations in mice

Anna García-Serra, Marija Radosevic, Anika Pupak, et al.

Neurol Neuroimmunol Neuroinflamm 2021;8;
DOI 10.1212/NXI.0000000000000915

SUPPLEMENTAL MATERIAL

1. Animal care
2. Infusion of IgG and assessment of transplacental transfer of antibodies
3. Processing of brain and blood samples
4. Antibody determination in blood from pregnant mice and fetuses
5. Determination of human IgG, NMDAR clusters, and cortical plate thickness in fetal brain tissue
6. Immunoprecipitation of fetal brain tissue
7. Determination of human IgG, levels of NMDAR clusters, synaptic density, cortical layer thickness, and microglial activation in offspring
8. DiOlistic staining and confocal imaging for dendritic complexity (Sholl analysis) and spine morphology analysis
9. Hippocampal long-term potentiation (LTP) and paired-pulse facilitation
10. Neurobehavioral assessment in postnatal and adult stages
11. Novel object location (NOL) test
12. Prepulse inhibition of the acoustic startle response (PPI) test
13. Nest building (NB) test
14. Social interaction test (SIT)
15. Accelerating Rotarod (ARR) test

1. Animal care

Pregnant C57BL/6J mice (9 weeks old, 25-30 g, Charles River) were housed in a specific pathogen-free facility in cages of five until pregnancy day 16 (E16), at which time they were caged alone. The room was maintained at controlled temperature (21 ± 1°C) and humidity (55 ± 10%) with illumination at 12:12 light: dark cycles and *ad libitum* access to food and water. Randomly selected representative offspring from every litter were separated by sex on postnatal day 21, and kept in the same caging conditions as described above until the indicated time points (i.e., postnatal days 21, 70 or 155). Overall, 54 pregnant female mice, 165 fetuses and 187 pups were used for behavioral, electrophysiological, morphological, and synaptic brain studies.

2. Infusion of IgG and assessment of transplacental transfer of antibodies

Pooled IgG (800µg) from patients or controls was injected via tail vein to pregnant mice on days 14, 15 and 16 (E14, E15 and E16) of gestation (figure 1A). These experiments were planned according to the window of time in which the neonatal receptor (FcRn), which allows IgG transplacental transfer is expressed in placental tissue, and the immature fetal blood-brain barrier

(BBB) does not restrict the crossing of IgG (e.g., around gestational day 16 the BBB becomes significantly more restrictive to maternal antibody penetration into the fetal brain).[1]

3. Processing of brain and blood samples

In subsets of mice, blood and brain from fetuses/offspring were collected on days 16, 17 and 18 of gestation, and on postnatal days 21, 70 and 155 (figure 1A). Blood samples from pregnant mice were also collected on the indicated gestational days. Blood samples were centrifuged to obtain serum. Brains were fixed with 4% paraformaldehyde for 1 hour, cryopreserved in 40% glucose for 48 hours, embedded in optimal cutting temperature compound and snapped frozen in isopentane chilled with liquid nitrogen. Representative brains from fetuses were kept fresh frozen for immunoprecipitation studies.

4. Antibody determination in blood from pregnant mice and fetuses

The presence of patients' NMDAR antibodies in serum of pregnant mice and fetuses was confirmed using immunolabeling of live rat hippocampal neurons in culture (serum dilution, 1:5; for 1 hour at 4°C), and also with CBA with fixed HEK293T cells expressing GluN1/2B subunits of the NMDAR (serum dilution 1:10, incubation at 4°C, overnight), as reported.[2] After washing, neurons were fixed with 4% paraformaldehyde and incubated with Alexa Fluor 488 goat anti-human IgG (A11013, diluted 1:500 from Invitrogen, Carlsbad, CA, USA) for 1 hour at 4°C. The same secondary antibody and duration of incubation was used for CBA. Coverslips were mounted and scanned under a Zeiss LSM 710 confocal microscope (Carl Zeiss GmbH, Jena, Germany). Antibody titration was obtained by serial antibody dilution using the indicated CBA.

5. Determination of human IgG, NMDAR clusters, and cortical plate thickness in fetal brain tissue

To determine whether human NMDAR antibodies injected to pregnant mice reached the brain of fetuses, 5 μm-thick fetal brain sections were immunostained for human IgG using Alexa Fluor 488 goat anti-human IgG, as above. Quantification of fluorescence intensity in the brain was done using the public domain Fiji ImageJ software (*http://fiji.sc/Fiji*). Background was subtracted and intensity normalized by area. Median intensity of IgG immunostaining in control animals was defined as 100%.

To determine the effects of patients' antibodies on total cell-surface and synaptic NMDAR clusters and postsynaptic density protein 95 (PSD95), non-permeabilized 5 μm-thick sections were blocked with 1% bovine serum albumin (BSA) for 30 minutes at room temperature (RT), incubated with human CSF containing NMDAR antibodies (used as primary antibody) for 2 hours at RT, washed with PBS, permeabilized with Triton X-100 0.3% for 10 minutes at RT, and incubated with rabbit polyclonal antibody against PSD95 (diluted 1:250, Ab18258, Abcam, Cambridge, UK) overnight at 4°C. Next day, the slides were washed and incubated with the corresponding secondary antibodies (Alexa Fluor 488 goat anti-human IgG, A11013, and Alexa Fluor 594 goat anti-rabbit IgG, A11012; both 1:500, Invitrogen, Carlsbad, CA, USA) for 1 hour at RT, as reported.[3] Slides were then mounted as described above and results scanned under a Zeiss LSM710 confocal microscope. Standardized z-stacks including 50 optical images were acquired from five different areas of the developing hippocampus. Images were then deconvolved using theoretical point spread functions of Huygens Professional 17.04 software (Scientific Volume Imaging, Hilversum, NL). For cluster density analysis a spot detection algorithm from Imaris 8.1 software (Oxford instruments, Belfast, UK) was used. Density of clusters was

expressed as spots/μm^3. Three-dimensional colocalization of clusters (e.g. NMDAR and PSD95) was done using a spot colocalization algorithm implemented in Imaris. Synaptic localization was defined as colocalization of NMDAR with PSD95. Synaptic NMDAR cluster density was expressed as colocalized spots/μm^3, and was normalized to the median cluster density of brains of fetuses exposed to controls' IgG (100%).

The thickness of the cortical plate was measured using DAPI-stained fetal sagittal brain sections, and quantified using Fiji ImageJ software.

6. Immunoprecipitation of fetal brain tissue

In order to confirm that the human antibody detected in fetal brains was specifically bound to NMDAR, homogenates of brain tissue were washed, incubated with protein A/G sepharose beads, precipitated, run in a gel, and blotted with a commercial GluN1 polyclonal rabbit antibody (G8913, 1:200, Sigma-Aldrich, St. Louis, MO, USA).

7. Determination of human IgG, levels of NMDAR clusters, synaptic density, cortical layer thickness, and microglial activation in offspring

The presence of human IgG in the brain of offspring (postnatal days 21 and 70), and density of NMDAR (postnatal days 21, 70, and 155) were determined as indicated above for fetal brains. In this case, NMDAR clusters were quantified from a total of 15 images acquired from CA1, CA3 and dentate gyrus of hippocampus (five different areas per region).

The density of glutamatergic synapses (postnatal days 21 and 70) was assessed with immunohistochemistry using pre- and postsynaptic markers: anti-Bassoon (1:250, SySy 141 003) and anti-Homer1 (1:250, SySy 160 004) for 2 hours at RT, both from (Synaptic Systems,

Goettingen, Germany), followed by incubation with the corresponding secondary antibodies (Alexa Fluor 594 goat anti-rabbit IgG, A11012; and Alexa Fluor 488 goat anti-guinea pig IgG, A11073; both diluted 1:500, Invitrogen) for 1 hour at RT. Acquisition and quantification of synaptic markers density were performed as above.

Cortical layer thickness was measured in sections of brains obtained on postnatal days 21, 70 and 155, and immunostained with specific cortical layer markers including a monoclonal mouse anti-CUTL1 (1:100, ab54583, Abcam) for layers II-IV, and a polyclonal sheep anti-FoxP2 (1:40, AF5647, R&D systems, Minneapolis, MN, USA) for layer VI, overnight at 4°C. Secondary antibodies included Alexa Fluor 488 goat anti-mouse IgG and Alexa Fluor 594 donkey anti-sheep IgG (A11001 and A11016, both 1:500, Invitrogen) for 2 hours at RT. Images were acquired with a Zeiss LSM710 confocal microscope and the layers' thickness was determined as described above for the fetal cortical plate. Cell density in CUTL1-labeled layers was measured on brain sections from postnatal day 21 using DAPI staining with spots algorithm in Imaris software.

Microglial activation was assessed in sections of brain (postnatal days 21, 70 and 155) with a monoclonal rat antibody against CD68 (pan-macrophage marker, 1:800, MCA1957GA, Bio-Rad, Hercules, CA, USA), and a polyclonal rabbit antibody against Iba-1 (activated microglia, 1:1000, 019-19741, Wako Chemicals, Neuss, Germany). Incubations were done overnight at 4°C, followed by incubation with secondary antibodies (Alexa Fluor 488 goat anti-rat IgG, A11006, and Alexa Fluor 594 goat anti-rabbit IgG, A11012, both diluted 1:1000, Invitrogen) for 2 hours at RT. Samples were mounted and scanned as above and the CD68- or Iba-1-stained surface density was quantified using Imaris software.

8. DiOlistic staining and confocal imaging for dendritic complexity (Sholl analysis) and spine morphology analysis

Cortical and hippocampal neurons from fixed brains of animals on postnatal days 21 and 70 were labeled using the Helios Gene Gun System (165-2431, Bio-Rad) as described.[4] Briefly, a suspension containing 3 mg of DiI (Molecular Probes, Eugene, OR, USA) dissolved in 100 μl of methylene chloride (Sigma-Aldrich) and mixed with 50 mg of tungsten particles (1.7 mm diameter; Bio-Rad) was spread on a glass slide and air-dried. The mixture was resuspended in 8 ml distilled water and sonicated. Subsequently, the mixture was drawn into Tefzel tubing (Bio-Rad), and then removed to allow tube drying during 5 minutes under nitrogen gas flow. The tube was then cut into 13-mm pieces to be used as gun cartridges. One hundred eighty μm coronal sections of 1.5% paraformaldehyde-fixed brain samples were shot at 80 psi through a membrane filter of 3 μm pore size and 8×10 pores/cm^2 (Millipore, Burlington, MA, USA) to deliver dye-coated particles in the cortex or the hippocampus. Sections were stored at RT in PBS for 3 hours protected from light and then incubated with DAPI, and mounted in Mowiol to be acquired.

The dendritic complexity was examined with Sholl analysis[5] in cortical and CA1 hippocampal pyramidal neurons imaged using a Zeiss LSM710 confocal microscope. Briefly, images were segmented, and the Imaris-implemented filament tracer algorithm was applied to obtain the dendritic traces. The images were then thresholded to a binary mask and saved as Tiff files. The Sholl intersection profile was obtained by counting the number of dendritic branches at a step distance of 10 μm from the soma using ImageJ software.[5]

The spine morphology analysis was examined in DiI-labeled segments of apical secondary dendrites of cortical and CA1 hippocampal pyramidal neurons. Confocal z-stacks including the entire volume of the dendrite were taken with a digital zoom of 5 and a lateral

resolution of 1024 × 1024 pixels. Images were deconvolved in order to improve contrast and resolution using Huygens Professional software. Quantification of mushroom-shaped dendritic spines was performed with the spine classification algorithm implemented in Imaris software.

9. Hippocampal long-term potentiation (LTP) and paired-pulse facilitation

Subsets of mice on postnatal days 18-23 and 70-80 were deeply anesthetized with isoflurane and decapitated. Brains were removed in ice-cold, high sucrose extracellular artificial cerebrospinal fluid (aCSF1, in mM: 206 sucrose, 1.3 KCl, 1 $CaCl_2$, 10 $MgSO_4$, 26 $NaHCO_3$, 11 glucose, 1.25 NaH_2PO_4; purged with 95% CO_2/5% O_2, pH 7.4), and subdivided into hemispheres. Thick (380 µm) coronal slices of hippocampus were obtained with a vibratome (VT1000S; Leica Microsystems, Wetzlar, Germany) and transferred into an incubation beaker with extracellular aCSF appropriate for neurophysiological recordings (aCSF2, in mM: 119 NaCl, 2.5 KCl, 2.5 $CaCl_2$, 1.25 NaH_2PO_4, 1.5 $MgSO_4$, 25 $NaHCO_3$, 11 glucose, purged with 95% CO_2/5% O_2, pH 7.4). Slices were kept at 32°C for 1 hour and subsequently at RT for at least 1 additional hour. For field potential measurements, single slices were then transferred into a measurement chamber perfused with aCSF2 at 2 ml/minute at 28-30°C (controls' IgG: postnatal days 18-23, number of acute slices n = 6, prepared from brain hemisections of five mice; days 70-80 n = 7 from hemisections of five mice; patients' IgG: postnatal days 18-23 n = 5 prepared from brain hemisections of five mice, days 70-80 n = 10 from hemisections of five mice). A bipolar stimulation electrode (Platinum-Iridium stereotrode, PI2ST30.1A5, Science Products GmbH, Hofheim, Germany) was placed in the Schaffer collateral pathway.[6] Recording electrodes were made with a puller (P-1000, Sutter Instrument Company, Novato, CA, USA) from thick-walled borosilicate glass with a diameter of 1.5 mm (BF150-86-10, Sutter Instrument). The recording

electrode filled with aCSF2 was placed in the dendritic branching of the CA1 region for local field potential measurement (field excitatory postsynaptic potential, fEPSP). A stimulus isolation unit A385 (World Precision Instruments, Sarasota, FL, USA) was used to elicit stimulation currents between 25-700 μA. Before baseline recordings for long-term potentiation (LTP), input-output curves were recorded for each slice at 0.03 Hz. The stimulation current was then adjusted in each recording to evoke fEPSPs at which the slope was at 50-60% of maximally evoked fEPSP slope value. After baseline recording for 30 minutes with 0.03 Hz, LTP was induced by theta-burst stimulation (TBS; 10 theta bursts of four pulses of 100 Hz with an interstimulus interval of 200 ms, repeated seven times with 0.03 Hz). After LTP induction, fEPSPs were recorded for 1 additional hour with 0.03 Hz. Recordings with unstable baseline measurements (variations higher than 20% in baseline fEPSPs) were discarded. Paired-pulse fEPSPs in the test pathway were measured before baseline recordings with an interstimulus interval of 50 ms. All recordings were amplified and stored using amplifier AxonClamp P2 (Molecular Devices, San José, CA, USA). Traces were analyzed using Axon pClamp software (Molecular Devices, version 10.6).

10. Neurobehavioral assessment in postnatal and adult stages

From birth to weaning (breastfeeding withdrawal on postnatal day 21) mice were assessed daily for achievement of developmental milestones using a modified Fox battery, similar to that previously reported.[7] This includes body weight, ear detachment, eye opening, skin color change, fur growth, tactile rooting and auditory startle responses, open field test (locomotion), and innate reflexes (i.e., surface body righting and negative geotaxis). The schedule used for assessment of developmental milestones is shown in figure e-1A.

From weaning to adulthood (155 days) subsets of mice underwent a battery of behavioral tests consisting of locomotor activity (LocAct), novel object location (NOL), prepulse inhibition of acoustic startling reflex (PPI), nest building (NB), social interaction (SIT), accelerating rotarod (ARR), and tail suspension (TST) tests, at 1, 2 and 4 months of age (figure e-1B). Selection and timing of these tasks were based on findings in our previously reported animal model of passive transfer of NMDAR antibodies in adult mice.[3] All experiments were performed during the light phase and by researchers blinded to the animals' experimental conditions. Locomotor activity assessment and tail suspension tests were performed as previously reported.[6] Details on NOL, PPI, nest building, social interaction, and rotarod tasks are provided in the following sections.

11. Novel object location (NOL) test

Animals were habituated to an empty, squared arena with visual cues, and underwent two daily trials of 15 minutes each, for four days. The day of the test, animals were placed into the arena in presence of two equal objects positioned at two opposite corners and they were allowed to explore the objects for 9 minutes (familiarization phase). After a retention time of three hours, animals were reintroduced to the arena, where one of the objects had been moved to a different corner. The animal was allowed to explore the objects for 9 minutes (test phase) and the time of exploration of each object was recorded. A discrimination index (NOL Index) was calculated using the following formula: Time of exploration of the moved object minus time of exploration of the not moved object, divided by total time of exploration of both objects. A higher discrimination index indicates a better memory of the position of both objects. Object exploration is defined as any exploratory behavior triggered by the presence of the object (sniffing, biting, touching) with the orientation of the nose toward the object within a distance of < 2 cm.[8]

12. Prepulse inhibition of the acoustic startle response (PPI) test

The PPI is a classic paradigm to measure alterations in sensorimotor gating, which have been shown to occur in models of psychotic-like behavior.[9] For this study, mice were restrained using a plexiglass cylinder placed within a startle box (Panlab, Barcelona) following a modification of an existing protocol.[10] After 5 minutes of habituation, a series of 10 trials of pulses (8 KHz. 115 dB, 40 miliseconds [ms]) was administered and the startle response (SR) was measured for 1000 ms (intertrial interval 29 seconds) in order to establish the basal response. The animal was subsequently exposed to a total of 40 trials randomly administered and equally divided into 4 different stimuli: pulse alone (8 KHz, 115 dB, 40 ms), prepulse alone (10 KHz, 80 dB, 20 ms), prepulse-pulse, and no stimulus (absence of pulse). Both habituation and test were always performed in presence of background white noise (60 dB) and light. The amount of inhibition of the SR due to the administration of the prepulse prior to the pulse was calculated as:

$$\text{SR inhibition (\%)} = 1 - \left(\frac{\text{average SR following prepulse} - \text{pulse stimulus}}{\text{average SR following pulse alone stimulus}}\right) \text{x}100$$

13. Nest building (NB) test

Nest building test was performed introducing 9 grams of nestlet material (Ancare, Bellmore, NY, USA) overnight in the cage of previously individualized mice. The next day the nest is scored as previously described,[11] and unused nestlet material is weighted.

14. Social interaction test (SIT)

Social memory was evaluated by the five-trial social interaction test, based on an habituation/dishabituation paradigm previously reported.[12] Briefly, after the experimental mouse has been kept alone for one week, a mouse of same sex and similar age (intruder) is introduced in the cage of the experimental mouse for 1 minute, and then removed. The same intruder exposure is performed for 1 minute in 4 different trials separated by 10 minutes' intertrial intervals. In the fifth trial, the intruder is changed for a different mouse for 1 minute. Trials are recorded and the total amount of time the experimental mouse interacts with the other mouse in each 1-minute trial is measured. Development of social memory is indicated by a reduction of exploration time during the interactions with the same animal (trials 1-4) and increase of exploration time during the interaction with a new animal in trial 5.[13]

15. Accelerating Rotarod (ARR) test

Balance and motor coordination were assessed in an accelerating-mode Rotarod (Panlab, Harvard Apparatus) as reported[14] with some modifications. Briefly, mice were previously habituated to the apparatus at a constant speed of 4 rpm for two trials with 1.5 hours of intertrial period in one day. The next day, animals were placed on the Rotarod at accelerating conditions of four to 40 rpm in 300 seconds and two trials per day with 1.5 hours of intertrial period for three consecutive days. Latency to fall was measured. Longer times on the rotarod indicate better balance and motor coordination.[15]

16. Table e-1: Summary of tests obtained on postnatal days 21, 70, and 155

		Day 21	Day 70*	Day 155
NMDAR clusters, dendritic and synaptic changes, and microglial activation	Cortical layers II-IV width	↓	N	-
	Dendritic arborization	↑	N	-
	Mushroom-shaped spine density Homer1/Bassoon colocalization cluster density	↓	N	-
	Total NMDAR cluster density	↓	↓	N
	Synaptic NMDAR cluster density	↓	N	N
	Microglial activation	↑	↑	N
Hippocampal electrophysiology	Synaptic plasticity (LTP)	↓	N	-
Neurodevelopment and behavior	Innate reflexes (Surface righting and negative geotaxis)	Delayed	N	N
	Eye opening	Delayed	N	N
	Spatial memory	Abn	N	N
	Nest building	Abn	N	N
	Social memory	Abn	N	N
	Balance and motor coordination	Abn	Abn	N
	Behavioral despair (Depressive-like behavior)	-	Abn	N

17. Supplemental figure e-1: Developmental milestones assessment and batteries of behavioral tests used in the offspring

Panel **A:** Diagram of the modified Fox battery showing the tests and days of assessment (grey boxes) from birth (day 0) to day 21.

Panel **B**: Schedule of behavioral tests used in offspring. After the habituation (Hab) period, mice underwent locomotor activity assessment (LocAct), novel object location (NOL), prepulse inhibition of acoustic startle response (PPI), nest building (NB), social interaction (SIT), and accelerating rotarod (ARR) tests at one, two and four months of age. Tail suspension test (TST, brown) was performed at two and four months of age, as it is a final point task.

18. Supplemental figure e-2: Intrauterine exposure to patients' IgG transiently impairs hippocampal LTP in the young offspring

Panel **A:** Example traces of individual recordings showing baseline recordings before LTP induction (grey, light blue traces) and after LTP (black, dark blue traces). Slope and peak amplitude of fEPSPs are increased after theta burst stimulation (TBS) in hippocampus of 21 day postnatal mice that were exposed *in utero* to controls' IgG. In contrast, manifestation of LTP is strongly impaired in mice exposed *in utero* to patients' IgG.

Panel **B:** Time course of fEPSP recordings demonstrating robust changes in fEPSP slope in hippocampus of 21 day postnatal mice that were exposed *in utero* to controls' IgG (n = 6 recordings from 5 animals, black dots) and mice exposed *in utero* to patients' IgG (n = 5 recordings from 5 animals, blue dots), which is stable throughout the recording period after TBS (arrow). In animals exposed *in utero* to patients' IgG the induction of synaptic LTP is markedly impaired. Average fEPSP values are presented as mean ± SEM.

Panel **C**: Quantitative analysis of the fEPSP slope in hippocampus of 21 day postnatal mice that were exposed *in utero* to patients' IgG compared to those exposed to controls' IgG. Mean fEPSP slope before TBS was defined as 100% and post-TBS fEPSP slope data was normalized to it for each group. The number of animals is the same as in panel B. The box plots show the median, 25th, and 75th percentiles; whiskers indicate minimum and maximum values. Significance of treatment effect was assessed by independent sample *t*-test. *** $P < 0.001$.

Panels **D**, **E**, and **F** show similar studies as above on slices of hippocampus of mice at postnatal day 70. Note that LTP formation in mice exposed *in utero* to patients' IgG is restored on postnatal day 70. In **E** and **F,** n = 7 recordings from 5 mice exposed *in utero* to controls' IgG (black dots); n = 10 recordings from 5 mice exposed *in utero* to patients' IgG (blue dots)

SUPPLEMENTAL REFERENCES

1. Braniste V, Al-Asmakh M, Kowal C, et al. The gut microbiota influences blood-brain barrier permeability in mice. Sci Transl Med 2014;6:263ra158.

2. Dalmau J, Gleichman AJ, Hughes EG, et al. Anti-NMDA-receptor encephalitis: case series and analysis of the effects of antibodies. Lancet Neurol 2008;7:1091-1098.

3. Planaguma J, Leypoldt F, Mannara F, et al. Human N-methyl D-aspartate receptor antibodies alter memory and behaviour in mice. Brain 2015;138:94-109.

4. Brito V, Giralt A, Enriquez-Barreto L, et al. Neurotrophin receptor p75(NTR) mediates Huntington's disease-associated synaptic and memory dysfunction. J Clin Invest 2014;124:4411-4428.

5. Ferreira TA, Blackman AV, Oyrer J, et al. Neuronal morphometry directly from bitmap images. Nat Methods 2014;11:982-984.

6. Planaguma J, Haselmann H, Mannara F, et al. Ephrin-B2 prevents N-methyl-D-aspartate receptor antibody effects on memory and neuroplasticity. Ann Neurol 2016;80:388-400.

7. Hill JM, Lim MA, Stone MM. Developmental milestones in the newborn mouse. In: Gozes I, ed. Neuromethods. Totowa, NJ: Humana Press, 2008: 131-149.

8. Mannara F, Radosevic M, Planaguma J, et al. Allosteric modulation of NMDA receptors prevents the antibody effects of patients with anti-NMDA recepotr encephalitis. Brain 2020.

9. Jones CA, Watson DJ, Fone KC. Animal models of schizophrenia. Br J Pharmacol 2011;164:1162-1194.

10. Moy SS, Perez A, Koller BH, Duncan GE. Amphetamine-induced disruption of prepulse inhibition in mice with reduced NMDA receptor function. Brain Res 2006;1089:186-194.

11. Gaskill BN, Karas AZ, Garner JP, Pritchett-Corning KR. Nest building as an indicator of health and welfare in laboratory mice. J Vis Exp 2013:51012.

12. Thor DH, Holloway WR. Social memory of the male laboratory rat. J Comp and Physiol Psychol 1982;96:1000-1006.

13. Ferguson JN, Young LJ, Hearn EF, Matzuk MM, Insel TR, Winslow JT. Social amnesia in mice lacking the oxytocin gene. Nat Genet 2000;25:284-288.

14. Puigdellivol M, Cherubini M, Brito V, et al. A role for Kalirin-7 in corticostriatal synaptic dysfunction in Huntington's disease. Hum Mol Genet 2015;24:7265-7285.

15. Jones BJ, Roberts DJ. The quantiative measurement of motor inco-ordination in naive mice using an acelerating rotarod. J Pharm Pharmacol 1968;20:302-304.

Supplemental figure e-1

A

Days 0 – 21	0	1	2	3	4	5	6	7	8	9	10	11	12	13	14	15	16	17	18	19	20	21
Weight																						
Eye opening																						
Ear detachment																						
Surface righting																						
Negative geotaxis																						
Rooting																						
Auditory startle																						
Open field transversal																						

B

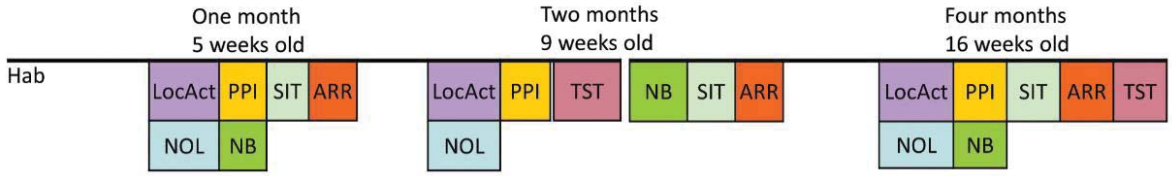

Supplemental figure e-2

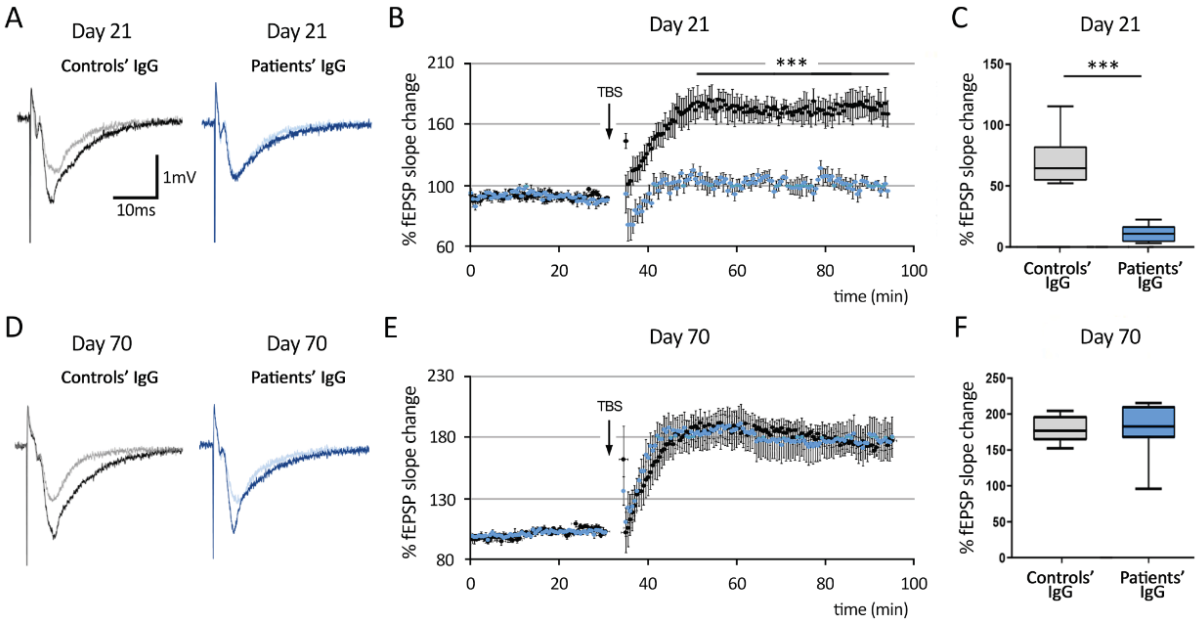

Paper III (in press)

Blocking placental IgG transfer prevents NMDAR antibody effects in newborn mice

Anna García-Serra, Marija Radosevic, José Ríos, Esther Aguilar, Estibaliz Maudes, Jon Landa, Lidia Sabater, Eugenia Martínez-Hernandez, Jesús Planagumà,* and Josep Dalmau*
*These are joint senior authors

Neurol Neuroimmunol Neuroinflamm. 2021

Impact factor JCR 2021 (percentile): The available IF from 2019 is 7.724 (D1)

Blocking placental IgG transfer prevents NMDAR antibody effects in newborn mice

Anna García-Serra, MSc,[1] Marija Radosevic, PhD,[1] José Ríos, MSc,[2,3] Esther Aguilar, BS,[1] Estibaliz Maudes, MSc,[1] Jon Landa, MSc,[1] Lidia Sabater, PhD,[1] Eugenia Martínez-Hernández, MD, PhD,[1] Jesús Planagumà, PhD,[1]* and Josep Dalmau, MD, PhD,[1,4,5]*

From the [1]Institut d'Investigacions Biomèdiques August Pi i Sunyer (IDIBAPS), Hospital Clínic, Universitat de Barcelona, Barcelona, Spain; [2]Medical Statistics Core Facility, IDIBAPS and Hospital Clínic, Barcelona, Spain; [3]Biostatistics Unit, Faculty of Medicine, Universitat Autònoma de Barcelona, Barcelona, Spain; [4]Department of Neurology, University of Pennsylvania, Philadelphia, PA, USA; and [5]Institució Catalana de Recerca i Estudis Avançats (ICREA), Barcelona, Spain

*These authors have equally contributed as senior authors

Running head: FcRn blockade abrogates NMDAR antibody effects

Number of characters in title: 79; in running head: 46

Keywords: animal model; anti-NMDAR encephalitis; pregnancy; IgG transplacental transfer; FcRn blockade.

Number of words in abstract: 236; introduction: 398; discussion: 720; body of the manuscript: 3446. Number of color figures: 5.

Address correspondence to Dr Dalmau, Department of Neurology, IDIBAPS-Hospital Clínic, Universitat de Barcelona, c/ Villarroel 170, 08036 Barcelona, Spain. E-mail: jdalmau@clinic.cat

ABSTRACT

Objective: To determine in a mouse model whether neonatal Fc receptor (FcRn) blockade prevents the placental transfer of IgG derived from patients with anti-*N*-methyl-D-aspartate receptor (NMDAR) encephalitis and their pathogenic effects on the fetuses and offspring.

Methods: Pregnant C57BL/6J mice were administered via tail vein FcRn antibody (FcRn-ab) or saline solution six hours prior to administration of patients' or controls' IgG on days 14, 15 and 16 of gestation. Three experimental groups were established: mice receiving controls' IgG, patients' IgG, or patients' IgG along with pre-treatment with FcRn-ab. Immunohistochemical staining, confocal microscopy, hippocampal long-term potentiation (LTP), and standardized developmental and behavioral tasks were used to assess the efficacy of treatment with FcRn-ab.

Results: In pregnant mice that received patients' IgG, treatment with FcRn-ab prevented the IgG from reaching the fetal brain, abrogating the decrease of NMDAR clusters and the reduction of cortical plate thickness that were observed in fetuses from untreated pregnant mice. Moreover, among the offspring of mothers that received patients' IgG, those whose mothers were treated with FcRn-ab did not develop the alterations that occurred in offspring of untreated mothers, including impairment in hippocampal plasticity, delay in innate reflexes, and visuospatial memory deficits.

Interpretation: FcRn blockade prevents placental transfer of IgG from patients with anti-NMDAR encephalitis and abrogates the synaptic and neurodevelopmental alterations caused by patients' antibodies. This model has potential therapeutic implications for other antibody-mediated diseases of the central nervous system during pregnancy.

Abbreviations: BBB = blood-brain barrier, CSF = cerebrospinal fluid, Fc = fragment, crystallizable of IgG antibodies, FcRn = neonatal Fc receptor of IgG, FcRn-ab = FcRn antibody, IgG = class G immunoglobulin, LTP = long-term potentiation, NMDAR = *N*-methyl-D-aspartate receptor, NOL = novel object location, PD = postnatal day, PSD95 = postsynaptic density protein 95, TBS = theta-burst stimulation.

INTRODUCTION

Anti-NMDA receptor (NMDAR) encephalitis is a neuronal antibody-mediated disease that associates with prominent neuropsychiatric symptoms.[1] Although the incidence of this disorder is unknown (estimated ~1.5 per million persons), it is considered the most frequent neuronal antibody-mediated encephalitis.[2] Most clinical series show that 60-80% of patients are women of childbearing age[3–5] who sometimes develop the encephalitis during pregnancy.[6,7] In these cases, the severity of the maternal encephalitis (seizures, abnormal movements, coma, hypoventilation, or autonomic instability)[6,8] is an important risk factor for obstetric complications and potential brain damage of the fetuses and newborns.[7]

There is the additional concern that patient's NMDAR antibodies can reach the fetal brain and cause synaptic and neurodevelopmental alterations. These antibodies are pathogenic, as demonstrated in several experimental models. For instance, in cultured live neurons patients' antibodies cause a robust reduction of NMDAR clusters along with a decrease of NMDAR-mediated currents;[9–11] and in a mouse model of cerebroventricular transfer of patients' cerebrospinal fluid (CSF) containing NMDAR antibodies, these alterations resulted in severe impairment of long-term plasticity, visuospatial memory deficits, depressive-like and psychotic-like behaviors.[12–14]

Animal studies examining placental transfer of NMDAR antibodies have reported potentially harmful effects in the offspring. Peritoneal injections of a patient-derived monoclonal antibody to pregnant mice caused high neonatal mortality and long-lasting deficits in the offspring.[15] In another animal model, maternofetal transfer of IgG from patients with anti-NMDAR encephalitis resulted in NMDAR synaptic changes, delayed neurodevelopment, and behavioral deficits that progressively resolved after birth.[16] These latest findings resemble the transient symptoms described in some newborns from patients with anti-NMDAR encephalitis.[7,17]

The FcRn receptor is responsible for the transport of IgG through the placenta and for extending serum IgG half-life after birth.[18] Treatment with a monoclonal antibody able to block IgG binding to the FcRn ameliorated the severity of symptoms in experimental animal models of myasthenia gravis.[19] In another study, administration of the same FcRn antibody (FcRn-ab) to immunized pregnant mice prevented pathogenic IgG-induced fetal and neonatal immune thrombocytopenia (FNIT) in the delivered neonates.[20] A similar model using plasma from patients with myasthenia gravis and acetylcholine receptor antibodies prevented antibody-mediated systemic complications in fetuses (arthrogryposis multiplex congenita).[21] Yet it is unknown whether this approach may work with an antibody-mediated disease of the central nervous system. Here, we examined the potential therapeutic use of FcRn blockade in a previously established mouse model of placental transfer of IgG from patients with anti-NMDAR encephalitis.

MATERIALS AND METHODS

Human serum samples, IgG purification, and immunoabsorption

IgG was isolated by ammonium sulfate-precipitation from serum of 7 patients with anti-NMDAR encephalitis and serum of 7 healthy blood donors. All patients with anti-NMDAR encephalitis were women (median age 20 years, range 16-26) with classical anti-NMDAR encephalitis; none of the patients had teratoma, and in all instances serum samples were obtained before treatment. The presence of NMDAR antibodies was determined with rat brain tissue immunohistochemistry and a cell-based assay (CBA) with human embryonic kidney (HEK) 293T cells expressing GluN1 and GluN2B receptor subunits, as reported.[1] The absence of other brain-specific antibodies was established using previously reported experiments[13,22] in which patients' NMDAR antibodies were immunoabsorbed, resulting in abrogation of patients' IgG effects in cultured neurons.[23]

Animals

Pregnant C57BL/6J mice (9 weeks old, 25-30 g, Charles River) were housed in cages of five until pregnancy day 16 (E16), at which time they were caged alone in previously reported room conditions.[16] Representative offspring from every litter were separated by sex on postnatal day 21, and kept in the same caging conditions until the indicated time points (i.e., postnatal days 21, or 43). Overall, 21 pregnant female mice, 22 fetuses and 91 pups were used for behavioral, electrophysiological, morphological, and synaptic brain studies.

Standard Protocol Approvals, Registrations, and Patient Consents

Written informed consent was obtained from all patients; the study was approved by the local institutional review board at Hospital Clínic de Barcelona (registration number HCB/2018/0192). All procedures were approved by the Local Ethical Committee of the University of Barcelona

following European (2010/63/UE) and Spanish (RD 53/2013) regulations about the use and care of experimental animals.

Infusion of human IgG and FcRn-ab to pregnant mice

Pooled IgG (800 µg) from patients or controls was injected via tail vein to pregnant mice on days 14, 15 and 16 (E14, E15 and E16) of gestation (Figure 1), as previously reported.[16] Mouse monoclonal FcRn-ab (3 mg/kg, GTX14550, GeneTex, Irvine, CA) or sterile saline solution was injected via tail vein on the same days of injection E14, E15 and E16, six hours prior to the human IgG administration in order to potentially block FcRn-mediated transplacental transfer of IgG. Three experimental groups were established: pregnant mice injected with controls' IgG, or injected with patients' IgG; or with patients' IgG and treated with FcRn-ab. These experiments were planned according to the window of time in which the FcRn is expressed in placental tissue, and the immature fetal blood-brain barrier (BBB) does not restrict the crossing of IgG (e.g., around gestational day 16 the BBB becomes significantly more restrictive to maternal antibody penetration into the fetal brain) as shown by us and others.[16,24] FcRn-ab administration schedule was based on the findings from a passive transfer rat model of autoimmune myasthenia gravis that used the same monoclonal antibody.[19] The dosage was adapted from the 5 mg/kg intraperitoneally used in the FNIT mouse model[20] to a lower dose of 3 mg/Kg since FcRn-ab administration route was changed to intravenous in order to avoid possible fetal damage.

Processing of brain and blood samples

In subsets of mice, brain and blood from fetuses and blood from pregnant mice were collected on day 17 of gestation (E17, Figure 1). Fetal brains were fixed with 4% paraformaldehyde for 1

hour, and cryopreserved in 40% glucose for 48 hours. Then, brains were embedded in optimal cutting temperature compound and snapped frozen in isopentane chilled with liquid nitrogen. Blood samples were centrifuged to obtain serum.

Antibody determination in blood from pregnant mice

The presence of human NMDAR antibodies in blood from pregnant mice was demonstrated by CBA with fixed HEK293T cells expressing GluN1/2B subunits of the NMDAR, as reported.[1] Briefly, transfected HEK cells were blocked and coincubated with the collected serum sample (1:10) and with a commercial GluN1 monoclonal mouse antibody (MAB363, 1:20.000, Sigma-Aldrich, St. Louis, MO) at 4°C overnight. Then, cells were washed and immunolabelled with Alexa Fluor 488 goat anti-human IgG (A11013) and Alexa Fluor 594 goat anti-mouse IgG (A11005; both diluted 1:1000, from ThermoFisher, Waltham, MA) as secondary antibodies for 1 hour at room temperature (RT). After washing, coverslips were mounted and scanned under a Zeiss LSM 710 confocal microscope (Carl Zeiss GmbH, Jena, Germany).

Determination of human IgG, NMDAR clusters and cortical plate thickness in fetal brains

To determine whether FcRn blockade prevented human NMDAR antibodies injected to pregnant mice from reaching the brain of fetuses, E17 brain tissue sections were blocked with 1% bovine serum albumin for 1 hour at RT and then incubated with the same Alexa Fluor 488 goat anti-human IgG as above diluted at 1:1000 for 2 hours at RT. The fluorescence intensity in the developing hippocampus was quantified using Imaris suite v.8.1 software (Oxford Instruments, Belfast, UK). Mean intensity of IgG immunostaining in control animals was defined as 100%.[16]

To determine whether treatment of pregnant mice with FcRn-ab abrogated the effects of patients' antibodies on the number of clusters of NMDAR and PSD95 in fetuses, non-permeabilized 5 μm-thick brain sections were blocked as above, and serially incubated with a human CSF NMDAR-antibody sample (1:20, used as primary antibody) for 2 hours at RT and the secondary Alexa Fluor 488 goat anti-human IgG (1:1000, A-11013, ThermoFisher) for 1 hour at RT. Tissue sections were then permeabilized with 0.3% Triton X-100 for 10 minutes at RT, and serially incubated with rabbit polyclonal anti-PSD95 (1:250, ab18258 Abcam, Cambridge, UK) overnight at 4°C, and the corresponding secondary Alexa Fluor 594 goat anti-rabbit IgG (1:1000, A-11012, ThermoFisher) for 1 hour at RT. Slides were then mounted with ProLong Gold antifade reagent, containing 6-diamidino-2-phenylindole dihydrochloride (DAPI, P36935; ThermoFisher) and results scanned with Zeiss LSM710 confocal microscope (Carl Zeiss) with EC-Plan NEOFLUAR CS 100×/1.3 NA oil objective. Standardized z-stacks including 25 optical images were acquired from five different areas of the developing hippocampus. Images were then deconvolved using theoretical point spread functions of Huygens Professional 17.04 software (Scientific Volume Imaging, Hilversum, NL). The median density of clusters of NMDAR or PSD95 was obtained using a spot detection algorithm from Imaris 8.1 software (Oxford instruments, Belfast, UK), and the cluster density expressed as spots/μm^3. Three-dimensional colocalization of clusters (e.g. NMDAR and PSD95) was done using a spot colocalization algorithm implemented in Imaris. Synaptic localization was defined as colocalization of NMDAR with PSD95 and expressed as colocalized spots/μm^3. For each experimental group, the median cluster density of total cell-surface and synaptic NMDAR, and PSD95 were normalized to that of brains of fetuses exposed to controls' IgG (100%).

The effects of FcRn-ab treatment on the thickness of the cortical plate were examined in DAPI-stained E17 fetal sagittal brain sections, acquired by confocal microscopy, and quantified using Fiji ImageJ software (*http://fiji.sc/Fiji*) as previously reported.[12,16]

Field potential recordings and analysis of hippocampal long-term potentiation (LTP) and paired-pulse facilitation

Acute sections of hippocampus obtained on postnatal days 19-23 were used to determine long-term plasticity by the classical paradigm of theta-burst stimulation (TBS) at the Schaffer collateral and field potential recording at the CA1 dendritic area. We recently reported this technique applied to the current model of placental transfer of NMDAR antibodies.[16,23]

Neurobehavioral assessment in postnatal and early adult stages

From birth to postnatal day 12 mice were assessed daily for achievement of innate reflexes on alternate days, i.e., surface body righting on postnatal days 1, 3, 5, 7, 9 and 11; and negative geotaxis on postnatal days 2, 4, 6, 8, 10 and 12; from a simplified Fox battery for developmental milestones previously reported.[25]

After breastfeeding withdrawal at postnatal day 21, subsets of mice underwent a battery of behavioral tests consisting of novel object location test (NOL, postnatal day 35), and locomotor activity assessment (LocAct, postnatal day 36) around 1 month of age. Selection and timing of these tasks were based on findings from our previously reported animal model of placental transfer of NMDAR antibodies.[16] All experiments were performed by researchers blinded to animals' experimental conditions, as reported.[13,16]

Statistical analysis

Comparison of human IgG intensity in brain of fetuses among the three experimental groups was performed with one-way ANOVA with Tukey's correction for multiple comparisons. Comparison of confocal densities of NMDAR and PSD95 clusters, and cortical plate thickness among the three experimental groups was analyzed with Welch's ANOVA test and Dunnett T3 corrections for multiple comparisons of small n groups (lower than 50) comparing normally-distributed non-homoscedastic populations. Comparison of fEPSP slope recordings in mice born to mothers from the indicated experimental groups was assessed by Kruskall-Wallis test comparing ranks (as populations were not normally distributed according to D'Agostino-Pearson test) with Dunn's corrections for multiple comparisons. For behavioral paradigms, longitudinal analyses were performed by Generalized Estimated Equations (GEE) using an AR(1) matrix in order to account for intra-individual correlations. All models include litter size, group and interaction group-by-time as fixed factors. Pair-wise comparison in interaction factor was used to analyze differences between group time-by-time, showed as estimated means and their 95% confidence intervals (95%CI). Mean values of fEPSP slope change recordings and of times for developmental reflexes were presented with standard error of the mean (± SEM). All experiments were assessed for outliers with ROUT method applying Q = 1%. In all statistical analyses we used a two-sided type I error of 5%. All tests were done using GraphPad Prism (Version 8, San Diego, CA) or SPSS (Version 25, IBM Corp., Armonk, NY) for GEE models.

Data availability

Data supporting these findings are available upon reasonable request.

RESULTS

Treatment with FcRn-ab prevents placental transfer of human IgG

Serum samples of E17 pregnant mice that received patients' IgG, but not those that received controls' IgG, showed human IgG binding to HEK293T cells expressing NMDARs. These antibodies were detectable in serum of pregnant mice that received patients' IgG regardless of whether they had been treated or not a few hours earlier with FcRn-ab (Figure 2A). In contrast, only serum samples from E17 fetuses whose mothers had received patients' IgG but were not treated with FcRn-ab harbored NMDAR antibodies (Figure 2B). Moreover, on day E17, these fetuses showed a significant increase in human IgG fluorescence in the developing hippocampus compared with fetuses of mothers that received the same patients' IgG but were treated with FcRn-ab ($p<0.0001$) or the fetuses of mothers that received controls' IgG ($p<0.0001$) (Figure 2C-F). These findings show that treatment with FcRn-ab resulted in an effective blockade of placental transfer of human NMDAR antibodies.

FcRn-ab administration to pregnant mice abrogates patients' IgG-mediated reduction of NMDAR clusters and thinning of the cortical plate in fetal brain

Analysis of the density of NMDAR clusters showed that fetuses from mothers that received patients' IgG without pre-treatment with FcRn-ab had a significant decrease of cluster density of total cell-surface and synaptic NMDARs compared to fetuses of mothers that received controls' IgG (72,95% total and 78,63% synaptic clusters vs 100% total and synaptic clusters in controls; both, $p<0.0001$) as expected from this model.[16] This decrease of NMDAR clusters was largely prevented when the mothers were treated with FcRn-ab (fetuses from FcRn-ab treated mothers

94,17% total and 102,4% synaptic NMDAR clusters vs the indicated values of fetuses from non-treated mothers, $p<0.0001$) (Figure 3A-C). Patients' IgG also caused a significant thinning of the fetal cortical plate on E17 (fetuses from mothers that received patients' IgG, 15,54% thinner plate compared with fetuses from mothers that received controls' IgG, 100%; $p=0.0004$). This thinning of the plate was abrogated in fetuses of mothers that received patients' IgG but were pretreated with FcRn-ab (fetuses from FcRn-ab treated mothers 103% vs the indicated value of fetuses from non-treated mothers, $p=0.0002$) (Figure 3D and E).

Treatment of pregnant mice with FcRn-ab prevents the impairment of hippocampal LTP caused by patients' IgG in the young offspring

Assessment of field excitatory postsynaptic potentials (fEPSPs) showed that on postnatal day 21, mice that had been exposed *in utero* to patients' IgG had a significant impairment in hippocampal LTP formation compared with mice exposed *in utero* to controls' IgG ($p<0.0001$). In contrast, mice whose mothers received the same patients' IgG but were treated with FcRn-ab did not show impairment of LTP (FcRn-ab treated vs. non-treated mothers, $p<0.0001$) (Figure 4A-C). Paired-pulsed facilitation was not affected by patients' IgG, as previously reported in this model[16] (data not shown). Overall, these experiments show severe impairment of postsynaptic, but not presynaptic, plasticity in animals exposed *in utero* to patients' IgG and that these antibody effects were abrogated when the mothers were treated with FcRn-ab.

Treatment of pregnant mice with FcRn-ab prevents the developmental delay in innate reflexes caused by patients' IgG in newborns

To determine whether FcRn-ab also prevented neurodevelopmental abnormalities, we assessed the neurodevelopment of newborns whose mothers received during gestation patients' IgG with or without FcRn-ab treatment. Newborn pups exposed *in utero* to patients' IgG, but not to controls' IgG, showed longer times for proper body righting (Figure 5A, postnatal days 5 and 9) and for completing a 180°-turn in the negative geotaxis reflex test (Figure 5B, postnatal days 6, 8 and 10). These neurodevelopmental delayed alterations induced by patients' IgG did not occur in the young offspring of mothers treated with FcRn-ab (Figure 5A and B).

Blockade of placental transfer of patients' IgG prevents behavioral alterations in early adulthood

We then compared the effects of patients' IgG on the behavior of mice whose mothers were treated or not with FcRn-ab. At 1 month of age, mice exposed *in utero* to patients' IgG, but not those exposed to controls' IgG, showed a significant decrease in the NOL index, indicating an impairment in visuospatial memory ($p=0.049$) (Figure 5C). In contrast, mice whose mothers were treated with FcRn-ab did not develop this memory deficit (FcRn-ab treated vs. non-treated mothers, $p=0.019$). No significant difference in motor activity was noted among the different groups, including local (Figure 5D), horizontal and vertical (rearing) activities (data not shown). Overall, these findings confirm those of our previous study[16] and demonstrate that in this animal model the alterations of memory caused by patients' IgG can be prevented by blocking the placental transfer of antibodies with FcRn-ab.

DISCUSSION

We have used a mouse model of placental transfer of IgG from patients with anti-NMDAR encephalitis to show that FcRn-ab administration blocked the materno-fetal IgG transfer and prevented the alterations previously reported in this model, which include, (1) a decrease of the cluster density of total cell-surface and synaptic NMDARs in the fetus, (2) thinning of the cortical plate in the developing brain, (3) delay in neonatal developmental reflexes, (4) impairment of hippocampal LTP in newborns, and (5) deficit in visuospatial memory in the offspring.[16]

The FcRn is an Fc IgG receptor responsible for preventing early lysosomal IgG degradation in vascular endothelial cells, therefore extending the half-life of IgG in serum.[18] FcRn-IgG interactions are pH-dependent: at slightly acidic pH environments (e.g. in early endosomes) IgG undergoes a conformational change that enables its Fc region to bind the FcRn; while at physiological pH in the cell surface FcRn-bound IgG is released back into circulation.[26–28] This FcRn mechanism also mediates placental IgG transcytosis , allowing passive humoral immunization from mother to fetus during pregnancy.[29] Moreover, a similar mechanism of transcytosis applies to other cell barriers such as the intestinal epithelium,[26] or the blood-brain barrier.[30]

FcRn blocking strategies are of special interest for the treatment of autoimmune diseases in which the autoantibodies are pathogenic. For example, in preclinical studies monoclonal FcRn-abs were able to reduce IgG serum half-life and decrease the severity of symptoms in animal models of autoimmune arthritis,[31] myasthenia gravis,[19] and epidermolysis bullosa acquisita.[32]

In pregnant patients with autoantibody-mediated diseases, pathogenic IgG antibodies are also transferred via placental FcRn to fetus. Blockade of FcRn-IgG binding using a monoclonal

FcRn-ab prevented IgG from reaching fetal circulation in an *ex vivo* perfusion model of human placenta.[33] Furthermore, a previous animal model of antibody-mediated fetal and neonatal immune thrombocytopenia showed that treatment of the mothers with a FcRn-ab prevented the pathogenic effects of the antibodies in the pups.[20] Despite the differences in the experimental design and location of the target antigens (periphery vs central nervous system), our data resembles that of the FNIT model, since FcRn blockade with the same FcRn-ab prevented the pathogenic effects of NMDAR antibodies in mice fetuses and newborns.

Our study has limitations; the current model lacks the inflammatory component associated with anti-NMDAR encephalitis which can potentially alter the placental transfer of patients' antibodies or directly affect the developing fetal brain. Thus, future studies should address if FcRn inhibitors such as the FcRn-ab used here, work similarly in presence of systemic inflammation. Moreover, the FcRn expressed in the BBB facilitates IgG efflux from brain to blood.[30,34] Therefore, one can speculate that blocking the FcRn of a well-developed BBB can potentially increase the amount of pathogenic antibodies in the brain; however, in the pregnancy model the pathogenic antibodies have to reach the brain from systemic blood, which in turn it is largely prevented by the mature BBB.

The use of FcRn-abs has already reached clinical trial stage. Rozanolixizumab, a high affinity FcRn IgG4 antibody, and M281, also known as nipocalimab, are currently in phase III (NCT03971422) and phase II trials (NCT03772587) for the treatment of myasthenia gravis.[35,36] Nipocalimab, an IgG1 antibody with a high safety profile[37] is currently used in a phase II study (NCT03842189) in pregnant women at high risk for early onset severe hemolytic disease of the fetus and newborn.[38] However, efficiently blocking placental IgG transfer may lead to a transient hypogammaglobulinemia in the infant. If so, this newborn with reduced maternal protective

antibodies would be more prone to infections until its own immune system restores IgG levels, at around 6 months of age, as reported in pregnancies of patients with genetic primary immunodeficiencies[39] or in those with immunosuppressive treatment during pregnancy (e.g., rituximab).[40] Although no signs of infection were observed in the newborn mice that received FcRn-ab in our model, the possibility of IgG replacement therapy in the infants should be considered.

Overall, our findings and experience from ongoing clinical trials support the potential therapeutic use of FcRn blockade in pregnant patients with anti-NMDAR encephalitis. Similar implications are likely applicable to other antibody-mediated encephalitis. Tasks for the future are to determine the effects of NMDAR antibodies in models of active immunization (which should be accompanied by inflammation), the frequency of synaptic, developmental, and behavioral alterations in the offspring, and whether they can be prevented by FcRn blockade.

ACKNOWLEDGEMENTS

This study was funded by Plan Nacional de I+D+I and cofinanced by the Instituto de Salud Carlos III (ISCIII) – Subdirección General de Evaluación y Fomento de la Investigación Sanitaria and the Fondo Europeo de Desarrollo Regional (FEDER) (FIS PI20/00197, J.D; PI20/00820, J.P); Project Integrative of Excellence (PIE 16/00014) and Juan Rodés grant (JR17/00012, E.M-H); Centro de Investigación Biomédica en Red de Enfermedades Raras (CIBERER; #CB15/00010); "La Caixa" Foundation (ID 100010434, under the agreement LCF/PR/HR17/52150001); The Safra Foundation (J.D), and Fundació CELLEX (J.D); Centres

de Recerca de Catalunya (CERCA) program, Pla Estratègic de Recerca i Innovació en Salut (PERIS, SLT002/16/00346, J.P) and Agència de Gestió d'Ajuts Universitaris i de Recerca (FI-AGAUR) grant program (2020 FI_B2 00208, A.G-S) by La Generalitat de Catalunya (J.R); and Basque Government Doctoral Fellowship Program (PRE_2020_2_0219; E.M).

AUTHOR CONTRIBUTIONS

E.M.-H., J.P., and J.D. were responsible for conception and design of the study. A.G.-S., J.R., E.M., and J.L. were responsible for acquisition and analysis of animal behavior. A.G.-S., E.A., L.S., and J.P. were responsible for acquisition and analysis of immunohistochemistry and confocal microscopy. M.R, and A.G-S. were responsible for acquisition and analysis of electrophysiological studies. A.G.-S. and J.D. were responsible for drafting of the manuscript, and J.P. for the figures. J.P. and J.D. share seniority.

POTENTIAL CONFLICTS OF INTEREST

J.D. receives royalties from Athena Diagnostics for the use of Ma2 as an autoantibody test and from Euroimmun for the use of NMDA, $GABA_B$ receptor, $GABA_A$ receptor, DPPX and IgLON5 as autoantibody tests.

FIGURE LEGENDS

Figure 1. Experimental design

Intravenous injection of FcRn-ab (or saline solution) was performed on gestational days E14, E15, and E16; six hours before the administration of controls' or patients' IgG on these days.

Fetal brain samples were collected on E17 for immunohistochemical studies of NMDAR cluster density and cortical plate thickness. Electrophysiology to determine hippocampal long-term potentiation was performed on postnatal day 21. Newborns were assessed daily for neurodevelopmental milestones of innate reflexes from birth until day 12 on alternate days (surface righting [postnatal days 1, 3, 5, 7, 9 and 11] and negative geotaxis [days 2, 4, 6, 8, 10 and 12]). After breastfeeding withdrawal (day 21), mice underwent a simplified battery of behavioral tests at 1 month of age including novel object location task, and locomotor activity measurement. Gestational period is marked in light gray and postnatal period in dark gray.

Figure 2. Treatment with FcRn-ab blocks the placental transfer of intravenously administered patients' IgG, and their presence in fetal brain

A-B: Representative images of HEK293T cells expressing NMDARs immunolabeled with human IgG contained in serum of pregnant mice injected with controls' IgG or patients' IgG with or without pre-treatment with FcRn-ab (**A**), and from serum of their fetuses (**B**) (all studies done on day E17). Scale bar = 10 μm.

C-E: Representative human IgG immunolabeling in E17 fetal brain sections of animals whose mothers were administered controls' IgG (**C**), patients' IgG (**D**), or patients' IgG along with pre-treatment with FcRn-ab (**E**); the two insets (small squares in developing hippocampus) are shown enlarged on the right of each panel. Scale bar whole brain = 50 μm, insets = 10 μm.

F: Quantification of human IgG immunofluorescence intensity in the developing hippocampus of E17 fetal brains whose mothers were administered controls' IgG, patients' IgG, or patients' IgG along with pre-treatment with FcRn-ab. Controls' IgG, n = 8; patients' IgG, n = 7; patients' IgG treated with FcRn-ab, n = 7. Mean intensity of IgG immunofluorescence in brain of mice

exposed to controls' IgG was defined as 100%. Data presented in box plots show the median, 25th, and 75th percentiles; whiskers indicate minimum and maximum. Significance of treatment effect was assessed by one-way ANOVA and multiple comparisons with Tukey's corrections. **** $P < 0.0001$.

Figure 3. FcRn-ab administration to pregnant mice abrogates patients' IgG-mediated reduction of NMDAR clusters and thinning of the cortical plate in fetal brain

A: Representative three-dimensional projections and analysis of the density of total cell-surface NMDAR clusters (green), PSD95 (red), and synaptic NMDAR clusters (white, defined as those that colocalized with PSD95) in the developing hippocampus area in E17 animals whose mothers received controls' IgG, patients' IgG, or patients' IgG along with pre-treatment with FcRn-ab. Scale bar = 2 μm.

B – C: Quantification of total cell-surface (**B**) and synaptic (**C**) NMDAR cluster density in brains obtained on gestational day E17 from animals whose mothers received controls' IgG, patients' IgG, or patients' IgG along with pre-treatment with FcRn-ab. Median of NMDAR clusters in mice exposed to controls' IgG was defined as 100%. Controls' IgG, n = 7; patients' IgG, n = 7; patients' IgG along with pre-treatment with FcRn-ab, n = 6.

D: Representative cortical plate thickness (stained with DAPI) in E17 brains of fetuses whose mothers received controls' IgG, patients' IgG, or patients' IgG along with pre-treatment with FcRn-ab. Scale bars = 100 μm.

E: Quantification of cortical plate thickness in E17 brains of fetuses whose mothers received controls' IgG, patients' IgG, or patients' IgG along with pre-treatment with FcRn-ab. Controls'

IgG, n = 8; patients' IgG, n = 7; patients' IgG along with pre-treatment with FcRn-ab, n = 7. Mean thickness of cortical plate or the indicated cortical layers in mice exposed *in utero* to controls' IgG was defined as 100%.

Data presented in box plots show the median, 25th, and 75th percentiles; whiskers indicate minimum and maximum. Significance of treatment effect was assessed by Welch's ANOVA test and Dunnett T3 corrections for multiple comparisons. *** $P < 0.001$, **** $P < 0.0001$.

Figure 4. Treatment of pregnant mice with FcRn-ab prevents the impairment of hippocampal LTP caused by patients' IgG in young offspring

A: Example traces of individual recordings showing baseline recordings before LTP induction (grey, light blue, pink traces) and after LTP (black, dark blue, red traces). Slope and peak amplitude of fEPSPs are increased after theta-burst stimulation (TBS) in hippocampus of postnatal day 21 mice whose mothers received controls' IgG. In contrast, manifestation of LTP is strongly impaired in mice whose mothers received patients' IgG, and therefore were exposed *in utero* to patients' IgG. Note that in mice whose mothers received the same patients' IgG but were treated with FcRn-ab, the slope and peak amplitude of fEPSPs are similar to those of controls.

B: Time course of fEPSP recordings demonstrating a robust increase in fEPSP slope in hippocampus of postnatal day 21 mice whose mothers received controls' IgG (n = 6 recordings from 5 animals, grey dots) or patients' IgG along with pre-treatment with FcRn-ab (n = 5 recordings from 5 animals, pink dots), compared with that of mice whose mothers received patients' IgG but were not treated with FcRn-ab (n = 5 recordings from 5 animals, blue dots); the indicated changes were stable throughout the recording period after TBS (arrow). In animals

exposed *in utero* to patients' IgG the induction of LTP is markedly impaired. Average fEPSP values are presented as mean ± SEM.

C: Quantitative analysis of the fEPSP slope in hippocampus of 21 day postnatal mice whose mothers received controls' IgG, patients' IgG, or patients' IgG along with pre-treatment with FcRn-ab. Mean fEPSP slope before TBS was defined as 100% and post-TBS fEPSP slope data was normalized to it for each group. The number of animals is the same as in panel B. The box plots show the median, 25th, and 75th percentiles; whiskers indicate minimum and maximum values. Significance of treatment effect was assessed by Kruskall-Wallis test with Dunn's corrections for multiple comparisons. **** $P < 0.0001$.

Figure 5. Treatment of pregnant mice with FcRn-ab prevents developmental delay in innate reflexes and behavioral alterations caused by patients' IgG in offspring

A-B: Developmental milestones assessment (from birth to day 12) of innate reflexes in mice whose mothers were administered controls' IgG (black), patients' IgG (blue), or patients' IgG along with pre-treatment with FcRn-ab (red). (**A**) Time needed for body righting using the surface righting reflex test (days 1, 3, 5, 7, 9 and 11), and (**B**) time needed for 180° turning to "head up" position using the negative geotaxis reflex (days 2, 4, 6, 8, 10 and 12). Number of mice whose mothers received controls' IgG = 30; number of mice whose mothers received patients' IgG = 25, number of mice whose mothers received patients' IgG and were treated with FcRn-ab = 35. Data are represented as mean ± SEM. Significance of treatment effect was assessed with estimated means and (95%CI) by a GEE adjusted model. Controls' IgG vs. patients' IgG: ** $P < 0.01$, *** $P < 0.001$. Patients' IgG vs. patients' IgG along with pre-treatment with FcRn-ab: ## $P < 0.01$, ### $P < 0.001$.

C-D: Behavioral tests performed at one month of age including novel object location index (**C**) and number of local activity events from the locomotor activity assessment (**D**). Number of mice whose mothers received controls' IgG = 25; mice whose mothers received patients' IgG = 17, and mice whose mothers received patients' IgG along with pre-treatment with FcRn-ab = 31. Data are represented as box plots with median, 25th, and 75th percentiles; whiskers indicate minimum and maximum values. Significance of treatment effect was assessed with estimated means and (95%CI) by GEE model. $*P < 0.05$.

REFERENCES

1. Dalmau J, Gleichman AJ, Hughes EG, et al. Anti-NMDA-receptor encephalitis: case series and analysis of the effects of antibodies. Lancet Neurol. 2008;7(12):1091–1098.
2. Dalmau J, Armangué T, Planagumà J, et al. An update on anti-NMDA receptor encephalitis for neurologists and psychiatrists: mechanisms and models. Lancet Neurol. 2019;18:1045–1057.
3. Irani SR, Bera K, Waters P, et al. N-methyl-d-aspartate antibody encephalitis: Temporal progression of clinical and paraclinical observations in a predominantly non-paraneoplastic disorder of both sexes. Brain 2010;133(6):1655–1667.
4. Titulaer MJ, McCracken L, Gabilondo I, et al. Treatment and prognostic factors for long-term outcome in patients with anti-NMDA receptor encephalitis: An observational cohort study. Lancet Neurol. 2013;12:157–165.
5. Viaccoz A, Desestret V, Ducray F, et al. Clinical specificities of adult male patients with NMDA receptor antibodies encephalitis. Neurology 2014;82:556–563.
6. Kumar MA, Jain A, Dechant VE, et al. Anti-N-methyl-D-aspartate receptor encephalitis during pregnancy. Arch. Neurol. 2010;67:884–887.
7. Joubert B, García-Serra A, Planagumà J, et al. Pregnancy outcomes in anti-NMDA receptor encephalitis: Case series. Neurol. Neuroimmunol. neuroinflammation 2020;7(3):e668.
8. Xiao X, Gui S, Bai P, et al. Anti-NMDA-receptor encephalitis during pregnancy: A case report and literature review. J. Obstet. Gynaecol. Res. 2017;43:768–774.
9. Hughes EG, Peng X, Gleichman AJ, et al. Cellular and Synaptic Mechanisms of Anti-NMDA Receptor Encephalitis. J. Neurosci. 2010;30:5866–5875.
10. Mikasova L, De Rossi P, Bouchet D, et al. Disrupted surface cross-talk between NMDA and Ephrin-B2 receptors in anti-NMDA encephalitis. Brain 2012;135:1606–1621.
11. Moscato EH, Peng X, Jain A, et al. Acute mechanisms underlying antibody effects in anti-N-methyl-D-aspartate receptor encephalitis. Ann. Neurol. 2014;76(1):108–119.

12. Planagumà J, Leypoldt F, Mannara F, et al. Human N-methyl D-aspartate receptor antibodies alter memory and behaviour in mice. Brain 2015;138:94–109.
13. Planagumà J, Haselmann H, Mannara F, et al. Ephrin-B2 prevents N-methyl-D-aspartate receptor antibody effects on memory and neuroplasticity. Ann. Neurol. 2016;80:388–400.
14. Carceles-Cordon M, Mannara F, Aguilar E, et al. NMDAR Antibodies Alter Dopamine Receptors and Cause Psychotic Behavior in Mice. Ann. Neurol. 2020;88(3):603–613.
15. Jurek B, Chayka M, Kreye J, et al. Human gestational N-methyl-D-aspartate receptor autoantibodies impair neonatal murine brain function. Ann. Neurol. 2019;86:656–670.
16. García-Serra A, Radosevic M, Pupak A, et al. Placental transfer of NMDAR antibodies causes reversible alterations in mice. Neurol. Neuroimmunol. neuroinflammation 2021;8(1):e915.
17. Hilderink M, Titulaer MJ, Schreurs MWJ, et al. Transient anti-nmdar encephalitis in a newborn infant due to transplacental transmission. Neurol. Neuroimmunol. neuroinflammation 2015;2:1–2.
18. Roopenian DC, Christianson GJ, Sproule TJ, et al. The MHC Class I-Like IgG Receptor Controls Perinatal IgG Transport, IgG Homeostasis, and Fate of IgG-Fc-Coupled Drugs. J. Immunol. 2003;170(7):3528–3533.
19. Liu L, Garcia AM, Santoro H, et al. Amelioration of Experimental Autoimmune Myasthenia Gravis in Rats by Neonatal FcR Blockade. J. Immunol. 2007;178:5390–5398.
20. Chen P, Li C, Lang S, et al. Animal model of fetal and neonatal immune thrombocytopenia: Role of neonatal Fc receptor in the pathogenesis and therapy. Blood 2010;116(18):3660–3668.
21. Coutinho E, Jacobson L, Shock A, et al. Inhibition of maternal-to-fetal transfer of IgG antibodies by FcRn blockade in a mouse model of arthrogryposis multiplex congenita. Neurol. - Neuroimmunol. Neuroinflammation 2021;8:e1011.
22. Moscato EH, Jain A, Peng X, et al. Mechanisms underlying autoimmune synaptic encephalitis leading to disorders of memory, behavior and cognition: Insights from molecular, cellular and synaptic studies. Eur. J. Neurosci. 2010;32(2):298–309.
23. Mannara F, Radosevic M, Planagumà J, et al. Allosteric modulation of NMDA receptors prevents the antibody effects of patients with anti-NMDAR encephalitis. Brain 2020;143(9):2709–2720.
24. Braniste V, Al-Asmakh M, Kowal C, et al. The gut microbiota influences blood-brain barrier permeability in mice. Sci. Transl. Med. 2014;6:263ra158.
25. Hill JM, Lim MA, Stone MM. Developmental Milestones in the Newborn Mouse. In: Gozes I, editor. Neuromethods. Totowa, NJ: Humana Press; 2008 p. 131–149.
26. Simister NE, Rees AR. Isolation and characterization of an Fc receptor from neonatal rat small intestine. Eur. J. Immunol. 1985;15(7):733–738.
27. Jones EA, Waldmann TA. The mechanism of intestinal uptake and transcellular transport of IgG in the neonatal rat. J. Clin. Invest. 1972;51:2916–2927.
28. Rodewald R. pH-dependent binding of immunoglobulins to intestinal cells of the neonatal rat. J. Cell Biol. 1976;71:666–669.
29. Simister NE, Story CM, Chen HL, Hunt JS. An IgG-transporting Fc receptor expressed in the syncytiotrophoblast of human placenta. Eur. J. Immunol. 1996;26:1527–1531.
30. Zhang Y, Pardridge WM. Mediated efflux of IgG molecules from brain to blood across the blood-brain barrier. J. Neuroimmunol. 2001;114(1–2):168–172.
31. Petkova SB, Akilesh S, Sproule TJ, et al. Enhanced half-life of genetically engineered

human IgG1 antibodies in a humanized FcRn mouse model: Potential application in humorally mediated autoimmune disease. Int. Immunol. 2006;18:1759–1769.
32. Kasprick A, Hofrichter M, Smith B, et al. Treatment with anti-neonatal Fc receptor (FcRn) antibody ameliorates experimental epidermolysis bullosa acquisita in mice. Br. J. Pharmacol. 2020;177:2381–2392.
33. Roy S, Nanovskaya T, Patrikeeva S, et al. M281, an anti-FcRn antibody, inhibits IgG transfer in a human ex vivo placental perfusion model. Am. J. Obstet. Gynecol. 2019;220(5):498.e1-498.e9.
34. Cooper PR, Ciambrone GJ, Kliwinski CM, et al. Efflux of monoclonal antibodies from rat brain by neonatal Fc receptor, FcRn. Brain Res. 2013;1534:13–21.
35. Momenta Pharmaceuticals Inc. A Study to Test Efficacy and Safety of Rozanolixizumab in Adult Patients With Generalized Myasthenia Gravis [Internet]. 2019.Available from: https://clinicaltrials.gov/ct2/show/NCT03971422
36. Momenta Pharmaceuticals Inc. A Study to Evaluate the Safety, Tolerability, Efficacy, Pharmacokinetics and Pharmacodynamics of M281 Administered to Adults With Generalized Myasthenia Gravis [Internet]. 2018.Available from: https://clinicaltrials.gov/ct2/show/NCT03772587?term=M281&rank=5
37. Ling LE, Hillson JL, Tiessen RG, et al. M281, an Anti-FcRn Antibody: Pharmacodynamics, Pharmacokinetics, and Safety Across the Full Range of IgG Reduction in a First-in-Human Study. Clin. Pharmacol. Ther. 2018;105:1031–1039.
38. Momenta Pharmaceuticals Inc. A Study to Evaluate the Safety, Efficacy, Pharmacokinetics and Pharmacodynamics of M281 Administered to Pregnant Women at High Risk for Early Onset Severe Hemolytic Disease of the Fetus and Newborn (HDFN) [Internet]. 2019.Available from: https://clinicaltrials.gov/ct2/show/NCT03842189?term=M281&rank=2
39. Sheikhbahaei S, Sherkat R, Camacho-Ordonez N, et al. Pregnancy, child bearing and prevention of giving birth to the affected children in patients with primary immunodeficiency disease; A case-series. BMC Pregnancy Childbirth 2018;18(1):299.
40. Mandal PK, Dolai TK, Bagchi B, et al. B Cell Suppression in Newborn Following Treatment of Pregnant Diffuse Large B-cell Lymphoma Patient with Rituximab Containing Regimen. Indian J. Pediatr. 2014;81(10):1092–1094.

Figure 1

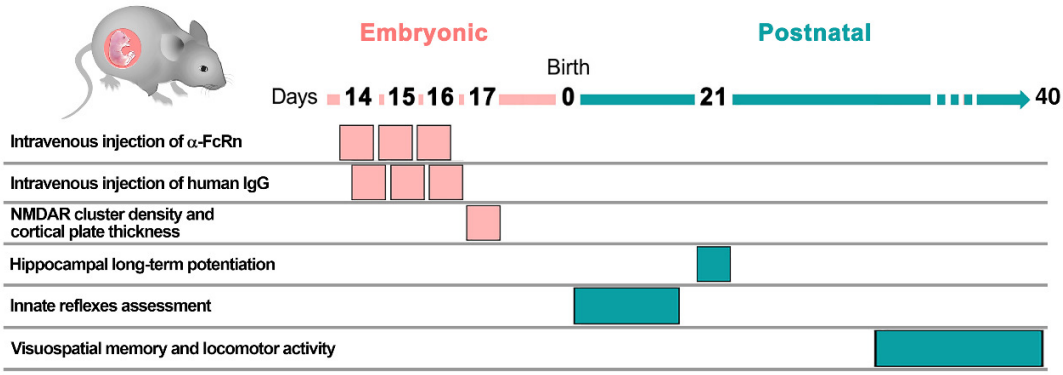
Embryonic
Postnatal
Birth
Days
14
15
16
17
0
21
40
Intravenous injection of α-FcRn
Intravenous injection of human IgG
NMDAR cluster density and cortical plate thickness
Hippocampal long-term potentiation
Innate reflexes assessment
Visuospatial memory and locomotor activity

Figure 2

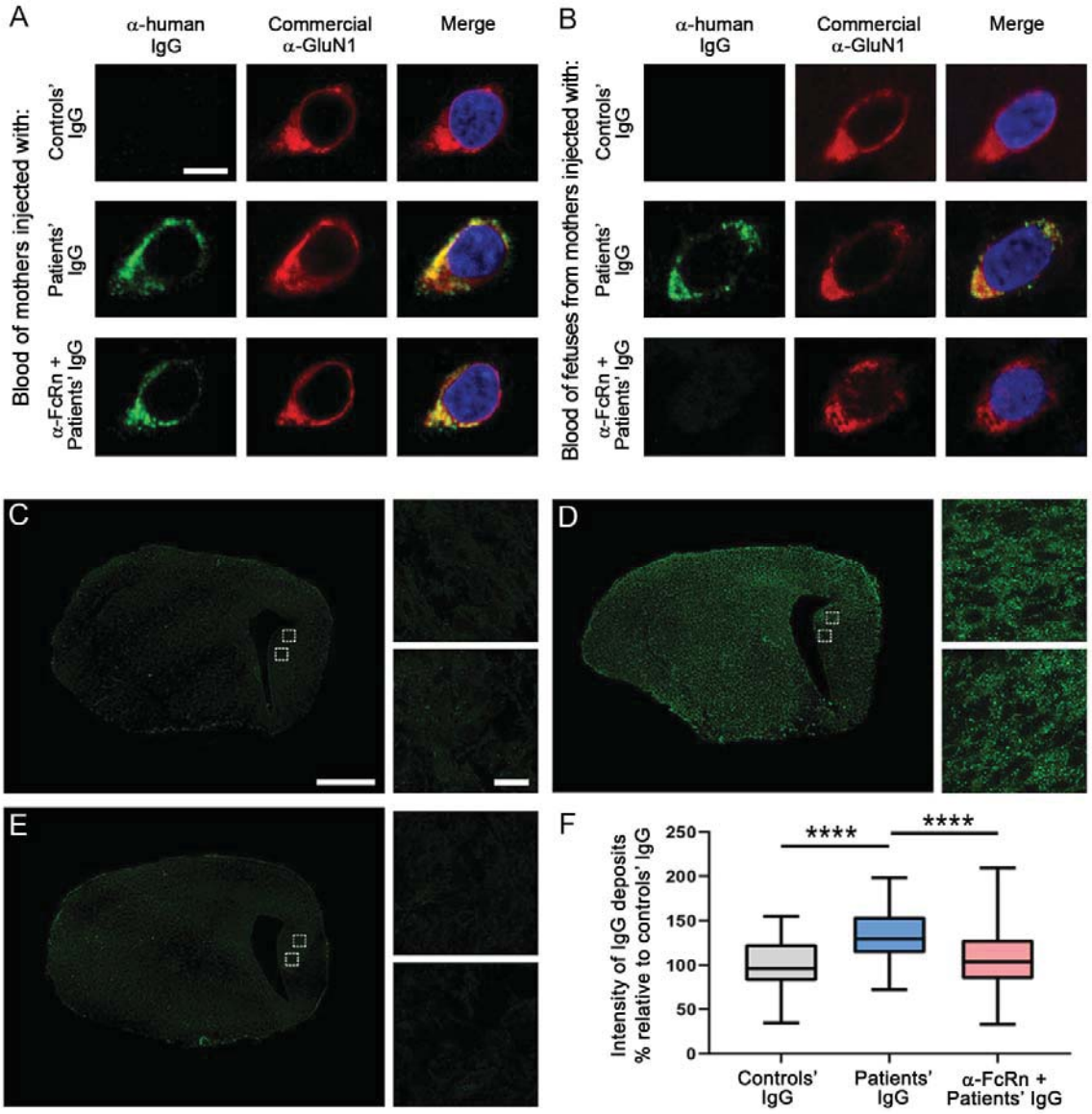
A
α-human IgG
Commercial α-GluN1
Merge
Blood of mothers injected with:
Controls' IgG
Patients' IgG
α-FcRn + Patients' IgG
B
α-human IgG
Commercial α-GluN1
Merge
Blood of fetuses from mothers injected with:
Controls' IgG
Patients' IgG
α-FcRn + Patients' IgG
C
D
E
F
Intensity of IgG deposits % relative to controls' IgG
250
200
150
100
50
0
****
****
Controls' IgG
Patients' IgG
α-FcRn + Patients' IgG

Figure 3

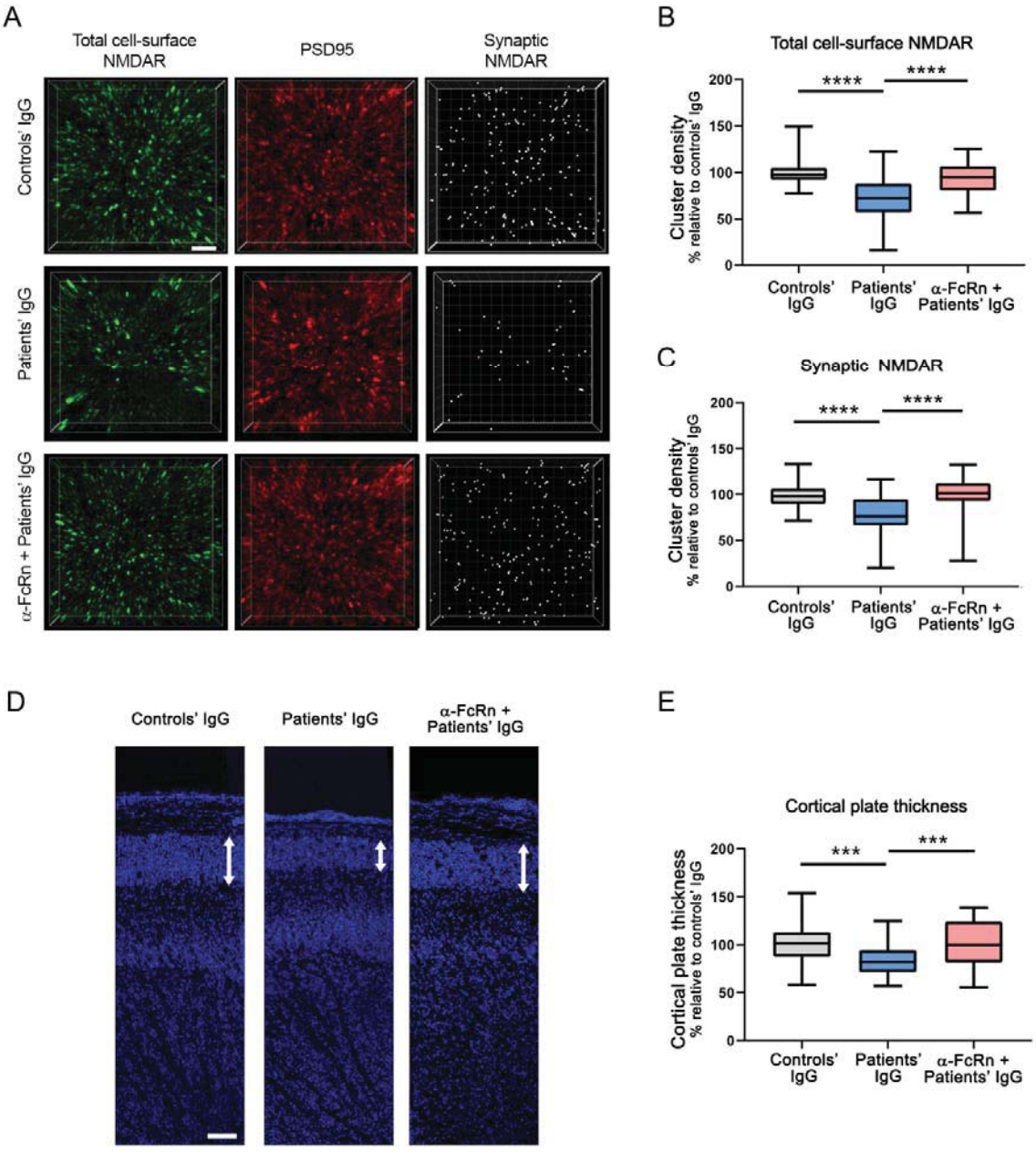
A
Total cell-surface NMDAR
PSD95
Synaptic NMDAR
Controls' IgG
Patients' IgG
α-FcRn + Patients' IgG
B
Total cell-surface NMDAR
Cluster density
% relative to controls' IgG
****
****
Controls' IgG
Patients' IgG
α-FcRn + Patients' IgG
C
Synaptic NMDAR
Cluster density
% relative to controls' IgG
****
****
Controls' IgG
Patients' IgG
α-FcRn + Patients' IgG
D
Controls' IgG
Patients' IgG
α-FcRn + Patients' IgG
E
Cortical plate thickness
Cortical plate thickness
% relative to controls' IgG
***
***
Controls' IgG
Patients' IgG
α-FcRn + Patients' IgG

Figure 4

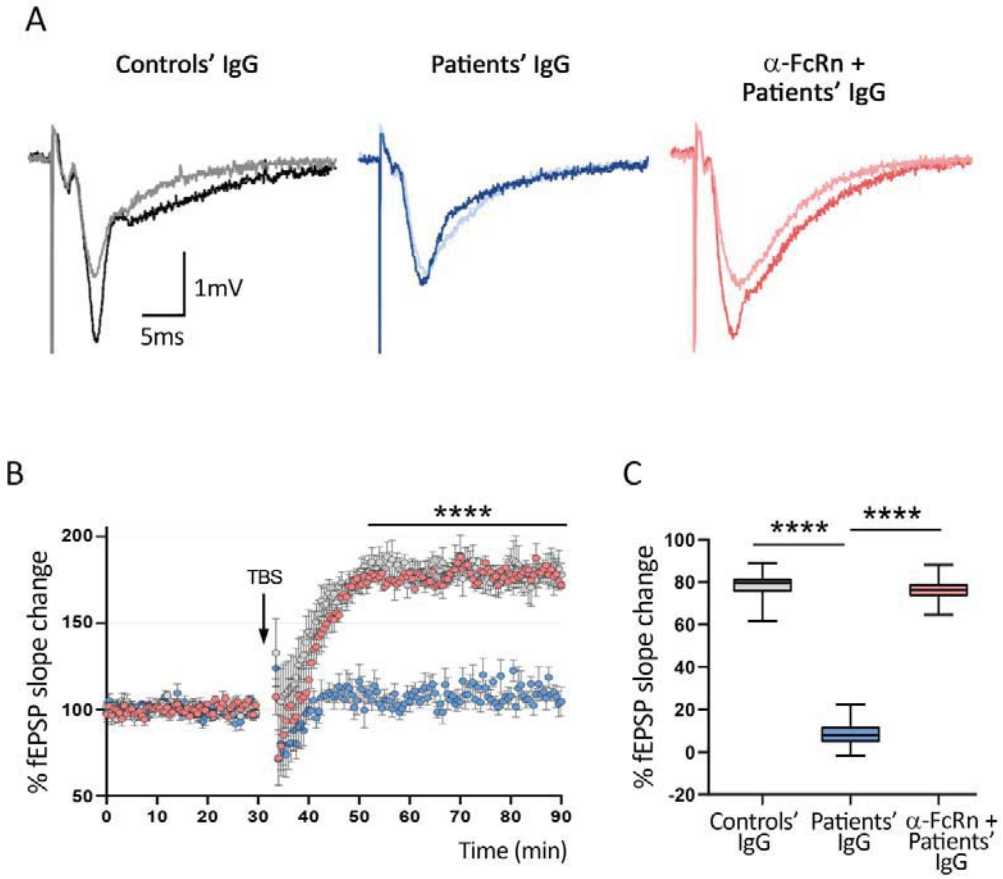
A
Controls' IgG
Patients' IgG
α-FcRn +
Patients' IgG
1mV
5ms
B
****
TBS
% fEPSP slope change
200
150
100
50
0
10
20
30
40
50
60
70
80
90
Time (min)
C
****
****
% fEPSP slope change
100
80
60
40
20
0
-20
Controls' IgG
Patients' IgG
α-FcRn +
Patients' IgG

Figure 5

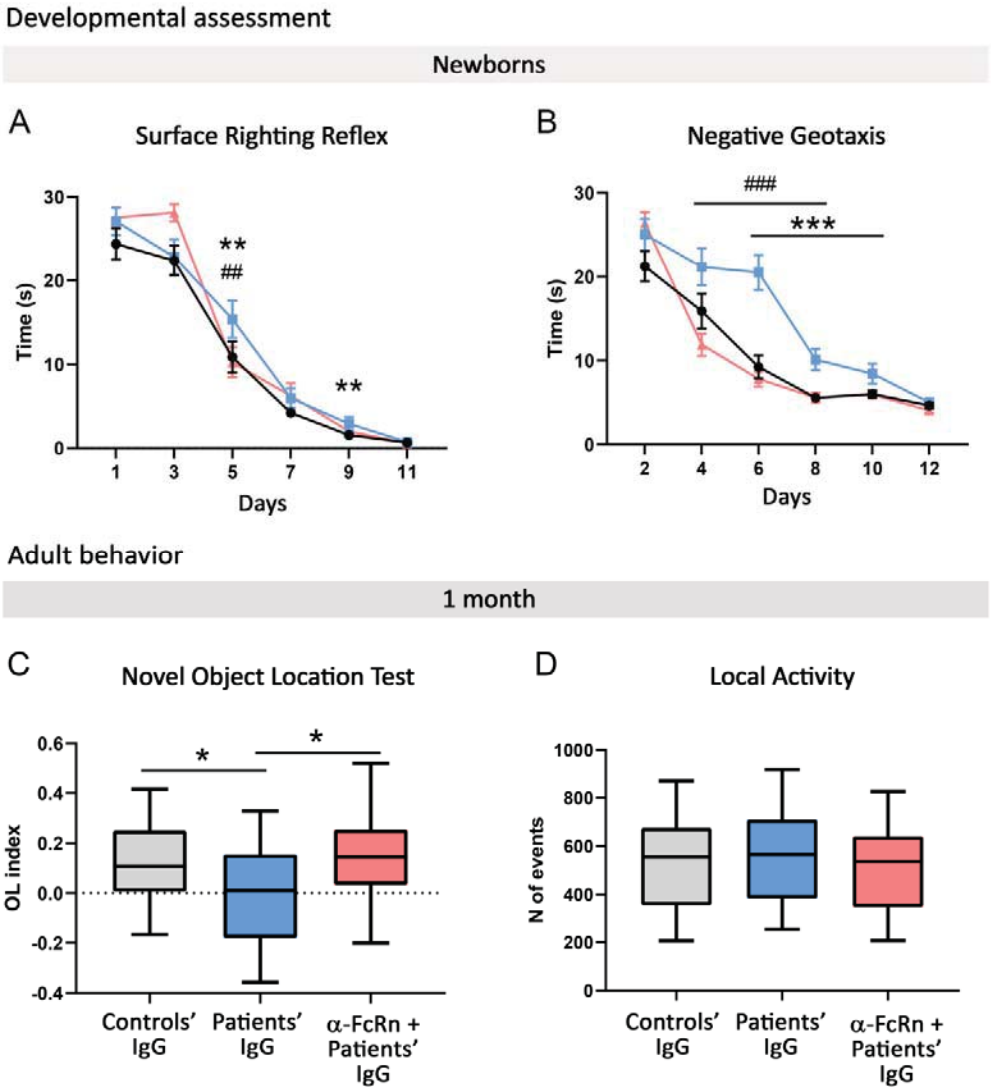
Developmental assessment
Newborns
A
Surface Righting Reflex
Time (s)
Days
**
##
**
B
Negative Geotaxis
###
***
Time (s)
Days
Adult behavior
1 month
C
Novel Object Location Test
OL index
*
*
Controls' IgG
Patients' IgG
α-FcRn + Patients' IgG
D
Local Activity
N of events
Controls' IgG
Patients' IgG
α-FcRn + Patients' IgG

Paper IV

Allosteric modulation of NMDA receptors prevents the antibody effects of patients with anti-NMDAR encephalitis

Francesco Mannara,* Marija Radosevic,* Jesús Planagumà,* David Soto, Esther Aguilar, Anna García-Serra, Estibaliz Maudes, Marta Pedreño, Steven Paul, James Doherty, Michael Quirk, Jing Dai, Xavier Gasull, Mike Lewis, # and Josep Dalmau#

*,#These authors contributed equally to this work

Brain. 2020 Sep 1;143(9):2709-2720

Impact factor JCR 2020 (percentile): The available IF from 2019 is 11.337 (D1)

doi:10.1093/brain/awaa195 BRAIN 2020: 143; 2709–2720 | 2709

BRAIN
A JOURNAL OF NEUROLOGY

Allosteric modulation of NMDA receptors prevents the antibody effects of patients with anti-NMDAR encephalitis

Francesco Mannara,[1,*] Marija Radosevic,[1,*] Jesús Planagumà,[1,*] David Soto,[1,2] Esther Aguilar,[1] Anna García-Serra,[1] Estibaliz Maudes,[1] Marta Pedreño,[1] Steven Paul,[3,4] James Doherty,[3] Michael Quirk,[3] Jing Dai,[3] Xavier Gasull,[1,2] Mike Lewis[3,#] and Josep Dalmau[1,5,6,#]

*,#These authors contributed equally to this work.

Anti-*N*-methyl-D-aspartate receptor (NMDAR) encephalitis is an immune-mediated disease characterized by a complex neuropsychiatric syndrome in association with an antibody-mediated decrease of NMDAR. About 85% of patients respond to immunotherapy (and removal of an associated tumour if it applies), but it often takes several months or more than 1 year for patients to recover. There are no complementary treatments, beyond immunotherapy, to accelerate this recovery. Previous studies showed that SGE-301, a synthetic analogue of 24(S)-hydroxycholesterol, which is a potent and selective positive allosteric modulator of NMDAR, reverted the memory deficit caused by phencyclidine (a non-competitive antagonist of NMDAR), and prevented the NMDAR dysfunction caused by patients' NMDAR antibodies in cultured neurons. An advantage of SGE-301 is that it is optimized for systemic delivery such that plasma and brain exposures are sufficient to modulate NMDAR activity. Here, we used SGE-301 to confirm that in cultured neurons it prevented the antibody-mediated reduction of receptors, and then we applied it to a previously reported mouse model of passive cerebroventricular transfer of patient's CSF antibodies. Four groups were established: mice receiving continuous (14-day) infusion of patients' or controls' CSF, treated with daily subcutaneous administration of SGE-301 or vehicle (no drug). The effects on memory were examined with the novel object location test at different time points, and the effects on synaptic levels of NMDAR (assessed with confocal microscopy) and plasticity (long-term potentiation) were examined in the hippocampus on Day 18, which in this model corresponds to the last day of maximal clinical and synaptic alterations. As expected, mice infused with patient's CSF antibodies, but not those infused with controls' CSF, and treated with vehicle developed severe memory deficit without locomotor alteration, accompanied by a decrease of NMDAR clusters and impairment of long-term potentiation. All antibody-mediated pathogenic effects (memory, synaptic NMDAR, long-term potentiation) were prevented in the animals treated with SGE-301, despite this compound not antagonizing antibody binding. Additional investigations on the potential mechanisms related to these SGE-301 effects showed that (i) in cultured neurons SGE-301 prolonged the decay time of NMDAR-dependent spontaneous excitatory postsynaptic currents suggesting a prolonged open time of the channel; and (ii) it significantly decreased, without fully preventing, the internalization of antibody-bound receptors suggesting that additional, yet unclear mechanisms, contribute in keeping unchanged the surface NMDAR density. Overall, these findings suggest that SGE-301, or similar NMDAR modulators, could potentially serve as complementary treatment for anti-NMDAR encephalitis and deserve future investigations.

1 Institut d'Investigacions Biomèdiques August Pi i Sunyer (IDIBAPS), Hospital Clínic, Universitat de Barcelona, Barcelona, Spain
2 Laboratori de Neurofisiologia, Departament de Biomedicina, Facultat de Medicina i Ciències de la Salut, Institut de Neurociències, Universitat de Barcelona, Barcelona, Spain
3 Sage Therapeutics, Cambridge, MA, USA

Received December 5, 2019. Revised April 3, 2020. Accepted April 22, 2020. Advance access publication August 24, 2020

4 Departments of Psychiatry and Neurology, Washington University School of Medicine, St Louis, USA
5 Department of Neurology, University of Pennsylvania, Philadelphia, USA
6 Institució Catalana de Recerca i Estudis Avançats (ICREA), Barcelona, Spain

Correspondence to: Josep Dalmau, MD, PhD
IDIBAPS-Hospital Clínic, Universitat de Barcelona, Department of Neurology, c/Villarroel 170, 08036 Barcelona, Spain
E-mail: jdalmau@clinic.cat

Keywords: animal model; anti-NMDAR encephalitis; SGE-301; treatment

Abbreviations: EPSC = excitatory postsynaptic current; fEPSP = field excitatory postsynaptic potential; LTP = long-term potentiation; NMDAR = NMDA receptor; PAM = positive allosteric modulator; SGE-301 = $\Delta^{5,6}$-3β-oxy-nor-cholenyl-dimethylcarbinol; TBS = theta-burst stimulation

Introduction

Anti-NMDA receptor (NMDAR) encephalitis is an immune-mediated disease characterized by a complex neuropsychiatric syndrome and the presence of CSF antibodies against the GluN1 subunit of NMDARs (Dalmau *et al.*, 2008). The disorder can be triggered by systemic tumours, usually a teratoma of the ovary, and less frequently by herpes simplex encephalitis (Armangue *et al.*, 2018), but in many cases no trigger is identified. At disease onset patients develop psychosis, insomnia, abnormal movements, seizures, decreased level of consciousness, dysautonomia, or coma, which in about 85% of cases respond to immunotherapy and removal of the tumour when it applies (Titulaer *et al.*, 2013; Viaccoz *et al.*, 2014). However, it often takes several months or more than 1 year for patients to return to most of their activities. During the process of recovery the clinical features are different from those of the acute stage, including impairment of attention, memory, executive functions, or behaviour (Dalmau *et al.*, 2011; Finke *et al.*, 2012; Peer *et al.*, 2017). The reasons for this slow clinical recovery are unclear but may include a persisting immune activation against NMDAR within the CNS, a severe impairment of synaptic function and long-term plasticity, a limited blood–brain barrier penetration of current immunotherapies, or a combination of these factors. Studies examining the effects of patients NMDAR antibodies in cultured neurons (Hughes *et al.*, 2010; Mikasova *et al.*, 2012) or mice (Planaguma *et al.*, 2015, 2016) have shown that they mediate a broad loss of surface NMDARs, regardless of synaptic localization or subunit composition (Warikoo *et al.*, 2018), leading to impairment of synaptic plasticity and memory (Planaguma *et al.*, 2015, 2016).

In some respects, the treatment paradigm of anti-NMDAR encephalitis resembles that of antibody-mediated diseases of the neuromuscular junction, such as myasthenia gravis or the Lambert-Eaton myasthenic syndrome (LEMS), where despite evidence that several immunotherapies are effective, most patients need additional treatment for a faster or sustained improvement. These treatments are addressed to compensate or overcome the mechanisms altered by the autoantibodies, for example, acetylcholinesterase inhibitors (pyridostigmine) in myasthenia gravis, or the presynaptic potassium channel blocker (3,4-diaminopyridine) in LEMS (Newsom-Davis, 2003; Wirtz *et al.*, 2010). In studies using cultured neurons (Mikasova *et al.*, 2012; Planaguma *et al.*, 2016) or passive transfer of patient's CSF NMDAR antibodies to mice (Planaguma *et al.*, 2016), a soluble form of ephrin-B2 (an agonist of the ephrin-B2 receptor that clusters and retains NMDARs at the synapse) was able to antagonize all antibody-mediated effects including NMDAR internalization and impairments of long-term plasticity and visuospatial memory. As a proof-of-principle, this finding showed that interfering with the antibody-mediated mechanisms could potentially be used as a complementary treatment with immunotherapy (Mikasova *et al.*, 2012); however, ephrin-B2 was administered intraventricularly and there are no available ephrin-B2 agonists that cross the blood–brain barrier.

There is evidence that a major brain-derived cholesterol metabolite, 24(S)-hydroxycholesterol [24(S)-HC], is a very potent, direct, and selective positive allosteric modulator (PAM) of NMDARs (Paul *et al.*, 2013). In hippocampal slices, application of 24(S)-HC enhanced the ability of subthreshold stimuli to induce long-term potentiation (LTP), and reversed the LTP deficits caused by the NMDAR channel blocker, ketamine. Several synthetic analogues of 24(S)-HC such as $\Delta^{5,6}$-3β-oxy-nor-cholenyl-dimethylcarbinol (SGE-201) or SGE-301 shared similar mechanisms of action (Paul *et al.*, 2013). In rats, the administration of SGE-301 reverted the memory deficit caused by phencyclidine, a non-competitive NMDAR antagonist (Paul *et al.*, 2013). Moreover, application of SGE-301 to cultures of neurons exposed to CSF antibodies from patients with anti-NMDAR encephalitis prevented the antibody-mediated dysfunction of NMDARs (Warikoo *et al.*, 2018). An advantage of this compound is that it is optimized for systemic delivery such that plasma and brain exposures are sufficient to modulate activity in preclinical models of NMDAR hypofunction (Paul *et al.*, 2013). These findings led us to investigate whether SGE-301 was able to prevent the antibody-mediated reduction of NMDAR and memory impairment observed in a previously reported model of cerebroventricular transfer of patient's CSF antibodies.

Materials and methods

Animals, surgery, and patients' CSF

Seventy-six male C57BL/6J mice (Charles River), 8–10 weeks old (25–30 g) were used for the studies including, memory and locomotor activity ($n = 47$ mice), confocal immunohistochemistry assessment of levels of NMDAR and other synaptic proteins, and electrophysiological studies ($n = 29$ mice). Animal care, anaesthesia, insertion of bilateral ventricular catheters (PlasticsOne, model 3280PD-2.0; coordinates: 0.2 mm posterior and ± 1.00 mm lateral from bregma, depth 2.2 mm), and connection of each catheter to a subcutaneous osmotic pump for continuous infusion of CSF (Alzet; volume 100 µl, flow rate 0.25 µl/h for 14 days) have been reported (Planaguma *et al.*, 2015). The CSF infused was pooled from samples of 10 patients with high titre IgG GluN1 antibodies (all > 1:320), and 10 patients with normal pressure hydrocephalus without NMDAR antibodies (control samples).

The presence of NMDAR antibodies in patient's CSF (and absence in controls' CSF) was examined with three different techniques: brain tissue immunohistochemistry, HEK293T cells expressing NMDAR, and cultured neurons, as reported (Ances *et al.*, 2005; Dalmau *et al.*, 2008). Patients' and controls' CSF were then pooled in two different samples and filtered (Amicon Ultracel 30K, Sigma-Aldrich), dialysed against phosphate-buffered saline (PBS), and normalized to a physiological concentration of 2 mg IgG/dl (Planaguma *et al.*, 2016). The absence of other antibodies in pooled patient's CSF was confirmed using an aliquot immunoabsorbed with HEK293T expressing GluN1, showing: (i) abrogation of reactivity with mouse brain and HEK293T cells expressing NMDARs; and (ii) abrogation of NMDAR internalization (Supplementary Fig. 1).

Written informed consent was obtained from all patients. The study was approved by the local institutional review board (Hospital Clínic, HCB/2018/0192), and animal studies were approved by the Local Ethical Committee of the University of Barcelona following European (2010/63/UE) and Spanish (RD 53/2013) regulations about the use and care of experimental animals.

Preparation and treatment with SGE-301

SGE-301 is a potent allosteric modulator of NMDAR that has been characterized previously (Paul *et al.*, 2013). For the current studies, we adopted a subcutaneous administration paradigm (versus intraperitoneal) to minimize interaction with the centrally fixed osmotic minipumps. Therefore, we ran plasma and brain pharmacokinetic studies to measure exposures of SGE-301 present at the time of *in vivo* testing. The method of determination of plasma and brain concentration of SGE-301 is described in the Supplementary material. At 1 h, we achieved 1954 ± 157 ng/ml plasma and 523 ± 86 ng/g brain exposures. At 4 h, we achieved 985 ± 173 ng/ml plasma and 1350 ± 120 ng/g brain exposures (Supplementary Fig. 2). These exposures are similar to those reported after intraperitoneal administration (Paul *et al.*, 2013).

For studies with cultured neurons, lyophilized SGE-301 was weighted and dissolved in dimethyl sulphoxide (DMSO) to a stock concentration of 10 mM; the solution was then sonicated for 1 h at 40°C and used at a working concentration of 10 µM. For studies using mice, lyophilized SGE-301 was weighed and dissolved in a solution of 30% 2-hydroxypropyl-β-cyclodextrin (HPBCD, Sigma-Aldrich) in distilled water. The solution was then vortexed for 5 min, sonicated for 40 min, and stirred for 2 h at 50°C. After adjusting the pH to 5.5–7.0, working aliquots were prepared and kept frozen at –20°C. A similar solution of 30% HPBCD in distilled water, but without drug, served as control (vehicle). Aliquots with or without drug were thawed and vortexed for 2 min before use.

Experimental design

Four experimental groups were established including mice infused with patients' or controls' CSF along with subcutaneous administration of SGE-301 (10 mg/kg) or vehicle (Fig. 1A). The administration of SGE-301 began on Day 1 (coinciding with Day 1 of infusion of CSF) until Day 18 (4 days after the infusion of CSF had stopped), which was the last day with maximal memory deficits and reduction of NMDAR synaptic clusters observed in this model (Planaguma *et al.*, 2015). The selected animal tasks (novel object location; locomotor activity) and the timing of the tasks (Fig. 1B) were based on previous experience with this model, showing that patient's CSF NMDAR antibodies caused a progressive decrease of visuospatial memory until Day 18, subsequently followed by progressive recovery several days after the antibody infusion stopped (Planaguma *et al.*, 2015). In contrast, patient antibodies did not significantly alter the locomotor activity (included here as control, and to ensure that animals did not have motor limitations in exploring the objects). All tasks were performed by researchers blinded to experimental conditions.

Immunohistochemistry and confocal microscopy

Techniques related to immunolabelling of live cultures of dissociated rodent hippocampal neurons, immunoabsorption of patient samples with GluN1-expressing HEK cells, brain tissue processing, and quantitative brain tissue immunoperoxidase staining, have previously been reported (Planaguma *et al.*, 2015). To determine the effects of patient antibodies in cultured rat hippocampal neurons, 17-day *in vitro* cultures were exposed to patient or controls' CSF (diluted 1:100) along with 10 µM SGE-301 or vehicle for 24 or 48 h, and the cell surface clusters of NMDAR, PSD95, phospho-S295-PSD95, and the co-localization of NMDAR/PSD95 (representing synaptic NMDAR) were quantified with specific biomarkers and confocal microscopy (Supplementary material). Determination of antibody-bound internalized NMDAR was carried out as previously reported (Moscato *et al.*, 2014) (Supplementary material).

To determine the effects of patient antibodies on the number of clusters of NMDAR and PSD95, non-permeabilized 5-µm thick brain sections (obtained on Day 18, Fig. 1B) were blocked with 5% goat serum, and serially incubated with a human CSF NMDAR-antibody sample (1:20, used as primary antibody) for 2 h at room temperature and the secondary Alexa Fluor® 488 goat anti-human IgG (1:1000, A-11013, ThermoFisher) for 1 h at room temperature. Tissue sections were then permeabilized with 0.3% Triton™ X-100 for 10 min at room temperature, and serially incubated with rabbit polyclonal anti-PSD95 (1:250, ab18258 Abcam) overnight at 4°C, and the corresponding secondary Alexa Fluor® 594 goat anti-rabbit IgG (1:1000, A-11012, ThermoFisher) for 1 h at room temperature. Slides

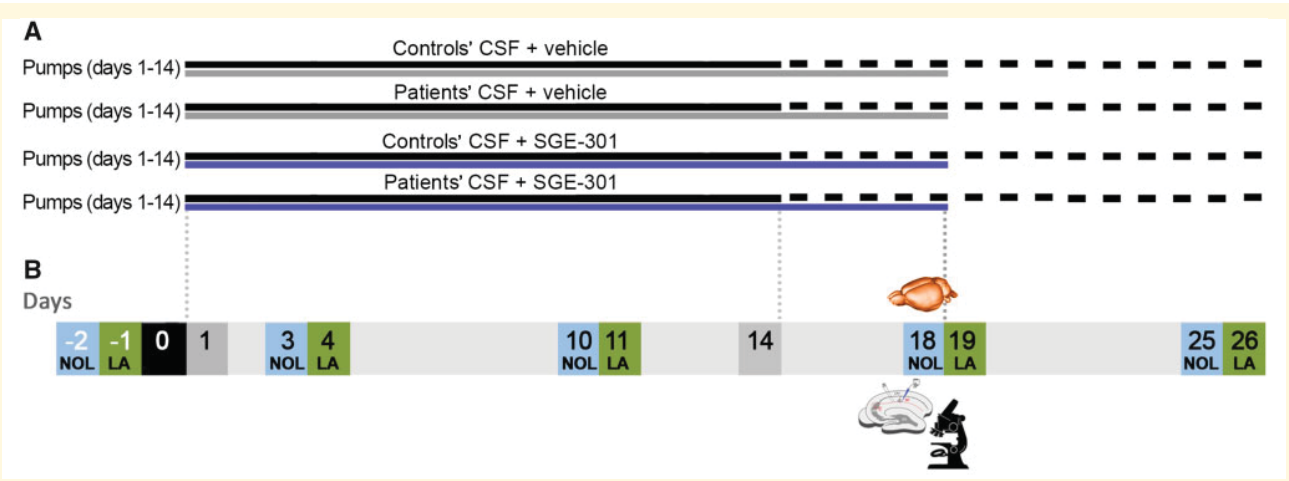

Figure 1 Experimental design. (**A**) Four experimental groups of mice were used, including mice treated with continuous cerebroventricular infusion of control or patients' CSF for 14 days along with daily subcutaneous injection of vehicle (30% HPBCD) or SGE-301 (10 mg/kg diluted in vehicle) for 18 days. (**B**) Timing of memory and locomotor tasks. Novel object location (NOL) and locomotor activity (LA) tests were begun before the surgical implantation of ventricular catheters and osmotic pumps. The same tests were applied on Days 3–4, 10–11, 18–19 and 25–26 after surgery. The effects of antibodies from patients on the levels of NMDARs and synaptic plasticity were examined on subsets of mice sacrificed on Day 18, which is the date of maximal effects reported in this model (Planaguma *et al.*, 2015).

were then mounted with ProLong™ Gold antifade reagent for 4 min, containing 6-diamidino-2-phenylindole dihydrochloride (DAPI, P36935; ThermoFisher) and results scanned with Zeiss LSM710 confocal microscope (Carl Zeiss) with EC-Plan NEOFLUAR CS 100×/1.3 NA oil objective. For each animal, five identical image stacks in three hippocampal areas (CA1, CA3 and dentate gyrus; total 15 image stacks) were acquired as reported (Planaguma *et al.*, 2015). Each *z*-stack comprised 50 optical images that were deconvolved with AutoQuantX3 (Bitplane, Oxford Instruments). The mean density of clusters of NMDAR or PSD95 was obtained using a spot detection algorithm from Imaris suite 7.6.4 (Bitplane), and the cluster density expressed as spots/mm^3. The clusters of NMDAR that co-localized with PSD95 were defined as synaptic. For each experimental group, the mean cluster densities of NMDAR or PSD95 were normalized with the corresponding values in control animals (infused with controls' CSF and treated with vehicle).

To determine the levels of synaptic phospho-S295-PSD95 in brain tissue, 5-µm thick brain sections permeabilized as above and blocked with 5% goat serum and 1% bovine serum albumin (BSA) were incubated with rabbit anti-phospho-S295-PSD95 (1:200, ab76108, Abcam) and mouse anti-PSD95 (diluted 1:200, 124 011, Synaptic Systems) for 1 h. Slides were then washed and incubated with Alexa Fluor® 488 goat anti-rabbit IgG and Alexa Fluor® 594 goat anti-mouse IgG (both diluted 1:500, A-11034, A-11032, ThermoFisher). Results were scanned as above, and the cluster density of phospho-S295-PSD95 and PSD95 was determined with Imaris (Bitplane) software.

Electrophysiological studies

Preparation of acute hippocampal slices on Day 18 (Fig. 1B) and field potential recordings and analysis were performed as reported (Planaguma *et al.*, 2016) (Supplementary material).

To determine the effects of chronic exposure to SGE-301 on NMDAR currents we treated 18 days *in vitro* (div) cultures of hippocampal neurons with controls' CSF (diluted 1:100) or controls' CSF + SGE-301 (10 µM) for 48 h prior to whole-cell patch clamp recordings of spontaneous NMDAR-mediated excitatory postsynaptic currents (sEPSCs) (Supplementary material).

Memory and locomotor activity tasks

Visuospatial memory was assessed with the novel object location discrimination index, and the locomotor activity was automatically determined using locomotor activity boxes (11 × 21 × 18 cm, Imetronic) for 1 h (Planaguma *et al.*, 2015) (Supplementary material).

Statistical analysis

Data from behavioural studies (novel object location and locomotor activity) were analysed using repeated-measures two-way ANOVA. Human IgG intensities from different brain regions and confocal cluster densities of NMDAR and PSD95 on cultured neurons and brain tissue were analysed using one-way ANOVA. Density levels of phospho-S295-PSD95 in cultured neurons and brain tissue were assessed with unpaired *t*-test. The electrophysiological data were assessed by one-way ANOVA (LTP and paired-pulse facilitation: PP2/PP1 ratios) and unpaired *t*-test (paired-pulse facilitation: analysis of increase of PP2 slope compared with PP1 in each of the experimental groups independent of each other). A P-value < 0.05 was considered significant. All ANOVA tests included *post hoc* analyses with Bonferroni correction for multiple testing. Analysis of NMDAR-mediated spontaneous EPSCs in cultures of neurons chronically exposed to SGE-301 was performed with Student's *t*-tests. Statistical analyses were performed with GraphPad Prism v.6 (La Jolla, CA, USA).

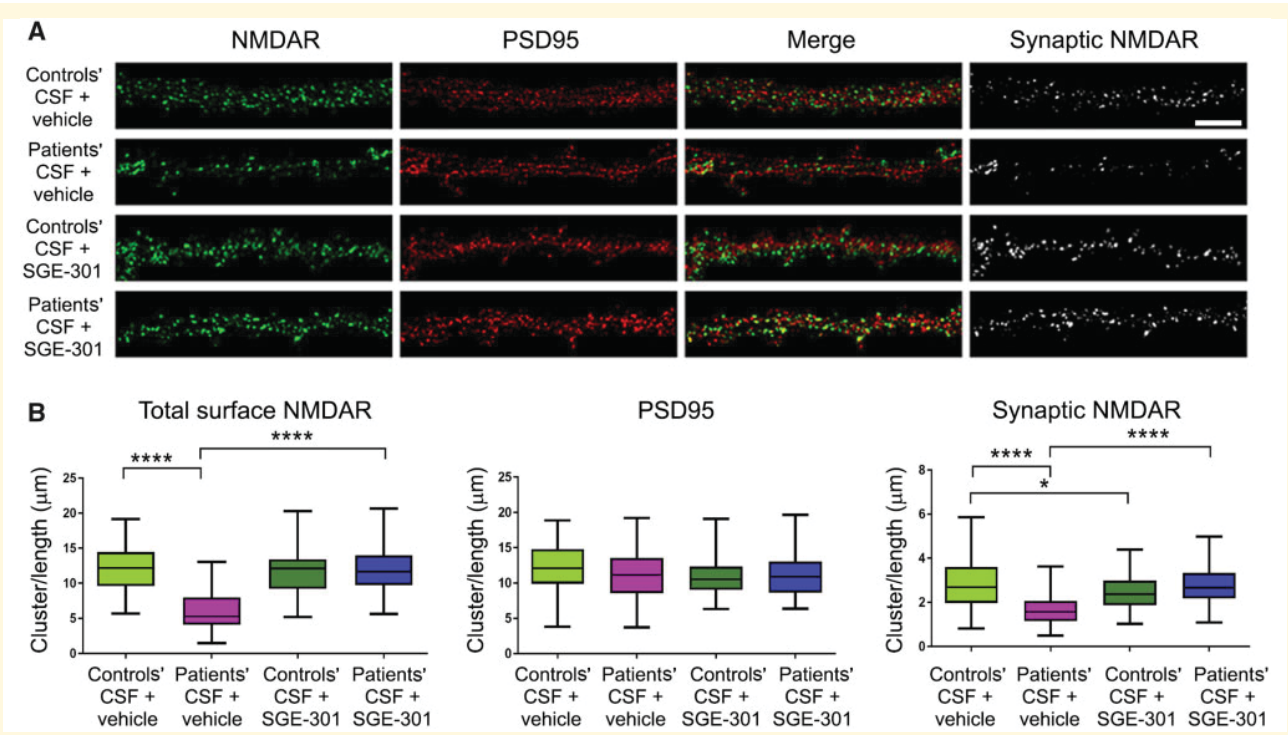

Figure 2 Treatment with SGE-301 prevents the reduction of NMDARs caused by patients' antibodies in cultured neurons. (**A**) Representative dendrites of hippocampal neurons immunostained for surface NMDAR (green) and PSD95 (red) after 24 h treatment with patients' CSF or controls' CSF, each with either vehicle or SGE-301. Synaptic NMDARs are defined as those that co-localize with PSD95 (white channel). Scale bars = 10 µm. (**B**) Quantification of the density of surface and synaptic NMDAR. Cultures co-treated with patients' CSF antibodies and vehicle showed a significant decrease of total cell surface and synaptic NMDARs without affecting the density of PSD95. In contrast, cultures co-treated with the same patients' CSF and SGE-301 did not show reduction of NMDARs. No effects on total cell surface NMDARs were noted in neurons treated with CSF from controls with vehicle or SGE-301, although the presence of SGE-301 was associated with a mild reduction of synaptic NMDARs. The density of PSD95 was not affected by any of these conditions. $n = 15$ dendrites per condition, three independent experiments. Box plots show the median, and 25th and 75th percentiles; whiskers indicate the minimum and maximum values. Significance of treatment effect was assessed by one-way ANOVA ($P < 0.0001$ for NMDAR, synaptic NMDAR) with Bonferroni *post hoc* correction: *$P < 0.05$; ****$P < 0.0001$. Additional information is available in Supplementary Table 1.

Data availability

The authors confirm that the data supporting the findings of this study are available within the article and its Supplementary material.

Results

Treatment with SGE-301 prevents the pathogenic effects of antibodies in cultured neurons

We and others have previously reported that NMDAR antibodies of patients cause a reduction of the clusters of synaptic and extrasynaptic NMDARs in cultured neurons (Hughes *et al.*, 2010; Mikasova *et al.*, 2012), and in an animal model of cerebroventricular infusion of patients' CSF (Planaguma *et al.*, 2015). Here, we first used cultured neurons to determine whether the antibody effects were prevented by SGE-301. As expected, neurons treated with patients' CSF and vehicle showed a significant decrease of total cell surface and synaptic NMDAR clusters compared with neurons treated with controls' CSF and vehicle. However, neurons treated with the same patients' CSF antibodies along with SGE-301, instead of vehicle, showed no significant change of the levels of total cell surface or synaptic NMDARs (Fig. 2). To determine whether this was due to abrogation of receptor internalization, we quantified the clusters of antibody-bound internalized NMDAR (Moscato *et al.*, 2014) showing that treatment with SGE-301 significantly reduced the levels of internalized antibody-bound receptors, but did not completely abolish the internalization (Supplementary Fig. 3). Overall, these findings show that SGE-301 prevents the antibody-mediated decrease of cell-surface NMDAR, and suggest that this treatment effect is due to a reduction of internalized antibody-bound receptors along with additional, yet unclear mechanisms, which overall keep the clusters of surface receptors similar to control levels.

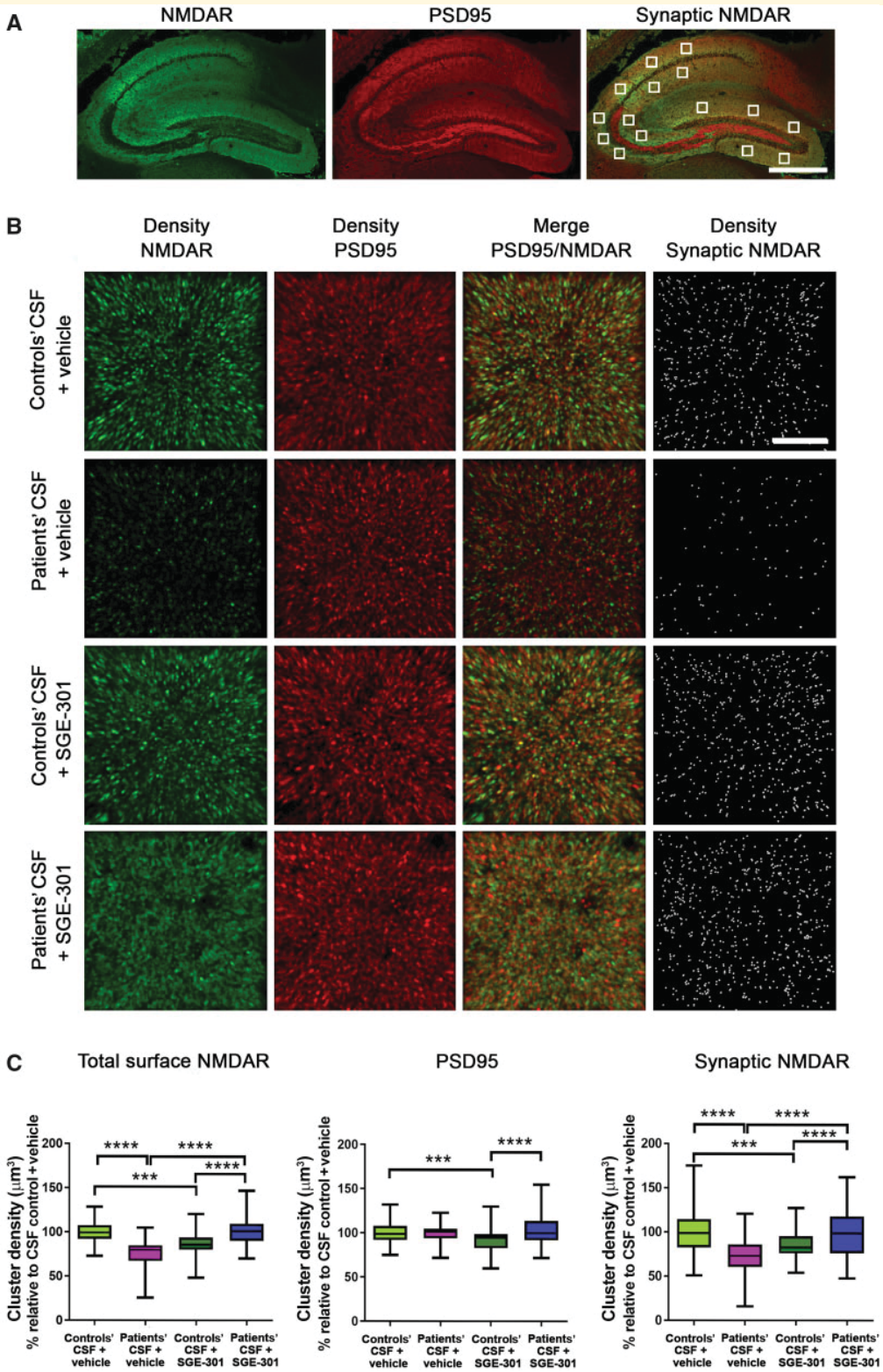

Figure 3 Treatment with SGE-301 prevents the reduction of NMDARs caused by patients' antibodies in hippocampus. (**A**) Hippocampus of mouse immunolabelled for NMDAR and PSD95. Images were merged (synaptic NMDAR, yellow colour) and post-processed to demonstrate co-localizing clusters. White squares indicate the analysed areas in CA1, CA3, and dentate gyrus. Each square is a 3D stack of 50 sections. Scale bar = 500 µm. (**B**) 3D projection and analysis of the density of total cell surface NMDAR clusters, PSD95, and synaptic NMDAR clusters (defined as those that co-localized with PSD95). Each 3D projection is a representative CA1 square region (as those shown in **A**) of an animal representative of each experimental condition infused with control or patients' CSF along with SGE-301 or vehicle. Merged

(continued)

Neurons treated for 24 h with controls' CSF and SGE-301 showed a mild decrease of synaptic NMDAR clusters. To explore the cause of this decrease of synaptic NMDAR we examined the effects of a longer (48 h) neuronal exposure to SGE-301, which demonstrated a decrease of synaptic and extrasynaptic NMDAR clusters (Supplementary Fig. 4A). Considering that phosphorylation of Ser295 enhances the accumulation of PSD95 and that Ser295 phosphorylation is suppressed by chronic NMDAR activation (Kim *et al.*, 2007), we determined whether SGE-301 changed the levels of phospho-S295-PSD95. This experiment showed a reduction of phospho-S295-PSD95 without significant decrease of total PSD95 (Supplementary Fig. 4B). A similar reduction of phospho-S295-PSD95 was obtained when cultured neurons were incubated with bicuculline, as reported (Kim *et al.*, 2007), and used here as control (Supplementary Fig. 4C). These findings indicate that prolonged neuronal exposure to SGE-301 leads to a reduction of NMDARs accompanied by a decrease of phospho-S295-PSD95, suggesting the presence of compensatory changes to the positive modulation of NMDAR.

To determine the effects of chronic exposure to SGE-301 on NMDAR currents we treated hippocampal neuronal cultures with controls' CSF (diluted 1:100) or controls' CSF + SGE-301 (10 μM) for 48 h prior to whole-cell patch clamp recordings of NMDAR-mediated spontaneous EPSCs. Recordings revealed that SGE-301 did not modify the amplitude or frequency of spontaneous EPSC (Supplementary Fig. 5) but significantly slowed the decay phase of the spontaneous EPSC, as shown by a longer decay time constant (262.0 ± 37.3 ms versus 368.6 ± 49.8 ms; $P < 0.05$; Supplementary Fig. 5B). These findings suggest that SGE-301 enhances NMDAR-mediated EPSCs by slowing their decay phase, most probably by increasing the channel's open time and thus decreasing NMDAR's deactivation time.

Treatment with SGE-301 prevents the antibody-mediated reduction of NMDAR in mice

We next assessed whether SGE-301 antagonized the antibody effects in the hippocampus of mice infused with patients' CSF antibodies. Fifteen hippocampal areas with 50 optical *z*-sections per area, representing 750 optical sections per animal (five animals per experimental group), were investigated (Fig. 3A). Animals infused with patients' CSF and treated with vehicle showed a significant decrease of the density of total and synaptic NMDAR clusters compared with animals infused with controls' CSF and treated with vehicle or SGE-301. Similarly, as observed with cultured neurons, the pathogenic effect of patients' CSF antibodies was prevented in the group of animals that received the same patients' CSF but were treated with SGE-301 instead of vehicle (Fig. 3B and C). To assess whether the treatment effect of SGE-301 was due to a direct interference with patient's antibody binding to NMDARs, we determined the intensity of human IgG bound to hippocampus in mice representative of the four experimental groups. This study showed that SGE-301 did not modify the intensity of patients' CSF IgG present in hippocampus suggesting that the drug did not block the binding of the antibody to NMDARs (Supplementary Fig. 6).

An additional finding of these studies was that in control conditions (e.g. animals not infused with antibodies) chronic administration of SGE-301 caused a decrease of total cell surface and synaptic NMDAR clusters as well as a decrease of PSD95, as shown by comparison of the groups of animals treated with controls' CSF with or without SGE-301 (Fig. 3C). Moreover, the hippocampus of mice infused with controls' CSF and chronically treated with SGE-301 had a significant decrease of Ser295 phosphorylated PSD95 and total PSD95 compared with animals not treated with SGE-301 (Supplementary Fig. 7). Overall, these studies showed that subcutaneous administration of SGE-301 prevented the antibody-mediated reduction of synaptic and extrasynaptic clusters of NMDARs, and that in control conditions (animals not infused with NMDAR antibodies) SGE-301 led to a decrease of levels of NMDAR and PSD95 suggesting, as with the experiments with neurons, the presence of compensatory mechanisms to the positive modulatory effect of SGE-301 on NMDARs.

Treatment with SGE-301 prevents the impairment of LTP caused by NMDAR antibodies of patients

Acute brain slices from mice infused with patient or controls' CSF treated with SGE-301 or vehicle, were used to record field excitatory postsynaptic potentials (fEPSPs) in the CA1 region of the hippocampus (Fig. 4A). Animals infused with patients' CSF showed a significant reduction of LTP compared with animals infused with controls' CSF, as shown by

Figure 3 Continued
images [merge: PSD95 (red)/NMDAR (green)] were postprocessed and used to calculate the density of clusters (density = spots/μm^3). Scale bar = 2 μm. (**C**) Quantification of the density of total (*left*) and synaptic (*right*) NMDAR clusters, and total PSD95 at Day 18 in a pooled analysis of hippocampal areas (CA1, CA3, and dentate gyrus). Mean density of clusters in animals treated with controls' CSF + vehicle was defined as 100%. For each condition, five animals were examined (15 hippocampal areas per animal). Box plots show the median, and 25th and 75th percentile; whiskers indicate the minimum or maximum values. Significance of treatment effect was assessed by one-way ANOVA ($P = 0.0001$) and *post hoc* analysis with Bonferroni correction; ***$P < 0.001$; ****$P < 0.0001$. Additional information is available in Supplementary Table 1.

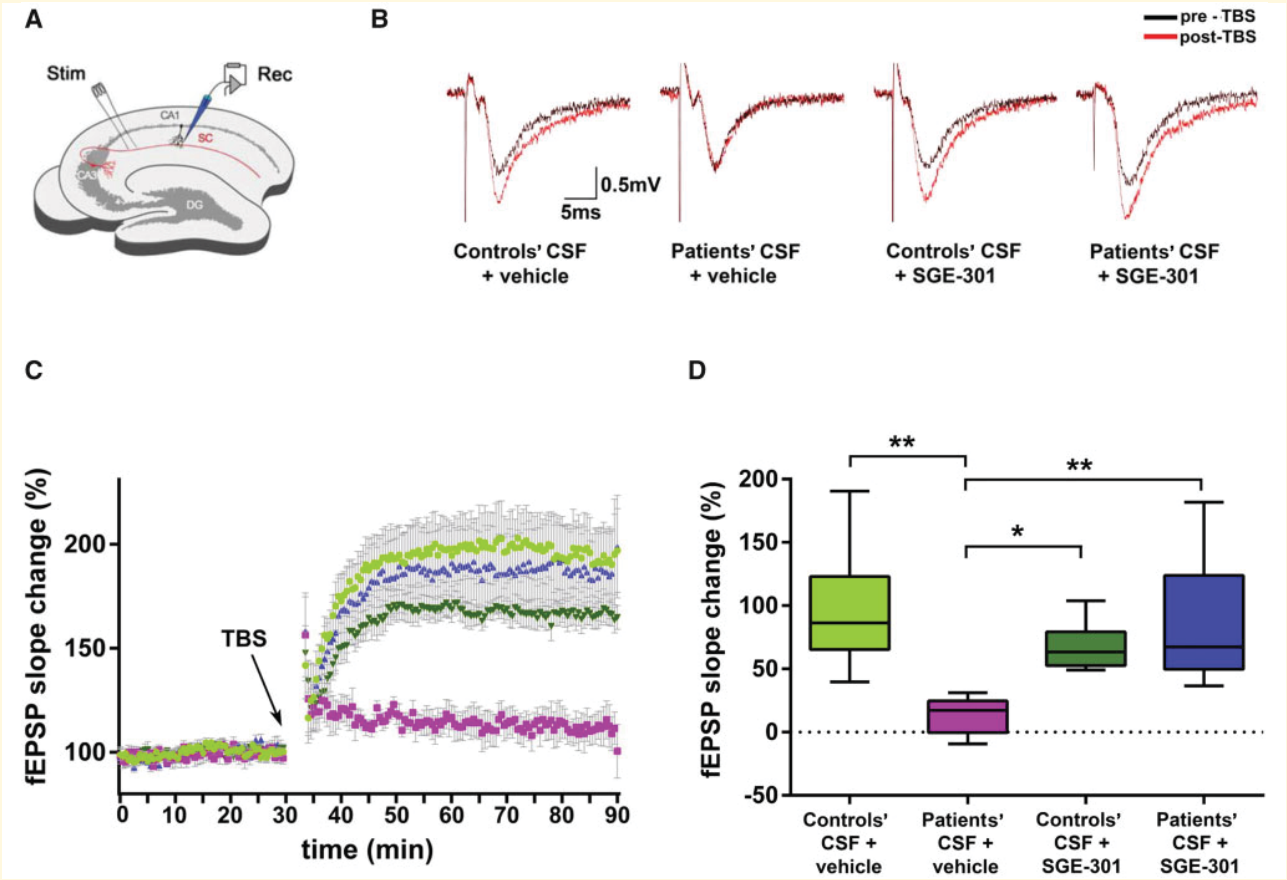

Figure 4 Treatment with SGE-301 prevents the impairment of LTP caused by NMDAR antibodies from patients. (**A**) The Schaffer collateral pathway (SC, red) was stimulated (Stim) and field potentials were recorded (Rec) in the CA1 region of the hippocampus. LTP was induced by TBS. CA = cornu ammonis; DG = dentate gyrus. (**B**) Example traces of individual recordings showing baseline fEPSPs before LTP induction (black traces) and after LTP (red traces). Slope and peak amplitude of fEPSPs are increased after TBS in mice infused with controls' CSF and treated with vehicle or SGE-301, and are strongly impaired in animals infused with patients' CSF and treated with vehicle. In mice infused with patients' CSF and treated with SGE-301 the increase of slope is improved. Note that initial peak amplitude of fEPSP may vary within individual recordings. (**C**) Time course of fEPSP recordings demonstrating robust changes in fEPSP slope in the animals infused with controls' CSF treated with vehicle ($n = 8$ recordings from seven animals, light green), or treated with SGE-301 ($n = 10$ recordings from seven animals, dark green), which was stable throughout the recording period after TBS (arrow). In animals infused with patients' CSF and treated with vehicle ($n = 6$ recordings from five animals, pink) the induction of LTP was markedly impaired. In contrast, animals infused with the same patients' CSF and treated with SGE-301 ($n = 7$ recordings from six animals, blue) show resolved effects on synaptic plasticity after LTP induction. The fEPSP values of all animals for each of the groups are presented as mean ± standard error of the mean (SEM). (**D**) Quantification of fEPSP slope change showing a significant reduction of fEPSP slope in animals infused with patients' CSF and treated with vehicle compared with the other groups of animals. Note that animals infused with patients' CSF and treated with SGE-301 did not show reduction of fEPSP slope. The number of recordings and animals used are the same as those indicated in **C**. Box plots show the median, 25th and 75th percentiles; whiskers indicate minimum and maximum values. Significance was assessed by one-way ANOVA ($P < 0.01$) and Bonferroni *post hoc* correction test was applied: *$P < 0.05$; **$P < 0.01$. Additional information is available in Supplementary Table 1.

analysis of fEPSP slope change (Fig. 4B and C). Quantitative analysis showing median changes in slope values during the stable period post-theta-burst stimulation (TBS) (from Minutes 15 to 60, of 60 min after TBS) showed a reduced potentiation of fEPSP in mice infused with patients' CSF compared with those infused with controls' CSF (Fig. 4D). Treatment with SGE-301 prevented patients' CSF antibody-mediated impairment of LTP (Fig. 4C and D). Compared with these findings, animals infused with controls' CSF, with or without treatment with SGE-301, did not show impairment of LTP, although the control group treated with SGE-301 showed a non-significant reduction of fEPSP slope change (Fig. 4C). This finding probably reflects the decreased density of NMDAR clusters noted in the confocal analysis of effects of SGE-301 in animals infused with controls' CSF (Fig. 3C).

In contrast to the severe reduction of hippocampal LTP, short-term plasticity was not affected in animals infused

with patients' CSF antibodies, as expected from the experience with previous studies (Planaguma *et al.*, 2016). Indeed, fEPSP recordings following a standard paired-pulse protocol showed significant facilitation consistent with increased presynaptic release probability (Supplementary Fig. 8A and B). This effect was similar in the four experimental groups (Supplementary Fig. 8C). Overall, these studies showed a severe impairment of postsynaptic, but not presynaptic, plasticity after TBS in animals infused with CSF from patients, but not in animals infused with the same patients' CSF and simultaneously treated with SGE-301.

Treatment with SGE-301 prevents memory loss caused by NMDAR antibodies from patients

Mice infused with patients' CSF and treated with daily subcutaneous administration of vehicle developed a progressive decrease of the novel object location index, with maximal deficit on Days 10 and 18 (4 days after stopping the antibody infusion), followed by progressive memory improvement until reaching the baseline pre-infusion level on Day 25 (Fig. 5, pink line) (Planaguma *et al.*, 2015). In contrast, mice infused with the same patients' CSF but treated with daily subcutaneous injections of SGE-301 instead of vehicle, showed no alteration of the novel object location index (Fig. 5, blue line); these findings were similar to those of mice infused with controls' CSF treated with SGE-301 or vehicle (Fig. 5, light and dark green lines). The total time of exploration of the two objects (not moved + novel location) was similar in animals of the four experimental groups (Supplementary Fig. 9A). The locomotor activity was also similar in the four groups of animals (Supplementary Fig. 9B–D). Overall, these findings showed that daily subcutaneous administration of SGE-301 prevented the hippocampal memory impairment caused by NMDAR antibodies from patients in this animal model.

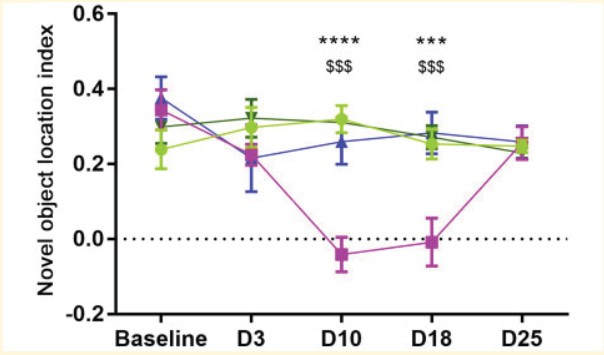

Figure 5 SGE-301 prevented the visuospatial memory deficits caused by NMDAR antibodies from patients. Mice infused with patients' CSF antibodies and treated with vehicle (pink line) showed a significant reduction of the novel object location index. This memory deficit was prevented in the group of mice infused with the same patients' CSF antibodies but treated with SGE-301 (blue line). No significant memory changes were noted in the groups of mice infused with controls' CSF and treated with vehicle (light green line) or SGE-301 (dark green line). Number of animals: controls' CSF + vehicle = 11; patients' CSF + vehicle = 10; controls' CSF + SGE-301 = 12; patients' CSF + SGE-301 = 10. A higher index represents better visuospatial memory. Data are presented as mean ± SEM. Significance of assessment was performed by repeated-measures two-way ANOVA ($P < 0.0001$) with Bonferroni *post hoc* correction. Patient's CSF + vehicle versus controls' CSF + vehicle: $^{****}P < 0.0001$, $^{***}P < 0.001$. Patient CSF + vehicle versus patients' CSF + SGE-301: $^{\$\$\$}P < 0.001$. Additional information is available in Supplementary Table 1.

Discussion

In this proof-of-concept study we show that a synthetic analogue (SGE-301) of the brain-derived cholesterol metabolite 24(S)-HC prevented the pathogenic effects of antibodies from patients with anti-NMDAR encephalitis in hippocampal neuronal cultures and in a previously reported model of cerebroventricular transfer of antibodies (Planaguma *et al.*, 2015, 2016). These findings and the good brain concentration after subcutaneous dosing suggest that oxysterol-based NMDAR PAMs could serve as potential treatments for anti-NMDAR encephalitis.

Like steroids, oxysterols are well recognized signalling molecules that interact with membrane-bound as well as soluble intracellular receptors (Radhakrishnan *et al.*, 2007). In particular, 24-hydroxylated oxysterol, such as 24 (S)-HC and the synthetic analogues, SGE-201 and SGE-301, are known for a striking selectivity for NMDARs (Paul *et al.*, 2013; Linsenbardt *et al.*, 2014). The enzyme involved in synthesis of 24(S)-HC (cholesterol 24-hydroxylase; CYP46A1) is expressed predominantly in the endoplasmic reticulum of neurons and dendrites (Ramirez *et al.*, 2008) and its deficiency causes severe impairment of hippocampal LTP and memory in mice (Kotti *et al.*, 2006). Using slices of hippocampus of rats, previous studies showed that application of 24(S)-HC or synthetic oxysterols (SGE-201 or SGE-301) reversed the LTP inhibition caused by ketamine (a non-competitive antagonist of NMDAR) (Paul *et al.*, 2013). In rats, the impairment of memory and active social interactions caused by phencyclidine (PCP), a non-competitive antagonist of NMDARs, were significantly improved by SGE-301 (Paul *et al.*, 2013). These findings, together with results from our studies, suggest that SGE-301 prevents the NMDAR hypofunction caused by pharmacological antagonists as well as by immune-mediated mechanisms.

Studies with chimeric GluN-GluK subunits suggest that GluN transmembrane domains are critical for oxysterol modulation (Wilding *et al.*, 2016), which would be consistent with the lipophilic nature of these modulators. SGE-301 increases channel open probability, potentiating NMDAR function, and appears to bind to a site independent of other allosteric modulators of NMDAR function (Paul *et al.*,

2013; Wilding *et al.*, 2016). In a previous study in which cultured rat hippocampal neurons were exposed for 48 h to patients' CSF NMDAR antibodies or controls' CSF and during the last 24 h each condition was treated with SGE-301 or vehicle, those that were treated with SGE-301 showed increased NMDAR function compared with those treated with vehicle (Warikoo *et al.*, 2018). Similar to our observed prolonged spontaneous EPSCs duration after SGE-301 (Supplementary Fig. 5), the authors found an increase of NMDAR function in the neurons exposed to controls' CSF and treated with SGE-301, which was attributed to an increase in open probability of NMDAR (Warikoo *et al.*, 2018). These findings led to the suggestion that SGE-301 does not interfere directly with the patient's antibody-mediated internalization of NMDARs (Warikoo *et al.*, 2018). However, the authors did not consider that the maximal antibody-mediated reduction of NMDARs in cultured neurons occurs within the first 12–24 h of incubation (before SGE-301 was applied); afterwards, the clusters of NMDARs remain decreased for as long as the antibodies are present in the media (Moscato *et al.*, 2014; Ladepeche *et al.*, 2018). Our current data show that when CSF antibodies from patients were co-applied with SGE-301 to cultures of neurons, the expected antibody-mediated effects were prevented and the NMDAR clusters were not decreased. Similar findings occurred in the animal model, showing that the density of total cell surface and synaptic NMDAR clusters in mice infused with patients' CSF and treated with SGE-301 was not significantly different from that of control mice (infused with controls' CSF and treated with vehicle). In contrast, animals infused with CSF from patients but not treated with SGE-301 showed the expected significant reduction of NMDARs. This reduction of NMDAR was associated with severe impairment of LTP and visuospatial memory, which were prevented when animals were simultaneously treated with SGE-301.

We noted that mice infused with controls' CSF and treated with SGE-301 compared with mice infused with the same controls' CSF and treated with vehicle, showed a decrease of total cell surface and synaptic NMDAR clusters. A similar effect was noted in neuronal cultures treated for 48 h with controls' CSF and SGE-301. We postulated that this finding represents a compensatory mechanism to the chronic PAM activity of SGE-301. Studies have shown that phosphorylation of Ser295 enhances the accumulation of PSD95 and that phospho-S295-PSD95 is suppressed by chronic NMDAR activation (Kim *et al.*, 2007). In line with these studies, we found that mice infused with controls' CSF and chronically treated with SGE-301 had lower amounts of phospho-S295-PSD95 and PSD95 compared with mice treated with vehicle. Neuronal cultures treated for 48 h with SGE-301 showed an effect in the same direction, including a reduction of phospho-S295-PSD95 that was more intense than that of total PSD95. Similar mechanisms induced by the chronic PAM effect of SGE-301 may be involved in the change, although not significant, in fEPSP slope after induction of LTP in control animals treated with SGE-301 compared with those treated with vehicle.

Data from this and a previous study (Planaguma *et al.*, 2016) show that antibodies from patients do not affect paired-pulse facilitation, suggesting that presynaptic neurotransmitter release is unaffected in all experimental groups and that postsynaptic mechanisms are responsible for the decrease of LTP in animals treated with patients' CSF. In another report using hippocampal neuronal cultures, antibodies from patients specifically decreased NMDAR-mediated currents (along with a specific reduction of NMDAR clusters) without affecting AMPA receptor-mediated currents (Hughes *et al.*, 2010). These studies, along with the selective SGE-301 PAM effect on NMDAR (Paul *et al.*, 2013), suggest that the impairment of LTP (and its prevention by SGE-301) in animals infused with patients' CSF is via modulation of NMDAR.

The exact molecular mechanisms by which SGE-301 prevents the effects of patient antibodies are unknown. We found that SGE-301 does not block the binding of antibodies from patients to hippocampus, suggesting several alternative mechanisms, such as interference with antibody-induced internalization of receptors, increase of recruitment of NMDARs, or both. In preliminary studies with cultured neurons treated with antibodies from patients, we found that SGE-301 significantly decreased (without fully preventing) antibody-mediated NMDAR internalization, suggesting that in this setting, a recruitment of NMDARs to the cell surface and synapse may be facilitated by the drug.

Our study design does not allow for the assessment of whether SGE-301 reverses the antibody-mediated decrease of NMDAR and associated memory deficit because animals infused with antibodies from patients were simultaneously treated with SGE-301, and they did not develop any of those alterations. Although previous studies showed that application of SGE-301 to neuronal cultures exposed to patient antibodies for 24 h accelerated the recovery from the antibody effects (Warikoo *et al.*, 2018), it is unclear if SGE-301 would fully reverse symptoms already established and if so, how long it would take to recovery. It is also unclear whether SGE-301 would be effective for symptoms other than memory impairment; future animal models reproducing the entire repertoire of symptoms in the acute and chronic stage of the disease would facilitate these studies. Finally, there is evidence that SGE-301 and similar PAMs potentiate the NMDAR responses for many minutes beyond their presence in the media, a feature attributed to their strong lipophilicity or potential intracellular accumulation (Paul *et al.*, 2013; Warikoo *et al.*, 2018). Therefore, a dosing less frequent than that used in our model (e.g. every other day instead of daily dosing) may result in the same beneficial effects.

The experience with current treatment approaches to anti-NMDAR encephalitis and the outcome of most patients emphasizes the importance of our findings. During the acute stage of anti-NMDAR encephalitis,

patients often require intensive immunotherapy, anti-epileptics, psychoactive medications, and intensive care support, along with tumour removal if this applies (Titulaer *et al.*, 2013). This stage is usually followed by a protracted process of recovery in which symptoms of the acute phase (psychosis, seizures, abnormal movements, decreased level of consciousness) are no longer present, and the patient is at home or in a rehabilitation centre showing other symptoms such as deficit of memory, attention, cognition, abnormal behaviour, or executive dysfunction (Finke *et al.*, 2012, 2013; Titulaer *et al.*, 2013). Our model, in which the local transfer of human NMDAR antibodies into the mouse cerebroventricular system predominantly affects hippocampal NMDAR (Planaguma *et al.*, 2015), provides a proof-of-principle that targeting the antibody-related mechanisms as complementary treatment for anti-NMDAR encephalitis may mitigate or shorten the process of recovery. In preliminary studies, SAGE-718 (a PAM closely related to SGE-301 designed for oral bioavailability and once daily dosing) showed a good tolerability profile in healthy volunteers in a double-blind, placebo-controlled phase 1 single ascending dose study (Koenig *et al.*, 2019) and is currently being used in a trial for Huntington's disease (which, at early stages, appears to associate with reduced NMDAR function). The tasks for the future are to better understand the underlying mechanisms by which SGE-301 prevents patient antibody effects, assess the ability of this compound to reverse established symptoms, and determine its optimal dosing and frequency of treatment.

Acknowledgements

We thank Mercedes Alba, Eva Caballero, and Araceli Mellado-Berguillos (IDIBAPS, Hospital Clínic, University of Barcelona) for their technical support.

Funding

This study was funded by Plan Nacional de I + D + I and cofinanced by the Instituto de Salud Carlos III (ISCIII)—Subdirección General de Evaluación y Formento de la Investigación Sanitaria—and the Fondo Europeo de Desarrollo Regional (ISCIII-FEDER; 17/00234 and 17/00296); Project Integrative of Excellence (PIE 16/00014); Centro de Investigación Biomédica en Red de Enfermedades Raras (CIBERER, #CB15/00010); RETICs Oftared RD16/0008/0014 (X.G.); "la Caixa" Foundation (ID 100010434, under the agreement LCF/PR/HR17/52150001); The Safra Foundation (J.D.), and Fundació CELLEX (J.D.); BFU2017-83317-P (D.S.); Pla Estratègic de Recerca i Innovació en Salut (PERIS, SLT002/16/00346, J.P.); and Agència de Gestió d Ajuts Universitaris i de Recerca (FI-AGAUR) grant program by the Generalitat de Catalunya (2019FI_B1 00212, A.G.-S.), Basque Goverment Doctoral Fellowship Program, PRE-2019-1-0255 (E.M.), and Maria de Maeztu MDM-2017-0729 to Institut de Neurociencies.

Competing interests

J.D. receives royalties from Athena Diagnostics for the use of Ma2 as an autoantibody test and from Euroimmun for the use of NMDA as an antibody test. He received a licensing fee from Euroimmun for the use of $GABA_B$ receptor, $GABA_A$ receptor, DPPX and IgLON5 as autoantibody tests; he has received a research grant from Sage Therapeutics. S.P., J.D., M.Q., J.D., and M.L. work at Sage Therapeutics.

Supplementary material

Supplementary material is available at *Brain* online.

References

Ances BM, Vitaliani R, Taylor RA, Liebeskind DS, Voloschin A, Houghton DJ, et al. Treatment-responsive limbic encephalitis identified by neuropil antibodies: MRI and PET correlates. Brain 2005; 128: 1764–77.

Armangue T, Spatola M, Vlagea A, Mattozzi S, Carceles-Cordon M, Martinez-Heras E, et al. Frequency, symptoms, risk factors, and outcomes of autoimmune encephalitis after herpes simplex encephalitis: a prospective observational study and retrospective analysis. Lancet Neurol 2018; 17: 760–72.

Dalmau J, Gleichman AJ, Hughes EG, Rossi JE, Peng X, Lai M, et al. Anti-NMDA-receptor encephalitis: case series and analysis of the effects of antibodies. Lancet Neurol 2008; 7: 1091–8.

Dalmau J, Lancaster E, Martinez-Hernandez E, Rosenfeld MR, Balice-Gordon R. Clinical experience and laboratory investigations in patients with anti-NMDAR encephalitis. Lancet Neurol 2011; 10: 63–74.

Finke C, Kopp UA, Pruss H, Dalmau J, Wandinger KP, Ploner CJ. Cognitive deficits following anti-NMDA receptor encephalitis. J Neurol Neurosurg Psychiatry 2012; 83: 195–8.

Finke C, Kopp UA, Scheel M, Pech LM, Soemmer C, Schlichting J, et al. Functional and structural brain changes in anti-N-methyl-D-aspartate receptor encephalitis. Ann Neurol 2013; 74: 284–96.

Hughes EG, Peng X, Gleichman AJ, Lai M, Zhou L, Tsou R, et al. Cellular and synaptic mechanisms of anti-NMDA receptor encephalitis. J Neurosci 2010; 30: 5866–75.

Kim MJ, Futai K, Jo J, Hayashi Y, Cho K, Sheng M. Synaptic accumulation of PSD-95 and synaptic function regulated by phosphorylation of serine-295 of PSD-95. Neuron 2007; 56: 488–502.

Koenig A, Murck H, Paskavitz J, Hoffmann E, Li S, Silber C, et al. Double-blind, placebo-controlled phase 1 single ascending dose study of SAHE-718. International College of Neuropsychopharmacology (CINP) 2019 Congress. Athens, Greece; 2019.

Kotti TJ, Ramirez DM, Pfeiffer BE, Huber KM, Russell DW. Brain cholesterol turnover required for geranylgeraniol production and learning in mice. Proc Natl Acad Sci USA 2006; 103: 3869–74.

Ladepeche L, Planaguma J, Thakur S, Suarez I, Hara M, Borbely JS, et al. NMDA receptor autoantibodies in autoimmune encephalitis cause a subunit-specific nanoscale redistribution of NMDA receptors. Cell Rep 2018; 23: 3759–68.

Linsenbardt AJ, Taylor A, Emnett CM, Doherty JJ, Krishnan K, Covey DF, et al. Different oxysterols have opposing actions at N-methyl-D-aspartate receptors. Neuropharmacology 2014; 85: 232–42.

Mikasova L, De Rossi PBouchet D, Georges F, Rogemond V, Didelot A, et al. Disrupted surface cross-talk between NMDA and Ephrin-B2 receptors in anti-NMDA encephalitis. Brain 2012; 135: 1606–21.

Moscato EH, Peng X, Jain A, Parsons TD, Dalmau J, Balice-Gordon RJ. Acute mechanisms underlying antibody effects in anti-N-methyl-D-aspartate receptor encephalitis. Ann Neurol 2014; 76: 108–19.

Newsom-Davis J. Therapy in myasthenia gravis and Lambert-Eaton myasthenic syndrome. Semin Neurol 2003; 23: 191–8.

Paul SM, Doherty JJ, Robichaud AJ, Belfort GM, Chow BY, Hammond RS, et al. The major brain cholesterol metabolite 24(S)-hydroxycholesterol is a potent allosteric modulator of N-methyl-D-aspartate receptors. J Neurosci 2013; 33: 17290–300.

Peer M, Pruss H, Ben-Dayan I, Paul F, Arzy S, Finke C. Functional connectivity of large-scale brain networks in patients with anti-NMDA receptor encephalitis: an observational study. Lancet Psychiatry 2017; 4: 768–74.

Planaguma J, Haselmann H, Mannara F, Petit-Pedrol M, Grunewald B, Aguilar E, et al. Ephrin-B2 prevents N-methyl-D-aspartate receptor antibody effects on memory and neuroplasticity. Ann Neurol 2016; 80: 388–400.

Planaguma J, Leypoldt F, Mannara F, Gutierrez-Cuesta J, Martin-Garcia E, Aguilar E, et al. Human N-methyl D-aspartate receptor antibodies alter memory and behaviour in mice. Brain 2015; 138: 94–109.

Radhakrishnan A, Ikeda Y, Kwon HJ, Brown MS, Goldstein JL. Sterol-regulated transport of SREBPs from endoplasmic reticulum to Golgi: oxysterols block transport by binding to Insig. Proc Natl Acad Sci USA 2007; 104: 6511–8.

Ramirez DM, Andersson S, Russell DW. Neuronal expression and subcellular localization of cholesterol 24-hydroxylase in the mouse brain. J Comp Neurol 2008; 507: 1676–93.

Titulaer MJ, McCracken L, Gabilondo I, Armangue T, Glaser C, Iizuka T, et al. Treatment and prognostic factors for long-term outcome in patients with anti-NMDA receptor encephalitis: an observational cohort study. Lancet Neurol 2013; 12: 157–65.

Viaccoz A, Desestret V, Ducray F, Picard G, Cavillon G, Rogemond V, et al. Clinical specificities of adult male patients with NMDA receptor antibodies encephalitis. Neurology 2014; 82: 556–63.

Warikoo N, Brunwasser SJ, Benz A, Shu HJ, Paul SM, Lewis M, et al. Positive allosteric modulation as a potential therapeutic strategy in anti-NMDA receptor encephalitis. J Neurosci 2018; 38: 3218–29.

Wilding TJ, Lopez MN, Huettner JE. Chimeric glutamate receptor subunits reveal the transmembrane domain is sufficient for NMDA receptor pore properties but some positive allosteric modulators require additional domains. J Neurosci 2016; 36: 8815–25.

Wirtz PW, Titulaer MJ, Gerven JM, Verschuuren JJ. 3,4-diaminopyridine for the treatment of Lambert-Eaton myasthenic syndrome. Expert Rev Clin Immunol 2010; 6: 867–74.

SUPPLEMENTARY INFORMATION

Determination of plasma and brain concentration of SGE-301

SGE-301 was measured using liquid-liquid extraction and quantified by LC-MS/MS. Brain tissue was first diluted and homogenized at a ratio of 3 mL of PBS to 1 g of tissue. Five microliters of internal standard in methanol solution was added to 50 μL of plasma or brain homogenate sample. Calibrators and assay quality controls were made by spiking SGE-301 into control mouse plasma or brain homogenate and preparing them as samples. One hundred fifty-five microliters of sample was then mixed with 200 μL of deionized water and extracted with 1 mL of methyl-t-butyl ether. The organic layer was separated from the water layer and evaporated to dryness under nitrogen at 50°C for 15 minutes. The dry residue was reconstituted in 100 μL of 50% acetonitrile + 0.1% formic acid in deionized water. Five microliters of reconstituted sample was injected on an ACE 3 Phenyl-300 50 x 1 mm HPLC column. Gradient elution was performed using an Eksigent LC200 HPLC system running a water:acetonitrile gradient from 50% acetonitrile to 95% acetonitrile over 2.3 minutes at 100 μL/min.

Analyte detection was performed using a Sciex API4000 mass spectrometer running selected reaction monitoring of the analyte and internal standard in positive ion mode using a TurboV electrospray ion source. Sample concentrations were determined using the peak area ratio of analyte to internal standard and the least squares linear regression equation from the standard curve. Assay acceptance criteria for each LC-MS/MS run were +/- 20% accuracy compared to the nominal spiked concentration and +/- 20% CV.

Immunofluorescence and confocal studies with cultured live neurons

Primary hippocampal neurons were obtained from day 18 embryos of Wistar rats, as reported (Hughes *et al.*, 2010). Dissociated neurons were seeded on coverslips and grown in Corning® 35 mm x 10 mm dishes (Sigma-Aldrich, St Louis , MI, US) containing 1 ml of Neurobasal medium + B-27 Supplement (ThermoFisher, Waltham, MA, US). Seventeen-day *in vitro* cultures were then treated with patients' or controls' CSF (final

dilution 1:25 in the indicated media) along with SGE-301 (10 μM) or vehicle (control) for 24 hours at 37°C. After washing with PBS, neurons were serially incubated with a human CSF NMDAR antibody sample (1:100, used as primary antibody) for 1 hour at 4°C, and the secondary antibody Alexa Fluor 488 goat anti-human IgG (A-11013 1:1000, ThermoFisher) for 1 hour at 4°C. Neurons were then washed with PBS, fixed with 4% paraformaldehyde, permeabilized with 0.3% Triton TM X-100, blocked with 1% BSA for 30 minutes, and serially incubated with rabbit anti-PSD95 (1:200, ab18258 Abcam, Cambridge, UK) overnight at 4°C, and the corresponding secondary antibody Alexa Fluor 594 goat anti-rabbit IgG (1:1000, A11012, ThermoFisher) for 1 hour at 4°C. Slides were mounted with ProLong Gold antifade reagent for 4 minutes, containing 6-diamidino-2-phenylindole dihydrochloride (DAPI, P36935; ThermoFisher) and results scanned with a Zeiss LSM 710 confocal microscope with EC-Plan NEOFLUAR CS 100×/1.3 NA oil immersion objective. For spot analysis we performed image deconvolution using the AutoQuantX3 software (Bitplane, Oxford Instruments, Abingdon, UK) followed by automatic segmentation using the spot detection algorithm from Imaris suite 7.6.4 (Bitplane). Synaptic localization was defined as colocalization of NMDAR with postsynaptic PSD95, applying an algorithm for spot colocalization of NMDAR and PSD95 using Imaris 7.6.4 (Bitplane). The density of spots was indicated as number of puncta per μm-length of dendrite.

To determine the clusters of internalized antibody-bound receptors, neurons were treated as above with patients' CSF with SGE-301 or vehicle. Then neurons were washed with PBS, incubated with excess (1:20) secondary anti-human IgG Alexa Fluor 594 (red fluorescence, ThermoFisher) for 1 hour at 4°C, washed, fixed, permeabilized as above, and incubated with Alexa Fluor 488 goat anti-human IgG (1:1000, green fluorescence ThermoFisher) for 1 hour at 4°C. Slides were then mounted and the green fluorescence clusters quantified as above.

To determine whether prolonged treatment with SGE-301 modified the levels of NMDAR and phospho-S295-PSD95, neurons were treated as above for 48 hours with controls' CSF and SGE-301 or vehicle. Clusters of cell-surface synaptic and extrasynaptic NMDAR were immunolabeled as indicated, and neurons were then fixed and permeabilized as above and serially incubated with rabbit anti-phospho-S295-PSD95 (1:200, ab76108, Abcam) and mouse anti-PSD95 (1:200, 124 011, Synaptic Systems, Goettingen, Germany) overnight at 4°C, followed by the secondary antibodies Alexa Fluor 488 goat anti-rabbit IgG and Alexa Fluor 594 goat anti-mouse IgG (A-11034, A-11032, ThermoFisher) both at 1:500 dilution. Slides were then mounted and scanned, and the density of NMDARs, phospho-S295-PSD95 and PSD95 clusters was determined as above. Neurons treated for 24 hours with 25 μM bicuculline (#14340, Sigma-Aldrich), which is an antagonist of GABAa receptor that causes an increase of the levels of phospho-S295-PSD95 (Kim *et al.*, 2007) were used as control for this assay.

Electrophysiological studies

LTP and paired pulse facilitation in acute sections of hippocampus

Eighteen to 19 days after activation of the osmotic pumps and daily injection of drug or vehicle, mice were deeply anesthetized with isofluorane and decapitated. Brains were removed in ice-cold, high-sucrose extracellular artificial cerebrospinal fluid (aCSF1, in mM; 206 sucrose, 1.3 KCl, 1 $CaCl_2$, 10 $MgSO_4$, 26 $NaHCO_3$, 11 glucose, 1.25 NH_2PO_4, purged with 95% CO_2/5% O_2, pH 7.4) and subdivided into the hemispheres. Thick (380 μm) coronal slices of hippocampus were obtained with a vibratome (VT1000S; Leica Microsystems, Wetzlar, Germany) and transferred into an incubation beaker with extracellular aCSF appropriate for neurophysiological recordings (aCSF2, in mM; 119 NaCl, 2.5 KCl, 2.5 $CaCl_2$, 1.25 NaH_2PO_4, 1.5 $MgSO_4$, 25 $NaHCO_3$, 11 glucose, purged with 95 % CO_2/5 % O_2, pH 7.4). Slices were kept at 32°C for 1 hour and subsequently at RT for at least 1 additional hour. For field potential measurements, single slices were then transferred into a measurement chamber perfused with aCSF2 at 2 ml/min

at 28-30°C (controls' CSF + vehicle: number of acute slices n = 8 prepared from brain hemisections of seven mice; patients' CSF + vehicle: n = 6 from hemisections of five mice; controls' CSF + SGE-301: n = 10 from hemisections of seven mice; patients' CSF + SGE-301: n = 7 from hemisections of six mice). A bipolar stimulation electrode (Platinum-Iridium stereotrode, PI2ST30.1A5, Science Products, Hofheim, Germany) was placed in the Schaffer collateral pathway. Recording electrodes were made with a puller (P-1000, Shutter Instrument Company, Novato, CA, US) from thick-walled borosilicate glass with a diameter of 1.5 mm (Sutter Instruments). The recording electrode filled with aCSF2 was placed in the dendritic branching of the CA1 region for local field potential measurement (field excitatory postsynaptic potential, fEPSP). A stimulus isolation unit A385 (World Precision Instruments, Hertfordshire, UK) was used to elicit stimulation currents between 25-700 μA. Before baseline recordings for long-term potentiation (LTP), input-output (IO) curves were recorded for each slice at 0.03 Hz. The stimulation current was then adjusted in each recording to evoke fEPSPs at which the slope was at 50-60 % of maximally evoked fEPSP slope value. After baseline recording for 30 minutes with 0.03 Hz, LTP was induced by theta-burst stimulation (TBS; 10 theta bursts of four pulses of 100 Hz with an interstimulus interval of 200 ms repeated seven times with 0.03 Hz). After LTP induction, fEPSPs were recorded for 1 additional hour with 0.03 Hz. Paired-pulse fEPSPs in the test pathway were measured before baseline recordings with an interstimulus interval of 50 ms (controls' CSF + vehicle: number of acute slices n= 20 prepared from brain hemisections of eight mice; patients' CSF + vehicle: n = 12 from hemisections of six mice; controls' CSF + SGE-301: n = 17 from hemisections of eight mice; patients' CSF + SGE-301: n = 14 from hemisections of seven mice). All recordings were amplified and stored using amplifier AxoClamp 2B (Molecular Devices, San Jose, CA, US). Traces were analyzed using Axon pClamp software (Molecular Devices, version 10.6).

NMDAR-mediated spontaneous excitatory postsynaptic currents (sEPSC) in cultured neurons

To determine the effects of chronic exposure to SGE-301 on NMDAR currents we treated 18 days in vitro (d.i.v.) hippocampal neuronal cultures with controls' CSF (diluted 1:100) or controls' CSF + SGE-301 (10 μM) for 48h prior to whole-cell patch clamp recordings of spontaneous NMDAR-mediated excitatory postsynaptic currents (sEPSCs). Recordings were made using thin-walled electrodes with a resistance of 3-5 MΩ, giving a final series resistance of 5-15 MΩ. Extracellular solution contained (in mM): 130 NaCl, 3.5 KCl, 2 $CaCl_2$, 15 glucose, 20 sorbitol and 10 HEPES, (Mg^{2+}-free); osmolarity 300 mOsm/Kg and pH 7.4 with NaOH. In order to isolate NMDAR component, 100μM picrotoxin and 50μM NBQX were added to block $GABA_A$R-mediated IPSCs and AMPAR-mediated EPSCs, respectively. Intracellular pipette solution contained (in mM): 116 K-Gluconate, 6 KCl, 8 NaCl, 0.2 EGTA, 2 MgATP, 0.3 Na_3GTP and 10 HEPES; pH 7.25 with KOH. QX-314 at 2.5 mM was included into the pipette solution to block action potential firing in the recorded neuron. Spontaneous EPSCs were acquired at 2 kHz and filtered at 1 kHz at a holding potential of –70 mV. EPSCs were measured in periods ranging from 10 to 30 minutes. In experiments where the acute effect of SGE-301 was tested, a baseline period of 5 minutes in the absence of the drug was recorded followed by application of 10μM SGE-301 to the bath solution and a 10-15 minutes recording period after drug application. pClamp10/Clampfit10.6 software (Molecular Devices) were used to record, detect and analyze the amplitude, decay time constant and instantaneous frequency (from single sEPSCs).

Novel object location and locomotor activity

Both tasks were administered one day before surgical implantation of osmotic pumps and ventricular catheters, and once per week for four weeks after surgery (Fig. 1B).

Novel object location (NOL)

Animals were habituated to an empty, squared arena (45x45x40 cm, Panlab, Barcelona, Spain) with visual cues, and underwent two daily trials of 15 minutes each, for four days. The day of the test, animals were placed into the arena in presence of two equal objects positioned at two opposite corners and they were allowed to freely explore them for 9 minutes (familiarization phase). After a retention time of 3 hours, animals were returned to the arena, where one of the objects had been moved to a different corner. The animal was allowed to explore both objects for 9 minutes (test phase) and the time of exploration of each object was recorded. A discrimination index (NOL Index) was calculated using the following formula: Time of exploration of the moved object minus time of exploration of the not moved object divided by total time of exploration of both objects. A higher discrimination index indicates a better memory of the position of both objects. Object exploration is defined as any exploratory behavior triggered by the presence of the object (sniffing, biting, touching…) with the orientation of the nose toward the object within a distance of < 2 cm.

Locomotor activity

Animals were placed in locomotor activity boxes (11x21x18 cm, Imetronic, Passac, France) for 1 hour. The boxes are equipped with two rows of photocell beams that allow the measurement of small movements of the animal in each side of the box (local motor activity), the number of displacements from one side to the other of the box (horizontal activity) and the number of vertical explorations (rearings).

SUPPL FIG. 1: Absence of antibodies other than NMDAR in patients' CSF

Panels A and B show the immunostaining of rat brain by the pooled patients' CSF used in all experimental studies before (A) and after (B) immunoabsorption with NMDAR-expressing HEK293T cells. Scale bars = 200 μm.

Panels C-F show the immunolabeling of NMDAR-expressing HEK293T cells and neurons by the pooled patients' CSF before (C and D) and after (E and F) immunoabsorption with NMDAR-expressing HEK293T cells. Scale bars = 10 μm.

Panel G shows the effect of pooled patients' CSF antibodies on the density of total cell surface and synaptic NMDAR clusters before (not absorbed) and after (absorbed) immunoabsorption with NMDAR-expressing HEK293T cells. Note that the pooled patients' CSF causes the expected decrease of total cell surface and synaptic NMDAR, and that these effects are abrogated after immunoabsorption with NMDAR-expressing HEK cells. Box plots show the median, 25^{th} and 75^{th} percentiles; whiskers indicate the minimum or maximum values. Significance was assessed by one-way ANOVA ($p < 0.01$) and Bonferroni *post-hoc* correction test was applied: $^{**}p < 0.01$, $^{***}p < 0.001$, $^{****}p < 0.0001$.

SUPPL FIG. 2: Plasma and brain exposures of SGE-301 after subcutaneous administration

For all *in vivo* experiments, animals were administered 10 mg/kg SGE-301 via subcutaneous administration. Plasma and brain levels achieved after subcutaneous (SC) administration were similar to those previously reported after intraperitoneal (IP) administration (Paul *et al.*, 2013). Data points represent mean ± SEM levels of SGE-301. N= 4 mice per time point and matrix (e.g., 4 plasma 1 hour, 4 brain 1 hour, 4 plasma 4 hours, 4 brain 4 hours for a total of 16 animals).

SUPPL FIG. 3: SGE-301 decreases the number of antibody-bound internalized NMDAR

Panel A: Representative dendrites of neurons treated for 48 hours with patients' CSF with vehicle or SGE-301, showing the internalized antibody-bound NMDAR. Note that treatment with SGE-301 does not completely abrogate the internalization of receptors, Scale bars= 10 μm.

Panel B: Quantification of internalized clusters of antibody-bound receptors. There is a significant decrease of internalized receptors.

n = 20 dendrites per condition. Box plots show the median, 25^{th} and 75^{th} percentiles; whiskers indicate the whiskers indicate the minimum or maximum values. Significance of treatment effect was assessed by unpaired *t-test*. ****p <0,0001.

SUPPL FIG. 4: Cultures of rat hippocampal neurons treated for 48 hours with SGE-301 show a reduction of clusters of NMDAR and phospho-S295-PSD95

Panel A: Quantification of clusters of synaptic and extrasynaptic NMDAR in hippocampal cultures of neurons treated with controls' CSF along with vehicle or SGE-301. The presence of SGE-301 led to a significant reduction of clusters of NMDAR. Total surface NMDAR **p = 0.0020; synaptic NMDAR **p= 0.0085.

Panel B: Quantification of clusters of phospho-S295-PSD95 and PSD95 in hippocampal cultures of neurons treated with controls' CSF along with vehicle or SGE-301. The presence of SGE-301 leads to a significant reduction of phospho-S295-PSD95, $^{**}p < 0.01$. In this setting, SGE-301did not lead to a significant reduction of PSD95 (in contrast to the indicated reduction of PSD95 observed in mice hippocampus chronically treated with SGE-301, shown in Supplementary Fig. 5).

Panel C: Quantification of clusters of phospho-S295-PSD95 and PSD95 in hippocampal cultures of neurons treated with bicuculline. In this setting, bicuculline caused a significant reduction of phospho-S295-PSD95, as reported (Kim *et al.*, 2007). *$p < 0.05$

For all studies, n = 20 dendrites per condition. Box plots show the median, 25^{th} and 75^{th} percentiles; whiskers indicate the whiskers indicate the minimum or maximum values. Significance of treatment effect was assessed by unpaired *t-test*.

SUPPL FIG. 5: SGE-301 slows the decay phase of NMDAR-mediated spontaneous excitatory post-synaptic currents (sEPSC)

Panel A: Representative traces from spontaneous NMDAR-mediated EPSCs (sEPSC) recordings from hippocampal neuronal cultures treated with controls' CSF (light green trace) or controls´ CSF and SGE-301 (dark green) for 48h prior to recordings. sEPSCs were recorded at −70 mV in the presence of NBQX and picrotoxin and in the absence of TTX. Co-treatment with SGE-301 did not modify sEPSC amplitude or frequency but slowed the recovery (increase in decay time constant). Right inset shows a superposition of two sEPSCs to illustrate the longer duration of sEPSC in neurons treated with SGE-301.

Panel B: Mean amplitude, decay time constant (tau) and instantaneous frequency of NMDAR-mediated sEPSCs from neurons treated with controls´ CSF (ligh green columns; n=15 neurons) or controls´ CSF and SGE-301 (dark green columns; n=13). Controls' CSF vs controls' CSF + SGE-301: *$p < 0.05$ Student's t-test.

SUPPL FIG. 6: Administration of SGE-301 does not change the amount of patients' IgG present in mice hippocampus

Quantification of intensity of human IgG present in hippocampus of mice sacrificed on day 18. Mice infused with patients' CSF and treated with vehicle or SGE-301 show the same amount of IgG in the hippocampus, suggesting that SGE-301 does not block the binding of patients' antibodies to NMDAR. For all quantifications, mean intensity of IgG-immunostaining in the group of mice infused with controls' CSF and treated with vehicle was defined as 100%. Five animals of each experimental group were examined. Box plots show the median, 25^{th} and 75^{th} percentiles; whiskers indicate the minimum or maximum values.. Significance of treatment effect was assessed by one-way ANOVA ($p < 0.0001$) and *post-hoc* analyses were performed with Bonferroni correction; $*p < 0.05$.

SUPPL FIG. 7: Subcutaneous administration of SGE-301 leads in control mice to a reduction of clusters of phospho-S295-PSD95 and PSD95

Cluster density analysis of phospho-S295-PSD95 and PSD95 in brain tissue of animals infused with controls' CSF treated with vehicle or SGE-301. Note that animals treated with SGE-301 show a reduction of clusters of phospho-S295-PSD95 as well as PSD95. Five animals for each experimental group were examined. Box plots show the median, 25^{th} and 75^{th} percentiles; whiskers indicate whiskers indicate the minimum or maximum values. Significance of treatment effect was assessed by unpaired *t-test*; $****p < 0.0001$.

SUPPL FIG. 8: Paired-pulse facilitation is unaffected in animals infused with patients CSF and treated with or without SGE-301

Panel A: Example traces of fEPSPs in paired-pulse facilitation protocol applied to the Schaffer collateral - CA1 synaptic region. The fEPSP slope and amplitude in response to second stimulus (grey) are increased compared to the fEPSP slope and amplitude after the first stimulus (black) in all four groups of animals.

Panel B: Mean slope values of the fEPSPs in the response to the first (1st) and second (2nd) stimulus. All four experimental groups of animals show a significant increase in the fEPSP slope upon second stimulus. Controls' CSF + vehicle (n= 20 recordings from eight animals, light green); patients' CSF + vehicle (n= 12 recordings from six animals, pink); controls' CSF + SGE-301 (n= 17 recordings from eight animals, dark green); patients' CSF + SGE-301 (n= 14 recordings from seven animals, blue). Data are shown as mean ± SEM. Significance of the slope increase was assessed by unpaired *t-test*; $*p < 0.05$, $**p < 0.01$, $****p < 0.0001$. Interstimulus interval is 50 ms.

Panel C: Paired-pulse facilitation, calculated as P2/P1 (pulse 2/pulse 1) fEPSP slope ratio, with interstimulus interval of 50 ms, is not significantly altered in any of the experimental groups of animals when compared with that of the group infused with controls' CSF + vehicle. The number of recordings and animals used are the same as those indicated in B. The significance of the results was assessed by one-way ANOVA ($p > 0.05$, not significant). Box plots show the median, 25^{th} and 75^{th} percentiles; whiskers indicate the 10^{th} and 90^{th} percentile.

SUPPL FIG. 9: Total time of exploration and locomotor activity were not affected by treatment with SGE-301

Panel A: The total time of exploration of the two objects presented in each NOL test session was similar in the four experimental groups of animals. Animals infused with controls' CSF and treated with vehicle (n = 11, light green); animals infused with patients' CSF and treated with vehicle (n = 10, pink); animals infused with controls' CSF and treated with SGE-301 (n = 12, dark green), and animals infused with patients' CSF and treated with SGE-301 (n = 10, blue). Data are presented as mean ± SEM.

Panels B-D: The locomotor activity was similar in the four experimental groups of animals, including measurement of local movements (B), displacement from one side to the other of the cage (C), and vertical explorations or rearings (D). Each colored line indicates the same experimental condition described in panel A. Number of animals: infused with controls' CSF and treated with vehicle, n = 11; infused with patients' CSF and treated with vehicle, n = 11; infused with controls' CSF and treated with SGE-301, n = 12, and infused with patients' CSF and treated with SGE-301, n = 11.

Supplementary Table: Values and statistics for figures 2-5

Fig 2 (Cluster density (cultures of hippocampal neurons))					
Total NMDAR	**A**) Controls' CSF + vehicle	**B**) Patients' CSF + vehicle	**C**) Controls' CSF + SGE-301	**D**) Patients' CSF + SGE-301	
Median	12.17	5.23	12.1	11.66	A vs B p<0.0001
75% Percentile	14.46	7.97	13.41	13.99	B vs D p<0.0001
25% Percentile	9.59	4.07	9.18	9.71	
PSD95	**A**) Controls' CSF + vehicle	**B**) Patients' CSF + vehicle	**C**) Controls' CSF + SGE-301	**D**) Patients' CSF + SGE-301	
Median	12.09	11.12	10.56	10.88	
75% Percentile	14.81	13.58	12.34	13.03	
25% Percentile	9.88	8.55	9.04	8.65	
Synaptic NMDAR	**A**) Controls' CSF + vehicle	**B**) Patients' CSF + vehicle	**C**) Controls' CSF + SGE-301	**D**) Patients' CSF + SGE-301	
Median	2.69	1.56	2.38	2.66	A vs B p<0.0001
75% Percentile	3.6	2.06	2.99	3.34	A vs C p<0.0001
25% Percentile	1.97	1.15	1.87	2.18	B vs D p<0.0170
Fig 3 (Cluster density (Brain tissue))					
Total NMDAR	**A**) Controls' CSF + vehicle	**B**) Patients' CSF + vehicle	**C**) Controls' CSF + SGE-301	**D**) Patients' CSF + SGE-301	A vs B p<0.0001
Median	99.27	79.69	85.61	101.1	A vs C p=0.0001
75% Percentile	107.5	84.7	93.81	109.3	B vs D p<0.0001
25% Percentile	91.99	67.17	80.15	89.94	C vs D p<0.0001
PSD95	**A**) Controls' CSF + vehicle	**B**) Patients' CSF + vehicle	**C**) Controls' CSF + SGE-301	**D**) Patients' CSF + SGE-301	
Median	98.91	101.4	94.91	99.91	A vs C p=0.0003
75% Percentile	107.9	104.9	98.91	113.9	C vs D p<0.0001
25% Percentile	91.91	93.91	82.92	91.91	
Synaptic NMDAR	**A**) Controls' CSF + vehicle	**B**) Patients' CSF + vehicle	**C**) Controls' CSF + SGE-301	**D**) Patients' CSF + SGE-301	A vs B p<0.0001
Median	98.56	73.12	82.66	98.56	A vs C p=0.0009
75% Percentile	114.5	85.84	95.38	117.6	B vs D p<0.0001
25% Percentile	82.66	60.41	76.3	76.3	C vs D p<0.0001
Fig 4 (fEPSP slope change %)					
	A) Controls' CSF + vehicle	**B**) Patients' CSF + vehicle	**C**) Controls' CSF + SGE-301	**D**) Patients' CSF + SGE-301	
Median	86,41	17,2	63,5	67,37	A vs B p=0.0013
75% Percentile	123,1	24,73	79,27	123,9	B vs D p=0.0060
25% Percentile	65,26	-0,4091	52,53	49,77	B vs C p=0.0443
Fig 5 (Novel Object Location Index)					
Baseline	**A**) Controls' CSF + vehicle	**B**) Patients' CSF + vehicle	**C**) Controls' CSF + SGE-301	**D**) Patients' CSF + SGE-301	
Mean	0,239	0,345	0,299	0,376	
SEM	0,052	0,053	0,044	0,056	
N	11	10	12	10	
D3	**A**) Controls' CSF + vehicle	**B**) Patients' CSF + vehicle	**C**) Controls' CSF + SGE-301	**D**) Patients' CSF + SGE-301	
Mean	0,298	0,225	0,322	0,216	
SEM	0,053	0,028	0,050	0,089	
N	11	10	12	10	
D10	**A**) Controls' CSF + vehicle	**B**) Patients' CSF + vehicle	**C**) Controls' CSF + SGE-301	**D**) Patients' CSF + SGE-301	
Mean	0,320	-0,041	0,311	0,260	A vs B p<0.0001
SEM	0,036	0,046	0,015	0,060	B vs D p=0.0001
N	11	10	12	10	B vs C p<0.0001
D18	**A**) Controls' CSF + vehicle	**B**) Patients' CSF + vehicle	**C**) Controls' CSF + SGE-301	**D**) Patients' CSF + SGE-301	
Mean	0,254	-0,008	0,272	0,283	A vs B p=0.0007
SEM	0,040	0,063	0,031	0,055	B vs D p=0.0002
N	11	10	12	10	B vs C p=0.0002
D25	**A**) Controls' CSF + vehicle	**B**) Patients' CSF + vehicle	**C**) Controls' CSF + SGE-301	**D**) Patients' CSF + SGE-301	
Mean	0,248	0,256	0,230	0,259	
SEM	0,017	0,044	0,015	0,043	
N	11	10	12	10	

REFERENCES

Hughes EG, Peng X, Gleichman AJ, Lai M, Zhou L, Tsou R, *et al.* Cellular and synaptic mechanisms of anti-NMDA receptor encephalitis. J Neurosci 2010; 30: 5866-75.

Kim MJ, Futai K, Jo J, Hayashi Y, Cho K, Sheng M. Synaptic accumulation of PSD-95 and synaptic function regulated by phosphorylation of serine-295 of PSD-95. Neuron 2007; 56: 488-502.

Paul SM, Doherty JJ, Robichaud AJ, Belfort GM, Chow BY, Hammond RS, *et al.* The major brain cholesterol metabolite 24(S)-hydroxycholesterol is a potent allosteric modulator of N-methyl-D-aspartate receptors. J Neurosci 2013; 33: 17290-300.

SUPPL FIGURE 1

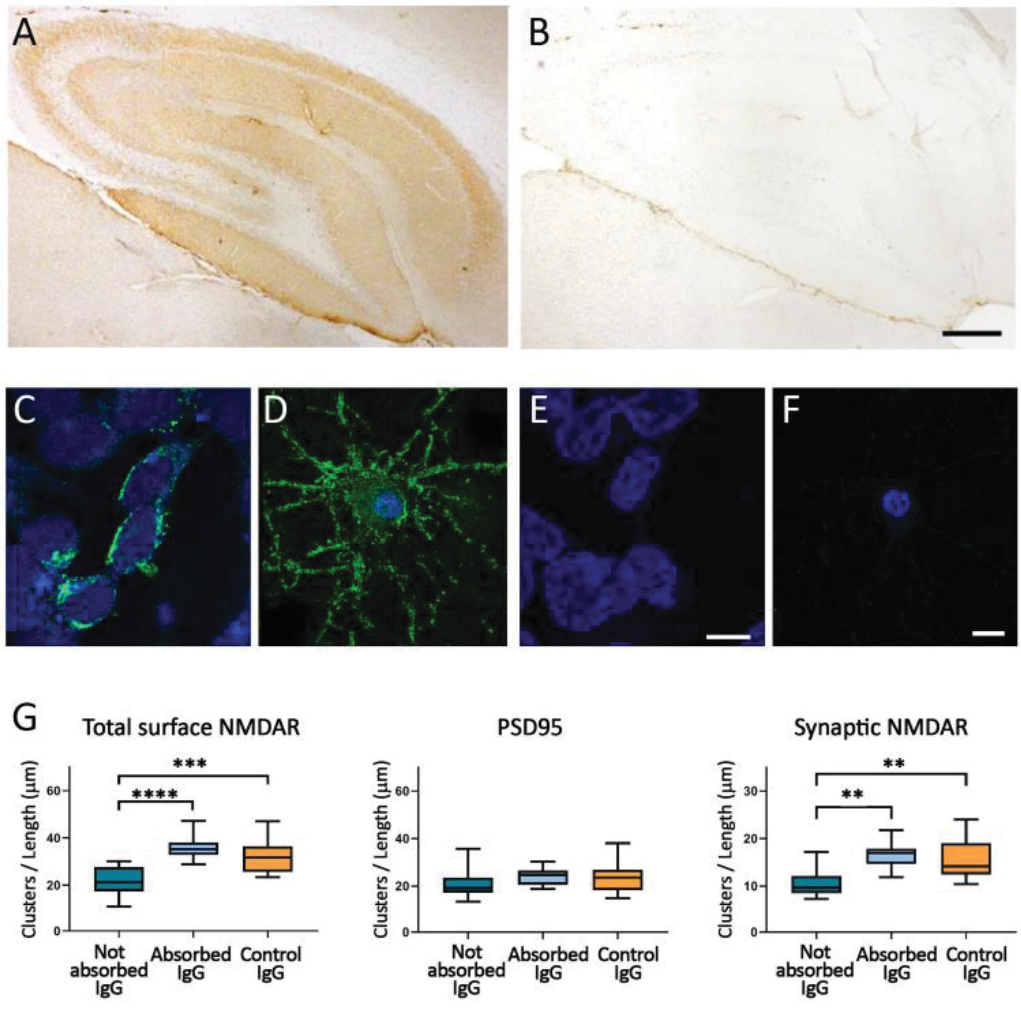

SUPPL FIGURE 2

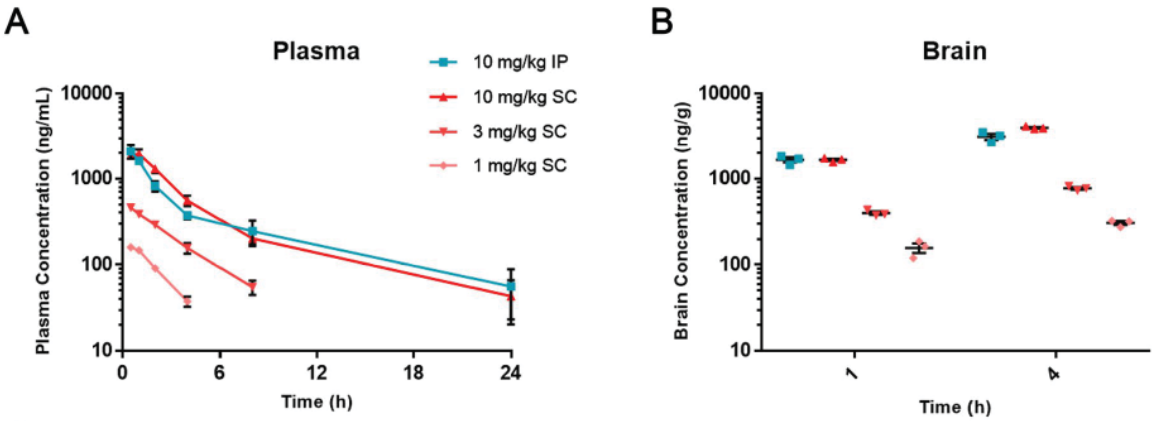

C

		10 mg/kg IP	10 mg/kg SC	3 mg/kg SC	1 mg/kg SC
C_{max}	ng/mL	2190	2083	462	164
T_{max}	h	0.67	0.83	0.50	0.67
$T_{1/2}$	h	5.4	4.3	2.5	1.5
AUC_{last}	ng*h/mL	6487	7340	1491	355

SUPPL FIGURE 3

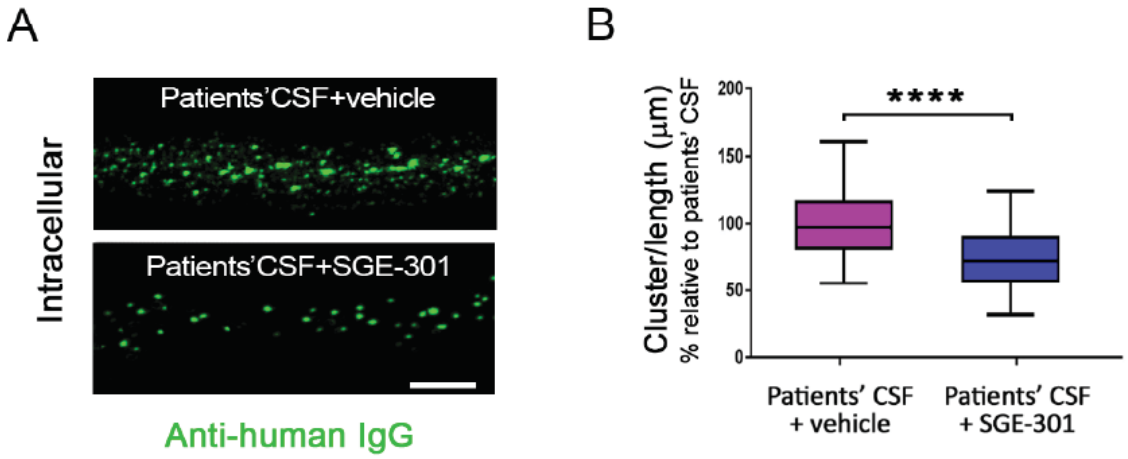

SUPPL FIGURE 4

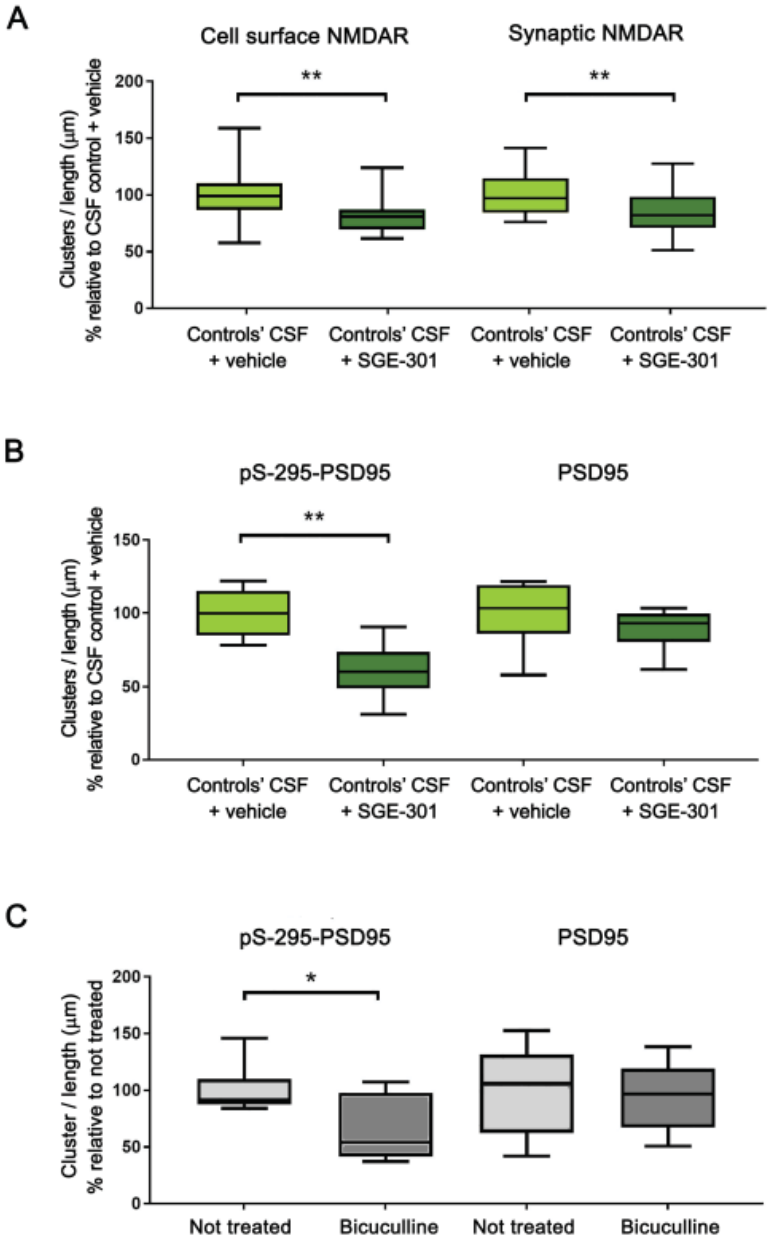

SUPPL FIGURE 5

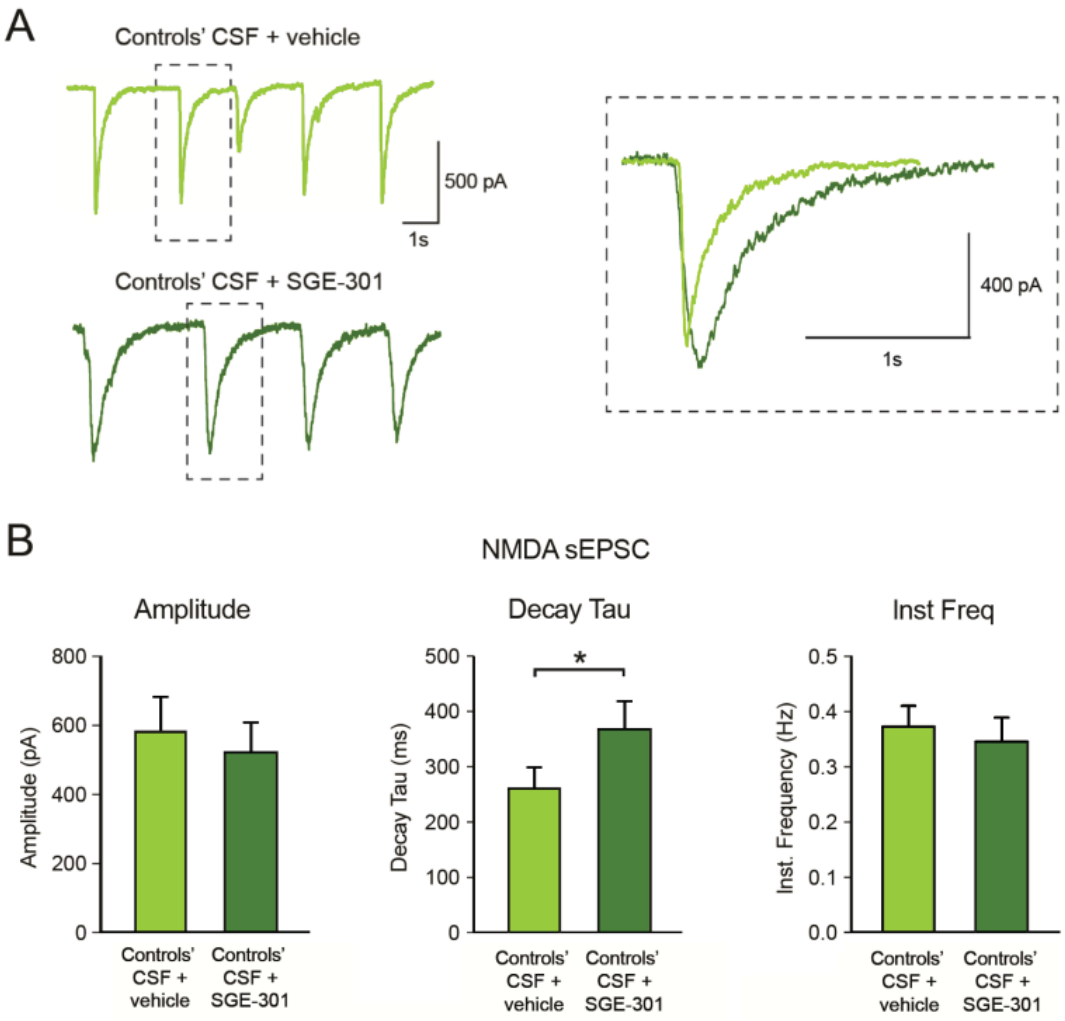

SUPPL FIGURE 6

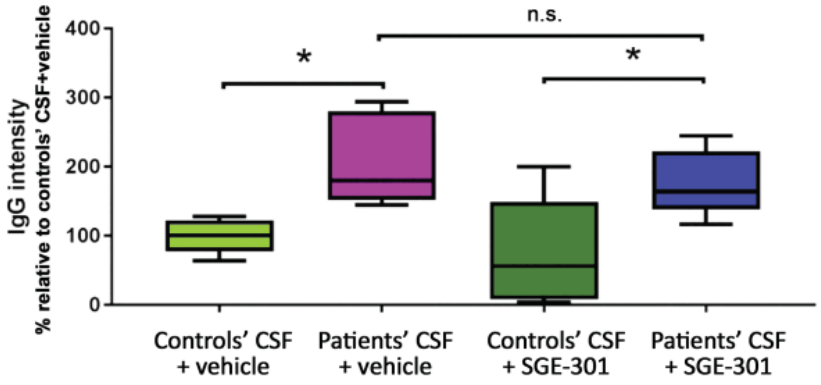

SUPPL FIGURE 7

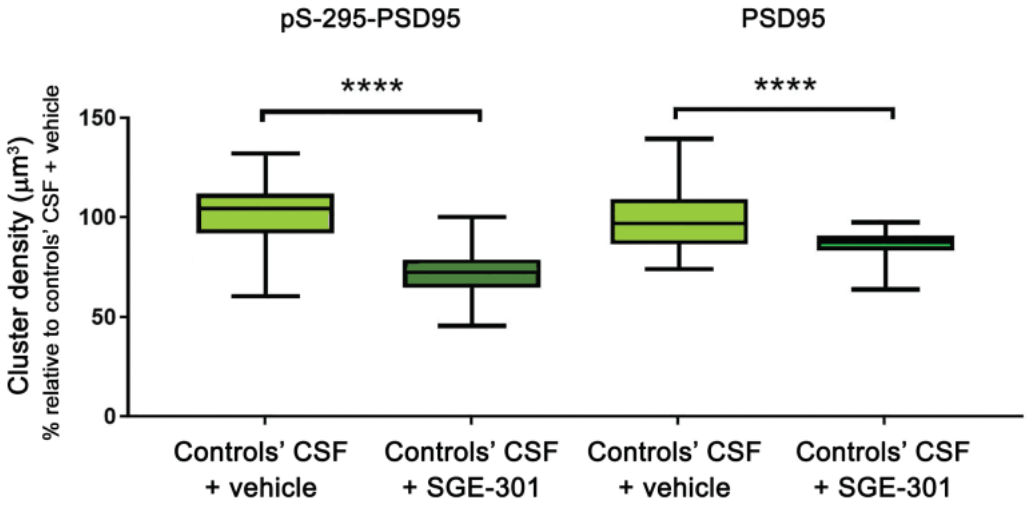

SUPPL FIGURE 8

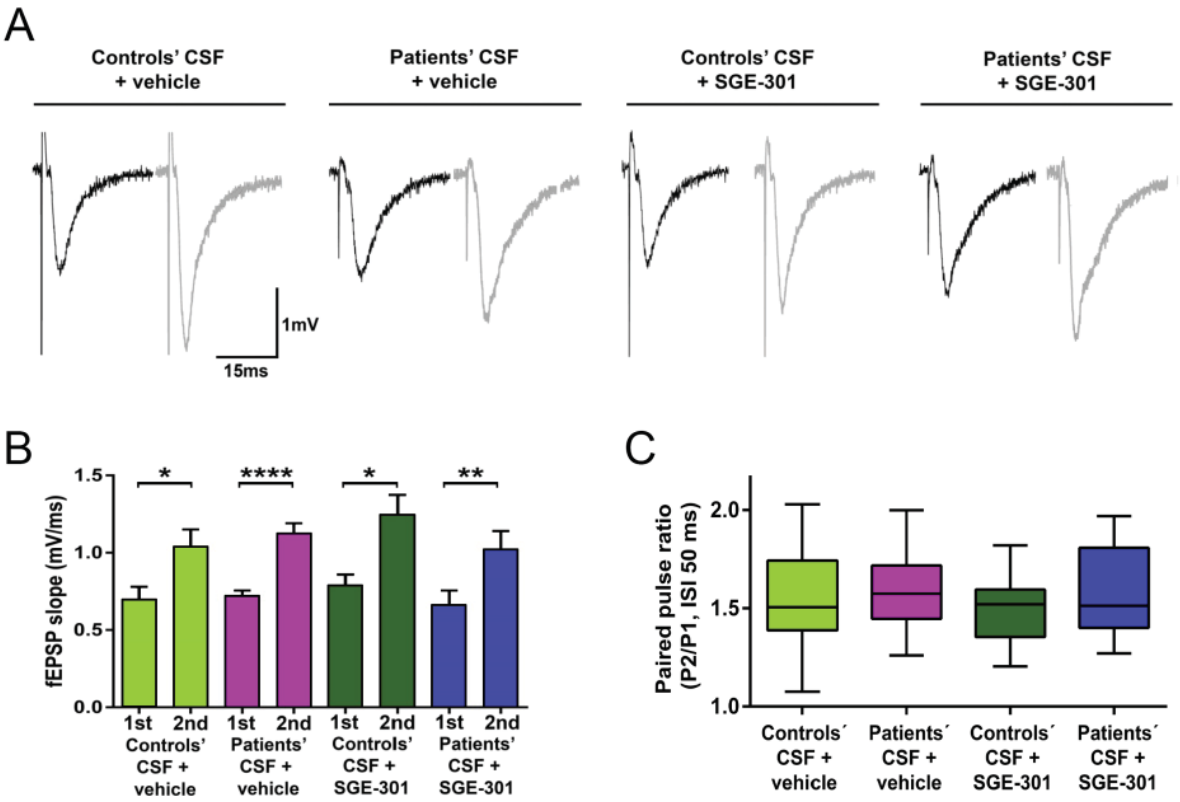

SUPPL FIGURE 9

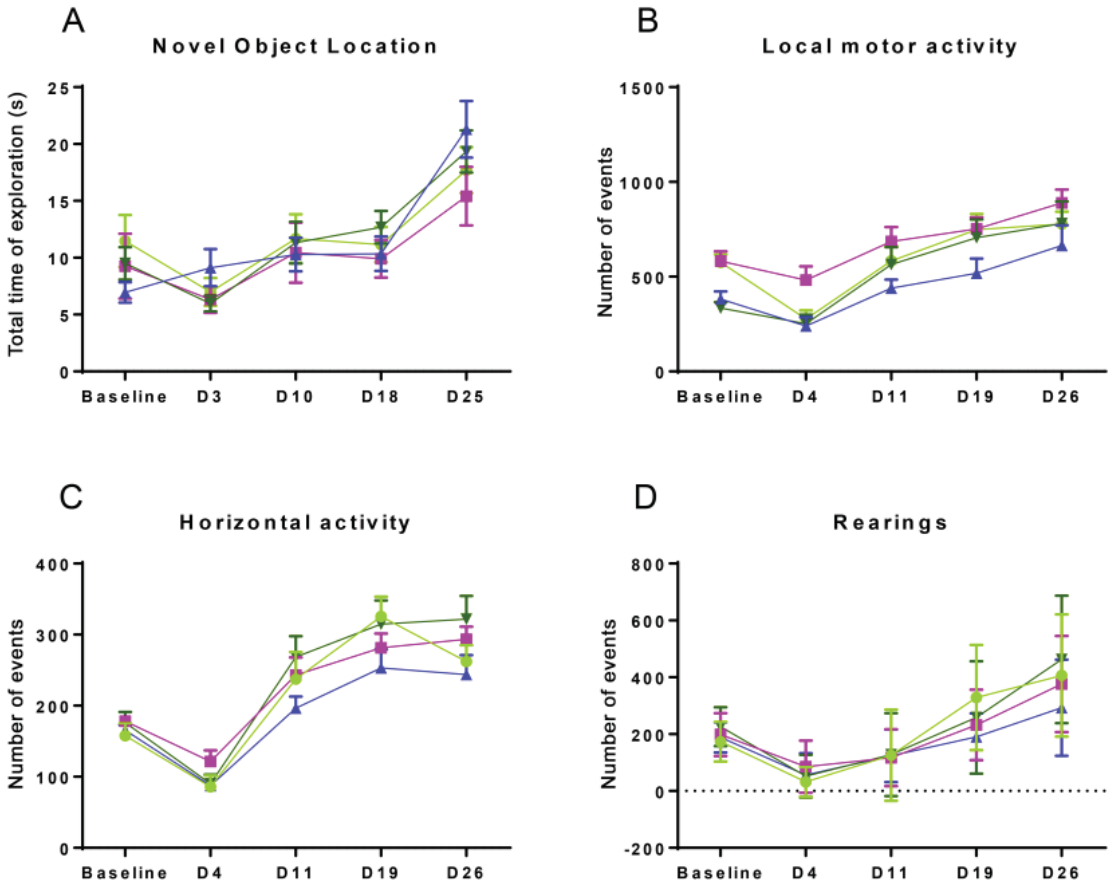

DISCUSSION

Anti-N-methyl-D-aspartate receptor (NMDAR) encephalitis is a severe autoantibody-mediated disease that associates with prominent neuropsychiatric symptoms.[84] Its identification fifteen years ago revealed a new category of autoimmune neurological diseases of previously unknown etiology, and since then, laboratory investigations on antibody pathogenicity have completely changed their clinical diagnosis, converting autoimmune encephalopathies from potentially lethal to now treatable diseases.[4]

Animal modeling of antibody-mediated encephalitis has been crucial to establish a causal link between the presence of autoantibodies in patients' CSF and the cognitive and behavioral alterations that patients develop. Indeed, the pioneering mouse model of anti-NMDAR encephalitis by passive cerebroventricular infusion of patients' antibodies reproduced memory deficits, depressive-like behavior,[11,12] and psychotic-like behavior[204] in mice that resembled the symptoms of the human disease.[84] As the most common antibody-mediated encephalitis, anti-NMDAR encephalitis has been, and is likely to remain, the spearhead of *in vivo* studies for other antibody-mediated diseases of the CNS, such as anti-AMPAR[205] or anti-LGI1 encephalitis.[16]

Anti-NMDAR encephalitis predominantly affects young women and patients' antibodies are of the IgG class;[85,93] thus, they can be transferred across the placenta in pregnant patients with anti-NMDAR encephalitis and potentially be detrimental for the fetus/newborn. Therefore, to study the effects of *in utero* exposure to antibodies from patients with anti-NMDAR encephalitis, the first and second objectives of this thesis emerged.

The **first objective** (**paper I**) of my thesis was to retrospectively collect clinical data from cases of anti-NMDAR encephalitis during pregnancy (both from consultations to our group and the literature) to report the effects of the disease and the outcome in patients and their babies.

The work for the **second objective** (**paper II**) occurred simultaneously; which consisted in the development of an animal model of placental transfer of IgG antibodies from patients with anti-NMDAR encephalitis by intravenous administration of patients' IgG to pregnant mice. This model allowed to further determine their potential pathogenic effects in neurodevelopment and behavior, and synaptic function in the fetus and offspring.

In **paper I**,[206] collected clinical data revealed that most infants from pregnant women with anti-NMDAR encephalitis were healthy at birth (with common premature birth), and all of those who had assessable follow-up (7–96 months) had normal development. Only 3 of 16 infants from mothers with anti-NMDAR encephalitis have been reported to present neonatal encephalopathy with transient neurological/respiratory symptoms.[197,207,208]

In **paper II**,[209] we demonstrated that patients' IgG infused to pregnant mice reached the fetal brain, and caused multiple alterations ranging from NMDAR synaptic changes to delayed neurodevelopment and behavioral deficits in the offspring, and that all these alterations progressively resolved after birth. The spontaneous reversibility of the patients' antibody-mediated alterations in our model of placental transfer of IgG (**paper II**) resembled the good outcome reported in the case series (**paper I**). Furthermore, the use of the animal model provided insight into the underlying synaptic and morphological mechanisms behind transient neurodevelopmental and behavioral alterations, such as reduction of NMDAR clusters, decreased thickness of cortical layers with increased cellular compaction, increased dendritic arborization accompanied by a reduction of mature (mushroom-shaped) dendritic spines and synaptic density, increased microglial activation, and impairment of hippocampal long-term plasticity.

As expected from previous experience with the animal model of infusion of patients' IgG into the cerebroventricular system of adult mice,[11,12] in the brain of fetuses *in utero* exposed to patients' IgG we observed a robust antibody-mediated decrease in NMDAR clusters (**paper II**). These effects occurred quickly (noted two days after injecting the antibodies to pregnant mice), and the reduction of NMDAR clusters and impairment of memory and hippocampal long-term plasticity were detectable during the first postnatal month.

In our immune-mediated model, the brain of mice exposed *in utero* to patients' IgG had decreased thickness of cortical layers II–IV along with increased cell density in the upper cortical layers that likely contributed to the restoration of the cortical layer thickness after postnatal day 21 (**paper II**). These findings are somewhat similar to those obtained in a model of genetic disruption of MeCP2 in the Rett syndrome model with a total rescue of cortical thickness after treatment with mirtazapine during postnatal day 28–42;[210] or in another model based on a constitutive reduction in central serotonin (VMAT2$^{sert\text{-}cre}$ mice), in which the total cortical thickness reduction at postnatal day 7 spontaneously recovered by day 14.[211]

In addition, we showed that hippocampal and cortical neurons from mice exposed *in utero* to patients' IgG showed an increase in dendritic arborization accompanied by a reduction of mature (mushroom-shaped) dendritic spines and synaptic density, which likely contributed to the impairment of hippocampal LTP. The effect of NMDAR hypofunction on dendritic arborization and the morphology of the spines is not well understood. In a cortex-specific GluN1 knockout model, the cortical neurons in layer IV elaborated exuberant dendritic specializations;[212] however, in a study using MK801 (an NMDAR antagonist) during early postnatal development, there was a transient decrease in dendritic arborization in

hippocampal pyramidal neurons that reversed when MK801 was discontinued.[213] Our findings resemble those of the cortex-specific GluN1 knockout, although in our immune model the alterations were reversible.

We believe that the increased dendritic arborization observed in animals exposed *in utero* to patients' IgG was likely caused by the reduction of NMDAR levels along with increased microglial activation compared to controls. Any perinatal immune challenge such as the binding of antibodies to NMDAR in the fetal brain can result in microglial activation[214] and consequently affect microglia-mediated synaptic pruning. For instance, impaired microglia-neuron interactions in CX3CR1-deficient mice showed delayed synaptic functional maturation[215] and immature and redundant connectivity. These alterations were attributed to reduced synaptic pruning[216] and spontaneously reverted by postnatal days 30–40,[215,216] similar to our findings.

In contrast to our findings, another mouse model of transplacental transfer of a human-derived NMDAR monoclonal antibody showed higher neonatal mortality (27%) compared to controls, impairment of native reflexes, and long-lasting neuropathologic alterations without evidence of reversibility.[199] We did not observe increased neonatal mortality, and the symptoms and developmental alterations spontaneously improved. The reasons for the discrepancies between the models are unclear. It is likely that compared to our model in which we used serum NMDAR antibodies representative of several patients, the lack of NMDAR antibodies repertoire in the monoclonal antibody model is less representative of the disease. Furthermore, the outcome of infants from pregnant patients with anti-NMDAR encephalitis (**paper I**) is remarkably different from that obtained with the mouse monoclonal antibody model.[199]

Despite the spontaneous reversibility of alterations, findings in our model (**paper II**) do not allow generalization of the notion that anti-NMDAR encephalitis during pregnancy does not represent a risk for serious effects in the offspring. In fact, our model lacks systemic inflammation and does not associate with encephalitis of the mothers, which in our experience (**paper I**) is the most important risk factor for obstetric complications and potential brain damage of the newborns. Limitations of **paper I** include the retrospective nature of the analysis and the small number of cases available. Therefore, future studies of pregnant patients who develop anti-NMDAR encephalitis with close follow-up of the babies are needed to determine the frequency of deficits and the timing of improvement.

The low frequency of antibody-mediated complications in newborns of patients with anti-NMDAR encephalitis may also be related to the timings of IgG placental transfer and BBB restriction properties for IgG crossing into the brain. In humans, placental transfer of maternal antibodies starts at 12–13 weeks of pregnancy[111,217,218] that is approximately the same time the BBB of the fetus starts to become more restrictive to the passage of albumin (and likely Igs) to the brain.[158] It is unknown whether the presence of maternal encephalitis or systemic inflammation might affect this time window, the function of the fetal BBB, or directly damage the developing fetal brain. Therefore, further studies on the potential effect of autoantibodies in a mouse model of autoimmune encephalitis by active immunization are needed.

Overall, results from translational research in **papers I** and **II** showed that patients who develop anti-NMDAR encephalitis during pregnancy or become pregnant during recovery often have obstetrical complications, but most of the newborns are healthy and appear to have normal development, and that in our mouse model placental transfer of these IgG caused severe but reversible synaptic and neurodevelopmental alterations.

These findings led us to explore how to abrogate the alterations produced in mice *in utero* exposed to patients' IgG in paper II. The FcRn is an Fc IgG receptor responsible for extending the half-life of IgG in serum[219] and for IgG transcytosis across the placenta during pregnancy.[111] In pregnant patients with autoantibody-mediated diseases pathogenic IgG antibodies are also transferred via placental FcRn from mother to fetus. Altogether, the **third objective** (**paper III**) of my thesis consisted in investigating whether treatment with an FcRn inhibitor prevented the placental transfer of patients' IgG and abrogated the antibody-mediated alterations in the same mouse model of placental transfer of IgG from patients with anti-NMDAR encephalitis

In **paper III**, we showed that the administration of a monoclonal FcRn antibody able to interfere with FcRn-IgG binding blocked the materno-fetal IgG transfer and prevented the pathogenic effects of NMDAR antibodies in mice fetuses and newborns previously reported in paper II, which include, (1) a decrease of the number of clusters of total cell-surface and synaptic NMDARs in the fetus, (2) reduction of the cortical plate thickness in the developing brain, (3) delay in neonatal developmental reflexes, (4) impairment of hippocampal long-term potentiation in newborns, and (5) deficit in visuospatial memory in the offspring.[209]

Blockade of FcRn-IgG binding using a monoclonal FcRn antibody prevented IgG from reaching fetal circulation in an *ex vivo* perfusion model of human placenta.[220] Furthermore, a previous animal model of antibody-mediated fetal and neonatal immune thrombocytopenia (FNIT) showed that treatment of the mothers with a FcRn antibody prevented the pathogenic effects

of the antibodies in the pups.[145] Despite the differences in the experimental design and location of the target antigens (periphery vs. CNS), our current data resembles that of the FNIT model, since blockade of FcRn with the same FcRn antibody prevented the pathogenic effects of NMDAR antibodies in mice fetuses and newborns. In addition, in a similar model using plasma from patients with myasthenia gravis and AChR antibodies treatment with another monoclonal FcRn antibody prevented the systemic complications of these antibodies in the fetus (arthrogryposis multiplex congenita).[221]

These novel strategies are promising for systemic antibody-mediated diseases. For instance, the use of FcRn antibodies has already reached clinical trial stage. Rozanolixizumab, a high affinity FcRn IgG4 antibody, and M281, also known as nipocalimab, are currently in phase III (NCT03971422) and phase II trials (NCT03772587) for the treatment of myasthenia gravis.[222,223] Nipocalimab, an IgG1 antibody with a high safety profile[224] is currently used in a phase II study (NCT03842189) in pregnant women at high risk for early onset severe hemolytic disease of the fetus and newborn.[225] However, efficiently blocking placental transfer of IgG may lead to a transient hypogammaglobulinemia of the infant. If so, this newborn with reduced maternal protective antibodies would be more prone to infections until its own immune system restores IgG levels, at around 6 months of age, as reported in cases of pregnant patients with genetic primary immunodeficiencies[226] or in those that received immunosuppressive treatment during pregnancy (e.g., rituximab).[227] Although no signs of infection were observed in the newborn mice that received FcRn antibody in our model, the possibility of IgG transient replacement therapy in the infants should be considered.

Moreover, in autoantibody-mediated diseases of the CNS there is an additional concern: the FcRn is also expressed in the BBB where it facilitates the transport of IgG from brain to blood.[127,228] Therefore, the efficacy of FcRn inhibitors should also be further studied in animal models of these diseases by active immunization before developing conclusions about their applicability in the clinics.

Given that it often takes several months or more than one year for treated patients with anti-NMDAR encephalitis to return to most of their activities, novel therapeutic strategies for a faster improvement are of interest. Thus, the fourth objective of this thesis was to study the potential therapeutic use of SGE-301, an oxysterol-based positive allosteric modulator of NMDAR, in a reported mouse model of passive cerebroventricular transfer of patients' CSF antibodies.

In **paper IV**,[229] I participated in the study of the potential therapeutic use of SGE-301, which is a very potent, direct, and selective positive allosteric modulator (PAM) of NMDARs, in a previous mouse model of anti-NMDAR encephalitis. In the reported model, passive transfer of patients' CSF antibodies into the cerebroventricular system of mice resulted in decrease of synaptic levels of these receptors, impairment of synaptic plasticity, and memory deficits.[11,12]

Findings from **paper IV** provided proof-of-concept that SGE-301, a synthetic analogue of a brain-derived cholesterol metabolite, prevented the pathogenic effects of antibodies from patients with anti-NMDAR encephalitis in hippocampal neuronal cultures and in a previously reported model of cerebroventricular transfer of antibodies.[11,12] SGE-301 increases channel open probability, potentiating NMDAR function.[230] Our findings in neurons and mice treated with SGE-301 are in line with previous studies in which SGE-301 prevented the antibody-mediated dysfunction of NMDARs in cultures of neurons exposed to CSF antibodies from patients with anti-NMDAR encephalitis,[231] or its administration in rats reverted the memory deficit caused by phencyclidine, a non-competitive NMDAR antagonist.[230] Despite the demonstration that SGE-301 does not interfere with the binding of patients' antibodies to NMDAR, the exact molecular mechanisms by which this PAM prevents the pathogenic effects of the antibodies are unknown.

Our study design does not allow for the assessment of whether SGE-301 reverses the antibody-mediated decrease of NMDAR and associated memory deficit because animals infused with patients' antibodies were simultaneously treated with SGE-301, and they did not develop any of those alterations. Previous studies showed that application of SGE-301 to neuronal cultures exposed to patient's antibodies for 24 hours accelerated the recovery from the antibody effects.[231] Currently, there is work in progress to determine whether SGE-301 is able to reverse symptoms and synaptic alterations already caused by patients' antibodies.

These findings and the good brain concentration after subcutaneous dosing suggest that oxysterol-based PAMs of NMDAR could serve as potential adjuvant treatment to mitigate or shorten the recovery in anti-NMDAR encephalitis. In preliminary studies, SAGE-718 (a PAM closely related to SGE-301 designed for oral bioavailability and once daily dosing) showed a good tolerability profile in healthy volunteers in a double-blind, placebo-controlled phase 1 single ascending dose study[232] and is currently being used in a trial for Huntington's disease (which, at early stages, appears to associate with reduced NMDAR function). The tasks for the future are to better understand the underlying mechanisms by which SGE-301 prevents patients' antibody-mediated effects, assess the ability of this compound to reverse already established symptoms, and determine its optimal dosing and frequency of treatment.

Overall, results from **paper IV** showed that daily subcutaneous administration of SGE-301 in the indicated animal model of cerebroventricular transfer of patients' NMDAR antibodies prevented the hippocampal memory impairment and all paradigms of synaptic alterations (decreased of NMDAR, impairment of LTP) consistently observed in this model when untreated.

CONCLUSIONS

General conclusions

Animal models are extremely valuable and useful research tools that enable the study of the pathogenesis or potential treatment strategies for complex diseases that involve several body systems. Anti-NMDAR encephalitis is the main neuronal antibody-mediated disease known to date. Therefore, animal models of this disease provide an experimental approach to investigate the pathogenicity of patients' antibodies and to explore novel strategies for this and similar autoimmune diseases.

Specific Conclusions

1. IgG antibodies from patients with anti-NMADR encephalitis intravenously injected to pregnant mice are transferred across the placenta, reach fetal brain and cause synaptic, functional and morphological alterations likely responsible for the delay in neurodevelopment and behavioral alterations after birth that spontaneously reverted without further implications in mature adulthood.

2. Findings in our model are in accordance with clinical experience: in pregnant patients with anti-NMDAR encephalitis, fetal exposure to maternal NMDAR antibodies infrequently associates with overt neurologic deficits, and in such cases, alterations in the infant are transient.

3. FcRn blocking with a specific monoclonal antibody in pregnant mice prevents placental transfer of IgG from anti-NMDAR encephalitis patients and abrogates the synaptic and neurodevelopmental alterations caused by patients' IgG in offspring, providing evidence of therapeutic potential in antibody-mediated diseases of the CNS during pregnancy.

4. SGE-301, or similar oxysterol-based PAMs of NMDAR, antagonizes the pathogenic effects of CSF antibodies from patients with anti-NMDAR encephalitis and could potentially serve as adjuvant treatment for the disease beyond immunotherapy.

REFERENCES

1 Graus F, Titulaer MJ, Balu R, *et al.* A clinical approach to diagnosis of autoimmune encephalitis. *Lancet Neurol* 2016; **15**: 391–404.

2 Smitt PS, Kinoshita A, De Leeuw B, *et al.* Paraneoplastic Cerebellar Ataxia Due to Autoantibodies against a Glutamate Receptor. *N Engl J Med* 2000; **342**: 21–7.

3 Sabater L, Gaig C, Gelpi E, *et al.* A novel non-rapid-eye movement and rapid-eye-movement parasomnia with sleep breathing disorder associated with antibodies to IgLON5: A case series, characterisation of the antigen, and post-mortem study. *Lancet Neurol* 2014; **13**: 575–86.

4 Dalmau J, Geis C, Graus F. Autoantibodies to Synaptic Receptors and Neuronal Cell Surface Proteins in Autoimmune Diseases of the Central Nervous System. *Physiol Rev* 2017; **97**: 839–87.

5 Ances BM, Vitaliani R, Taylor RA, *et al.* Treatment-responsive limbic encephalitis identified by neuropil antibodies: MRI and PET correlates. *Brain* 2005; **128**: 1764–77.

6 Vincent A, Buckley C, Schott JM, *et al.* Potassium channel antibody-associated encephalopathy: A potentially immunotherapy-responsive form of limbic encephalitis. *Brain* 2004; **127**: 701–12.

7 Landa J, Guasp M, Petit-Pedrol M, *et al.* Seizure-related 6 homolog like 2 autoimmunity: Neurologic syndrome and antibody effects. *Neurol Neuroimmunol Neuroinflamm* 2021; **8**: e916.

8 Ruiz-García R, Martínez-Hernández E, Joubert B, *et al.* Paraneoplastic cerebellar ataxia and antibodies to metabotropic glutamate receptor 2. *Neurol Neuroimmunol Neuroinflamm* 2020; **7**: e658.

9 Hughes EG, Peng X, Gleichman AJ, *et al.* Cellular and Synaptic Mechanisms of Anti-NMDA Receptor Encephalitis. *J Neurosci* 2010; **30**: 5866–75.

10 Mikasova L, De Rossi P, Bouchet D, *et al.* Disrupted surface cross-talk between NMDA and Ephrin-B2 receptors in anti-NMDA encephalitis. *Brain* 2012; **135**: 1606–21.

11 Planagumà J, Leypoldt F, Mannara F, *et al.* Human N-methyl D-aspartate receptor antibodies alter memory and behaviour in mice. *Brain* 2015; **138**: 94–109.

12 Planagumà J, Haselmann H, Mannara F, *et al.* Ephrin-B2 prevents N-methyl-D-aspartate receptor antibody effects on memory and neuroplasticity. *Ann Neurol* 2016; **80**: 388–400.

13 Peng X, Hughes EG, Moscato EH, Parsons TD, Dalmau J, Balice-Gordon RJ. Cellular plasticity induced by anti-α-amino-3-hydroxy-5-methyl-4-isoxazolepropionic acid (AMPA) receptor encephalitis antibodies. *Ann Neurol* 2015; **77**: 381–98.

14 Lancaster E, Lai M, Peng X, *et al.* Antibodies to the GABAB receptor in limbic encephalitis with seizures: case series and characterisation of the antigen. *Lancet Neurol* 2010; **9**: 67–76.

15 Ohkawa T, Fukata Y, Yamasaki M, *et al.* Autoantibodies to epilepsy-related LGI1 in limbic encephalitis neutralize LGI1-ADAM22 interaction and reduce synaptic AMPA receptors. *J Neurosci* 2013; **33**: 18161–74.

16 Petit-Pedrol M, Sell J, Planagumà J, *et al.* LGI1 antibodies alter Kv1.1 and AMPA receptors changing synaptic excitability, plasticity and memory. *Brain* 2018; **141**: 3144–59.

17 Pinatel D, Hivert B, Boucraut J, *et al.* Inhibitory axons are targeted in hippocampal cell culture by anti-Caspr2 autoantibodies associated with limbic encephalitis. *Front Cell Neurosci* 2015; **9**: 265.

18 Petit-Pedrol M, Armangue T, Peng X, *et al.* Encephalitis with refractory seizures, status epilepticus, and antibodies to the GABAAreceptor: A case series, characterisation of the antigen, and analysis of the effects of antibodies. *Lancet Neurol* 2014; **13**: 276–86.

19 Hara M, Ariño H, Petit-Pedrol M, *et al.* DPPX antibody-associated encephalitis Main syndrome and antibody effects. *Neurology* 2017; **88**: 1340–8.

20 Sinmaz N, Tea F, Pilli D, *et al.* Dopamine-2 receptor extracellular N-terminus regulates receptor surface availability and is the target of human pathogenic antibodies from children with movement and psychiatric disorders. *Acta Neuropathol Commun* 2016; **4**: 126.

21 Spatola M, Sabater L, Planagumà J, *et al.* Encephalitis with mGluR5 antibodies: Symptoms and antibody effects. *Neurology* 2018; **90**: e1964–72.

22 Gresa-Arribas N, Planagumà J, Petit-Pedrol M, *et al.* Human neurexin-3α antibodies associate with encephalitis and alter synapse development. *Neurology* 2016; **86**: 2235–42.

23 Landa J, Gaig C, Plagumà J, *et al.* Effects of IgLON5 Antibodies on Neuronal Cytoskeleton: A Link between Autoimmunity and Neurodegeneration. *Ann Neurol* 2020; **88**: 1023–7.

24 Werner C, Pauli M, Doose S, *et al.* Human autoantibodies to amphiphysin induce defective presynaptic vesicle dynamics and composition. *Brain* 2016; **139**: 365–79.

25 Sommer C, Weishaupt A, Brinkhoff J, *et al.* Paraneoplastic stiff-person syndrome: Passive transfer to rats by means of IgG antibodies to amphiphysin. *Lancet* 2005; **365**: 1406–11.

26 De Graaff E, Maat P, Hulsenboom E, *et al.* Identification of delta/notch-like epidermal growth factor-related receptor as the Tr antigen in paraneoplastic cerebellar degeneration. *Ann Neurol* 2012; **71**: 815–24.

27 Coesmans M, Sillevis Smitt PA, Linden DJ, *et al.* Mechanisms underlying cerebellar motor deficits due to mGluR1-autoantibodies. *Ann Neurol* 2003; **53**: 325–36.

28 Pinto A, Gillard S, Moss F, *et al.* Human autoantibodies specific for the α1A calcium channel subunit reduce both P-type and Q-type calcium currents in cerebellar neurons. *Proc Natl Acad Sci U S A* 1998; **95**: 8328–33.

29 Liao YJ, Safa P, Chen YR, Sobel RA, Boyden ES, Tsien RW. Anti-Ca2+ channel antibody attenuates Ca2+ currents and mimics cerebellar ataxia in vivo. *Proc Natl Acad Sci U S A* 2008; **105**: 2705–10.

30 Martín-García E, Mannara F, Gutiérrez-Cuesta J, *et al.* Intrathecal injection of P/Q type voltage-gated calcium channel antibodies from paraneoplastic cerebellar degeneration cause ataxia in mice. *J Neuroimmunol* 2013; **261**: 53–9.

31 Carvajal-González A, Leite MI, Waters P, *et al.* Glycine receptor antibodies in PERM and related syndromes: Characteristics, clinical features and outcomes. *Brain* 2014; **137**: 2178–92.

32 Crisp SJ, Dixon CL, Jacobson L, *et al.* Glycine receptor autoantibodies disrupt inhibitory neurotransmission. *Brain* 2019; **142**: 3398–410.

33 Rauschenberger V, von Wardenburg N, Schaefer N, *et al.* Glycine Receptor Autoantibodies Impair Receptor Function and Induce Motor Dysfunction. *Ann Neurol* 2020; **88**: 544–61.

34 Landa J, Guasp M, Míguez-Cabello F, *et al.* Encephalitis with Autoantibodies against the Glutamate Kainate Receptors GluK2. *Ann Neurol* 2021. DOI:10.1002/ana.26098.

35 Dalmau J. NMDA receptor encephalitis and other antibody-mediated disorders of the synapse. *Neurology* 2016; **87**: 2471–82.

36 Darnell RB, Posner JB. Paraneoplastic Syndromes Involving the Nervous System. *N Engl J Med* 2003; **349**: 1543–54.

37 Graus F, Dalmau J. Paraneoplastic neurological syndromes in the era of immune-checkpoint inhibitors. *Nat Rev Clin Oncol* 2019; **16**: 535–48.

38 Graus F, Keime-Guibert F, Reñe R, *et al.* Anti-Hu-associated paraneoplastic encephalomyelitis: Analysis of 200 patients. *Brain* 2001; **124**: 1138–48.

39 Albert ML, Austin LM, Darnell RB. Detection and treatment of activated T cells in the cerebrospinal fluid of patients with paraneoplastic cerebellar degeneration. *Ann Neurol* 2000; **47**: 9–17.

40 Graus F, Delattre JY, Antoine JC, *et al.* Recommended diagnostic criteria for paraneoplastic neurological syndromes. *J Neurol Neurosurg Psychiatry* 2004; **75**: 1135–40.

41 Antoine JC, Cinotti L, Tilikete C, *et al.* [18F]fluorodeoxyglucose positron emission tomography in the diagnosis of cancer in patients paraneoplastic neurological syndrome and anti-Hu antibodies. *Ann Neurol* 2000; **48**: 105–8.

42 Titulaer MJ, Wirtz PW, Willems LNA, Van Kralingen KW, Smitt PAES, Verschuuren JJGM. Screening for small-cell lung cancer: A follow-up study of patients with Lambert-Eaton myasthenic syndrome. *J Clin Oncol* 2008; **26**: 4276–81.

43 Titulaer MJ, Soffietti R, Dalmau J, *et al.* Screening for tumours in paraneoplastic syndromes: Report of an EFNS Task Force. *Eur J Neurol* 2011; **18**: 19-e3.

44 Peterson K, Rosenblum MK, Kotanides H, Posner JB. Paraneoplastic cerebellar degeneration: I.A clinical analysis of 55 anti–Yo antibody–positive patients. *Neurology* 1992; **42**: 1931–7.

45 Cooper R, Khakoo Y, Matthay KK, *et al.* Opsoclonus-myoclonus-ataxia syndrome in neuroblastoma: Histopathologic features - A report from the children's cancer group. *Med Pediatr Oncol* 2001; **36**: 623–9.

46 Rosenblum MK. Paraneoplasia and Autoimmunologic Injury of the Nervous System: The Anti-Hu Syndrome. *Brain Pathol* 1993; **3**: 199–212.

47 Albert ML, Darnell JC, Bender A, Francisco LM, Bhardwaj N, Darnell RB. Tumor-specific killer cells in paraneoplastic cerebellar degeneration. *Nat Med* 1998; **4**: 1321–4.

48 Bernal F, Graus F, Pifarré À, Saiz A, Benyahia B, Ribalta T. Immunohistochemical analysis of anti-Hu-associated paraneoplastic encephalomyelitis. *Acta Neuropathol* 2002; **103**: 509–15.

49 Bien CG, Vincent A, Barnett MH, *et al.* Immunopathology of autoantibody-associated encephalitides: Clues for pathogenesis. *Brain* 2012; **135**: 1622–38.

50 Blumenthal DT, Salzman KL, Digre KB, Jensen RL, Dunson WA, Dalmau J. Early pathologic findings and long-term improvement in anti-Ma2-associated encephalitis. *Neurology* 2006; **67**: 146–9.

51 Joseph CG, Darrah E, Shah AA, *et al.* Association of the autoimmune disease scleroderma with an immunologic response to cancer. *Science* 2014; **343**: 152–7.

52 Small M, Treilleux I, Couillault C, *et al.* Genetic alterations and tumor immune attack in Yo paraneoplastic cerebellar degeneration. *Acta Neuropathol* 2018; **135**: 569–79.

53 Corriveau RA, Huh GS, Shatz CJ. Regulation of class I MHC gene expression in the developing and mature CNS by neural activity. *Neuron* 1998; **21**: 505–20.

54 Dalmau J, Graus F, Villarejo A, *et al.* Clinical analysis of anti-Ma2-associated encephalitis. *Brain* 2004; **127**: 1831–44.

55 Pittock SJ, Lucchinetti CF, Lennon VA. Anti-neuronal nuclear autoantibody type 2: Paraneoplastic accompaniments. *Ann Neurol* 2003; **53**: 580–7.

56 Drlicek M, Bianchi G, Bogliun G, *et al.* Antibodies of the anti-Yo and anti-Ri type in the absence of paraneoplastic neurological syndromes: A long-term survey of ovarian cancer patients. *J Neurol* 1997; **244**: 85–9.

57 Monstad SE, Knudsen A, Salvesen HB, Aarseth JH, Vedeler CA. Onconeural antibodies in sera from patients with various types of tumours. *Cancer Immunol Immunother* 2009; **58**: 1797–802.

58 Titulaer MJ, Klooster R, Potman M, *et al.* SOX antibodies in small-cell lung cancer and Lambert-Eaton myasthenic syndrome: Frequency and relation with survival. *J Clin Oncol* 2009; **27**: 4260–7.

59 Graus F, Dalmau J, Reñé R, *et al.* Anti-Hu antibodies in patients with small-cell lung cancer: Association with complete response to therapy and improved survival. *J Clin Oncol* 1997; **15**: 2866–72.

60 Tanaka M, Tanaka K, Idezuka J, Tsuji S. Failure to detect cytotoxic T cell activity against recombinant Yo protein using autologous dendritic cells as the target in a patient with paraneoplastic cerebellar degeneration and anti-Yo antibody. *Exp Neurol* 1998; **150**: 337–8.

61 Croteau D, Owainati A, Dalmau J, Rogers LR. Response to cancer therapy in a patient with a paraneoplastic choreiform disorder. *Neurology* 2001; **57**: 719–22.

62 Vigliani MC, Palmucci L, Polo P, *et al.* Paraneoplastic opsoclonus-myoclonus associated with renal cell carcinoma and responsive to tumour ablation. *J Neurol Neurosurg Psychiatry* 2001; **70**: 814–5.

63 Altman AJ, Baehner RL. Favorable prognosis for survival in children with coincident opso-myoclonus and neuroblastoma. *Cancer* 1976; **37**: 846–52.

64 Maddison P, Newsom-Davis J, Mills KR, Souhami RL. Favourable prognosis in Lambert-Eaton myasthenic syndrome and small-cell lung carcinoma. *Lancet* 1999; **353**: 117–8.

65 Hiyama E, Yokoyama T, Ichikawa T, *et al.* Poor outcome in patients with advanced stage neuroblastoma and coincident opsomyoclonus syndrome. *Cancer* 1994; **74**: 1821–6.

66 Drachman DB, Adams RN, Josifek LF, Self SG. Functional Activities of Autoantibodies to Acetylcholine Receptors and the Clinical Severity of Myasthenia Gravis. *N Engl J Med* 1982; **307**: 769–75.

67 Nagel A, Engel AG, Lang B, Newsom-Davis J, Fukuoka T. Lambert-Eaton myasthenic syndrome IgG depletes presynaptic membrane active zone particles by antigenic modulation. *Ann Neurol* 1988; **24**: 552–8.

68 Dale HH, Feldberg W, Vogt M. Release of acetylcholine at voluntary motor nerve endings. *J Physiol* 1936; **86**: 353–80.

69 Liyanage Y, Hoch W, Beeson D, Vincent A. The agrin/muscle-specific kinase pathway: New targets for autoimmune and genetic disorders at the neuromuscular junction. *Muscle and Nerve* 2002; **25**: 4–16.

70 Vincent A. Unravelling the pathogenesis of myasthenia gravis. *Nat Rev Immunol* 2002; **2**: 797–804.

71 Drachman DB, Angus CW, Adams RN, Michelson JD, Hoffman GJ. Myasthenic Antibodies Cross-Link Acetylcholine Receptors to Accelerate Degradation. *N Engl J Med* 1978; **298**: 1116–22.

72 Waterman SA, Lang B, Newsom-Davis J. Effect of Lambert-Eaton myasthenic syndrome antibodies on autonomic neurons in the mouse. *Ann Neurol* 1997; **42**: 147–56.

73 Lang B, Vincent A. Autoimmune disorders of the neuromuscular junction. *Curr Opin Pharmacol* 2009; **9**: 336–40.

74 Drachman DB, McIntosh KR, Reim J, Balcer L. Strategies for Treatment of Myasthenia Gravis. *Ann N Y Acad Sci* 1993; **681**: 515–28.

75 Wirtz PW, Titulaer MJ, Van Gerven JMA, Verschuuren JJ. 3,4-diaminopyridine for the treatment of Lambert-Eaton myasthenic syndrome. *Expert Rev Clin Immunol* 2010; **6**: 867–74.

76 Roberts A, Perera S, Lang B, Vincent A, Newsom-Davis J. Paraneoplastic myasthenic syndrome IgG inhibits 45Ca 2+ flux in a human small cell carcinoma line. *Nature* 1985; **317**: 737–9.

77 Marx A, Kirchner T, Hoppe F, *et al.* Proteins with epitopes of the acetylcholine receptor in epithelial cell cultures of thymomas in myasthenia gravis. *Am J Pathol* 1989; **134**: 865–77.

78 Kornstein MJ, Asher O, Fuchs S. Acetylcholine receptor α-subunit and myogenin mRNAs in thymus and thymomas. *Am J Pathol* 1995; **146**: 1320–4.

79 Buckley C, Douek D, Newsom-Davis J, Vincent A, Willcox N. Mature, long-lived CD4+ and CD8+ T cells are generated by the thymoma in myasthenia gravis. *Ann Neurol* 2001; **50**: 64–72.

80 Hoffacker V, Schult A, Tiesinga JJ, *et al.* Thymomas alter the T-cell subset composition in the blood: A potential mechanism for thymoma-associated autoimmune disease. *Blood* 2000; **96**: 3872–9.

81 Vincent A, Willcox N, Hill M, Curnow J, MacLennan C, Beeson D. Determinant spreading and immune responses to acetylcholine receptors in myasthenia gravis. *Immunol Rev* 1998; **164**: 157–68.

82 Vitaliani R, Mason W, Ances B, Zwerdling T, Jiang Z, Dalmau J. Paraneoplastic encephalitis, psychiatric symptoms, and hypoventilation in ovarian teratoma. *Ann Neurol* 2005; **58**: 594–604.

83 Dalmau J, Tüzün E, Wu HY, *et al.* Paraneoplastic anti-N-methyl-D-aspartate receptor encephalitis associated with ovarian teratoma. *Ann Neurol* 2007; **61**: 25–36.

84 Dalmau J, Armangué T, Planagumà J, *et al.* An update on anti-NMDA receptor encephalitis for neurologists and psychiatrists: mechanisms and models. *Lancet Neurol* 2019; **18**: 1045–57.

85 Titulaer MJ, McCracken L, Gabilondo I, *et al.* Treatment and prognostic factors for long-term outcome in patients with anti-NMDA receptor encephalitis: An observational cohort study. *Lancet Neurol* 2013; **12**: 157–65.

86 Irani SR, Bera K, Waters P, *et al.* N-methyl-d-aspartate antibody encephalitis: Temporal progression of clinical and paraclinical observations in a predominantly non-paraneoplastic disorder of both sexes. *Brain* 2010; **133**: 1655–67.

87 Florance NR, Davis RL, Lam C, *et al.* Anti-N-methyl-D-aspartate receptor (NMDAR) encephalitis in children and adolescents. *Ann Neurol* 2009; **66**: 11–8.

88 Kayser MS, Dalmau J. Anti-NMDA receptor encephalitis, autoimmunity, and psychosis. *Schizophr Res* 2016; **176**: 36–40.

89 Dalmau J, Gleichman AJ, Hughes EG, *et al.* Anti-NMDA-receptor encephalitis: case series and analysis of the effects of antibodies. *Lancet Neurol* 2008; **7**: 1091–8.

90 Dalmau J, Graus F. Antibody-mediated encephalitis. *N Engl J Med* 2018; **378**: 840–51.

91 Moscato EH, Jain A, Peng X, Hughes EG, Dalmau J, Balice-Gordon RJ. Mechanisms underlying autoimmune synaptic encephalitis leading to disorders of memory, behavior and cognition: Insights from molecular, cellular and synaptic studies. *Eur J Neurosci* 2010; **32**: 298–309.

92 Gleichman AJ, Spruce LA, Dalmau J, Seeholzer SH, Lynch DR. Anti-NMDA receptor encephalitis antibody binding is dependent on amino acid identity of a small region within the GluN1 amino terminal domain. *J Neurosci* 2012; **32**: 11082–94.

93 Gresa-Arribas N, Titulaer MJ, Torrents A, *et al.* Antibody titres at diagnosis and during follow-up of anti-NMDA receptor encephalitis: A retrospective study. *Lancet Neurol* 2014; **13**: 167–77.

94 Tüzün E, Zhou L, Baehring JM, Bannykh S, Rosenfeld MR, Dalmau J. Evidence for antibody-mediated pathogenesis in anti-NMDAR encephalitis associated with ovarian teratoma. *Acta Neuropathol* 2009; **118**: 737–43.

95 Dabner M, McCluggage WG, Bundell C, *et al.* Ovarian teratoma associated with anti-n-methyl D-aspartate receptor encephalitis: A report of 5 cases documenting prominent intratumoral lymphoid infiltrates. *Int J Gynecol Pathol* 2012; **31**: 429–37.

96 Dalmau J, Lancaster E, Martinez-Hernandez E, Rosenfeld MR, Balice-Gordon R. Clinical experience and laboratory investigations in patients with anti-NMDAR encephalitis. *Lancet Neurol* 2011; **10**: 63–74.

97 Armangue T, Spatola M, Vlagea A, *et al.* Frequency, symptoms, risk factors, and outcomes of autoimmune encephalitis after herpes simplex encephalitis: a prospective observational study and retrospective analysis. *Lancet Neurol* 2018; **17**: 760–72.

98 Armangue T, Moris G, Cantarín-Extremera V, *et al.* Autoimmune post-herpes simplex encephalitis of adults and teenagers. *Neurology* 2015; **85**: 1736–43.

99 Armangue T, Leypoldt F, Málaga I, *et al.* Herpes simplex virus encephalitis is a trigger of brain autoimmunity. *Ann Neurol* 2014; **75**: 317–23.

100 Gabilondo I, Saiz A, Galán L, *et al.* Analysis of relapses in anti-NMDAR encephalitis. *Neurology* 2011; **77**: 996–9.

101 Roopenian DC, Akilesh S. FcRn: The neonatal Fc receptor comes of age. *Nat Rev Immunol* 2007; **7**: 715–25.

102 Low SC, Mezo AR. Inhibitors of the FcRn:IgG protein-protein interaction. *AAPS J* 2009; **11**: 432–4.

103 Spiegelberg HL, Fishkin BG. The catabolism of human G immunoglobulins of different heavy chain subclasses. 3. The catabolism of heavy chain disease proteins and of Fc fragments of myeloma proteins. *Clin Exp Immunol* 1972; **10**: 599–607.

104 Waldmann TA, Strober W. Metabolism of immunoglobulins. *Prog Allergy* 1969; **13**: 1–110.

105 Morphis LG, Gitlin D. Maturation of the maternofoetal transport system for human γ-globulin in the mouse. *Nature* 1970; **228**: 573.

106 Brambell FW. The transmission of immunity from mother to young and the catabolism of immunoglobulins. *Lancet* 1966; **2**: 1087–93.

107 Simister NE, Rees AR. Isolation and characterization of an Fc receptor from neonatal rat small intestine. *Eur J Immunol* 1985; **15**: 733–8.

108 Simister NE, Mostov KE. An Fc receptor structurally related to MHC class I antigens. *Nature* 1989; **337**: 184–7.

109 Jones EA, Waldmann TA. The mechanism of intestinal uptake and transcellular transport of IgG in the neonatal rat. *J Clin Invest* 1972; **51**: 2916–27.

110 Leach JL, Sedmak DD, Osborne JM, Rahill B, Lairmore MD, Anderson CL. Isolation from human placenta of the IgG transporter, FcRn, and localization to the syncytiotrophoblast: implications for maternal-fetal antibody transport. *J Immunol* 1996; **157**: 3317–22.

111 Simister NE, Story CM, Chen HL, Hunt JS. An IgG-transporting Fc receptor expressed in the syncytiotrophoblast of human placenta. *Eur J Immunol* 1996; **26**: 1527–31.

112 Rodewald R. pH-dependent binding of immunoglobulins to intestinal cells of the neonatal rat. *J Cell Biol* 1976; **71**: 666–70.

113 Burmeister WP, Huber AH, Bjorkman PJ. Crystal structure of the complex of rat neonatal Fc receptor with Fc. *Nature* 1994; **372**: 379–83.

114 Raghavan M, Bonagura VR, Morrison SL, Bjorkman PJ. Analysis of the pH Dependence of the Neonatal Fc Receptor/Immunoglobulin G Interaction Using Antibody and Receptor Variants. *Biochemistry* 1995; **34**: 14649–57.

115 Kim J -K, Tsen M -F, Ghetie V, Ward ES. Localization of the site of the murine IgG1 molecule that is involved in binding to the murine intestinal Fc receptor. *Eur J Immunol* 1994; **24**: 2429–34.

116 Martin WL, West AP, Gan L, Bjorkman PJ. Crystal structure at 2.8 Å of an FcRn/heterodimeric Fc complex: Mechanism of pH-dependent binding. *Mol Cell* 2001; **7**: 867–77.

117 Deisenhofer J. Crystallographic Refinement and Atomic Models of a Human Fc Fragment and Its Complex with Fragment B of Protein A from Staphylococcus aureus at 2.9- and 2.8-Å Resolution. *Biochemistry* 1981; **20**: 2361–70.

118 Kristoffersen BK. Human placental Feγ-binding proteins in the maternofetal transfer of IgG. *APMIS, Suppl* 1996; **104**: 5–36.

119 Ober RJ, Martinez C, Vaccaro C, Zhou J, Ward ES. Visualizing the Site and Dynamics of IgG Salvage by the MHC Class I-Related Receptor, FcRn. *J Immunol* 2004; **172**: 2021–9.

120 Ober RJ, Martinez C, Lai X, Zhou J, Ward ES. Exocytosis of IgG as mediated by the receptor, FcRn: An analysis at the single-molecule level. *Proc Natl Acad Sci U S A* 2004; **101**: 11076–81.

121 Ward ES, Zhou J, Ghetie V, Ober RJ. Evidence to support the cellular mechanism involved in serum IgG homeostasis in humans. *Int Immunol* 2003; **15**: 187–95.

122 Akilesh S, Christianson GJ, Roopenian DC, Shaw AS. Neonatal FcR Expression in Bone Marrow-Derived Cells Functions to Protect Serum IgG from Catabolism. *J Immunol* 2007; **179**: 4580–8.

123 Schlachetzki F, Zhu C, Pardridge WM. Expression of the neonatal Fc receptor (FcRn) at the blood-brain barrier. *J Neurochem* 2002; **81**: 203–6.

124 Mayer B, Kis Z, Kaján G, Frenyó L V., Hammarström L, Kacskovics I. The neonatal Fc receptor (FcRn) is expressed in the bovine lung. *Vet Immunol Immunopathol* 2004; **98**: 85–9.

125 Spiekermann GM, Finn PW, Sally Ward E, *et al.* Receptor-mediated immunoglobulin G transport across mucosal barriers in adult life: Functional expression of FcRn in the mammalian lung. *J Exp Med* 2002; **196**: 303–10.

126 Haymann JP, Levraud JP, Bouet S, *et al.* Characterization and localization of the neonatal Fc receptor in adult human kidney. *J Am Soc Nephrol* 2000; **11**: 632–9.

127 Zhang Y, Pardridge WM. Mediated efflux of IgG molecules from brain to blood across the blood-brain barrier. *J Neuroimmunol* 2001; **114**: 168–72.

128 Burmeister WP, Gastinel LN, Simister NE, Blum ML, Bjorkman PJ. Crystal structure at 2.2 Å resolution of the MHC-related neonatal Fc receptor. *Nature* 1994; **372**: 336–43.

129 Martin WL, Bjorkman PJ. Characterization of the 2:1 complex between the class I MHC-related Fc receptor and its Fc ligand in solution. *Biochemistry* 1999; **38**: 12639–47.

130 Huber AH, Kelley RF, Gastinel LN, Bjorkman PJ. Crystallization and stoichiometry of binding of a complex between a rat intestinal Fc receptor and Fc. *J Mol Biol* 1993; **230**: 1077–83.

131 Sánchez LM, Penny DM, Bjorkman PJ. Stoichiometry of the interaction between the major histocompatibility- complex-related Fc receptor and its Fc ligand. *Biochemistry* 1999; **38**: 9471–6.

132 West AP, Bjorkman PJ. Crystal structure and immunoglobulin G binding properties of the human major histocompatibility complex-related Fc receptor. *Biochemistry* 2000; **39**: 9698–708.

133 Ghetie V, Ward ES. Multiple roles for the major histocompatibility complex class I-related receptor FcRn. *Annu Rev Immunol* 2000; **18**: 739–66.

134 Patel P, Schutzer SE, Pyrsopoulos N. Immunobiology of hepatocarcinogenesis: Ways to go or almost there? *World J Gastrointest Pathophysiol* 2016; **7**: 242.

135 Brambell FWR, Hemmings WA, Morris IG. A theoretical model of γ-globulin catabolism. *Nature* 1964; **203**: 1352–5.

136 Palmeira P, Quinello C, Silveira-Lessa AL, Zago CA, Carneiro-Sampaio M. IgG placental transfer in healthy and pathological pregnancies. *Clin Dev Immunol* 2012; **2012**: 985646.

137 Midelfart Hoff J, Midelfart A. Maternal myasthenia gravis: a cause for arthrogryposis multiplex congenita. *J Child Orthop* 2015; **9**: 433–5.

138 Vanoni F, Lava SAG, Fossali EF, *et al.* Neonatal Systemic Lupus Erythematosus Syndrome: a Comprehensive Review. *Clin Rev Allergy Immunol* 2017; **53**: 469–76.

139 Parlowsky T, Welzel J, Amagai M, Zillikens D, Wygold T. Neonatal pemphigus vulgaris: IgG4 autoantibodies to desmoglein 3 induce skin blisters in newborns. *J Am Acad Dermatol* 2003; **48**: 623–5.

140 Reznikoff-Etievant MF. Management of Alloimmune Neonatal and Antenatal Thrombocytopenia. *Vox Sang* 1988; **55**: 193–201.

141 Bussel JB, Primiani A. Fetal and neonatal alloimmune thrombocytopenia: progress and ongoing debates. *Blood Rev* 2008; **22**: 33–52.

142 Jacobson L, Polizzi A, Morriss-Kay G, Vincent A. Plasma from human mothers of fetuses with severe arthrogryposis multiplex congenita causes deformities in mice. *J Clin Invest* 1999; **103**: 1031–8.

143 Lee JY, Huerta PT, Zhang J, *et al.* Neurotoxic autoantibodies mediate congenital cortical impairment of offspring in maternal lupus. *Nat Med* 2009; **15**: 91–6.

144 Nishie W, Sawamura D, Natsuga K, *et al.* A Novel Humanized Neonatal Autoimmune Blistering Skin Disease Model Induced by Maternally Transferred Antibodies. *J Immunol* 2009; **183**: 4088–93.

145 Chen P, Li C, Lang S, *et al.* Animal model of fetal and neonatal immune thrombocytopenia: Role of neonatal Fc receptor in the pathogenesis and therapy. *Blood* 2010; **116**: 3660–8.

146 Obermeier B, Daneman R, Ransohoff RM. Development, maintenance and disruption of the blood-brain barrier. *Nat Med* 2013; **19**: 1584–96.

147 Daneman R, Zhou L, Kebede AA, Barres BA. Pericytes are required for blood-brain barrier integrity during embryogenesis. *Nature* 2010; **468**: 562–6.

148 Allt G, Lawrenson JG. Pericytes: Cell biology and pathology. *Cells Tissues Organs* 2001; **169**: 1–11.

149 Winkler EA, Bell RD, Zlokovic B V. Central nervous system pericytes in health and disease. *Nat Neurosci* 2011; **14**: 1398–405.

150 Li F, Lan Y, Wang Y, *et al.* Endothelial Smad4 Maintains Cerebrovascular Integrity by Activating N-Cadherin through Cooperation with Notch. *Dev Cell* 2011; **20**: 291–302.

151 Lee SW, Kim WJ, Choi YK, *et al.* SSeCKS regulates angiogenesis and tight junction formation in blood-brain barrier. *Nat Med* 2003; **9**: 900–6.

152 Gee JR, Keller JN. Astrocytes: Regulation of brain homeostasis via apolipoprotein E. *Int J Biochem Cell Biol* 2005; **37**: 1145–50.

153 Shalaby F, Janet R, Yamaguchi TP, *et al.* Failure of blood-island formation and vasculogenesis in Flk-1-deficient mice. *Nature* 1995; **376**: 62–6.

154 Daneman R, Agalliu D, Zhou L, Kuhnert F, Kuo CJ, Barres BA. Wnt/β-catenin signaling is required for CNS, but not non-CNS, angiogenesis. *Proc Natl Acad Sci U S A* 2009; **106**: 641–6.

155 Logan CY, Nusse R. The Wnt signaling pathway in development and disease. *Annu Rev Cell Dev Biol* 2004; **20**: 781–810.

156 Stenman JM, Rajagopal J, Carroll TJ, Ishibashi M, McMahon J, McMahon AP. Canonical Wnt signaling regulates organ-specific assembly and differentiation of CNS vasculature. *Science* 2008; **322**: 1247–50.

157 Alvarez JI, Dodelet-Devillers A, Kebir H, *et al.* The hedgehog pathway promotes blood-brain barrier integrity and CNS immune quiescence. *Science* 2011; **334**: 1727–31.

158 Virgintino D, Errede M, Robertson D, *et al.* Immunolocalization of tight junction proteins in the adult and developing human brain. *Histochem Cell Biol* 2004; **122**: 51–9.

159 Traynelis SF, Wollmuth LP, McBain CJ, *et al.* Glutamate receptor ion channels: Structure, regulation, and function. *Pharmacol Rev* 2010; **62**: 405–96.

160 Jatzke C, Watanabe J, Wollmuth LP. Voltage and concentration dependence of Ca2+ permeability in recombinant glutamate receptor subtypes. *J Physiol* 2002; **538**: 25–39.

161 Lester RAJ, Clements JD, Westbrook GL, Jahr CE. Channel kinetics determine the time course of NMDA receptor-mediated synaptic currents. *Nature* 1990; **346**: 565–7.

162 Johnson JW, Ascher P. Glycine potentiates the NMDA response in cultured mouse brain neurons. *Nature* 1987; **325**: 529–31.

163 Kleckner NW, Dingledine R. Requirement for glycine in activation of NMDA receptors expressed in xenopus oocytes. *Science* 1988; **241**: 835–7.

164 Lerma J, Zukin RS, Bennett MVL. Glycine decreases desensitization of N-methyl-D-aspartate (NMDA) receptors expressed in Xenopus oocytes and is required for NMDA responses. *Proc Natl Acad Sci U S A* 1990; **87**: 2354–8.

165 Antonov SM, Johnson JW. Permeant ion regulation of N-methyl-D-aspartate receptor channel block by Mg2+. *Proc Natl Acad Sci U S A* 1999; **96**: 14571–6.

166 Bourne HR, Nicoll R. Molecular machines integrate coincident synaptic signals. *Cell* 1993; **72**: 65–75.

167 Laube B, Kuhse J, Betz H. Evidence for a tetrameric structure of recombinant NMDA receptors. *J Neurosci* 1998; **18**: 2954–61.

168 Karakas E, Furukawa H. Crystal structure of a heterotetrameric NMDA receptor ion channel. *Science* 2014; **344**: 992–7.

169 Tajima N, Karakas E, Grant T, *et al.* Activation of NMDA receptors and the mechanism of inhibition by ifenprodil. *Nature* 2016; **534**: 63–8.

170 Furukawa H, Singh SK, Mancusso R, Gouaux E. Subunit arrangement and function in NMDA receptors. *Nature* 2005; **438**: 185–92.

171 Yao Y, Mayer ML. Characterization of a soluble ligand binding domain of the NMDA receptor regulatory subunit NR3A. *J Neurosci* 2006; **26**: 4559–66.

172 Ehlers MD, Zhang S, Bernhardt JP, Huganir RL. Inactivation of NMDA receptors by direct interaction of calmodulin with the NR1 subunit. *Cell* 1996; **84**: 745–55.

173 Lee CH, Lü W, Michel JC, *et al.* NMDA receptor structures reveal subunit arrangement and pore architecture. *Nature* 2014; **511**: 191–7.

174 Monyer H, Sprengel R, Schoepfer R, *et al.* Heteromeric NMDA receptors: Molecular and functional distinction of subtypes. *Science* 1992; **256**: 1217–21.

175 Vicini S, Wang JF, Li JH, *et al.* Functional and pharmacological differences between recombinant N- methyl-D-aspartate receptors. *J Neurophysiol* 1998; **79**: 555–66.

176 Pérez-Otaño I, Schulteis CT, Contractor A, *et al.* Assembly with the NR1 subunit is required for surface expression of NR3A-containing NMDA receptors. *J Neurosci* 2001; **21**: 1228–37.

177 Hunt DL, Castillo PE. Synaptic plasticity of NMDA receptors: Mechanisms and functional implications. *Curr Opin Neurobiol* 2012; **22**: 496–508.

178 Hansen KB, Yi F, Perszyk RE, *et al.* Structure, function, and allosteric modulation of NMDA receptors. *J Gen Physiol* 2018; **150**: 1081–105.

179 Watanabe M, Inoue Y, Sakimura K, Mishina M. Developmental changes in distribution of nmda receptor channel subunit m rim as. *Neuroreport* 1992; **3**: 1138–40.

180 Monyer H, Burnashev N, Laurie DJ, Sakmann B, Seeburg PH. Developmental and regional expression in the rat brain and functional properties of four NMDA receptors. *Neuron* 1994; **12**: 529–40.

181 Akazawa C, Shigemoto R, Bessho Y, Nakanishi S, Mizuno N. Differential expression of five N-methyl-D-aspartate receptor subunit mRNAs in the cerebellum of developing and adult rats. *J Comp Neurol* 1994; **347**: 150–60.

182 Rauner C, Köhr G. Triheteromeric NR1/NR2A/NR2B receptors constitute the major N-methyl-D-aspartate receptor population in adult hippocampal synapses. *J Biol Chem* 2011; **286**: 7558–66.

183 Gray JA, Shi Y, Usui H, During MJ, Sakimura K, Nicoll RA. Distinct Modes of AMPA Receptor Suppression at Developing Synapses by GluN2A and GluN2B: Single-Cell NMDA Receptor Subunit Deletion In Vivo. *Neuron* 2011; **71**: 1085–101.

184 Graus F, Illa I, Agusti M, Ribalta T, Cruz-Sanchez F, Juarez C. Effect of intraventricular injection of an anti-Purkinje cell antibody (anti-Yo) in a guinea pig model. *J Neurol Sci* 1991; **106**: 82–7.

185 Moscato EH, Peng X, Jain A, Parsons TD, Dalmau J, Balice-Gordon RJ. Acute mechanisms underlying antibody effects in anti-N-methyl-D-aspartate receptor encephalitis. *Ann Neurol* 2014; **76**: 108–19.

186 Lu WY, Man HY, Ju W, Trimble WS, MacDonald JF, Wang YT. Activation of synaptic NMDA receptors induces membrane insertion of new AMPA receptors and LTP in cultured hippocampal neurons. *Neuron* 2001; **29**: 243–54.

187 Dalva MB, Takasu MA, Lin MZ, *et al.* EphB receptors interact with NMDA receptors and regulate excitatory synapse formation. *Cell* 2000; **103**: 945–56.

188 Henderson JT, Georgiou J, Jia Z, *et al.* The receptor tyrosine kinase EphB2 regulates NMDA-dependent synaptic function. *Neuron* 2001; **32**: 1041–56.

189 Kullander K, Klein R. Mechanisms and functions of Eph and ephrin signalling. *Nat Rev Mol Cell Biol* 2002; **3**: 475–86.

190 Lisabeth EM, Falivelli G, Pasquale EB. Eph receptor signaling and ephrins. *Cold Spring Harb Perspect Biol* 2013; **5**: a009159.

191 Grunwald IC, Korte M, Wolfer D, *et al.* Kinase-independent requirement of EphB2 receptors in hippocampal synaptic plasticity. *Neuron* 2001; **32**: 1027–40.

192 Rose NR, Bona C. Defining criteria for autoimmune diseases (Witebsky's postulates revisited). *Immunol Today* 1993; **14**: 426–30.

193 Leypoldt F, Höftberger R, Titulaer MJ, *et al.* Investigations on CXCL13 in anti-N-methyl-D-aspartate receptor encephalitis: A potential biomarker of treatment response. *JAMA Neurol* 2015; **72**: 180–6.

194 Martinez-Hernandez E, Horvath J, Shiloh-Malawsky Y, Sangha N, Martinez-Lage M, Dalmau J. Analysis of complement and plasma cells in the brain of patients with anti-NMDAR encephalitis. *Neurology* 2011; **77**: 589–93.

195 Huerta PT, Sun LD, Wilson MA, Tonegawa S. Formation of temporal memory requires NMDA receptors within CA1 pyramidal neurons. *Neuron* 2000; **25**: 473–80.

196 Tsien JZ, Huerta PT, Tonegawa S. The essential role of hippocampal CA1 NMDA receptor-dependent synaptic plasticity in spatial memory. *Cell* 1996; **87**: 1327–38.

197 Hilderink M, Titulaer MJ, Schreurs MWJ, Keizer K, Bunt JEH. Transient anti-nmdar encephalitis in a newborn infant due to transplacental transmission. *Neurol Neuroimmunol Neuroinflamm* 2015; **2**: 1–2.

198 Jagota P, Vincent A, Bhidayasiri R. Transplacental transfer of nmda receptor antibodies in an infant with cortical dysplasia. *Neurology* 2014; **82**: 1662–3.

199 Jurek B, Chayka M, Kreye J, *et al.* Human gestational N-methyl-D-aspartate receptor autoantibodies impair neonatal murine brain function. *Ann Neurol* 2019; **86**: 656–70.

200 Braniste V, Al-Asmakh M, Kowal C, *et al.* The gut microbiota influences blood-brain barrier permeability in mice. *Sci Transl Med* 2014; **6**: 263ra158.

201 Puighermanal E, Marsicano G, Busquets-Garcia A, Lutz B, Maldonado R, Ozaita A. Cannabinoid modulation of hippocampal long-term memory is mediated by mTOR signaling. *Nat Neurosci* 2009; **12**: 1152–8.

202 Ennaceur A. One-trial object recognition in rats and mice: Methodological and theoretical issues. *Behav Brain Res* 2010; **215**: 244–54.

203 Barker GRI, Warburton EC. When Is the Hippocampus Involved in Recognition Memory? *J Neurosci* 2011; **31**: 10721–31.

204 Carceles-Cordon M, Mannara F, Aguilar E, Castellanos A, Planagumà J, Dalmau J. NMDAR Antibodies Alter Dopamine Receptors and Cause Psychotic Behavior in Mice. *Ann Neurol* 2020; **88**: 603–13.

205 Haselmann H, Mannara F, Werner C, *et al.* Human Autoantibodies against the AMPA Receptor Subunit GluA2 Induce Receptor Reorganization and Memory Dysfunction. *Neuron* 2018; **100**: 91-105.e9.

206 Joubert B, García-Serra A, Planagumà J, *et al.* Pregnancy outcomes in anti-NMDA receptor encephalitis: Case series. *Neurol Neuroimmunol Neuroinflamm* 2020; **7**: e668.

207 Chourasia N, Watkins MW, Lankford JE, Kass JS, Kamdar A. An Infant Born to a Mother With Anti–N-Methyl-D-Aspartate Receptor Encephalitis. *Pediatr Neurol* 2018; **79**: 65–8.

208 Lamale-Smith LM, Moore GS, Guntupalli SR, Scott JB. Maternal-fetal transfer of anti-N-methyl-d-aspartate receptor antibodies. *Obstet Gynecol* 2015; **125**: 1056–8.

209 García-Serra A, Radosevic M, Pupak A, *et al.* Placental transfer of NMDAR antibodies causes reversible alterations in mice. *Neurol Neuroimmunol Neuroinflamm* 2021; **8**: e915.

210 Bittolo T, Raminelli CA, Deiana C, *et al.* Pharmacological treatment with mirtazapine rescues cortical atrophy and respiratory deficits in MeCP2 null mice. *Sci Rep* 2016; **6**: 1–14.

211 Narboux-Nême N, Angenard G, Mosienko V, *et al.* Postnatal growth defects in mice with constitutive depletion of central serotonin. *ACS Chem Neurosci* 2013; **4**: 171–81.

212 Datwani A, Iwasato T, Itohara S, Erzurumlu RS. NMDA receptor-dependent pattern transfer from afferents to postsynaptic cells and dendritic differentiation in the barrel cortex. *Mol Cell Neurosci* 2002; **21**: 477–92.

213 Elhardt M, Martinez L, Tejada-Simon MV. Neurochemical, behavioral and architectural changes after chronic inactivation of NMDA receptors in mice. *Neurosci Lett* 2010; **468**: 166–71.

214 Paolicelli RC, Ferretti MT. Function and dysfunction of microglia during brain development: Consequences for synapses and neural circuits. *Front Synaptic Neurosci* 2017; **9**: 1–17.

215 Hoshiko M, Arnoux I, Avignone E, Yamamoto N, Audinat E. Deficiency of the microglial receptor CX3CR1 impairs postnatal functional development of thalamocortical synapses in the barrel cortex. *J Neurosci* 2012; **32**: 15106–11.

216 Paolicelli RC, Bolasco G, Pagani F, *et al.* Synaptic pruning by microglia is necessary for normal brain development. *Science* 2011; **333**: 1456–8.

217 Malek A, Sager R, Kuhn P, Nicolaides KH, Schneider H. Evolution of maternofetal transport of immunoglobulins during human pregnancy. *Am J Reprod Immunol* 1996; **36**: 248–55.

218 Dancis J, Lind J, Oratz M, Smolens J, Vara P. Placental transfer of proteins in human gestation. *Am J Obstet Gynecol* 1961; **82**: 167–71.

219 Roopenian DC, Christianson GJ, Sproule TJ, *et al.* The MHC Class I-Like IgG Receptor Controls Perinatal IgG Transport, IgG Homeostasis, and Fate of IgG-Fc-Coupled Drugs. *J Immunol* 2003; **170**: 3528–33.

220 Roy S, Nanovskaya T, Patrikeeva S, *et al.* M281, an anti-FcRn antibody, inhibits IgG transfer in a human ex vivo placental perfusion model. *Am J Obstet Gynecol* 2019; **220**: 498.e1-498.e9.

221 Coutinho E, Jacobson L, Shock A, Smith B, Vernon A, Vincent A. Inhibition of maternal-to-fetal transfer of IgG antibodies by FcRn blockade in a mouse model of arthrogryposis multiplex congenita. *Neurol Neuroimmunol Neuroinflamm* 2021; **8**: e1011.

222 Momenta Pharmaceuticals Inc. A Study to Test Efficacy and Safety of Rozanolixizumab in Adult Patients With Generalized Myasthenia Gravis. 2019 https://clinicaltrials.gov/ct2/show/NCT03971422.

223 Momenta Pharmaceuticals Inc. A Study to Evaluate the Safety, Tolerability, Efficacy, Pharmacokinetics and Pharmacodynamics of M281 Administered to Adults With Generalized Myasthenia Gravis. 2018 https://clinicaltrials.gov/ct2/show/NCT03772587?term=M281&rank=5.

224 Ling LE, Hillson JL, Tiessen RG, *et al.* M281, an Anti-FcRn Antibody: Pharmacodynamics, Pharmacokinetics, and Safety Across the Full Range of IgG Reduction in a First-in-Human Study. *Clin Pharmacol Ther* 2018; **105**: 1031–9.

225 Momenta Pharmaceuticals Inc. A Study to Evaluate the Safety, Efficacy, Pharmacokinetics and Pharmacodynamics of M281 Administered to Pregnant Women at High Risk for Early Onset Severe Hemolytic Disease of the Fetus and Newborn (HDFN). 2019 https://clinicaltrials.gov/ct2/show/NCT03842189?term=M281&rank=2.

226 Sheikhbahaei S, Sherkat R, Camacho-Ordonez N, *et al.* Pregnancy, child bearing and prevention of giving birth to the affected children in patients with primary immunodeficiency disease; A case-series. *BMC Pregnancy Childbirth* 2018; **18**: 299.

227 Mandal PK, Dolai TK, Bagchi B, Ghosh MK, Bose S, Bhattacharyya M. B Cell Suppression in Newborn Following Treatment of Pregnant Diffuse Large B-cell Lymphoma Patient with Rituximab Containing Regimen. *Indian J Pediatr* 2014; **81**: 1092–4.

228 Cooper PR, Ciambrone GJ, Kliwinski CM, *et al.* Efflux of monoclonal antibodies from rat brain by neonatal Fc receptor, FcRn. *Brain Res* 2013; **1534**: 13–21.

229 Mannara F, Radosevic M, Planagumà J, *et al.* Allosteric modulation of NMDA receptors prevents the antibody effects of patients with anti-NMDAR encephalitis. *Brain* 2020; **143**: 2709–20.

230 Paul SM, Doherty JJ, Robichaud AJ, *et al.* The major brain cholesterol metabolite 24(S)-hydroxycholesterol is a potent allosteric modulator of N-Methyl-D-Aspartate receptors. *J Neurosci* 2013; **33**: 17290–300.

231 Warikoo N, Brunwasser SJ, Benz A, *et al.* Positive allosteric modulation as a potential therapeutic strategy in anti-NMDA receptor encephalitis. *J Neurosci* 2018; **38**: 3218–29.

232 Murck H, Paskavitz J, Hoffmann E, *et al.* P.165 Double-blind, placebo-controlled phase 1 single ascending dose study of sage-718. *Eur Neuropsychopharmacol* 2019; **29**: S128.

ANNEX

Other publications

- Martinez-Hernandez E, Guasp M, García-Serra A, Maudes E, Ariño H, Sepulveda M, Armangué T, Ramos AP, Ben-Hur T, Iizuka T, Saiz A, Graus F, Dalmau J. Clinical significance of anti-NMDAR concurrent with glial or neuronal surface antibodies. Neurology. 2020 Jun 2;94(22):e2302-e2310. doi: 10.1212/WNL.0000000000009239. Epub 2020 Mar 11. PMID: 32161029.

- Landa J, Guasp M, Míguez-Cabello F, Guimarães J, Mishima T, Oda F, Zipp F, Krajinovic V, Fuhr P, Honnorat J, Titulaer M, Simabukuro M, Planagumà J, Martínez-Hernández E, Armangué T, Saiz A, Gasull X, Soto D, Graus F, Sabater L, Dalmau J; GluK2 encephalitis study group. Encephalitis with Autoantibodies against the Glutamate Kainate Receptors GluK2. Ann Neurol. 2021 May 5. doi: 10.1002/ana.26098. Epub ahead of print. PMID: 33949707.

Acknowledgements/Agraïments

Crec que no és possible plasmar en paraules l'agraïment que sento per tot el caliu i el suport que he rebut. El doctorat han estat quatre anys en què ha passat de tot a la meva vida. He après moltíssim, i m'hi he deixat sang, suor, llàgrimes, i algun òrgan pel camí. Tinc la sensació d'haver après més de mi mateixa i de relació interpersonal que no pas de ciència, i mira que n'he après.

Primer de tot, moltes gràcies Josep, per haver confiat en mi des del primer dia i haver tingut prou paciència per ensenyar-me i compartir com vius i entens la ciència.

Jesús, moltes gràcies per l'oportunitat d'involucrar-me en els projectes i aprendre a cada pas.

Thank you, Myrna. You and I know that without you probably my path here would have been very very different.

A tot l'equip del laboratori amb qui he col·laborat més o menys i que heu anat apareixent o marxant durant aquest període de temps. Francesco, per introduir-me amb tant respecte al món de l'experimentació animal; Mar P., per tenir-te com a mentora llunyana en el procés acadèmic de doctorat; Marija, por hacer que trabajar contigo sea tan fácil; Lidia, pels teus consells biomoleculars i un limoncello deliciós; Eugenia, per la teva tremenda saviesa vital; Merche, per alegrar-nos la vida sent tu; Maria, per ser una peça clau indispensable i la complicitat; Esther, gracias por la implicación tanto profesional como personal, y poder hablar de Hume, de cómics o de lo que se tercie. Helena, Marta, Marianna, gracias por vuestra disposición a enseñar o echar una mano con una actitud siempre positiva.

Al club del café. Paula, los desayunos de los domingos que ha habido que venir han sabido mejor contigo. Bastien, je suis vraiment reconnaissant pour la scène partagée avec toi. Mar G, per alegrar-te tant genuïnament de qualsevol petit pas endavant. Jon, por los esquejes, qué tuerca eres, y todos los swingouts que nos quedan.

Estitxu, eskerrik asko, ederra. Por ser mi compitrueno, por estar codo con codo durante todo el proceso, dando apoyo logístico y emocional. Sin ti no hubiera aguantado ni tanto ni tan bien.

Ja que m'hi he passat tantíssimes hores, moltes gràcies a tot l'equip humà de l'estabulari, ho heu fet més fàcil; i en especial a en Pep. Gràcies per la teva càlida amabilitat des del primer moment i les recomanacions culturals al llarg de tota aquesta aventura.

Bioquímics, gràcies per seguir rient a les barbacoes com si les nostres vides no haguessin canviat tant des que vem acabar la uni. Helena, sé que poca gent empatitza amb el procés com tu,

gràcies per generar l'espai de compartir penes i glòries amb tant carinyo. Marc i Silvia, mi consejo de sabios, us estimo tant; la resta la sabeu de sobres, gràcies.

Aina, Yi, Vasilka i Marina, per haver fet llar d'una habitació a Sants.

A tota la gent amb qui he compartit part del camí, potser sense ser-ne conscients. Faig una llista ràpida intentant-me recordar de tothom: Anika Pupak, Eva Banús, Andrea Arcas, Alba Andrés, Mireia Tarrés, tota la gent de swing i de la Iguana per tanta i tanta felicitat, Anna Paredes, Rodrigo, Toni, Rubén, Chavero y Ana, Marian i Alex, Carol i companyia, Anne, Clara i Georgina, Fio, Sandra y Elena, Ibai, Júlia, Sílvia, Eduard i Roser, Clara i Gala, Laura Garcia, Silvia i Águeda, a La ciutat invisible, al Kop de mà; gràcies!

A la família, tete, tiets i tietes, avis y yayos, us estimo una barbaritat!

A la Sivi, cari-cari, per ser una ànima afí en aquesta bogeria que anomenem vida.

A la mama, pel seu amor i la seva fe incondicionals en mi i en la meva vàlua com a persona. T'estimo.

A mi padre, gracias por haberme escuchado tanto y vivido tan de cerca cada experimento, reto y triunfo, que un poquito son tuyos también. Te quiero.

I gràcies als pacients i a les famílies, sense la vostra col·laboració la recerca no seria possible.

"Sé que cierro con este libro un ciclo vital y se abre con su cierre un espacio dentro de mí que aún no existía. Un espacio de silencio, un espacio en el que mi salud mental ya no está en riesgo, un lugar en el que no quiero experimentar ni ser experimento. Quiero vivir intensamente, porque tampoco sé vivir de otra manera, y quiero, también, explorar ese silencio, el silencio que hay en mí. "

Brigitte Vasallo (1973-actualidad)
Escritora y activista antirracista, feminista y LGBTI española